2014

Characterization of Phosphatidylinositol 4,5-bisphosphate Regulation of the Electrogenic Na/Bicarbonate Cotransporter NBCe1

Ian Michael Thornell
University of Alabama at Birmingham

CHARACTERIZATION OF PHOSPHATIDYLINOSITOL 4,5-BISPHOSPHATE REGULATION OF THE ELECTROGENIC Na/BICARBONATE COTRANSPORTER NBCe1

by

IAN M. THORNELL

MARK O. BEVENSEE, COMMITTEE CHAIR
WALTER F. BORON
KEVIN L. KIRK
ROBIN AJ. LESTER
JACQUES I. WADICHE

A DISSERTATION

Submitted to the graduate faculty of The University of Alabama at Birmingham,
in partial fulfillment of the requirements for the degree of
Doctor of Philosophy

BIRMINGHAM, ALABAMA

2014

CHARACTERIZATION OF PHOSPHATIDYLINOSITOL 4,5-BISPHOSPHATE REGULATION OF THE ELECTROGENIC Na/BICARBONATE COTRANSPORTER NBCe1

IAN M. THORNELL

NEUROSCIENCE

ABSTRACT

The electrogenic Na/bicarbonate cotransporter (NBCe1) is an acid/base regulator that is also involved in coordinating epithelial ion transport. Splice variants of NBCe1 differ at their cytosolic amino- (N-) and/or carboxy- (C-) termini. These different cytosolic termini impart differential regulation for each variant. For example, the N-terminus of NBCe1-A is autostimulatory, whereas the N-terminus of NBCe1-B and -C is autoinhibitory. We examine the regulatory role of PIP_2 for NBCe1 splice variants. In the first study of this dissertation, we characterize the effect of increasing PIP_2 on the activity of NBCe1-A, -B, and -C expressed in *Xenopus laevis* oocytes. Injecting PIP_2 stimulated NBCe1-B and -C current by ~150% as monitored by the two-electrode voltage-clamp technique. The majority of this stimulation required PIP_2 hydrolysis to IP_3 and ER Ca^{2+} stores, and was mediated by a staurosporine-sensitive kinase. The second study focuses on the effect of PIP_2 itself on the activity of NBCe1 expressed in oocytes. The two-electrode voltage-clamp technique was used to control the activation of a co-expressed voltage sensitive phosphatase (VSP), that dephosphorylates PIP_2, and to monitor associated changes in the current of co-expressed NBCe1 variants. VSP activation by depolarizing an oocyte to +60 mV for 10 s inhibited NBCe1-B and -C by ~35%. When VSP was subsequently inactivated by repolarization to -60 mV, NBCe1 currents slowly recovered to baseline levels. Both NBCe1 currents and PIP_2 levels were simultaneously

monitored by the two-electrode voltage-clamp technique and confocal imaging of a PIP_2-binding pleckstrin homology conjugated to green fluorescent protein, respectively. The slow NBCe1 current recovery mirrored PIP_2 replenishment at the membrane. NBCe1 inhibition was not observed in the same experimental protocols with a catalytically dead VSP. These combined studies reveal that PIP_2 can regulate NBCe1 activity by a dual mechanism that involves both PIP_2 itself and the classic IP_3/Ca^{2+} pathway. This dissertation provides insight into how acid-base regulation can be tightly coupled to receptors that hydrolyze PIP_2, such as G_q-coupled receptors. Because PIP_2 is a ubiquitous signaling epicenter, the findings may have implications across many types of tissue.

Keywords: acid-base, bicarbonate, NBCe1, phospholipid, PIP_2, SLC4

DEDICATION

This dissertation is dedicated to my father, for promoting the value of an education and the pursuit of curiosity, and my mother, for being an exemplar of determination and resolve.

ACKNOWLEDGMENTS

I thank my mentor Dr. Mark Bevensee, whose guidance has transformed me from a graduate student into the conscientious scientist I am today. I also thank my committee members Dr. Mark Bevensee, Dr. Robin Lester, Dr. Jacques Wadiche, Dr. Kevin Kirk, Dr. Walter Boron and the late Dr. Dale Benos for their suggestions, comments, guidance, and enthusiasm. I thank Dr. Mark Bevensee, Dr. Lori McMahon, and Dr. Kent Keyser for their mentorship in teaching and for the opportunities they have given me to educate aspiring scientists. Finally, I thank the past and present members of the Bevensee Laboratory who have help me along the way, especially Jianping Wu and Xiaofen Liu for their time, patience, and training.

TABLE OF CONTENTS

Page

TABLE OF CONTENTS (CONTINUED)

Page

LIST OF TABLES

Table *Page*

INTRODUCTION

LIST OF FIGURES

Figure *Page*

INTRODUCTION

REGULATORS OF *Slc4* BICARBONATE TRANSPORTER ACITIVITY

PIP_2 HYDROLYSIS STIMULATES THE ELECTROGENIC Na/BICARBONATE COTRANSPORTER NBCe1-B AND -C VARIANTS EXPRESSED IN *XENOPUS LAEVIS* OOCYTES

LIST OF FIGURES (CONTINUED)

Figure *Page*

LIST OF FIGURES (CONTINUED)

Figure *Page*

PIP$_2$ DEGRADATION INHIBITS THE ELECTROGENIC Na/BICARBONATE COTRANSPORTER NBCe1-B AND -C VARIANTS EXPRESSED IN *XENOPUS* OOCYTES

DISCUSSION

INTRODUCTION

Intracellular pH (pH_i) regulation is vital for proper cell function because many cellular processes are pH-sensitive (Roos & Boron, 1981; Chesler, 2003; Vaughan-Jones *et al.*, 2009). Regarding pH-sensitive processes, a pioneering *in vitro* study demonstrated that acidic pH inhibits phosphorylase *a* activation of phosphorylase *b*—an enzyme that catalyzes mobilization of glucose from glycogen stores (Danforth, 1965). In a subsequent study, phosphofructokinase—the rate limiting glycolytic enzyme—was inhibited *in vitro* by lowering pH within the physiological range (Trivedi & Danforth, 1966). The pH sensitivity of these two ubiquitous enzymes highlights the influence of pH on cell biology. Additionally, a myriad of other proteins have pH sensitivity, such as ion channels [e.g., the N-methyl-d-aspartate receptor (Traynelis & Cull-Candy, 1990; Tang *et al.*, 1990), voltage-gated K^+, Na^+, and Ca^{2+} channels (Tombaugh & Somjen, 1996), and the acid-sensing ion channel (Waldmann *et al.*, 1997)]. Finally, the importance of pH regulation is reflected in genetic diseases of acid-base transporters (Alper, 2002)

The proton regulates proteins, for example through aqueous histidine residues. Histidine has a pKa of 6.8 and therefore histidine is readily protonated and deprotonated within the physiological pH_i range of 7.0 to 7.4 (Madshus, 1988). As pH_i decreases, histidine residues are protonated and the radical group is no longer charged. Subsequently, amino acids can change structure or lose catalytic activity.

The cell has various acid-base transporters to maintain the physiological pH_i range (Bevensee & Boron, 2007). These pH_i-regulating transporters are either acid loaders or acid extruders. The acid loaders lower the pH_i either by importing protons or extruding HCO_3^- or CO_3^{2-} across cell membranes. Conversely, acid extruders raise the pH_i either by extruding protons or importing HCO_3^- or CO_3^{2-} across cell membranes.

The *Solute carrier 4* (*Slc4*) gene encodes HCO_3^- transporters that are powerful regulators of pH (Alper, 2009; Parker & Boron, 2013). A single cell can employ several acid loading and acid extruding HCO_3^- transporters and even express different splice variants of the same member. We hypothesize that the aforementioned differential transporter regulation may explain the apparent redundancy in acid-base transporter expression. This idea is expanded on in Chapter 2. This dissertation examines the phospholipid phosphatidylinositol 4,5-bisphosphate (PIP_2) regulation of 3 splice variants—A, B, and C—of the electrogenic Na/HCO_3 cotransporter NBCe1. In this introductory chapter, I will provide an overview of NBCe1 and its regulation. I will then provide an overview of PIP_2 and its characterized interactions with other membrane channels and transporters. Finally, the goals of this dissertation are outlined and the results are briefly summarized.

Electrogenic Na/HCO_3 cotransporter, NBCe1

Cloned Variants

NBCe1 is an electrogenic Na^+-dependent cotransporter that is a member of the bicarbonate transporter superfamily, which includes other Na^+-dependent HCO_3^- transporters and the Na^+-independent anion exchangers, which are all encoded by *Slc4*

genes. NBCe1-A was the first Na^+-dependent HCO_3^- transporter functionally described (Boron & Boulpaep, 1983) and cloned (Romero *et al.*, 1997). Subsequently, NBCe1 cDNA from different tissue, including additional splice variants, were cloned from various animals (Table 1). NBCe1-B, -C, and -E are transcribed from a promoter upstream of exon 1 (Abuladze *et al.*, 2000). This sequence translates into an NBCe1 protein with an 85 residue N-terminus that is different from NBCe1-A and -D (Figure 1). The 43 residue N-terminus of NBCe1-A and -D arises from an alternative promoter in intron 3 (Abuladze *et al.*, 2000). The 61 residue C-terminus of NBCe1-C, which arises from a 97-base pair deletion, is distinct from the other variants' 46 residue C-terminus (Bevensee *et al.*, 2000). Both NBCe1-D and -E are missing 9 amino acid residues between the variable N-terminus and the putative transmembrane domains. This 9 residue extraction arises from an unidentified splicing mechanism in exon 6 (Liu *et al.*, 2011). NBCe1-D and -E clones are presumed to be functional, but have not been expressed and functionally characterized (Parker & Boron, 2013). This dissertation focuses on PIP_2 regulation of the characterized NBCe1 variants (-A, -B, and -C).

NBCe1 Physiology

NBCe1 cotransports 1 Na^+ and either 2 or 3 HCO_3^- ions [alternatively 1 CO_3^{2-} or 1 CO_3^{2-} and 1 HCO_3^- (Lee *et al.*, 2011)]. Because NBCe1 transports 2 or 3 base equivalents, NBCe1activity and associated regulation plays an important role in pH homeostasis. In addition, NBCe1 variants have specific roles in acid-base and solute transport in different cell-types. Some examples are summarized below.

Renal Proximal Tubule. The first Na^+-dependent HCO_3^- transporter was identified in the salamander proximal renal tubule (Boron & Boulpaep, 1983). In the proximal tubule, NBCe1-A contributes to ~90% of the HCO_3^- reabsorption. Briefly, protons are secreted from the apical membrane by a proton pump and the Na-H exchanger NHE3. These protons combine with tubular HCO_3^- to form CO_2 and H_2O due to the presence of the apical membrane tethered carbonic anhydrase IV (CA IV). Gaseous CO_2 diffuses across the apical membrane into the tubule cell, where it undergoes CA II catalyzed hydrolysis to reform HCO_3^- and protons. These protons are apically secreted and used for subsequent tubule reactions. The HCO_3^- formed inside the epithelial cell is the substrate for the basolateral NBCe1, which operates with a 1:3 stoichiometry and transports the HCO_3^- to the blood.

Pancreas. The exocrine role of the pancreas involves secreting digestive enzymes into the duodenum. These enzymes are kept inactive by maintaining a pancreatic fluid with a pH greater than 8.0. The pancreatic fluid has HCO_3^- concentrations as high as 70-75 mM for mice and rats; and ~150 mM for cats, guinea pigs and humans (Sinđić *et al.*, 2010). The majority of these large apical HCO_3^- secretions are maintained by NBCe1-B in the basolateral membrane of the duct cells (Muallem & Loessberg, 1990; Ishiguro *et al.*, 1996). The HCO_3^- is apically secreted through the channel cystic fibrosis transmembrane conductance regulator (CFTR) and SLC26 encoded proteins, which are Cl-HCO_3 exchangers, however their relative contributions to HCO_3^- secretion remain controversial (Steward & Ishiguro, 2009).

Basolateral and apical HCO_3^- transport is tightly coupled because pH_i does not change during apical HCO_3^- secretion (Steward & Ishiguro, 2009). This coordination

between basolateral and apical HCO_3^- transport highlights the importance of NBCe1 regulation in pancreatic duct cells. One signaling molecule pertinent to the pathways discussed in this dissertation is IRBIT (IP$_3$ receptor binding protein released with inositol-triphosphate, IP$_3$), which weakly binds to the IP$_3$ receptor and is released from the IP$_3$ receptor by increasing IP$_3$ concentrations. In mouse duct cells, IRBIT tonically stimulates HCO_3^- secretion (Yang *et al.*, 2009). IRBIT also stimulates NBCe1 (Shirakabe *et al.*, 2006) and potentially coordinates NBCe1 activity with apical HCO_3^- secretion (Yang *et al.*, 2009). Additionally, secretin and acetylcholine both increase apical HCO_3^- secretions (Evans *et al.*, 1996) and potentially NBCe1 either through IRBIT or the IP$_3$/Ca^{2+} pathway discussed in this dissertation. Crosstalk between all these aforementioned pathways is likely because apical and basolateral HCO_3^- transport are tightly coupled (Lee *et al.*, 2012).

Brain. The aforementioned pH sensitivity of ion channels make neuronal firing sensitive to changes in pH_o. In the hippocampus, pH_o affects the amplitude of neuronal population spikes [e.g. an alkaline shift increases the population spike amplitude and an acidic shift decreases the population spike amplitude (Balestrino & Somjen, 1988)]. NBCe1 is of particularly interest in regards to pH_o shifts because NBCe1 is electrogenic and responds to voltage changes (Chesler, 2003). NBCe1 has been characterized in both invertebrate glia (Deitmer & Schlue, 1987, 1989; Deitmer & Szatkowski, 1990) and mammalian astrocytes (O'Connor *et al.*, 1994; Pappas & Ransom, 1994; Bevensee *et al.*, 1997). In a model derived from experiments performed on the giant leech glia (Chesler, 1990) and supported by NBCe1 properties in mammalian astrocytes, action potential-induced NBCe1 stimulation dampens neuronal firing by lowering pH_o. Briefly, action

potential firing increases extracellular K^+, which depolarizes the astrocyte through inward rectifying K^+ channels. The degree of this stimulation will depend on the degree of action potential firing. For mice *in vivo*, a firing frequency of 10 Hz for 300 stimulations depolarizes astrocytes by ~10 mV (Chever *et al.*, 2010). However, because NBC activity is tightly coupled to the astrocyte membrane potential (Chesler, 2003), even this small depolarization is expected to stimulate the transporter. Increased NBCe1 activity siphons HCO_3^- from the extracellular space and drives CA IV- and CA XIV-mediated proton and HCO_3^- formation in the tortuous synaptic space, which decreases pH_o (Makani *et al.*, 2012). This decrease in pH_o inhibits voltage-gated channels and therefore inhibits neuronal firing. A functional NBCe1 is also in neurons (Majumdar *et al.*, 2008; Svichar *et al.*, 2011) and is expected to alter neuronal firing by voltage shifts in the neuron.

NBCe1 Regulation

Many NBCe1 regulators have been identified and are summarized in Chapter 2. The membrane phospholipid phosphatidylinositol 4,5-bisphosphate (PIP_2) is of particular interest because PIP_2 intersects several signaling cascades. Phospholipase C (PLC) hydrolyzes PIP_2 into 2nd messenger signaling molecules. However, as summarized in the subsequent section, PIP_2 also directly regulates ion channels and transporters. The KCNQ channel has even been demonstrated to be sensitive to both PLC-generated second messengers and PIP_2 per se in the same cell type. The ubiquitously expressed Na-H exchanger, NHE1, was the first pH_i regulating transporter characterized for PIP_2 sensitivity (Aharonovitz *et al.*, 2000). Subsequently, PIP_2 sensitivity has been characterized for NBCe1-A in an isolated membrane patch (Wu *et al.*, 2009). However, it

is unclear if this form of regulation is preserved in the whole cell, if the other variants are regulated by PIP_2, and if 2^{nd} messengers from PIP_2 hydrolysis also regulate NBCe1.

Phosphatidylinositol 4,5-bisphosphate, PIP_2

PIP_2 is a phospholipid in the cell membrane that is synthesized from the precursor compound phosphatidylinositol (PI). PIs share a common structure that consists of two variable fatty acid tails in the membrane linked to a cytosolic inositol head group through glycerol and a phosphate. The inositol head group can be phosphorylated on the 3', 4', and/or 5' position. The predominant PIP found in the cell membrane is phosphorylated on the 4' and 5' position, $PI(4,5)P_2$,and only comprises 1% of anionic lipids in the whole cell. Using this percentage, cellular membrane PIP_2 is estimated to range from ~4-10 μM (McLaughlin *et al.*, 2002; Suh & Hille, 2008) and is about ~100 fold higher than the second most abundant PIPs, $PI(3,4)P_2$ and PIP_3 (Gamper & Shapiro, 2007). Although PIP_2 comprises only 1% of the anionic lipids, it is a hub for intracellular signaling. PIP_2 is a substrate for PLC (e.g., associated with G_q-coupled receptor signaling) and phosphatidylinositol 3-kinase (e.g., associated with growth factor receptor signaling). In addition, PIP_2 is a signaling molecule itself and regulates many cellular processes, including channels and transporters (Di Paolo & De Camilli, 2006; Balla, 2013).

Phospholipase C Signaling

Activated G_q-coupled receptors stimulate PLC activity, which hydrolyze PIP_2 to form the second messengers inositol trisphospate (IP_3) and diacylglycerol (DAG) (Berridge & Irvine, 1984). IP_3 binds and opens the IP_3 receptor on the ER, resulting in IP_3

receptor-mediated Ca^{2+} release (Clapham, 1995). DAG remains in the cell membrane and recruits the second messenger phosphokinase C (Hurley & Misra, 2000). These second messengers are known regulators of many channels and transporters.

PIP_2 Regulation of Ion Channels and Transporters

Discovery of PIP_2-sensitivity. PIP_2 stimulation of ion channels and transporters was first reported by Hilgemann and Ball for the Na^+-Ca^{2+} exchanger (NCX) and K_{ATP} channel in a patch of guinea pig cardiac myocyte (Hilgemann & Ball, 1996). It was observed that NCX- and K_{ATP}-associated currents quickly decayed (i.e., exhibited rundown) after patch excision. Rundown was rescued by applying Mg^{2+}-PIP_2 to the cytosolic face of the patch. To demonstrate PIP_2 specificity, applying Mg^{2+}-PIP_2 in the presence of exogenous PLC did not stimulate either transport protein. It was concluded that lipid kinases were inactivated when the patch was pulled. In turn, lipid phosphatases then dephosphorylated PIP_2. The lipid kinase activity was restored by adding ATP, which is the substrate for the lipid kinases that was lost when the membrane patch was pulled from the cell. These data were consistent with a novel form of PIP_2 regulation, where PIP_2 directly regulates channels or transporters.

Mechanism. Since this pioneering study, many channels and transporters have been demonstrated to be PIP_2 sensitive (Balla, 2013) and are predicted to share a general stimulation mechanism. Each PIP_2 molecule has an effective charge near -4 at a neutral pH (McLaughlin *et al.*, 2002). PIP_2's negative charge allows for electrostatic interaction with positive charges, such as positively charged amino acids (arginine, lysine, or histidine). Crystal structures of PIP_2 bound to K_{ir} or GIRK channels reveal that the

anionic charges of PIP_2 indeed bind to polybasic residues (Hansen *et al.*, 2011; Whorton & Mackinnon, 2011). Mechanistically, these crystal structures reveal that the cytosolic channel domains are more compressed in the presence vs. absence of PIP_2. PIP_2 binding to these K^+ channels causes a large 6 Å spring-like compression of the channel's cytosolic domain , which opens the inner helix gate and activates the channels.

Strategies to manipulate PIP_2. There are several experimental protocols used to test the PIP_2-sensitivity of channels and transporters. As stated above, Mg^{2+}/ATP-sensitive current rundown in a pulled membrane patch is a strong indicator of a PIP_2-sensitive transporter or ion channel. In membrane patch studies, investigators typically apply the water soluble short-chain $PI(4,5)P_2$ (8:0) because short-chain PIP_2 does not readily form micelles and rapidly incorporates into the membrane. This PIP_2 is designated short-chain because the unsaturated fatty acid tails each contain 8 carbons (i.e., 8 carbons:0 double bonds). The endogenous PIP_2 chain lengths vary, but tend to be much larger (e.g. brain PIP_2 is predominantly 22:4 and 18:0; AVANTI Polar Lipids). In the membrane patch, an electrostatic PIP_2-protein interaction is demonstrated by inhibiting the PIP_2-mediated stimulation with polyvalent cations (e.g., poly-lysine or neomycin). The polyvalent cations shield the -4 charge of PIP_2 and inhibit the interaction. PIP_2 antibodies may also be used to inhibit the interaction.

In whole cells, it is more difficult to manipulate PIP_2 levels because PIP_2 is in the inaccessible cytosolic leaflet. Additionally, manipulating PIP_2 also alters downstream cell signaling. For example, increasing PIP_2 can increase PLC-mediated PIP_2 hydrolysis (Nasuhoglu *et al.*, 2002; Thornell *et al.*, 2012) and decreasing PIP_2 has the potential to change ambient IP_3 signaling.

PIP_2 can be delivered to small cells by pipette dialysis in a whole-cell recording conformation and to larger cells by injection. A disadvantage for these techniques is reported PLC-mediated hydrolysis of PIP_2 for dialysis (Nasuhoglu *et al.*, 2002) and injection (Thornell *et al.*, 2012). If the assayed channel or transporter is sensitive to PLC-generated 2^{nd} messengers then the dialysis/injection data are inconclusive without several subsequent experiments to evaluate each pathway. Alternatively, histone-carrier complexes raise PIP_2 without mechanical membrane disruption (Ozaki *et al.*, 2000). Positively charged histones shuttle negatively charged PIP_2 into the cell, where PIP_2 is incorporate into the membrane. However, the histone-carrier technique also stimulates a PLC-mediated rise in Ca^{2+} (Ozaki *et al.*, 2000).

Wortmannin is a non-specific membrane permeable phosphatidylinositol 4-kinase (PI4K) inhibitor, which in turn inhibits PIP_2-sensitive channels (Suh & Hille, 2002; Ford *et al.*, 2003; Zhang *et al.*, 2003; Ding *et al.*, 2004; Lopes *et al.*, 2005). Wortmannin inhibits PI3K at low concentrations (e.g., 10 nM) and PI3K and PI4K at high concentrations (e.g., 10 μM). When cells are incubated with a high concentration of wortmannin to inhibit PI4K, catalyzed PIP_2 (phosphorylated, dephosphorylated, or hydrolyzed) is not resynthesized because PIP_2 substrates are not phosphorylated on their 4' position. Therefore, pre-incubation of cells with wortmannin lowers PIP_2 and inhibits PIP_2-sensitive current (Suh & Hille, 2002; Ford *et al.*, 2003; Lopes *et al.*, 2005). Wortmannin is now rarely used to evaluate PIP_2 sensitivity because of its non-specificity and development of more direct ways to alter PIP_2 levels.

The chemical dimerization technique specifically targets PIP_2. Chemical dimerization is a chemical-induced heterodimerization of two proteins that possess a

binding site for the chemical. For PIP_2 studies, protein domains from FK506 binding protein (FKBP) and from mTOR (FRB) are dimerized by rapamycin (or rapamycin analog) treatment (Suh *et al.*, 2006). FRB is conjugated to a plasma membrane anchoring domain and therefore is tethered to the inner leaflet of the plasma membrane. FKBP is conjugated to a PI5 lipid phosphatase and is cytosolic. Rapamycin treatment induces dimerization of the lipid phosphatase-conjugated FKBP to the membrane tethered FRB within ~20 s and lowers membrane PIP_2 (Suh *et al.*, 2006). Conversely, FKBP can be conjugated to PI5K. Rapamycin treatment induces dimerization of the lipid kinase-conjugated FKBP to the membrane tethered FRB and raises membrane PIP_2 (Suh *et al.*, 2006). Dimerization-induced changes in PIP_2 have been shown to regulate the K^+ channel KCNQ. In separate experiments, KCNQ-mediated current was either inhibited by dimerization of FRB and PI5 phosphatase-FKBP, or stimulated by dimerization of FRB and PI5 kinase-FKBP (Suh *et al.*, 2006).

Finally, PIP_2 levels can be decreased with a voltage-sensitive phosphate (VSP). VSP was first cloned from the ascidian *Ciona intestinalis* (Murata *et al.*, 2005) and later this clone was characterized in *Xenopus* oocytes (Murata & Okamura, 2007). VSP consists of a voltage-sensing S4 transmembrane domain tethered by linker residues to a phosphatase domain (Murata *et al.*, 2005; Murata & Okamura, 2007; Kohout *et al.*, 2010; Hobiger *et al.*, 2012). Depolarization causes a change in VSP conformation so that the phosphatase domain can dephosphorylate PIP_2. The phosphatase domain is homologous to the protein PTEN (phosphatase and tensin homolog) and dephosphorylates $PI(4,5)P_2$ to PI(4)P (Iwasaki *et al.*, 2008; Halaszovich *et al.*, 2009; Okamura *et al.*, 2009). The depolarization-induced activation of the phosphatase domain for Ci-VSP has a $V_{1/2}$ of 60

mV (Murata *et al.*, 2005). When expressed in *Xenopus* oocytes, depolarization-induced Ci-VSP activation decreases PIP_2 (Murata & Okamura, 2007). The magnitude of the PIP_2 decrease is dependent upon the density of VSP expression, which may vary with different batches of oocytes (Sakata *et al.*, 2011).

Co-expression of VSP with the PIP_2-sensitive channels KCNQ2/3 or K_{ir} 2.1 inhibits the channel-mediated current upon depolarization-induced VSP activation (Falkenburger *et al.*, 2010; Sakata *et al.*, 2011). When the cell is depolarized and VSP is active, repolarization to a potential where VSP is inactivate induces a slow recovery of the PIP_2 sensitive current with the same time course as PI5K-mediated PIP_2 resynthesis (Falkenburger *et al.*, 2010; Sakata *et al.*, 2011). Other VSPs have been cloned and characterized from the zebrafish *Danio rerio* (Hossain *et al.*, 2008) and the frogs *Xenopus laevis* and *Xenopus tropicalis* (Ratzan *et al.*, 2011) and differ in their voltage dependences. Note that the VSPs cloned from *Xenopus* are not expressed in their oocytes and do not lead to artificial results. VSP is a powerful tool for characterizing the PIP_2 sensitivity of channels and transporters because it is a 5'-specific phosphatase (i.e., VSP circumvents IP_3 signaling) and can be rapidly activated and inactivated in the same experiment.

Dual PIP_2 Signaling

PIP_2 can regulate membrane transport proteins in a dual fashion. For example, the K^+ channel KCNQ is inhibited by Ca^{2+} release downstream from PIP_2 hydrolysis (Gamper *et al.*, 2004) and PIP_2 per se (Suh & Hille, 2002; Zhang *et al.*, 2003; Winks *et al.*, 2005) in the same cell type. In the Ca^{2+} release pathway, there is no appreciable

decline in PIP_2 because a Ca^{2+} sensitive PI4K is activated (Brown *et al.*, 2007; Hughes *et al.*, 2007; Zaika *et al.*, 2011). The lack of Ca^{2+} release in the direct PIP_2 signaling pathway is due to either IRBIT tuning of IP_3 receptors, microdomain differences in IP_3 metabolism, the physical distance of PLC from the IP_3 receptor (Zaika *et al.*, 2011), or differences in the degree of G_q receptor activation (Dickson *et al.*, 2013) .

PIP_2 Regulation of NBCe1

Rat NBCe1-A is sensitive to PIP_2 when the transporter is expressed in *Xenopus laevis* (Wu *et al.*, 2009). Membrane macropatches pulled from these oocytes had an NBCe1-A current that rapidly inactivated (i.e. displayed rundown). Applying PIP_2 to the cytosolic membrane reduced NBCe1-A current rundown and stimulated NBCe1-A current. Cytosolic application of a phosphatase inhibitor cocktail (vanadate/0 Mg^{2+}/F^-) inhibited the observed rundown. The polycations spermine and neomycin inhibited the PIP_2-induced stimulation indicating the involvement of an electrostatic interaction.

Transiently transfected NBCe1-B is also regulated by PIP_2 when expressed in HeLa cells (Hong *et al.*, 2013). Delivery of PIP_2 by pipette or as a histone-carrier complex stimulated NBCe1-B and required 3 arginines within the IRBIT binding domain. However, as discussed in *Strategies to manipulate PIP_2*, these 2 strategies potentially stimulate PLC activity, which stimulates NBCe1-B as described in this dissertation.

Project Rationale and Summary

Because PIP_2 is a hub for intracellular signaling and is ubiquitously expressed in cells, it is important to characterize PIP_2 regulation of NBCe1 in a whole cell, where

other cytosolic regulatory proteins are present. This study is the first characterization of bimodal PIP_2 regulation of NBCe1 in an intact cell. For the first mode, we demonstrate a novel regulation for NBCe1-B and -C, but not NBCe1-A, which involves PIP_2 hydrolysis and subsequent Ca^{2+} release to activate a staurosporine-sensitive kinase. For the second mode, we demonstrate that NBCe1-B and -C are inhibited by a decrease in PIP_2 per se. Based on these results, PIP_2 can regulate NBCe1-B and -C by a dual mechanism, which is a novel finding for a transporter.

Chapter 2 Overview

In Chapter 2, we summarize the intracellular regulators of the cloned *Slc4* bicarbonate transporters. Relevant to this dissertation is the NBCe1 section, more specifically NBCe1 regulation by PIP_2.

Chapter 3 Overview

In Chapter 3, we demonstrate that injecting PIP_2 into NBCe1-expressing *Xenopus* oocytes stimulates NBCe1-B and -C, but not NBCe1-A. NBCe1 currents were monitored by 2-electrode voltage clamp technique. The PIP_2 injection-mediated stimulation was mimicked by IP_3 injection, Ca^{2+} influx, and G_q-receptor activation. In experiments that combined 2-electrode voltage clamp technique with a pH-sensing microelectrode, G_q activation stimulated NBCe1-C mediated pH_i recovery from an acid load.

Chapter 4 Overview

In Chapter 4, we characterize the PIP_2 sensitivity of NBCe1-B and -C in *Xenopus* oocytes co-expressing VSP. 2-electrode voltage clamp technique was used to monitor NBCe1 current and to activate VSP by depolarization and inactivate VSP by repolarization. VSP activation inhibited both NBCe1-B and -C. Upon repolarization, which inactivated VSP, NBCe1-B and -C current slowly recovered with a time constant similar to the time constant for PIP_2 resynthesis in these experiments. In experiments that combined 2-electrode voltage clamp technique with a pH-sensing microelectrode, depolarization (i.e. VSP activation) inhibited NBCe1-C mediated recovery from an acid load.

This dissertation is organized as followed. Chapter 2 provides a review of the cytosolic regulation of the cloned *Slc4* bicarbonate transporters. This review includes an in depth overview of NBCe1 regulators. This is followed by two original research articles demonstrating regulation of NBCe1 by PIP_2 hydrolysis (Chapter 3) and PIP_2 per se (Chapter 4). Results are discussed and future directions are presented in Chapter 5.

Table 1. Summary of NBCe1 cDNA clones

Variant	Animal	Tissue	Clone Name	References
NBCe1-A	Salamander	Kidney	NBC[1]	(Romero *et al.*, 1997)
	Human	Kidney	kNBC[2]	(Burnham *et al.*, 1997)
	Rat	Kidney	rNBC[3]	(Romero *et al.*, 1998)
			rNBC-1	(Burnham *et al.*, 1998)
NBCe1-B	Human	Pancreas	pNBC	(Abuladze *et al.*, 1998)
	Human	Heart	hhNBC	(Choi *et al.*, 1999)
	Rat	Pancreas	rpNBC	(Thévenod *et al.*, 1999)
	Rat	Brain	rb1[3]	(Bevensee *et al.*, 2000)
	Zebrafish	Tissue	zNBCe1	(Sussman *et al.*, 2009)
NBCe1-C	Rat	Brain	rb2[3]	(Bevensee *et al.*, 2000)
NBCe1-D	Mouse	Reproductive Tract	not named	(Liu *et al.*, 2011)
NBCe1-E	Mouse	Reproductive Tract	not named	(Liu *et al.*, 2011)

[1]renamed aNBC for clarity in subsequent literature
[2]renamed hkNBC for clarity in subsequent literature
[3]clones used for this dissertation

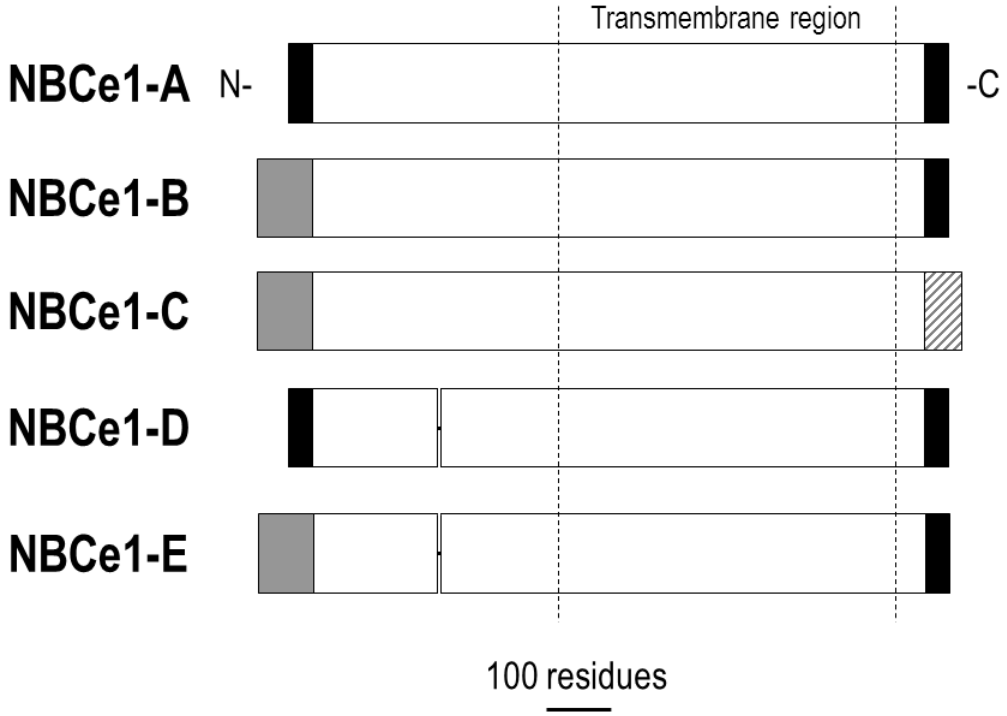

Figure 1. NBCe1 variant motifs. The cartoon represents each NBCe1 variant's primary amino acid sequence and shaded/absent regions represent variable regions. NBCe1-A and -D contain a different N-terminus from NBCe1-B, -C, and -E. NBCe1-C contains a unique C-terminus. Both NBCe1-D and -E are missing 9 amino acid residues (*removed above*) between the transmembrane region and the variable N-terminus. Modified with permission from Thornell *et al.* PIP_2 hydrolysis stimulates the electrogenic Na+-bicarbonate cotransporter NBCe1-B and -C variants expressed in *Xenopus laevis* oocytes. *J Physiol* 2012, 590:5993-6011.

REGULATORS OF *Slc4* BICARBONATE TRANSPORTER ACTIVITY

Ian M. Thornell and Mark O. Bevensee

In preparation for Acid-Base Sensing and Regulation: Molecular Mechanisms and Functional Implications in Health and Disease

Format adapted for dissertation

Abstract

The *Slc4* gene superfamily of cloned bicarbonate transporters is comprised of Anion Exchangers (AE1-4), Na-coupled Bicarbonate Transporters (NCBTs) including electrogenic Na/Bicarbonate Cotransporters (NBCe1 and NBCe2), electroneutral Na/Bicarbonate Cotransporters (NBCn1 and NBCn2), and the electroneutral Na-driven Cl-HCO_3 Exchanger (NDCBE), as well as a borate transporter (BTR1). Although these transporters are best known for regulating intracellular pH (pH_i) and contributing to steady-state pH_i, they are also involved in many physiological processes including CO_2 carriage by red blood cells and solute secretion/reabsorption across epithelia. From the standpoint of pH physiology, acid-base transporters function as either acid extruders or acid loaders, with the Slc4 proteins moving HCO_3^- either into or out of cells. However, according to results from both molecular and functional studies over the years, it is clear that multiple Slc4 proteins and/or associated splice variants with similar expected effects on pH_i are often found in the same tissue or cell. Such apparent redundancy is likely to be physiologically important. In addition to regulating pH_i, a HCO_3^- transporter contributes to a cell's ability to fine tune the intracellular regulation of the cotransported/exchanged ion(s) (e.g., Na^+ or Cl^-). In addition, functionally similar transporters or splice variants with different regulatory profiles will optimize pH physiology and solute transport under various conditions or within subcellular domains. Such optimization will depend on activated signaling pathways and transporter expression profiles. In this review, we will summarize and discuss both classical and more recently identified regulators of the Slc4 proteins. Some of these regulators include traditional second messengers (e.g., IP_3, cAMP, and Ca^{2+}), lipids (e.g., phosphoinositides), binding proteins (e.g., glycolytic

enzymes and the IP_3 receptor binding protein released with IP_3, IRBIT), autoregulatory domains (e.g., cytoplasmic amino termini), and less conventional regulators (e.g., Mg^{2+} and heat shock proteins). Where appropriate, we will address the physiological consequences of such regulation. The goal of this review is to provide a contemporary overview of Slc4 regulators that will provide insight into the diversity and physiological significance of multiple members within the *Slc4* gene superfamily.

Introduction

The *Solute carrier 4* (*Slc4*) gene products comprise the superfamily of bicarbonate transporters (BTs). BTs regulate intracellular pH (pH_i) and/or extracellular pH (pH_o) by either extruding or loading HCO_3^- (or CO_3^{2-}) into the cell. BTs are further characterized as either the Na^+-independent anion exchangers (AEs) or Na^+-dependent bicarbonate transporters (the NBTs). BTs not only contribute to the steady-state pH_i, but also contribute to secretion and reabsorption across epithelia. For example, the electrogenic Na/HCO_3 cotransporter, NBCe1-A, is responsible for HCO_3^- reabsorption in the renal proximal tubule (Boron & Boulpaep, 1983) and NBCe1-B contributes to HCO_3^- secretion in the pancreas (Muallem & Loessberg, 1990). BTs also have roles ancillary to pH_i regulation and epithelia. For example, the erythrocyte AE1 (eAE1) mediates the erythrocyte chloride shift, also known as the Hamburger shift, and NBCe1 elicits pH_o shifts in the nervous system that modulate neuronal firing.

One of the first transporter cDNAs be cloned was eAE1 (Kopito & Lodish, 1985). Subsequently, many BTs were cloned throughout the 1990s. From these cloning studies, it is apparent that each family member has several different splice variants. The most common alternative BT splicing occurs at the cytoplasmic amino (N-) terminus and/or the carboxy (C-) terminus. These variable termini serve as a potential target of differential regulation. As discussed below, the alternative splicing allows the cell to specifically control and fine tune HCO_3^- transport. In the BT field, there is considerable interest in understanding how *Slc4* family members and their variants are regulated, thereby leading to predictable physiological consequences.

Mechanisms of Differential Regulation

Intracellular signals set BT activity for a specific cell type. More specifically, the presence or absence of a signaling molecule may change activity for a single transporter. For instance, the presence of an intracellular protein found in cell *A*, but not cell *B*, imparts a more active transporter in cell *A* vs. cell *B* (Figure 1A). The signaling molecule may alter BTs apparent transport activity either by changing transporter velocity, expression, or stoichiometry.

Intracellular signals also dynamically regulate BT activity in response to a change in the cellular environment. For instance, a cell contains 3 pathways *A*, *B* and *C* and 2 acid extruding BT transporters *a* and *b* (Figure 1B). Activating pathway *A* stimulates transporter *a*, but not transporter *b*. Conversely, activating pathway *B* stimulates transporter *b*, but not transporter *a*. Each response increases bulk acid extrusion, but through different mechanisms and possibly act in distinct microdomains. In a third scenario, activation of pathway C stimulates both transporter *a* and transporter *b*. Such a signal could result from cellular acidification to maximize acid extrusion.

In this review, we compile what has been demonstrated in the BT regulation field for the cloned family members. We first briefly review BT molecular physiology and highlight areas pertinent to cell signaling. We then describe each family member by giving an overview and then summary of modes of regulation.

Molecular Physiology

The BT superfamily consists of 10 genes that encode SLC4 proteins. *Slc4* can be divided into the following three groups: Na^+-independent AEs, Na^+-dependent HCO_3^-

transporters, and the lesser characterized transporters. The AEs consist of AE1-3 (encoded by *Slc4a1-3*). These acid loaders exchange 1 Cl^- for 1 HCO_3^-, but can also transport sulfate . *Slc4a4-5* encodes NBCe1 and NBCe2. NBCes cotransport 1 Na^+ and either 2 or 3 HCO_3^- (alternatively, 1 CO_3^{2-} or 1 HCO_3^- and 1 CO_3^{2-}). The remaining members are electroneutral and complete the well-characterized members of the family. *Slc4a6* encodes the electroneutral Na^+/HCO_3^- cotransporter (NBCn1), which normally extrudes acid by cotransporting 1 Na^+ and 1 HCO_3^- into cells. *Slc4a8* encodes the Na^+ driven Cl^--HCO_3^- exchangers (NDCBE), which extrudes acid utilizing the electrochemical energy of 1 Na^+ into cells to drive the exchange of 2 HCO_3^- (or 1 CO_3^{2-}) into cells for 1 Cl^- out of cells. *Slc4a10* encodes the electroneutral Na^+/HCO_3^- cotransporter (NBCn2), which normally extrudes acid by cotransporting 1 Na^+ and 1 HCO_3^- into cells, but with an associated futile Cl^- self-exchange. The remaining 2 lesser characterized members include the *Slc4a9* encoded AE4, whose Na^+-dependence is controversial, and the *Slc4a11* encoded borate transporter. In this review, we focus on AE1, AE2, NBCe1, NBCn1, NDCBE and NBCn2 because they are the best known and understood.

The AEs are 28-34% homologous to the NBCs (Romero *et al.*, 2004) with the largest differences at the cytoplasmic N- and C-termini. These termini are potential targets for differential signaling. The crystal structures of the N-terminus of eAE1, which is resolved to 2.6 Å (Zhang *et al.*, 2000), and the N-terminus of NBCe1-A, which is resolved to 2.4 Å, both verify that these proteins dimerize through the N-terminus. However, until full transporter structures are crystallized, structure-function data from the cloned transporters will provide the best evidence for regions of transporter regulation.

This review summarizes our current knowledge of regulators of cloned BTs. We recommend the following reviews for a more in depth discussion of BT superfamily members outside the scope of regulation (Alper *et al.*, 2002; Romero *et al.*, 2004; Parker & Boron, 2013)

AE1 (*Slc4a1*)

The murine erythrocyte AE1 (eAE1) was not only the first BT cloned, but one of the first transporters cloned (Kopito & Lodish, 1985). eAE1 is commonly known as band 3 protein because AE1 was first identified as the third band of a electrophoresis gel of erythrocyte protein. The physiologically important function of AE1 is to exchange 1 Cl^- for 1 HCO_3^-.

In erythrocytes, AE1 is integral in the Jacobs—Stewart cycle. In brief, AE1 extrudes HCO_3^- formed by the carbonic anhydrase (CA)-mediated hydration of CO_2. The remaining protons are buffered by deoxyhemoglobin, allowing the erythrocyte to carry metabolically produced CO_2 to the lungs. The eAE1-mediated Cl^--HCO_3^- exchange is responsible for the Cl^- (Hamburger shift) observed in these cells during CO_2 uptake. Highlighting the importance of eAE1 in this process, eAE1 is about ¼ of all erythrocyte membrane protein.

AE1 is also densely expressed in the basolateral membrane of renal collecting duct α-intercalated cells. Kidney AE1 (kAE1) lacks the N-terminal 65-amino acid residues found in eAE1 (Figure 2). In the collecting duct, kAE1 contributes to net HCO_3^- reabsorption from the lumen to the blood. AE1 mRNA has also been detected in the heart

(Kudrycki *et al.*, 1990; Richards *et al.*, 1999) and colon where the protein's role is less defined.

AE2 is found in the basolateral membrane of most epithelia. Similar to AE1, AE2 has a 1:1 Cl^--HCO_3^- exchange stoichiometry. However, all the AE2 variant N-termini are much longer than AE1. Each of the 3 AE2 variants (Figure 3) results from an alternate promoter and are designated by the letter a, b, or c (e.g., AE2a). AE2b and AE2c may undergo further splicing to produce two additional variants designated 1 and 2 (e.g., AE2b1 or AE2b2). AE2a is ubiquitous among tissue types. AE2b is less ubiquitous and is densely expressed in stomach tissue. AE2c is expressed exclusively in stomach tissue (Wang *et al.*, 1996).

Carbonic Anhydrase

CA is an enzyme that catalyzes the net reversible reaction $CO_2 + H_2O \leftrightarrow H_2CO_3$, which is in rapid equilibrium with HCO_3^- and H^+. In the presence of CA, the rate of the hydration reaction is nearly limited by diffusion. AE1 contains a short carboxy terminus of 33 amino acids, where the binding site for cytosolic CA II has been proposed to mediate the protein-protein interaction.. According to the CA II metabolon hypothesis, proximity of CA II to AE1 allows for near instantaneous generation or removal of HCO_3^- to support high AE1 activity. However, binding of CA II to AE1 and its functional implication remain controversial.

There is experimental evidence that both supports and refutes the idea that CA and AE physically interact. Early evidence was consistent with a direct CA-AE interaction. For example, AE1 expressed in HEK293 cells appeared to be maximally

stimulated by endogenous CA II. AE1 was inhibited by co-expression of dominant negative CA II, the CA inhibitor acetazolamide, or mutation to the putative CA binding domain on AE1 (Sterling *et al.*, 2001). It appeared that AE1 was maximally stimulated by endogenous CA II because co-expression with wild type CA II did not further stimulate AE1.

Based on results from solid phase binding assays, the CA II stimulation was predicted to be through a direct interaction. The GST-conjugated AE1 C-terminus (33 amino acids) was incubated with CA II (Vince & Reithmeier, 1998). Binding was slow at physiological ionic strength and pH, but was increased with low ionic strength and low pH. Interaction was block by an antibody targeted to the C-terminus residues. The region of interaction was further characterized to AE1 amino acids 887-890 (DADD) by competition assay (Vince & Reithmeier, 2000). Briefly, GST-fused AE1 C-termini, previously shown to bind CA II, were allowed to interact with immobilized CA II. Non-tagged truncation or point mutants of the AE1 C-terminus were then incubated with the interacted GST-AE1 and CA II. A positive interaction was verified by a decrease in the tagged AE1 signal.

Later evidence was not consistent with AE1 binding of CA II. The binding assay experiment above were replicated using the AE1 C-terminus and the putative CA II binding C-termini of NBCe1 and NDCBE (Piermarini *et al.*, 2007). Consistent with other groups, GST-fused C-termini interacted with immobile CA II greater than GST alone. However, when the C-termini were immobilized, GST-alone interacted greater than any of the GST-tagged constructs. In experiments where non-tagged constructs were assayed with immobile CA II, there was no evidence of interaction. Alternatively, surface plasma

resonance was used to investigate transient interactions. Immobile CA II was able to bind the CA II inhibitor acetazolamide, but not any of the C-terminal constructs. The group concluded GST-tagged constructs as well as GST will interact with CA II in the immobile phase; however, non-tagged constructs will not interact. The authors did not rule out a CA II metabolon, but concluded that it would be independent of the putative C-terminus domain.

More recent evidence against direct binding of CA II to AE1 was performed in tsA201 cells co-transfected with CA II-CyPet and yPet-AE1 (Al-Samir *et al.*, 2013). These modifications are optimized FRET pairs. In initial experiments, single-channel confocal microscopy was used to obtain a cross-sectional distribution of each fluorophore conjugated protein. AE1 was found predominantly on the membrane. However, CAII was found homogenously expressed throughout the cell. In FRET experiments, CA II-CyPet and yPet-AE1 did not interact. As a positive control, AE1 conjugated to yPet at the N-terminus and CyPet at the C-terminus interacted.

In summary, CA stimulates AE1 transport by its catalytic action. However, the mechanism of action remains controversial. CA II may bind directly to the transporter to create a metabolon to optimize reaction turnover, or CA II may increase AE1 transport activity by increasing whole cell CA activity.

Glycophorin A

Glycophorin A (GPA) is a single membrane passing 131 amino acid sialoglycoprotein enriched in erythrocytes (for a review see Chasis & Mohandas, 1992), where GPA presents antigenic determinants of the MNS blood group. In *Xenopus laevis*

oocytes, co-expressing AE1 and GPA enhanced AE1-mediated $^{36}Cl^-$ uptake and expression (Groves & Tanner, 1992, 1994), whereas glycophorin B and C did not alter AE1 expression or AE1-mediated $^{36}Cl^-$ uptake (Groves & Tanner, 1992). GPA with mutations in extracellular residues 61-70 decreased AE1 activity, while GPA with various mutations in the cytoplasmic domain inhibited trafficking of AE1 to the cell surface (Young & Tanner, 2003). Based on erythrocytes lacking eAE1, GPA was also not present. These data are consistent with AE1 acting as a chaperone-like protein, recruiting GPA to the membrane, where GPA then stimulates AE1 (Hassoun *et al.*, 1998). From these data, there is an apparent mutual dependency between AE1 and GPA for proper expression of either protein.

Some AE1 mutations cause recessive distal renal tubular acidosis and homelytic anemia, but retain normal anion transport in the erythrocytes. When one such AE1 mutant, G701D, was expressed in oocytes, $^{36}Cl^-$ uptake and AE1 expression were reduced compared to wild-type AE1 (Tanphaichitr *et al.*, 1998; Young & Tanner, 2003). G701D co-expression with GPA rescued the AE1 expression and $^{36}Cl^-$ uptake. These data provided insight into why G701D has normal anion transport in GPA-expressing erythrocytes, but impaired anion transport in GPA-absent α-intercalated cells.

Glyceraldehyde 3-phosphate dehydrogenase

Glycolytic enzymes (e.g., glyceraldehyde-3-phosphate dehydrogenase, aldolase, phosphofructokinase, lactate dehydrogenase, or pyruvate kinase) bind to AE1 or AE1-associated proteins (Chu & Low, 2006; Campanella *et al.*, 2008). However, it is mostly not known how glycolytic enzyme binding can influence AE1 activity. The exception is

glyceraldehyde 3-phosphate dehydrogenase (GAPDH). GAPDH catalyzes the conversion of glyceraldehyde 3-phosphate to D-glycerate 1,3-bisphosphate in the sixth step of glycolysis. kAE1, but not a mutant truncated at the C-terminus by 11 residues, bound GAPDH in a yeast 2-hybrid hybrid screen (Su *et al.*, 2011). Furthermore, eAE1 from rat erythrocytes and kAE1 from rat liver each co-immunoprecipitated with GAPDH. Specifically, C-terminal residues 902DEYDE were implicated in this binding. GAPDH stimulated eAE1 function in MDCKI cells by increasing expression in the basolateral membrane (Su *et al.*, 2011).

In the aforementioned immunoprecipitation study performed on AE1, AE2 also interacted with GAPDH, presumably through the shared motif DEYDE (Su *et al.*, 2011) in the C-terminus. However, any consequence in AE2 activity has not been demonstrated.

Adaptor Protein-1

Adaptor Protein-1 (AP-1) tethers the interaction between clathrin and cargo proteins that exit the trans-Golgi network. Co-transfecting kAE1 and siRNA targeting the µ1A subunit of AP-1 inhibited kAE1 surface expression in HEK293T cells. Consistent with this finding, MDCK1 cell lines stably transfected with human kAE1 and transiently transfected with µ1A siRNA caused intracellular retention of AE1 (Almomani *et al.*, 2012). Basolateral targeting was rescued by co-transfecting an siRNA-resistant µ1A subunit and kAE1. In the same study, similar results were obtained with the µ1B subunit of AP-1. AP-1 stimulation of kAE1 was through the kAE1 C-terminus. kAE1 C-terminus bait (C-terminal 36 residues) bound to the µ1A subunit of AP-1 in a yeast two-hybrid

screen of a human kidney cDNA library (Sawasdee *et al.*, 2010). Binding was confirmed and assigned to residues 904YDEV based on mutagenesis studies.

Src-family Kinases

Src-family kinases are tyrosine kinases encoded by the *Src* gene. Src-mediated phosphorylation of both eAE1 and kAE1 are required for AE1 expression and therefore Src-family kinases stimulate AE1 activity (Yannoukakos *et al.*, 1991; Williamson *et al.*, 2008). In MDCKI cells, expressing kAE1 point mutants Y359 or Y904 caused intracellular retention of kAE1 (Williamson *et al.*, 2008). kAE1 Y359 and Y904 are phosphorylated after treatment with pervanadate, a phosphatase inhibitor. Src-family kinase inhibitors blocked the pervanadate-induced kAE1 phosphorylation and reduced kAE1 expression. Based on these data, the authors proposed that a change in tyrosine kinase/phosphatase balance in response to pH_i will alter kAE1 activity in α-intercalated cells (i.e., stimulate AE1 during metabolic acidosis and inhibit AE1 during metabolic alkalosis).

Protein 4.2

Protein 4.2 is an ATP-binding membrane protein found in erythrocytes. Co-expressing protein 4.2 and eAE1 in *Xenopus laevis* oocytes stimulated $^{36}Cl^-$ uptake (Toye *et al.*, 2005). In this study, protein 4.2 binds eAE1 as revealed by co-immunoprecipitation results, but it was unclear whether the stimulation was through increased AE1 expression or increased transporter activity. eAE1in turn served as a chaperone-like protein in

recruiting protein 4.2 to the membrane because mutant protein 4.2 that did not bind eAE1 were not present in the cell membrane.

Nephrin

Nephrin is a protein necessary for proper glomerular filtration and its expression is required for kAE1 expression in glomeruli. Nephrin-mediated kAE1 trafficking was first demonstrated in human glomeruli that are homologous for the nephrin mutation NPHS1FinMaj. These glomeruli did not express endogenous kAE1 (Wu *et al.*, 2010). When wild-type nephrin was transfected into the podocytes of the glomerulus, kAE1 expression was restored. kAE1 C-terminus bait (877-911) bind nephrin in a yeast two-hybrid screen of a human kidney cDNA library as confirmed by immunoprecipitation and co-localization studies. Nephrin expression was inhibited in AE1 knockout mice, a finding consistent with mutual regulation.

NBCe1 (*Slc4a4)*

NBCe1 variants are found in many tissue types where they are responsible for pH_i regulation as well as epithelial absorption and secretion. As depicted in Figure 4, NBCe1-A contains a different N-terminus than found in NBCe1-B/C and NBCe1-C contains a different C-terminus than found in NBCe1-A/B. NBCe1-D is nearly identical to NBCe1-A, but lacks the RMFSNPDNG amino acid sequence found in the N-terminus of NBCe1-A, -B, and -C. NBCe1-E is nearly identical to NBCe1-A, but lacks the aforementioned RMFSNPDNG amino acid sequence. NBCe1-D and -E have not been functionally assayed. NBCe1 variants have either a 1 Na^+:2 HCO_3^- or a 1:3 stoichiometry.

NBCe1-A plays a major role in HCO_3^- reabsorption in the proximal renal tubule. Filtered HCO_3^- and secreted H^+ in the tubule are converted to CO_2 and H_2O by luminal CA IV activity. Generated CO_2 in the tubule lumen diffuses into the epithelial cell. Inside the epithelial cell, CA II-mediated conversion of CO_2 produces H^+ and HCO_3^-. The H^+ is secreted into the tubule for subsequent reactions with more HCO_3^-. Intracellular HCO_3^- is reabsorbed into the blood via a basolateral NBCe1-A with a 1:3 stoichiometry (Soleimani *et al.*, 1987).

NBCe1-B and -C are usually located in the basolateral membrane of epithelial cells and coordinate HCO_3^- absorption and secretion [e.g., the pancreas NBCe1-B (Muallem & Loessberg, 1990) and airway epithelia (Garnett *et al.*, 2011; Shan *et al.*, 2012)]. In these epithelia, the electronegative NBCe1 in the basolateral membrane contributes to both the electrical and chemical gradient to drive apical HCO_3^- secretion. In addition to epithelial roles, NBCe1 is responsible for glial pH_i shifts associated with neuronal firing that alter pH_o (Chesler, 2003). Briefly, neuronal activity releases K^+ from neurons. The passive uptake of K^+ by glial cells depolarizes the glial membrane, stimulating HCO_3^- uptake via NBCe1-B/C in glia. NBCe1-associated HCO_3^- transport causes glial alkalinization, while acidifying the extracellular space.

Carbonic Anhydrase

Carbonic anhydrase (CA) lowers the activation energy of the slow reaction $H^+ + HCO_3^- \leftrightarrow CO_2 + H_2O$ so that the reaction is nearly diffusion limited. Expanding upon the observation that a stretch of residues within AE1 binds CA II *in vitro* (Vince & Reithmeier, 1998), an analogous stretch found in NBCe1-A (887DADD) was proposed to

bind CA II. As evaluated by isothermal titration calorimetry, the C-terminus of NBCe1-A has a binding constant for CA II of 160 nM (Gross *et al.*, 2002). Mutating the putative NBCe1-A binding domain inhibited the transporter when expressed in a NBCe1-free mouse proximal tubule cell line (Pushkin *et al.*, 2004). Two of these mutated residues, Asp 986 and Asp 988, are also involved in PKC-mediated phosphorylation, which has been proposed to change the stoichiometry of NBCe1-A (Gross *et al.*, 2002). It was hypothesized that CA II binds NBCe1-A when the transporter stoichiometry is 3:1 and is unbound following NBCe1 phosphorylation by cAMP at the C terminus. Additionally, expressing a catalytically reduced CA II mutant in HEK293 cells reduced the activity of co-expressed NBCe1-B (Alvarez *et al.*, 2003).

Similar to CAII regulation of AE1, CAII regulation of NBCe1 remains controversial. In the aforementioned CA II/NBCe1 studies, reducing CA II activity or mutating the putative CA II binding site on NBCe1 inhibited NBCe1 activity. However, injecting *Xenopus* oocytes with CA II protein failed to stimulate NBCe1-A (Lu *et al.*, 2006). CA II was functional in these experiments as evident by faster pH_i recoveries from CO_2-induced acidifications that were also inhibited by ethoxzolamide, a membrane permeant CA II inhibitor. In additional experiments, eGFP-NBCe1-A was fused to CA II and its activity was compared to eGFP-NBCe1-A. The CA II fused NBCe1 had no enhanced activity over control. This study demonstrated that in *Xenopus* oocytes, co-localization may not occur and increased CA II protein does not stimulate NBCe1-A.

Discrepancies in the results from this study and Pushkin *et al.* may arise from differences in NBCe1 stoichiometry due to the different cell types studied. It is well established that NBCe1-A has a 1:2 stoichiometry when expressed in *Xenopus* oocytes

(Heyer *et al.*, 1999), whereas Pushkin *et al.* studied CA II regulation of NBCe1-A in their proximal tubule cell-line, where NBCe1-A stoichiometry is 1:3 (Gross *et al.*, 2001*a*).

In a similar *Xenopus* oocyte study by Lu *et al.*, CA II stimulated both an NBCe1-A-mediated pH_i recovery and a current when oocytes were held at -40 mV (Schueler *et al.*, 2011). This stimulation was not apparent when the slope conductance was computed in the previous oocyte study (Lu *et al.*, 2006). One source of discrepancy may arise from the different timelines for injections and assays. CA binding does not appear to be a requirement because Scheuler *et al*. found that both CA I, which lacks the putative NBCe1-A binding domain, and CA III, which is missing residues in the putative binding domain, both stimulate NBCe1-A.

CA IV, an outer plasma membrane glycosylphosphatidylinositol-anchored CA, also stimulated NBCe1-B co-expressed in HEK293 cells (Alvarez *et al.*, 2003). CA IV binding and stimulation of NBCe1-B was dependent on residue G767 found in the fourth extracellular loop of NBCe1-B. Based on these conclusions, CA IV would be predicted to stimulate all NBCe1 variants because all extracellular domains of NBCe1 are conserved.

Autoregulation

When expressed in *Xenopus* oocytes, NBCe1-A has greater activity than NBCe1-B or -C (McAlear *et al.*, 2006). NBCe1-A differs from NBCe1-B and -C at the N-terminus (Figure 4) and therefore appears to contain an autostimulatory domain (ASD). Indeed, NBCe1-A is inhibited by truncating the N-terminus that differs between the variants. NBCe1-D is predicted to have an ASD because it contains the same N-terminus as NBCe1-A (Figure 4). Currently, there are no known regulators of the ASD. This

domain may be a splice-specific regulatory mechanism to promote high velocity HCO_3^- transport where needed in tissues such as kidney.

Similar autoregulation has been demonstrated for the N-terminus of NBCe1-B and -C. Truncating the N-terminus of NBCe1-B or -C resulted in a more active transporter (McAlear *et al.*, 2006). Furthermore, the activity of these truncated proteins was similar to that of the corresponding NBCe1-A truncation (i.e., all had similar whole oocyte currents). Therefore, the N-terminus of NBCe1-B or -C appears to contain an autoinhibitory domain (AID). NBCe1-E is predicted to have an ASD because it contains the same N-terminus as NBCe1-B and -C (Figure 4).

The specific C-terminus of NBCe1-C may also contribute to the AID based on two observations. First, expressing the NBCe1-B/C stimulator IRBIT (IP$_3$ receptor binding protein release with inositol 1,4,5-trisphosphate) in oocytes stimulated co-expressed NBCe1-C to a greater extent (i.e., more relief of the AID) than NBCe1-B (Thornell *et al.*, 2010). Second, IP_3-mediated stimulation was not completely abolished by N-terminus truncation of NBCe1-C (Thornell *et al.*, 2012). IP_3-mediated stimulation likely relieves the N-terminus AID because NBCe1-A was not stimulated. However, removal of the N-terminus AID from NBCe1-C resulted in a minimal, but significant IP_3-induced stimulation that required ER-store Ca^{2+}. Based on these observations, the C-terminus of NBCe1-C either contributes to the N-terminal-based AID or contains a relatively small and separate AID.

IRBIT-WNK/SPAK

IP_3 receptor binding protein release with inositol 1,4,5-trisphosphate (IRBIT) is a ubiquitous second messenger protein that binds to the IP_3 receptor and is competed off the receptor by an increase in intracellular IP_3 (Ando *et al.*, 2003). IRBIT released from IP_3 receptors is cytosolic and regulates other proteins, including NBCe1. IRBIT contains a binding domain for protein phosphatase-1 (PP-1) (Devogelaere *et al.*, 2007), which antagonizes WNK (with-no-lysine kinase)/SPAK (STE20/SPS1-related proline/alanine-rich kinase) signaling (Yang *et al.*, 2011). Human WNK/SPAK mutations cause hypertension and therefore play a major role in regulating epithelial electrolyte transport (Wilson *et al.*, 2001). Indeed, WNK/SPAK regulates many epithelial ion channels and transporters including the Na/K/2Cl cotransporter (Anselmo & Earnest, 2006), the epithelial sodium channel (Heise *et al.*, 2010), the cystic fibrosis transmembrane conductance regulator (Yang *et al.*, 2007), the renal outer medullary K^+ channel (He *et al.*, 2007), and NBCe1-B and -C (Yang *et al.*, 2009). Whereas IRBIT stimulates NBCe1-B and -C, WNK/SPAK inhibits these NBCs. It was hypothesized that once released from the IP_3 receptor, IRBIT antagonizes WNK/SPAK inhibition of NBCe1 by recruiting PP-1 (Yang *et al.*, 2009; Park *et al.*, 2012).

In *Xenopus* oocytes, human NBCe1-B was stimulated by co-expressing IRBIT (Shirakabe *et al.*, 2006). In similar oocyte co-expression experiments, IRBIT also stimulated rat NBCe1-B and -C currents (Parker *et al.*, 2007*b*; Thornell *et al.*, 2010). NBCe1-B binds IRBIT from a rat cerebellar homogenate and binding mutants do not stimulate NBCe1-B when co-expressed in oocytes (Shirakabe *et al.*, 2006). The specific N-terminus of NBCe1-B and -C was involved based on two observations. First, none of

the aforementioned groups observed an IRBIT stimulation of NBCe1-A. Second, IRBIT did not stimulate N-terminal truncations of either NBCe1-B or -C (Thornell *et al.*, 2010).

In a mutation study performed with HeLa cells, no single mutation to the putative IRBIT domain affected NBCe1 stimulation (Hong *et al.*, 2013). However, the NBCe1-B triple mutant R42A/R43A/R44A did not bind IRBIT and did not stimulate NBCe1-B. In summary, IRBIT binds to the N-terminus of NBCe1-B and -C and stimulates NBCe1 activity.

It was proposed that IRBIT acts through relief of the NBCe1-B and -C AID (Seki *et al.*, 2008). If this is true, then IRBIT-mediated NBCe1 stimulation should never exceed stimulation elicited by removing the AID. However it is difficult to achieve full IRBIT stimulation because IRBIT is inhibited by PP-1. To achieve maximal IRBIT stimulation, the Boron group mutated IRBIT's PP-1 binding site so that IRBIT was no longer inhibited by PP-1. The activity of NBCe1-B co-expressed with this super-IRBIT exceeded the activity of the N-terminal truncation of NBCe1-B, which did not contain the putative AID (Lee *et al.*, 2012*b*). The authors concluded that IRBIT did not stimulate NBCe1-B through relief of the AID exclusively. Alternatively, the AID's tertiary structure may include other parts of the transporter, such as a putative C-terminus AID as mentioned above.

In HeLa cells, NBCe1-B is inhibited by the WNK/SPAK pathway (Yang *et al.*, 2011; Hong *et al.*, 2013). Transfecting either WNK or kinase-dead WNK mutants inhibited NBCe1-B, consistent with WNK acting as a scaffold for an NBCe1 regulator such as SPAK (Yang *et al.*, 2011). Co-transfecting kinase-dead SPAK with WNK blocked the WNK-mediated inhibition. These data are consistent with WNK recruiting

SPAK to phosphorylate NBCe1-B and reduce NBCe1-B surface expression. The WNK/SPAK inhibition was antagonized by IRBIT recruitment of phosphatase PP1, but did not exert their regulation on the same NBCe1 region (Yang *et al.*, 2011; Hong *et al.*, 2013).

A major difference between the *Xenopus* oocyte expression system and the HeLa cell expression system was IRBIT's effect on NBCe1-B surface expression. Co-expression of IRBIT and NBCe1-B in *Xenopus* oocytes did not change surface NBCe1 protein assayed by confocal imaging (Shirakabe *et al.*, 2006), single-oocyte chemiluminescence (Thornell *et al.*, 2010), or biotinylation (Lee *et al.*, 2012*b*). However, IRBIT increased NBCe1-B surface expression in HeLa cells (Yang *et al.*, 2011). The basis of this discrepancy may be a less active WNK/SPAK pathway in oocytes vs. HeLa cells. If so, then the majority NBCe1-B would already be expressed on the oocyte membrane. Consistent with this explanation, co-expressing NBCe1-B and IRBIT in HeLa cells suppressed WNK/SPAK-mediated NBCe1 internalization and stimulated NBCe1-B by a WNK/SPAK-independent mechanism (Hong *et al.*, 2013)— mostly likely by direct NBCe1 stimulation as characterized in oocytes.

PIP_2

Phosphatidylinositol 4,5-bisphosphate (PIP_2) is a minor membrane phospholipid involved in many cellular processes including the regulation of channels and transporters (Di Paolo & De Camilli, 2006; Balla, 2013). PIP_2 stimulated rat kidney NBCe1-A in macropatches of *Xenopus* oocyte membrane (Wu *et al.*, 2009). NBCe1-A current rundown was reversed and stimulated by directly applying a fast membrane incorporating

short-chain PIP_2 to the patch. In addition, NBCe1-A current rundown was decreased by vanadate and 0 Mg^{2+} solutions. These data were consistent with an initial endogenous PIP_2-dependent transporter current that rapidly decayed due to Mg^{2+}-sensitive phosphatase activity. ATP stimulation of NBCe1-A as reported in a previous study may involve the same mechanism (Heyer *et al.*, 1999).

These previous findings in isolated patches have been extended to the whole *Xenopus* oocyte. Raising PIP_2 by injection is difficult because it is rapidly hydrolyzed to IP_3 by phospholipase C (PLC) (Thornell *et al.*, 2012). However, blocking PIP_2 hydrolysis by pretreating the oocyte with the PLC inhibitor U73122 resulted in a modest PIP_2 injection-induced stimulation of NBCe1-A, -B, and -C (Thornell *et al.*, 2012). Importantly, NBCe1-A was not stimulated by IP_3/Ca^{2+}, as described below, therefore the PIP_2-induced stimulation in these experiments was not the result of an incomplete PLC inhibition. Because there was only a small change in NBCe1 activity when PIP_2 was increased, decreasing PIP_2 may be a better assay for demonstrating the PIP_2 sensitivity of NBCe1.

A decrease in membrane PIP_2, without generation of IP_3, inhibited NBCe1-B and -C. In *Xenopus* oocytes, activation of a co-expressed 5' voltage-sensitive phosphatase (VSP) inhibited NBCe1-B and -C (Thornell & Bevensee, 2013). Where might PIP_2 bind? According to the crystal structure of Kir2.2- and GIRK2-PIP_2 interactions (Hansen *et al.*, 2011; Whorton & Mackinnon, 2011), these K^+ channels have a non-specific phospholipid domain within the transmembrane region, as well as a polycationic PIP_2 binding domain in the cytosol near one transmembrane domain. NBCe1 variants contain similar PIP_2 binding motifs including the sequences KDKKKKEDEKKKKKKK in the cytosolic C-

terminus, RKHRH in the cytosolic N-terminus, and RKEHKLKK before transmembrane domain 8 (TMD8). The region before TMD8 is of particular interest because TMD8 is involved in ion translocation (McAlear & Bevensee, 2006). An additional PIP_2 binding motif, RRRRRHKRK is found in the N-terminus of NBCe1-B and -C, but is unlikely to be the sole PIP_2 binding region because it is absent in the PIP_2 -sensitive NBCe1-A.

IP_3 and Ca^{2+}

In whole *Xenopus* oocytes, injecting PIP_2 stimulated NBCe1-B and -C, but not NBCe1-A currents (Thornell *et al.*, 2012). The majority of the PIP_2-induced stimulation was mediated by PIP_2 hydrolysis to IP_3/Ca^{2+} to activate a staurosporine-sensitive kinase (Thornell *et al.*, 2012). The kinase likely stimulated NBCe1 through phosphorylation of NBCe1 or an NBCe1 regulator to relieve the AID.

NBCe1-A expressed in *Xenopus* oocytes was neither sensitive to phospholipid injection nor Ca^{2+} influx through store-operated channels (Thornell *et al.*, 2012). However in a separate study, raising Ca^{2+} from 100 nM to 500 nM stimulated the slope conductance for rat NBCe1-A in a small fraction of macropatches. The stimulation was through a change in stoichiometry from 2:1 to 3:1 (Müller-Berger *et al.*, 2001). Discrepancies between these whole oocyte and patch studies are unknown, but may reflect differences in the whole oocyte vs. a membrane patch.

ANG-II, PKC, and Ca^{2+}

It is well established that endogenous and heterologous NBCe1-A are inhibited by high doses of angiotensin II (ANG-II) and are stimulated by low doses of ANG-II (Geibel

et al., 1990; Eiam-ong *et al.*, 1993; Coppola & Frömter, 1994; Ruiz *et al.*, 1995; Robey *et al.*, 2002; Zheng, 2003). The ANG-II-mediated NBCe1 signaling pathways remained loosely defined until the rat kidney NBCe1-A clone was expressed in *Xenopus* oocytes. In *Xenopus* oocytes, activation of the rat AT_{1A} inhibited co-expressed NBCe1-A depolarization-induced outward currents (Perry *et al.*, 2006). NBCe1-A associated with the calcium-insensitive phosphokinase C, PKCε, after high ANG-II treatment. However, the AT_{1A}-mediated NBCe1-A stimulation was inhibited by BAPTA. It was concluded that the high ANG-II concentration inhibited NBCe1-A surface expression by a calcium-insensitive PKC and a separate Ca^{2+} sensitive process. Further support for ANG-II-induced trafficking of NBCe1-A was the finding that high ANG-II caused an intracellular accumulation of GFP-conjugated NBCe1-A (Perry *et al.*, 2007). Furthermore, ANG-II-induced inhibition was irreversible after applying calmodulin inhibitors or monensin. The bimodal regulation of NBCe1-A by ANG-II was preserved in the above experiments because low ANG-II concentrations potentiated depolarized-induced NBC current in a Ca^{2+}-sensitive manner (Perry *et al.*, 2006).

Acetylcholine

Acetylcholine (ACh) is a signaling molecule that can activate either ionotropic or metabotropic receptors. Metabotropic ACh receptor activation is coupled to anion secretion in many epithelial cell types, such as acinar cells. Applying the ACh analog, carbachol, lowered membrane expression of NBCe1-A or NBCe1-B in acinar ParC5 cells (Perry *et al.*, 2009). Carbachol-induced inhibition was not through the variable N-terminus because carbachol lowered expression for both NBCe1-A and -B. This mode of

ACh regulation is likely cell-type specific because HEK293 cells expressing NBCe1-B were not affected by carbachol pre-incubation (Bachmann *et al.*, 2008).

cAMP

cAMP is a second messenger formed by the catalytic activity of adenylate cyclase upon ATP. It is well established that a hormone-induced increase in cAMP decreases renal tubular HCO_3^- absorption and increases pancreatic duct HCO_3^- secretion (Mckinney & Myers, 1980; Liu & Cogan, 1989; Ishiguro *et al.*, 1996*a*, 1996*b*; Kunimi *et al.*, 2000). However, the characterization of these cAMP-induced NBCe1 regulation cascades remains less established. The studies on NBCe1 clones detailed below have provided evidence that cAMP converts NBCe1 stoichiometry from 1:3 to 1:2 and increases NBCe1-B transport activity.

When transfected in mouse proximal tubule cells (mPT), which lacked endogenous NBCe1 activity, both mouse kidney NBCe1-A and pancreatic NBCe1-B had a 1:3 stoichiometry (Gross *et al.*, 2001*a*, 2001*b*). Applying the cell permeable cAMP analog, 8-bromo-cAMP, changed NBCe1-A stoichiometry from 1:3 to 1:2 (Gross *et al.*, 2001*b*). The change in stoichiometry required the phosphokinase A (PKA) mediated phosphorylation of S982. This finding was consistent with the inhibition of net HCO_3^- efflux noted in the proximal tubule in response to dopamine (Kunimi *et al.*, 2000) and parathyroid hormone (Mckinney & Myers, 1980), which both increase cAMP. In a separate study, applying 8-bromo-cAMP to pancreatic NBCe1-B expressing mPT cells changed NBCe1-B stoichiometry from 1:3 to 1:2 through PKA-mediated phosphorylation of S1026 (Gross *et al.*, 2003), which is homologous to residue 982 of NBCe1-A. Because

cAMP-mediated stoichiometry changes were conserved for both NBCe1-A and -B, this mode of regulation did not involve the variable N-terminus of NBCe1.

Interestingly, when transfected in the mouse pancreatic duct cell line mPEC, NBCe1-B had a 1:2 stoichiometry and NBCe1-A had a 1:3 stoichiometry (Gross *et al.*, 2003). Consistent with the previously described phosphorylation-induced change in stoichiometry, NBCe1-B residue S1026 is phosphorylated, but NBCe1-A S982 is not phosphorylated under basal conditions in mPEC cells. The kinase responsible for this differential phosphorylation state remains elusive. However, differential phosphorylation in mPEC cells likely involves the N-terminus because the C-terminus of NBCe1-A and -B are identical (Figure 4). In these mPEC cells, applying 8-bromo-cAMP changed the stoichiometry of NBCe1-A, as indicated by a change in reversal potential, but stimulated NBCe1-B activity, as indicated by an increase in slope conductance without a change in reversal potential. The NBCe1-B stimulation involved residue T49 located in the PKA phosphorylation site in the different N-terminus. This stimulation was also observed for pancreatic NBCe1-B expressed in mPT cells as indicated by a change in slope conductance in addition to the shift in reversal potential. These data provided insight into a potential basolateral NBCe1-B regulation pathway to support secretin-induced HCO_3^- secretion observed for pancreatic ducts (Ishiguro *et al.*, 1996*a*, 1996*b*).

Magnesium

Free cytosolic Mg^{2+} is estimated to vary physiologically from 0.5 mM to 0.7 mM and remains fairly constant under a variety of physiological conditions (Romani, 2007). Yamaguchi and Ishikawa expressed bovine NBCe1-B and monitored Na^+-dependent

HCO_3^- whole cell currents in both HEK293 and NIH3T3 cells while varying dialyzed Mg^{2+} concentrations (Yamaguchi & Ishikawa, 2008). For HEK293 cells, Mg^{2+} inhibited Na^+-dependent HCO_3^- currents with a K_i that was likely voltage-independent with values of 14.6 μM at -20 mV, 11.1 μM at +20 mV, and 10.9 μM at +40 mV. A similar Mg^{2+}-induced NBCe1-B inhibition was observed for NIH3T3 cells. The AID of NBCe1-B was involved because N-terminal truncation of NBCe1-B raised the K_i for Mg^{2+} to 300 μM.

In bovine parotid acinar cells, endogenous NBCe1-B was inhibited by Mg^{2+} with ~8-fold higher K_i values (Yamaguchi & Ishikawa, 2008). The rightward shift in K_i from the previous expression systems was likely due to cell-type specific regulation. For example, HEK293 stably transfected with NBCe1-B had a K_i for Mg^{2+}-induced NBCe1-B inhibition of 560 nM that was increased to 11 μM with IRBIT co-transfection (Yamaguchi & Ishikawa, 2012). The authors note that the K_i for Mg^{2+}-induced NBCe1-B inhibition for this HEK293 cell study (Yamaguchi & Ishikawa, 2012) was higher than the previous HEK293 cell study (Yamaguchi & Ishikawa, 2008), but there is currently no explanation for this finding.

Mg^{2+}-mediated inhibition of NBCe1-B was likely due to disruption of PIP_2 regulation of NBCe1. More specifically, the cationic Mg^{2+} likely screened the negative charges of PIP_2, which stimulate NBCe1. Consistent with this mechanism, other polyvalent cations neomycin (Yamaguchi & Ishikawa, 2008) and spermine (Yamaguchi & Ishikawa, 2012) increased the K_i for Mg^{2+}-induced NBCe1-B inhibition for NBCe1-B expressed in HEK293, NIH3T3, and for endogenous NBCe1-B in bovine parotid acinar cells.

Because $[Mg^{2+}]_i$ appears to be static, Mg^{2+} likely regulates NBCe1 by lowering the apparent NBCe1 affinity for PIP_2, possibly allowing for physiological PIP_2 regulation of NBCe1. Unlike NBCe1-B, Mg^{2+}-induced inhibition of NBCe1-A would not involve IRBIT because NBCe1-A does not bind IRBIT. This simplest interpretation is IRBIT bound to NBCe1-B stabilizes NBCe1's interaction with PIP_2 (i.e. raises the K_i for Mg^{2+} inhibition).

Chaperone stress 70 protein (STCH)

Chaperone stress 70 protein (STCH) is a microsomal-associated protein. Although a member of the 70 kDa heat-shock protein family, it is not activated by heat shock. STCH is expressed ubiquitously and activated by Ca^{2+}. Using a yeast 2-hybrid system, NBCe1-B was identified to bind with STCH (Bae *et al.*, 2013). When both constructs were co-expressed in *Xenopus* oocytes, STCH stimulated NBCe1-B current due to an increase in expression. NBCe1-B stimulation was not mediated by the shared NBCe1-B/C N-terminus because the N-terminal truncation mutant (Δ95aa) was also stimulated when co-expressed with STCH. SCTH-induced NBCe1-B stimulation was additive when co-expressed with IRBIT and therefore likely through a separate pathway. SCTH stimulation was confirmed in a human submandibular gland ductile cell line, HSG. siRNA knockdown of STCH in HSG cells, inhibited DIDS-sensitive pH_i recovery from an NH_4^+-induced acid-load and decreased membrane expression of NBCe1-B.

NBCn1 (*Slc4a7*)

NBCn1 variants are found in many tissue types and are regulators of pH_i. Additionally, NBCn1 is involved in coordinating epithelial absorption and secretion. There are 16 identified NBCn1 splice variants, NBCn1-A through -P. These splice variants are simplified by grouping variable regions into cassettes (Figure 5). Each functional variant contains 1 of 2 alternate N-termini and include or exclude previously defined cassette I, II, and/or IV in the N-terminus and/or cassette III in the C-terminus (Liu *et al.*, 2013).

In addition to pH_i regulation, NBCn1 is found in many epithelial cells and is involved in HCO_3^- absorption and secretion. Tissue-specific roles for NBCn1 have been identified by studying NBCn1 knockout mice and genomic data. Specifically, NBCn1 plays a major role in somatosensory perception. NBCn1 knockout mice exhibit blindness and hearing loss (Bok *et al.*, 2003; Lopez *et al.*, 2005). NBCn1 dysfunction has also been identified as a risk factor for hypertension (Ehret *et al.*, 2011), which is consistent with the mild hypertension identified in knockout mice (Boedtkjer *et al.*, 2011).

Autoregulation

Each NBCn1 cassette effects either membrane surface expression or transporter activity as monitored by pH_i recovery from an acid-load in a systematic oocyte expression study (Liu *et al.*, 2013). It was apparent that surface expression was regulated by the interactions of multiple cassettes and may not be attributed to a single cassette for cassettes I, II, and III. The MEAD residues of one variable N-terminus stimulated NBCn1 surface expression, but did not stimulate transporter activity as compared to the MERF

amino terminus. Cassette 1 did not stimulate NBCn1 activity; however cassette 1 was involved in expression interactions. NBCn1 activity was stimulated by cassette II by a factor of 3.8 and cassette III by a factor of 4.4. Cassette IV had the most dramatic regulatory effect and stimulated NBCn1 activity 10.6-fold and clearly inhibited NBCn1 membrane abundance by 55%.

Carbonic anhydrase

CA, as discussed above, is responsible for the rapid reversible conversion of CO_2 to HCO_3^-. CA II binding to NBCn1 is controversial. Similar to AE1, HEK293 cells co-expressing NBCn1 and a catalytically-reduced CA II mutant have a slower pH_i recovery from an acid load than NBCn1 expressing cells (Loiselle *et al.*, 2004). However, similar to evidence that AE1 does not bind CA II, as described above, non-tagged NBCn1 did not bind CA II (Piermarini *et al.*, 2007).

Calcineurin

Calcineurin is a calcium-dependent serine-threonine protein phosphatase found in many cell types (Rusnak & Mertz, 2000). A calcineurin-NBCn1 interaction was identified by a yeast 2-hybrid screen, using cassette II of NBCn1 as bait to screen a human skeletal muscle cDNA library (Danielsen *et al.*, 2013). Serial truncations and further mutations demonstrated that the interaction was dependent on the residues 94-99 (PTVVIHT—critical amino acids are underlined). The involvement of cassette II was verified in an additional study and calcineurin binding may induce a conformational change in NBCn1(Gill *et al.*, 2014). Functionally, calcineurin stimulated endogenous

NBCn1-B in rat mesenteric arteries (Danielsen *et al.*, 2013). In this study, calcineurin was activated prior to and during the acid load by elevating extracellular K^+ to raise intracellular Ca^{2+} through voltage-gated Ca^{2+} channels. In these experiments, recovery from the acid-load was inhibited to a similar extent by the Ca^{2+} chelator BAPTA and the calcineurin inhibitors FK506 and cyclosporine. Calcineurin stimulation required Ca^{2+} because the BAPTA and FK506 inhibition were non-additive. Based on the modular structure of NBCn1 (Boron *et al.*, 2009), this stimulation is most likely conserved in NBCn1-A, -B, -C, -D, and -H due to the inclusion of cassette II (Figure 5).

IRBIT

As described above, IRBIT is a signaling molecule released from IP_3 receptors when IP_3 concentrations increase (Ando *et al.*, 2003). IRBIT both interacted with and stimulated NBCn1-B (Parker *et al.*, 2007*b*). IRBIT likely binds all other NBCn1 variants because the characterized IRBIT binding domain in NBCe1-B and -C is present in all NBCn1 variants.

cAMP

cAMP is a second messenger that actives PKA, which phosphorylates many target proteins. NBCn1 expressed in HEK293 cells was inhibited by applying the PKC-activators forskolin or 8-bromoadenosine (Loiselle *et al.*, 2004). The inhibition was sensitive to the PKA inhibitor H89, however PKA did not alter NBCn1 phosphorylation. It was likely that PKA phosphorylated an intermediate NBCn1 regulatory protein.

PDZ domain containing proteins

Post synaptic density protein 95 (PSD-95) is a scaffolding protein found in the post synaptic density of neuronal dendrites. PSD-95 contains an SH3 domain, a catalytically-inactive guanylate kinase domain, and 3 PDZ domains, which interact with other PDZ containing proteins (e.g. the NDMA receptor)(Xu, 2011). NBCn1 contains a PDZ domain that binds PSD-95 as verified by co-immunoprecipitation. Co-expression of NBCn1 with PSD-95 did not stimulate HCO_3^- transport, but did stimulate NBCn1-associated channel-like conductance (Lee *et al.*, 2012*a*). Syntrophin γ2 is another cytosolic scaffolding protein that contains a PDZ domain and binds NBCn1 (Lee *et al.*, 2014). Co-expressing syntrophin γ2 with NBCn1 stimulated both HCO_3^- transport and the NBCn1-associated channel-like conductance.

NDCBE (*Slc4a8*)

NDCBE is present in many organs, but is most abundant in the brain, where it regulates neuronal firing (Sinning *et al.*, 2011). There are 5 NDCBE splice variants, NDCBE-A through -E (Figure 6). NDCBE-A and -B contain the same 16 residue N-terminus, but vary in their C-terminus. NDCBE-C is identical to NDCBE-A, but is truncated at the N-terminus by 54 residues. NDCBE-D is identical to NDCBE-B, but is truncated at the N-terminus by 54 residues. NDCBE-E is identical to NDCBE-B, but the 16 residue N-terminus of NDCBE-B is replaced by a unique 43 residue N-terminus. NDCBE-E is the only variant not tested for function, but is presumed to be functional (Parker & Boron, 2013).

Autoregulation

NDCBE-B, -D, and -E share a 17 amino acid C-terminal sequence (Figure 6). When expressed in *Xenopus* oocytes, NDCBE-B and -D have similar activities (Parker *et al.*, 2008). Truncation of the 17 amino acid C-terminus of NDCBE-B stimulated NDCBE-B to an activity level the same as NDCBE-A. These findings are consistent with an AID contained in the differential C-terminus region of NDCBE-B and -D.

IRBIT

IRBIT, as described above, binds to and regulates many BTs. IRBIT binds to NDCBE-B and stimulates HCO_3^- current (Parker *et al.*, 2007*b*). In an unpublished observation, NDCBE-D was not stimulated by IRBIT (Parker & Boron, 2013). Interestingly, NDCBE-D still contains the putative IRBIT-binding RRR sequence (residues 19-21). Therefore, IRBIT binding may involve determinants outside of the RRR sequence elucidated for NBCe1 (Hong *et al.*, 2013).

NBCn2 (*Slc4a10*)

NBCn2 is present throughout many organs, however specific roles in physiology have remained elusive due to difficulty characterizing NBCn2 transport and dysregulation of other transporters associated with the NBCn2 knockout mouse (Parker & Boron, 2013). There are 4 NBCn2 splice variants, NBCn2-A through -D (Figure 7). NBCn2-B and -D contain the 30 amino acid cassette A within the N-terminus. NBCn2-A and -B contain a 3 amino acid C-terminus, whereas NBCn2-C and -D contain a 21 amino acid C-terminus that has a PDZ domain.

Autoregulation

Truncation of the N-terminal 92 residues of NBCn2 increased transporter activity (Parker *et al.*, 2007*a*) and therefore this region of NBCn2 likely contains an AID. The variant for this study is unclear, but all NBCn2 variants contain these 92 residues and are predicted to have the AID (Figure 7). Although the inclusion of the AID is ubiquitous among variants, this AID may be differentially regulated through variable regions of NBCn2.

cAMP

In 3T3 cells expressing NBCn2-C, applying the forskolin to increase cAMP inhibited NBCn2-mediated pH_i recovery from an acid load (Lee *et al.*, 2006). The cAMP-induced inhibition of NBCn2 was likely through PKA because inhibition was mimicked by the cAMP analog, 8-bromo-cAMP, to activate PKA and the PKA inhibitory fragment 14-22 stimulated recovery. A similar inhibition of NBCn2-mediated pH_i recovery was observed after disrupting the actin cytoskeleton with cytochalasin B. A potential protein that may link cytoskeleton structure to NBCn2 is the ezrin binding protein 50 (EBP50), which contains PDZ domains and co-immunoprecipitated with transfected NBCn2-C for 3T3 cells. If cAMP-induced NBCn2 inhibition is indeed upstream an upstream regulator of the PDZ domain then cAMP would be predicted regulate NBCn2-C and -D.

IRBIT

IRBIT, as detailed for NBCe1, is a cytosolic signaling protein, which signals by competition off the IP_3 receptor in response to increases in IP3 (Ando *et al.*, 2003).

IRBIT both binds and stimulates NBCn2 (Parker *et al.*, 2007*a*, 2007*b*). However, this was due partly to an increase in expression (Parker *et al.*, 2007*a*), which was not observed for IRBIT over-expression experiments for NBCe1 (Shirakabe *et al.*, 2006; Thornell *et al.*, 2012; Lee *et al.*, 2012*b*). All other NBCn2 variants are likely stimulated by IRBIT because of the conserved IRBIT binding region shared with the characterized NBCe1.

Conclusion

The presence of different *Slc4* family members in addition to compensation mechanisms complicates studying endogenous regulatory mechanisms of *Slc4* members. We have summarized the characterized and predicted regulatory mechanisms for the cloned *Slc4* proteins. These data provide a foundation for *Slc4* regulation in different cell types.

Acknowledgements

This work was supported by an award from the American Heart Association (Southeast Affiliate, 0755255B to M.O.B), an award from the NIH/NINDS (R01 NS046653) and an award from the NIH/NIGMS (T32GM008111).

References

Almomani EY, King JC, Netsawang J, Yenchitsomanus P-T, Malasit P, Limjindaporn T, Alexander RT & Cordat E (2012). Adaptor protein 1 complexes regulate intracellular trafficking of the kidney anion exchanger 1 in epithelial cells. *Am J Physiol Cell Physiol* **303,** C554–66.

Alper S, Darman R, Chernova M & Dahl N (2002). The AE gene family of Cl/HCO_3^- exchangers. *J Nephrol* **15,** S41–53.

Al-Samir S, Papadopoulos S, Scheibe RJ, Meißner JD, Cartron J-P, Sly WS, Alper SL, Gros G & Endeward V (2013). Activity and distribution of intracellular carbonic anhydrase II and their effects on the transport activity of anion exchanger AE1/SLC4A1. *J Physiol* **591,** 4963–4982.

Alvarez BV, Loiselle FB, Supuran CT, Schwartz GJ & Casey JR (2003). Direct Extracellular Interaction between Carbonic Anhydrase IV and the Human NBC1 Sodium/Bicarbonate Co-transporters. *Biochemistry*12321–12329.

Ando H, Mizutani A, Matsu-ura T & Mikoshiba K (2003). IRBIT, a novel inositol 1,4,5-trisphosphate (IP_3) receptor-binding protein, is released from the IP_3 receptor upon IP_3 binding to the receptor. *J Biol Chem* **278,** 10602–10612.

Anselmo A & Earnest S (2006). WNK1 and OSR1 regulate the Na^+, K^+, $2Cl^-$ cotransporter in HeLa cells. *Proc Natl Acad Sci USA* **103,** 2–7.

Bachmann O, Franke K, Yu H, Riederer B, Li HC, Soleimani M, Manns MP & Seidler U (2008). cAMP-dependent and cholinergic regulation of the electrogenic intestinal/pancreatic Na^+/HCO3$^-$ cotransporter pNBC1 in human embryonic kidney (HEK293) cells. *BMC Cell Biol* **9,** 70.

Bae J-S, Koo N-Y, Namkoong E, Davies AJ, Choi S-K, Shin Y, Jin M, Hwang S-M, Mikoshiba K & Park K (2013). Chaperone stress 70 protein (STCH) binds and regulates two acid/base transporters NBCe1-B and NHE1. *J Biol Chem* **288,** 6295–6305.

Balla T (2013). Phosphoinositides: tiny lipids with giant impact on cell regulation. *Physiol Rev* **93,** 1019–1137.

Boedtkjer E, Praetorius J, Matchkov V V, Stankevicius E, Mogensen S, Füchtbauer AC, Simonsen U, Füchtbauer E-M & Aalkjaer C (2011). Disruption of Na^+,HCO_3^- cotransporter NBCn1 (slc4a7) inhibits NO-mediated vasorelaxation, smooth muscle Ca^{2+} sensitivity, and hypertension development in mice. *Circulation* **124,** 1819–1829.

Bok D et al. (2003). Blindness and auditory impairment caused by loss of the sodium bicarbonate cotransporter NBC3. *Nat Genet* **34,** 313–319.

Boron WF & Boulpaep EL (1983). Intracellular pH regulation in the renal proximal tubule of the salamander basolateral HCO_3 transport. *J Gen Physiol* **81,** 53–94.

Boron WF, Chen L & Parker MD (2009). Modular structure of sodium-coupled bicarbonate transporters. *J Exp Biol* **212,** 1697–1706.

Campanella ME, Chu H, Wandersee NJ, Peters LL, Mohandas N, Gilligan DM & Low PS (2008). Characterization of glycolytic enzyme interactions with murine

erythrocyte membranes in wild-type and membrane protein knockout mice. *Blood* **112,** 3900–3906.

Chasis JA & Mohandas N (1992). Red blood cell glycophorins. *Blood* **80,** 1869–1879.

Chesler M (2003). Regulation and modulation of pH in the brain. *Physiol Rev* **83,** 1183–1221.

Chu H & Low PS (2006). Mapping of glycolytic enzyme-binding sites on human erythrocyte band 3. *Biochem J* **400,** 143–151.

Coppola S & Frömter E (1994). An electrophysiological study of angiotensin II regulation of Na-HCO_3 cotransport and K^+ conductance in renal proximal tubules. I. Effect of picomolar concentrations. *Pflügers Arch Eur J Physiol* **427,** 143–150.

Danielsen AA, Parker MD, Lee S, Boron WF, Aalkjaer C & Boedtkjer E (2013). Splice cassette II of Na^+/HCO_3^- cotransporter NBCn1 (slc4a7) interacts with calcineurin A: implications for transporter activity and intracellular pH control during rat artery contractions. *J Biol Chem* **288,** 8146–8155.

Devogelaere B, Beullens M, Sammels E, Derua R, Waelkens E, van Lint J, Parys JB, Missiaen L, Bollen M & De Smedt H (2007). Protein phosphatase-1 is a novel regulator of the interaction between IRBIT and the inositol 1,4,5-trisphosphate receptor. *Biochem J* **407,** 303–311.

Ehret GB et al. (2011). Genetic variants in novel pathways influence blood pressure and cardiovascular disease risk. *Nature* **478,** 103–109.

Eiam-Ong S, Hilden SA, Johns CA & Madias NE (1993). Stimulation of basolateral Na^+-HCO_3^- cotransporter by angiotensin II in rabbit renal cortex. *Am J Physiol Ren Physiol* **265,** 195–203.

Garnett JP, Hickman E, Burrows R, Hegyi P, Tiszlavicz L, Cuthbert AW, Fong P & Gray M a (2011). Novel role for pendrin in orchestrating bicarbonate secretion in cystic fibrosis transmembrane conductance regulator (CFTR)-expressing airway serous cells. *J Biol Chem* **286,** 41069–41082.

Geibel J, Giebisch G & Boron WF (1990). Angiotensin II stimulates both Na^+-H^+ exchange and Na^+/HCO_3^- cotransport in the rabbit proximal tubule. *Proc Natl Acad Sci USA* **87,** 7917–7920.

Gill HS, Roush ED, Dutcher L & Patel S (2014). Direct evidence for calcineurin binding to the exon-7 loop of the sodium-bicarbonate cotransporter NBCn1. *Int J Biol Sci* **10,** 771–776.

Gross E, Fedotoff O, Pushkin A, Abuladze N, Newman D & Kurtz I (2003). Phosphorylation-induced modulation of pNBC1 function: distinct roles for the amino- and carboxy-termini. *J Physiol* **549,** 673–682.

Gross E, Hawkins K, Abuladze N, Pushkin A, Cotton CU, Hopfer U & Kurtz I (2001*a*). The stoichiometry of the electrogenic sodium bicarbonate cotransporter NBC1 is cell-type dependent. *J Physiol* **531,** 597–603.

Gross E, Hawkins K, Pushkin a, Sassani P, Dukkipati R, Abuladze N, Hopfer U & Kurtz I (2001*b*). Phosphorylation of Ser(982) in the sodium bicarbonate cotransporter kNBC1 shifts the HCO_3^-:Na^+ stoichiometry from 3:1 to 2:1 in murine proximal tubule cells. *J Physiol* **537,** 659–665.

Gross E, Pushkin A, Abuladze N, Fedotoff O & Kurtz I (2002). Regulation of the sodium bicarbonate cotransporter kNBC1 function: role of Asp986, Asp988 and kNBC1-carbonic anhydrase II binding. *J Physiol* **544,** 679–685.

Groves J & Tanner MJ (1994). The effects of glycophorin A on the expression of the human red cell anion transporter (band 3) in *Xenopus* oocytes. *J Membr Biol* **140,** 81–88.

Groves JD & Tanner MJ (1992). Glycophorin A facilitates the expression of human band 3-mediated anion transport in *Xenopus* oocytes. *J Biol Chem* **267,** 22163–22170.

Hansen SB, Tao X & MacKinnon R (2011). Structural basis of PIP_2 activation of the classical inward rectifier K^+ channel Kir2.2. *Nature* **477,** 495–498.

Hassoun H, Hanada T, Lutchman M, Sahr KE, Palek J, Hanspal M & Chishti a H (1998). Complete deficiency of glycophorin A in red blood cells from mice with targeted inactivation of the band 3 (AE1) gene. *Blood* **91,** 2146–2151.

He G, Wang H, Huang S & Huang C (2007). Intersectin links WNK kinases to endocytosis of ROMK1. *J Clin Invest* **117,** 1078–1087.

Heise CJ, Xu B, Deaton SL, Cha S-K, Cheng C-J, Earnest S, Sengupta S, Juang Y-C, Stippec S, Xu Y, Zhao Y, Huang C-L & Cobb MH (2010). Serum and glucocorticoid-induced kinase (SGK) 1 and the epithelial sodium channel are regulated by multiple with no lysine (WNK) family members. *J Biol Chem* **285,** 25161–25167.

Heyer M, Müller-Berger S, Romero MF, Boron WF & Frömter E (1999). Stoichiometry of the rat kidney Na^+-HCO_3^- cotransporter expressed in *Xenopus laevis* oocytes. *Pflügers Arch Eur J Physiol* **438,** 322–329.

Hong JH, Yang D, Shcheynikov N, Ohana E, Shin DM & Muallem S (2013). Convergence of IRBIT, phosphatidylinositol (4,5) bisphosphate, and WNK/SPAK

kinases in regulation of the Na^+-HCO_3^- cotransporters family. *Proc Natl Acad Sci USA* **110,** 4105–4110.

Ishiguro H, Steward MC, Lindsay ARG & Case RM (1996*a*). Accumulation of intracellular HCO_3^- by Na^+-HCO_3^- cotransport in interlobular ducts from guinea-pig pancreas. *J Physiol* **495,** 169–178.

Ishiguro H, Steward MC, Wilson RW & Case RM (1996*b*). Bicarbonate secretion in interlobular ducts from guinea-pig pancreas. *J Physiol* **495,** 179–191.

Kopito RR & Lodish HF (1985). Primary structure and transmembrane orientation of the murine anion exchange protein. *Nature* **316,** 234–238.

Kudrycki KE, Newman PR & Shull GE (1990). cDNA cloning and tissue distribution of mRNAs for two proteins that are related to the band 3 Cl^-/HCO_3^- exchanger. *J Biol Chem* **265,** 462–471.

Kunimi M, Seki G, Hara C, Taniguchi S, Uwatoko S, Goto a, Kimura S & Fujita T (2000). Dopamine inhibits renal Na^+:HCO_3^- cotransporter in rabbits and normotensive rats but not in spontaneously hypertensive rats. *Kidney Int* **57,** 534–543.

Lee HJ, Kwon MH, Lee S, Hall R a, Yun CC & Choi I (2014). Systematic family-wide analysis of sodium bicarbonate cotransporter NBCn1/SLC4A7 interactions with PDZ scaffold proteins. *Physiol Rep* **2,** 1–11.

Lee S, Yang HS, Kim E, Ju EJ, Kwon MH, Dudley RK, Smith Y, Yun CC & Choi I (2012*a*). PSD-95 interacts with NBCn1 and enhances channel-like activity without affecting Na/HCO_3 cotransport. *Cell Physiol Biochem* **30,** 1444–1455.

Lee SK, Boron WF & Parker MD (2012*b*). Relief of autoinhibition of the electrogenic Na-HCO_3 cotransporter NBCe1-B: role of IRBIT vs.amino-terminal truncation. *Am J Physiol Cell Physiol* **302,** C518–26.

Lee YS, Ouyang YB & Giffard RG (2006). Regulation of the rat brain Na^+-driven Cl^-/HCO_3^- exchanger involves protein kinase A and a multiprotein signaling complex. *FEBS Lett* **580,** 4865–4871.

Liu F & Cogan M (1989). Angiotensin II stimulates early proximal bicarbonate absorption in the rat by decreasing cyclic adenosine monophosphate. *J Clin Invest* **84,** 83–91.

Liu Y, Qin X, Wang DK, Guo YM, Gill HS, Morris N, Parker MD, Chen LM & Boron WF (2013). Effects of optional structural elements, including two alternative amino termini and a new splicing cassette IV, on the function of the sodium-bicarbonate cotransporter NBCn1 (SLC4A7). *J Physiol* **591,** 4983–5004.

Loiselle FB, Morgan PE, Alvarez B V & Casey JR (2004). Regulation of the human NBC3 Na^+/HCO_3^- cotransporter by carbonic anhydrase II and PKA. *Am J Physiol Cell Physiol* **286,** C1423–33.

Lopez I a, Acuna D, Galbraith G, Bok D, Ishiyama A, Liu W & Kurtz I (2005). Time course of auditory impairment in mice lacking the electroneutral sodium bicarbonate cotransporter NBC3 (slc4a7). *Brain Res Dev Brain Res* **160,** 63–77.

Lu J, Daly CM, Parker MD, Gill HS, Piermarini PM, Pelletier MF & Boron WF (2006). Effect of human carbonic anhydrase II on the activity of the human electrogenic Na/HCO_3 cotransporter NBCe1-A in *Xenopus* oocytes. *J Biol Chem* **281,** 19241–19250.

McAlear SD & Bevensee MO (2006). A cysteine-scanning mutagenesis study of transmembrane domain 8 of the electrogenic sodium/bicarbonate cotransporter NBCe1. *J Biol Chem* **281,** 32417–32427.

McAlear SD, Liu X, Williams JB, McNicholas-Bevensee CM & Bevensee MO (2006). Electrogenic Na/HCO_3 cotransporter (NBCe1) variants expressed in Xenopus oocytes: functional comparison and roles of the amino and carboxy termini. *J Gen Physiol* **127,** 639–658.

Mckinney TD & Myers P (1980). Bicarbonate transport by proximal tubules: effect of parathyroid hormone and dibutyryl cyclic AMP. *Am J Physiol Ren Physiol* **238,** F166–F174.

Muallem S & Loessberg P (1990). Intracellular pH-regulatory mechanisms in pancreatic acinar cells. I. Characterization of H^+ and HCO_3^- transporters. *J Biol Chem* **265,** 12806–12812.

Müller-Berger S, Ducoudret O, Diakov A & Frömter E (2001). The renal $Na\text{-}HCO_3^-$ cotransporter expressed in *Xenopus laevis* oocytes: change in stoichiometry in response to elevation of cytosolic Ca^{2+} concentration. *Pflügers Arch Eur J Physiol* **442,** 718–728.

Di Paolo G & De Camilli P (2006). Phosphoinositides in cell regulation and membrane dynamics. *Nature* **443,** 651–657.

Park S, Hong JH, Ohana E & Muallem S (2012). The WNK/SPAK and IRBIT/PP1 pathways in epithelial fluid and electrolyte transport. *Physiology (Bethesda)* **27,** 291–299.

Parker MD, Daly CM, Skelton LA & Boron WF (2007*a*). IRBIT functionally enhances the electroneutral Na-coupled bicarbonate transporter NCBE by sequestering an N-terminal autoinhibitory domain (Abstract). *FASEB J* **21,** A1285.

Parker MD, Skelton LA, Daly CM & Boron WF (2007*b*). IRBIT binds to and functionally enhances the electroneutral Na-coupled bicarbonate transporters NBCn1, NDCBE and NCBE (Abstract). *FASEB J* **21,** A1285.

Parker MD & Boron WF (2013). The divergence, actions, roles, and relatives of sodium-coupled bicarbonate transporters. *Physiol Rev* **93,** 803–959.

Parker MD, Bouyer P, Daly CM & Boron WF (2008). Cloning and characterization of novel human SLC4A8 gene products encoding Na^+-driven Cl^-/HCO_3^- exchanger variants NDCBE-A, -C, and -D. *Physiol Genomics* **34,** 265–276.

Perry C, Baker OJ, Reyland ME & Grichtchenko II (2009). $PKC_{\alpha\beta\gamma}$- and PKC_{δ}-dependent endocytosis of NBCe1-A and NBCe1-B in salivary parotid acinar cells. *Am J Physiol Cell Physiol* **297,** 1409–1423.

Perry C, Blaine J, Le H & Grichtchenko II (2006). PMA- and ANG II-induced PKC regulation of the renal Na^+-HCO_3^- cotransporter (hkNBCe1). *Am J Physiol Ren Physiol* **290,** 417–427.

Perry C, Le H & Grichtchenko II (2007). ANG II and calmodulin/CaMKII regulate surface expression and functional activity of NBCe1 via separate means. *Am J Physiol Ren Physiol* **293,** 68–77.

Piermarini PM, Kim EY & Boron WF (2007). Evidence against a direct interaction between intracellular carbonic anhydrase II and pure C-terminal domains of SLC4 bicarbonate transporters. *J Biol Chem* **282,** 1409–1421.

Pushkin A, Abuladze N, Gross E, Newman D, Tatishchev S, Lee I, Fedotoff O, Bondar G, Azimov R, Ngyuen M & Kurtz I (2004). Molecular mechanism of kNBC1-carbonic anhydrase II interaction in proximal tubule cells. *J Physiol* **559,** 55–65.

Richards SM, Jaconi ME, Vassort G & Pucéat M (1999). A spliced variant of AE1 gene encodes a truncated form of Band 3 in heart: the predominant anion exchanger in ventricular myocytes. *J Cell Sci* **112,** 1519–1528.

Robey RB, Ruiz OS, Espiritu DJ, Ibañez VC, Kear FT, Noboa OA, Bernardo AA & Arruda JA (2002). Angiotensin II stimulation of renal epithelial cell Na/HCO_3 cotransport activity: a central role for Src family kinase/classic MAPK pathway coupling. *J Membr Biol* **187,** 135–145.

Romani A (2007). Regulation of magnesium homeostasis and transport in mammalian cells. *Arch Biochem Biophys* **458,** 90–102.

Romero MF, Fulton CM & Boron WF (2004). The SLC4 family of HCO_3^- transporters. *Pflügers Arch Eur J Physiol* **447,** 495–509.

Ruiz O, Qiu Y, Wang L & Arruda J (1995). Regulation of the renal Na-HCO_3 cotransporter: IV. Mechanisms of the stimulatory effect of angiotensin II. *J Am Soc Nephrol* **6,** 1202–1208.

Rusnak F & Mertz P (2000). Calcineurin: form and function. *Physiol Rev* **80,** 1483–1521.

Sawasdee N, Junking M, Ngaojanlar P, Sukomon N, Ungsupravate D, Limjindaporn T, Akkarapatumwong V, Noisakran S & Yenchitsomanus PT (2010). Human kidney anion exchanger 1 interacts with adaptor-related protein complex 1 μ1A (AP-1 μ1A). *Biochem Biophys Res Commun* **401,** 85–91.

Schueler C, Becker HM, McKenna R & Deitmer JW (2011). Transport activity of the sodium bicarbonate cotransporter NBCe1 is enhanced by different isoforms of carbonic anhydrase. *PLoS One* **6,** e27167.

Seki G, Yamada H, Horita S, Suzuki M, Sekine T & Fujita T (2008). Activation and inactivation mechanisms of Na-HCO_3 cotransporter. *J Epithel Biol Pharmacol* **1,** 35–39.

Shan J, Liao J, Huang J, Robert R, Palmer ML, Fahrenkrug SC, O'Grady SM & Hanrahan JW (2012). Bicarbonate-dependent chloride transport drives fluid secretion by the human airway epithelial cell line Calu-3. *J Physiol* **590,** 5273–5297.

Shirakabe K, Priori G, Yamada H, Ando H, Horita S, Fujita T, Fujimoto I, Mizutani A, Seki G & Mikoshiba K (2006). IRBIT, an inositol 1,4,5-trisphosphate receptor-binding protein, specifically binds to and activates pancreas-type Na^+/HCO_3^- cotransporter 1 (pNBC1). *Proc Natl Acad Sci USA* **103,** 9542–9547.

Sinning A, Liebmann L, Kougioumtzes A, Westermann M, Bruehl C & Hübner C (2011). Synaptic glutamate release is modulated by the Na^+-driven Cl^-/HCO_3^- exchanger Slc4a8. *J Neurosci* **31,** 7300–7311.

Soleimani M, Grassi S & Aronson P (1987). Stoichiometry of Na^+-HCO_3^- cotransport in basolateral membrane vesicles isolated from rabbit renal cortex. *J Clin Invest* **79,** 1276–1280.

Sterling D, Reithmeier R & Casey J (2001). A transport metabolon. Functional interaction of carbonic anhydrase II and chloride/bicarbonate exchangers. *J Biol Chem* **276,** 47886–47894.

Su Y, Blake-Palmer KG, Fry AC, Best A, Brown ACN, Hiemstra TF, Horita S, Zhou A, Toye AM & Karet FE (2011). Glyceraldehyde 3-phosphate dehydrogenase is required for band 3 (anion exchanger 1) membrane residency in the mammalian kidney. *Am J Physiol Renal Physiol* **300,** F157–66.

Tanphaichitr VS, Sumboonnanonda A, Ideguchi H, Shayakul C, Brugnara C, Takao M, Veerakul G & Alper SL (1998). Novel AE1 Mutations in Recessive Distal Renal Tubular Acidosis. *J Clin Invest* **102,** 2173–2179.

Thornell IM & Bevensee MO (2013). Activating a voltage-sensitive 5' phosphatase (VSP) that decreases phosphatidylinositol 4,5-bisphosphate (PIP_2) inhibits electrogenic Na/bicarbonate cotransporter NBCe1-B and -C variants expressed in *Xenopus laevis* oocytes (Abstract). *FASEB J* **27,** 730.7.

Thornell IM, Wu J & Bevensee MO (2010). The IP_3 receptor-binding protein IRBIT reduces phosphatidylinositol 4,5-bisphosphate (PIP_2) stimulation of Na/bicarbonate cotransporter NBCe1 variants expressed in *Xenopus laevis* oocytes (Abstract). *FASEB J* **24,** 815.6.

Thornell IM, Wu J, Liu X & Bevensee MO (2012). PIP_2 hydrolysis stimulates electrogenic Na/bicarbonate cotransporter NBCe1-B and -C variants expressed in *Xenopus laevis* oocytes. *J Physiol* **590,** 5993–6011.

Toye AM, Ghosh S, Young MT, Jones GK, Sessions RB, Ramaugé M, Leclerc P, Basu J, Delaunay J & Tanner MJ (2005). Protein-4.2 association with band 3 (AE1, SLCA4) in *Xenopus* oocytes: effects of three natural protein-4.2 mutations associated with hemolytic anemia. *Blood* **105,** 4088–4095.

Vince J & Reithmeier R (1998). Carbonic anhydrase II binds to the carboxyl terminus of human band 3, the erythrocyte $C1^-/HCO_3^-$ exchanger. *J Biol Chem* **273,** 28430–28437.

Vince J & Reithmeier R (2000). Identification of the carbonic anhydrase II binding site in the Cl^-/HCO_3^- anion exchanger AE1. *Biochemistry* **39,** 5527–5533.

Wang Z, Schultheis PJ & Shull GE (1996). Three N-terminal variants of the AE2 Cl^-/HCO_3^- exchanger Are encoded by mRNAs transcribed from alternative promoters. *J Biol Chem* **271,** 7835–7843.

Whorton MR & Mackinnon R (2011). Crystal structure of the mammalian GIRK2 K^+ channel and gating regulation by G proteins, PIP_2, and sodium. *Cell* **147,** 199–208.

Williamson RC, Brown ACN, Mawby WJ & Toye AM (2008). Human kidney anion exchanger 1 localisation in MDCK cells is controlled by the phosphorylation status of two critical tyrosines. *J Cell Sci* **121,** 3422–3432.

Wilson FH, Disse-Nicodème S, Choate K, Ishikawa K, Nelson-Williams C, Desitter I, Gunel M, Milford DV, Lipkin GW, Achard JM, Feely MP, Dussol B, Berland Y, Unwin RJ, Mayan H, Simon DB, Farfel Z, Jeunemaitre X & Lifton RP (2001). Human hypertension caused by mutations in WNK kinases. *Science* **293,** 1107–1112.

Wu F, Saleem M a, Kampik NB, Satchwell TJ, Williamson RC, Blattner SM, Ni L, Toth T, White G, Young MT, Parker MD, Alper SL, Wagner C & Toye AM (2010). Anion exchanger 1 interacts with nephrin in podocytes. *J Am Soc Nephrol* **21,** 1456–1467.

Wu J, McNicholas CM & Bevensee MO (2009). Phosphatidylinositol 4,5-bisphosphate (PIP_2) stimulates the electrogenic Na/HCO_3 cotransporter NBCe1-A expressed in Xenopus oocytes. *Proc Natl Acad Sci USA* **106,** 14150–14155.

Xu W (2011). PSD-95-like membrane associated guanylate kinases (PSD-MAGUKs) and synaptic plasticity. *Curr Opin Neurobiol* **21,** 306–312.

Yamaguchi S & Ishikawa T (2008). The electrogenic Na^+-HCO_3^- cotransporter NBCe1-B is regulated by intracellular Mg^{2+}. *Biochem Biophys Res Commun* **376,** 100–104.

Yamaguchi S & Ishikawa T (2012). IRBIT reduces the apparent affinity for intracellular Mg^{2+} in inhibition of the electrogenic Na^+-HCO_3^- cotransporter NBCe1-B. *Biochem Biophys Res Commun* **424,** 433–438.

Yang C-L, Liu X, Paliege A, Zhu X, Bachmann S, Dawson DC & Ellison DH (2007). WNK1 and WNK4 modulate CFTR activity. *Biochem Biophys Res Commun* **353,** 535–540.

Yang D, Li Q, So I, Huang C, Ando H, Mizutani A, Seki G, Mikoshiba K, Thomas PJ & Muallem S (2011). IRBIT governs epithelial secretion in mice by antagonizing the WNK/SPAK kinase pathway. *J Clin Invest* **121,** 956-965.

Yang D, Shcheynikov N, Zeng W, Ohana E, So I, Ando H, Mizutani A, Mikoshiba K & Muallem S (2009). IRBIT coordinates epithelial fluid and HCO_3^- secretion by stimulating the transporters pNBC1 and CFTR in the murine pancreatic duct. **119,** 193–202.

Yannoukakos D, Meyer H, Vasseur C, Driancourt C, Wajcman H & Bursaux E (1991). Three regions of erythrocyte band 3 protein are phosphorylated on tyrosines: characterization of the phosphorylation sites by solid phase sequencing combined with capillary electrophoresis. *Biochim Biophys Acta - Biomembr* **1066,** 70–76.

Young MT & Tanner MJ (2003). Distinct regions of human glycophorin A enhance human red cell anion exchanger (band 3; AE1) transport function and surface trafficking. *J Biol Chem* **278,** 32954–32961.

Zhang D, Kiyatkin A, Bolin JT & Low PS (2000). Crystallographic structure and functional interpretation of the cytoplasmic domain of erythrocyte membrane band 3. *Blood* **96,** 2925–2933.

Zheng Y, Horita S, Hara C, Kunimi M, Yamada H, Sugaya T, Goto A, Fujita T & Seki G (2003). Biphasic regulation of renal proximal bicarbonate absorption by luminal AT_{1A} receptor. *J Am Soc Nephrol* **14,** 1116–1122.

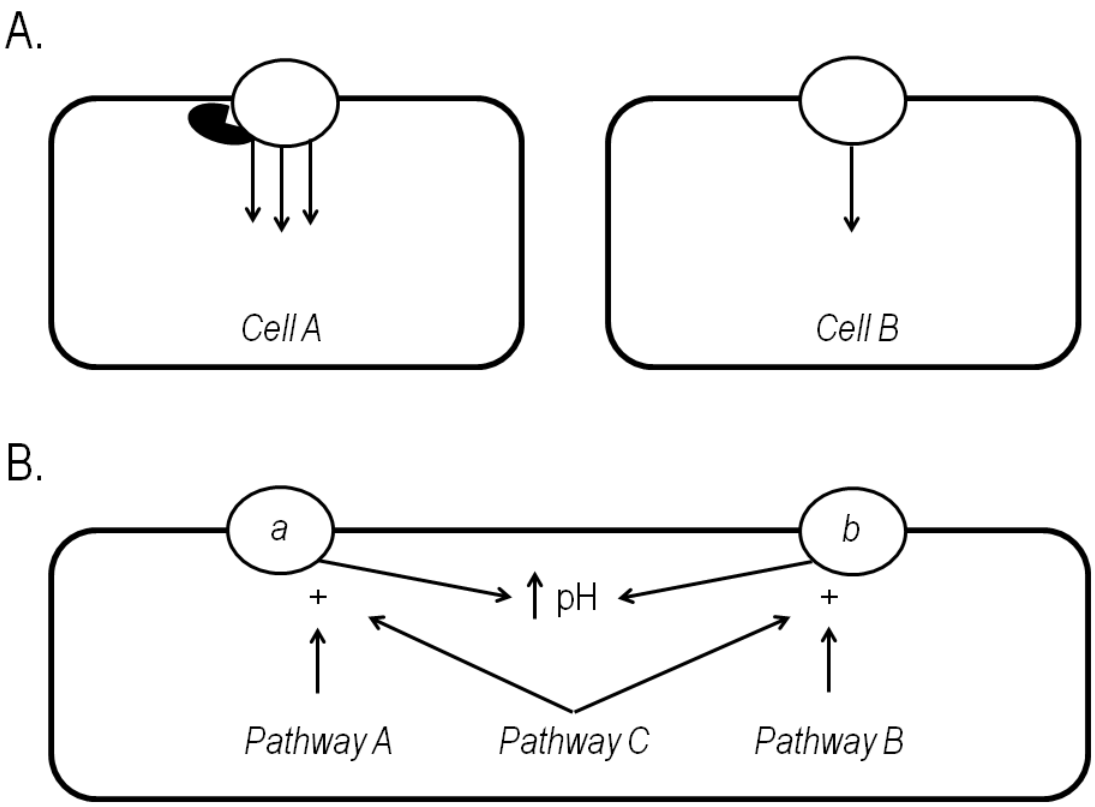

Figure 1. Models of differential regulation. (A) The same HCO_3^-transporter is expressed in Cell A and Cell B. Presence of signaling molecule in Cell A (filled molecule), vs. its absence in Cell B, imparts the transporter in Cell A with greater activity than Cell B. (B) A single cell expresses two different HCO_3^- transporters, which in this example are acid extruders. Activation of *Pathway A* stimulates transport *A*, but not transporter *B*. Activation of *Pathway B* stimulates transporter *B*, but not *A*. Activation of *Pathway C* stimulates both transporter *A* and *B*.

Figure 2. Amino acid sequence comparison of AE1 variants. kAE1 is homologous to eAE1 except for truncation at the N-proximal 65 residues of eAE1.

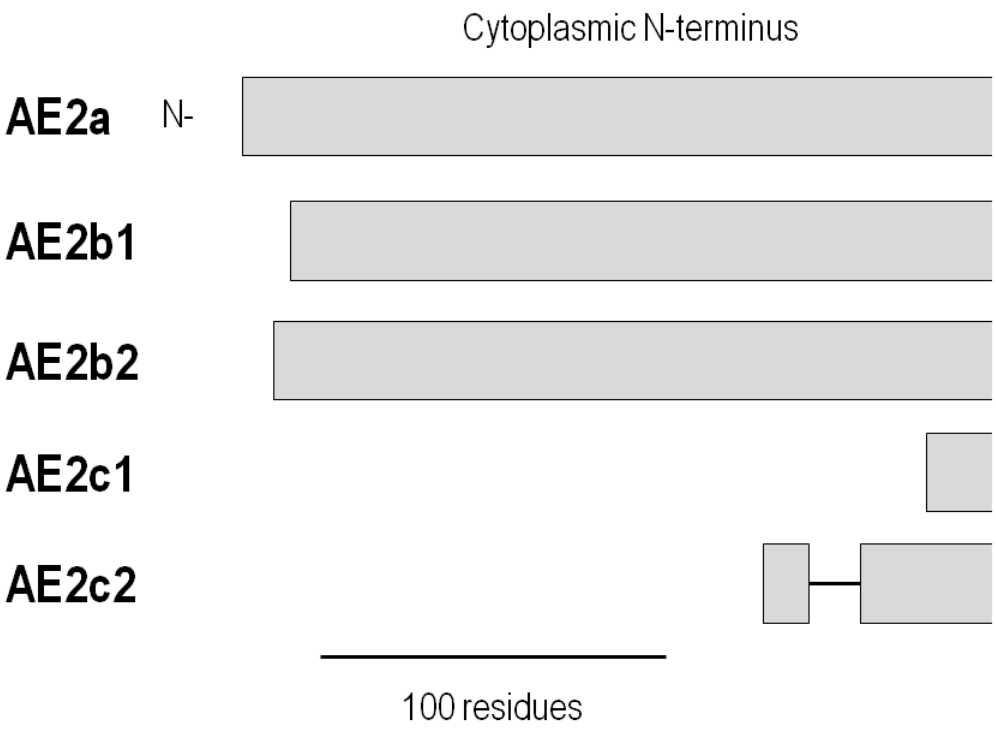

Figure 3. Amino acid sequence comparison of AE2 variants. AE2 variants are identical except for various truncations at the N-terminus. Only the variable N-terminus is shown.

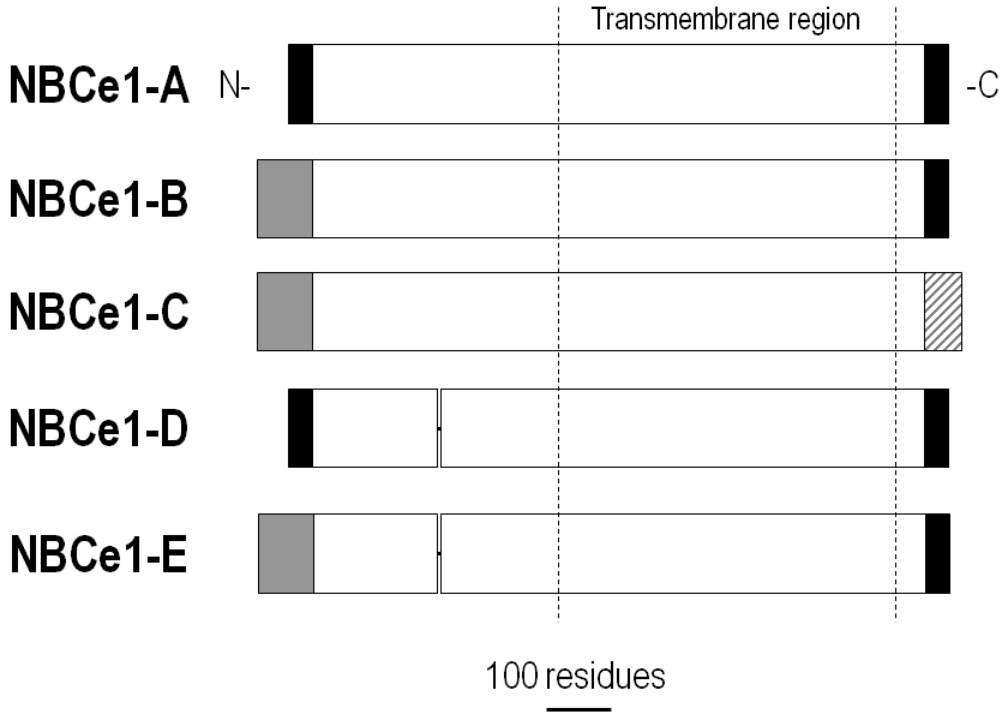

Figure 4. Amino acid sequence comparison of NBCe1 variants. NBCe1 variants are comprised of a variable N-terminus and C-terminus. In addition, NBCe1-D and -E are missing a 9 amino acid residue cassette. Modified with permission from Thornell *et al.* PIP_2 hydrolysis stimulates the electrogenic Na^+-bicarbonate cotransporter NBCe1-B and -C variants expressed in *Xenopus laevis* oocytes. *J Physiol* 2012, 590:5993-6011.

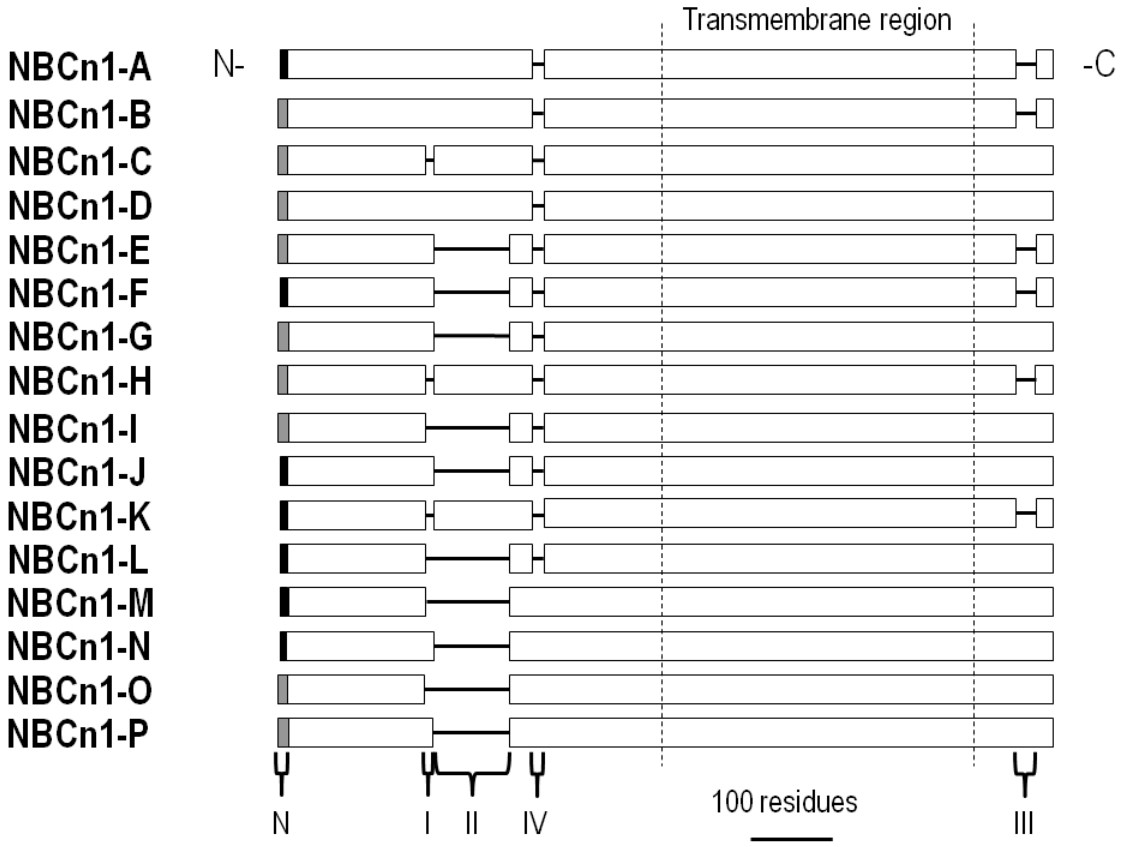

Figure 5. Amino acid sequence comparison of NBCn1 variants. NBCn1 variants are comprised of a variable N-termini (N). In addition, NBCn1 variants differ by the combinatorial inclusion of four different cassettes; cassette I, II, and IV in the N-terminus and cassette III in the C-terminus.

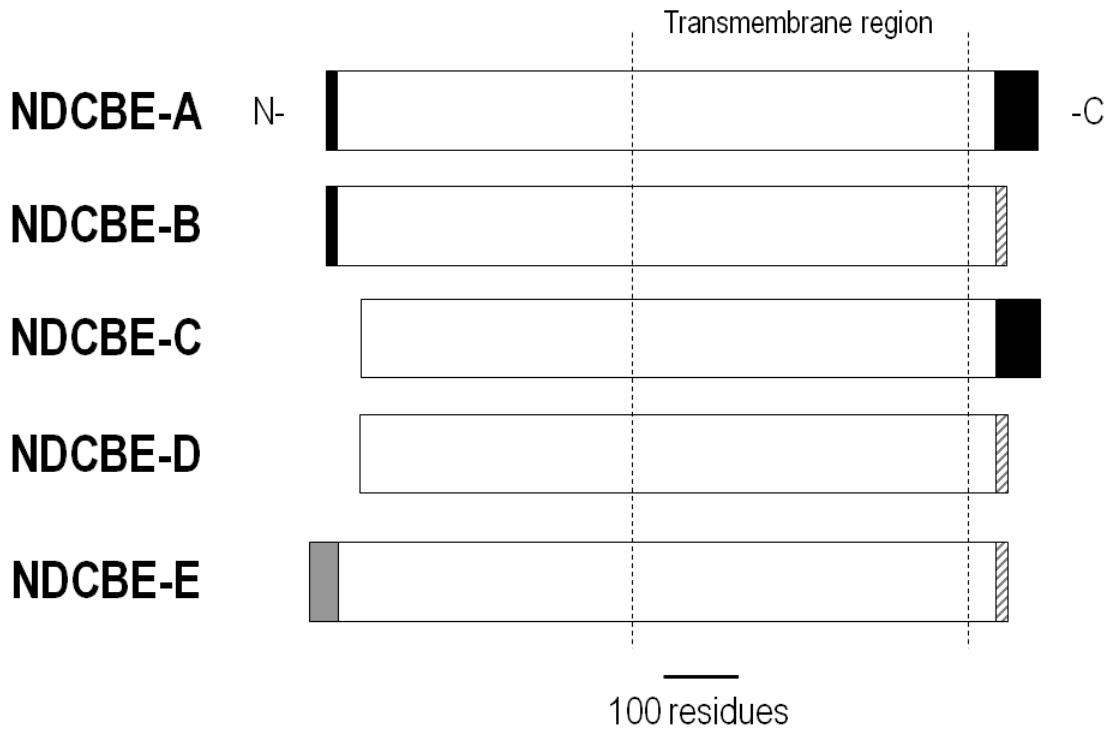

Figure 6. Amino acid sequence comparison of NDCBE variants. NDCBE-A and -B are comprised of a different N-terminus than NDCBE-E. NDCBE-C and -D are truncated at the N-terminus. All NDCBE variants are comprised of 1 of 2 alternate C-termini.

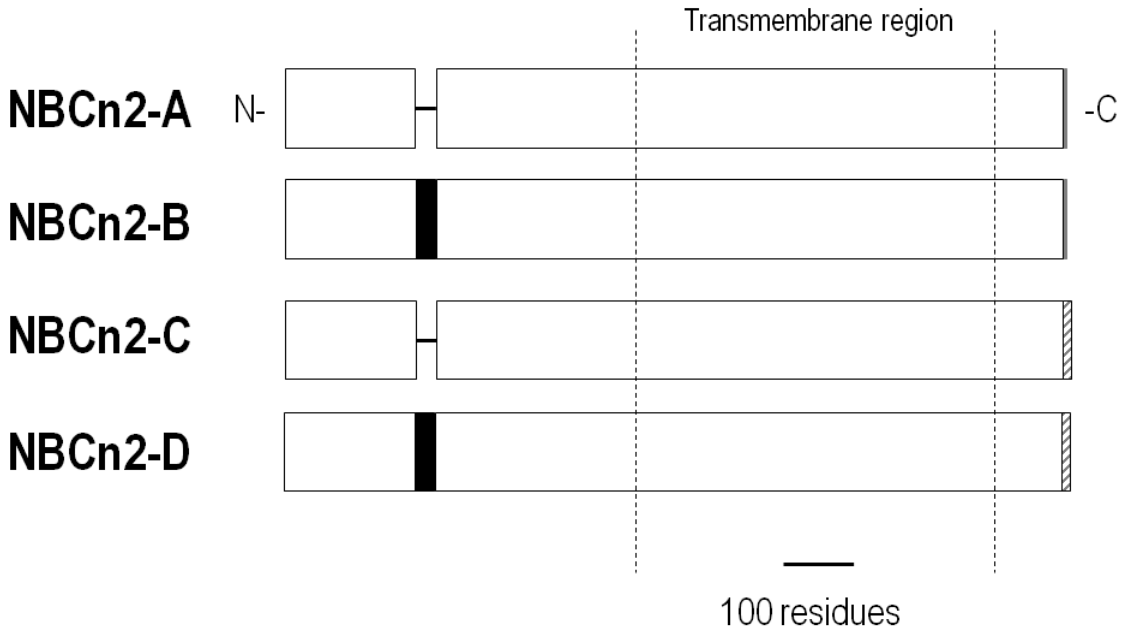

Figure 7. Amino acid sequence comparison of NBCn2 variants. NBCn2 variants are comprised of 1 of 2 different C-termini and either include or exclude a 30 amino acid cassette in the N-terminus.

PIP_2 HYDROLYSIS STIMULATES THE ELECTROGENIC Na/BICARBONATE COTRANSPORTER NBCe1-B AND -C VARIANTS EXPRESSED IN *XENOPUS LAEVIS* OOCYTES

by

IAN M. THORNELL, JIANPING WU, XIAOFEN LIU, AND MARK O. BEVENSEE

Journal of Physiology 590:5993-6011

Non-Technical Summary

The Na/bicarbonate cotransporter NBCe1 regulates cell and tissue pH, as well as ion movement across cell layers in organs such as kidney, gut, and pancreas. We previously showed that the signaling molecule PIP_2 stimulates the A variant of NBCe1 in a patch of biological membrane. In the current study, we characterize the effect of injecting PIP_2 into intact frog eggs expressing an NBCe1 variant (A, B, or C). PIP_2 stimulates the B and C variants, but not the A variant, through hydrolysis to IP_3. Stimulation requires an intracellular Ca^{2+} store and kinase activity. Results will contribute to our understanding of multiple HCO_3^--dependent transporters with different modes of regulation, as well as how molecules that stimulate specific membrane receptors lead to changes in cell/tissue pH, and perhaps how pathologies such as stroke and ischemia that lead to energy and ATP deficiency cause tissue acidosis.

Abstract

Electrogenic Na/bicarbonate cotransporter NBCe1 variants contribute to pH_i regulation, and promote ion reabsorption/secretion by many epithelia. Most Na-coupled bicarbonate transporter (NCBT) families such as NBCe1 contain variants with differences primarily at the cytosolic N and/or C termini that are likely to impart the transporters with different modes of regulation. For example, N-terminal regions of NBCe1 autoregulate activity. Our group previously reported that cytosolic phosphatidylinositol 4,5-bisphosphate (PIP_2) stimulates heterologously expressed rat NBCe1-A in inside-out macropatches excised from *Xenopus laevis* oocytes. In the current study on whole oocytes, we used the two-electrode voltage-clamp technique, as well as

pH- and voltage-sensitive microelectrodes, to characterize the effect of injecting PIP_2 on the activity of heterologously expressed NBCe1-A, -B, or -C. Injecting PIP_2 (10 μM estimated final) into voltage-clamped oocytes stimulated NBC-mediated, HCO_3^--induced outward currents by >100% for the B and C variants, but not for the A variant. The majority of this stimulation involved PIP_2 hydrolysis and endoplasmic reticulum (ER) Ca^{2+} release. Stimulation by PIP_2 injection was mimicked by injecting IP_3, but inhibited by either applying the phospholipase C (PLC) inhibitor U73112 or depleting ER Ca^{2+} with prolonged thapsigargin/EGTA treatment. Stimulating the activity of store-operated Ca^{2+} channels (SOCCs) to trigger a Ca^{2+} influx mimicked the PIP_2/IP_3 stimulation of the B and C variants. Activating the endogenous G_q protein-coupled receptor in oocytes with lysophosphatidic acid (LPA) also stimulated the B and C variants in a Ca^{2+}-dependent manner, although via an increase in surface expression for the B variant. In simultaneous voltage-clamp and pH_i studies on NBCe1-C-expressing oocytes, LPA increased the NBC-mediated pH_i-recovery rate from a CO_2-induced acid load by ~80%. Finally, the general kinase inhibitor staurosporine completely inhibited the IP_3-induced stimulation of NBCe1-C. In summary, injecting PIP_2 stimulates the activity of NBCe1-B and -C expressed in oocytes through an increase in IP_3/Ca^{2+} that involves a staurosporine-sensitive kinase. In conjunction with our previous macropatch findings, PIP_2 regulates NBCe1 through a dual pathway involving both a direct stimulatory effect of PIP_2 on at least NBCe1-A, as well as an indirect stimulatory effect of IP_3/Ca^{2+} on the B and C variants.

Abbreviations

AE, anion exchanger; BTR, bicarbonate transporter-related protein; DAG, diacylglycerol; GPCR, G-protein coupled receptor; HA, hemagglutinin; IRBIT, IP_3 receptor binding protein released with IP_3; I-V, current-voltage; LPA, lysophosphatidic acid; NBCe, electrogenic Na/bicarbonate cotransporter; NBCn, electroneutral Na/bicarbonate cotransporter; NCBT, Na-coupled bicarbonate transporter; NCBE, Na-driven Cl-bicarbonate exchanger; NDCBE, Na-driven Cl-bicarbonate exchanger; PIP_2, phosphatidylinositol 4,5-bisphosphate; PLC, phospholipase C; PKA, phosphokinase A; PKC, phosphokinase C; Pretx, pretreatment; SOC, single-oocyte chemiluminescence; SOCC, store-operated calcium channel; Tg, thapsigargin

Introduction

NCBTs are powerful regulators of pH_i, and also contribute to transepithelial Na^+ and HCO_3^- reabsorption and secretion in epithelia. NCBTs include the following paralogs in the *Slc4* gene family (Romero *et al.*, 2004): the electrogenic Na/HCO_3 cotransporters NBCe1 (*Slc4a4*) and NBCe2 (*Slc4a5*), the electroneutral Na/HCO_3 cotransporters NBCn1 (*Slc4a7*) and NBCn2/NCBE (*Slc4a10*), and the electroneutral Na-driven Cl-HCO_3 exchanger NDCBE (*Slc4a8*). Additional paralogs in the gene family include the anion exchangers AE1-4 (*Slc4a1-3,-9*), and the less characterized borate transporter BTR1 (*Slc4a11*).

The diversity of the *Slc4* gene family is further enriched by different variants of the aforementioned paralogs. Differences of each NCBT paralog are found at the cytoplasmic N- and/or C-termini. The one exception is NBCe2 with splice differences between predicted transmembrane domains 11 and 12. Regarding NBCe1, the A variant (NBCe1-A) contains 41 unique amino acids at the N terminus that arise from an alternate promoter in intron 3 of *Slc4a4* (Abuladze *et al.*, 2000). NBCe1-B is identical to NBCe1-A except for 85 N-terminal residues that replace the 41 N-terminal residues of the A variant (Fig. 1). In a similar fashion, NBCe1-C is identical to NBCe1-B except for 61 unique C-terminal residues (due to a 97 base-pair deletion near the 3′ open reading frame) that replace the 46 C-terminal residues of the B variant (Bevensee *et al.*, 2000). Recently, Liu *et al.* (2011) identified two additional NBCe1 splice variants that lack a 9-residue cassette in the cytoplasmic N terminus of either the A variant (NBCe1-D) or the B variant (NBCe1-E). In the current study, we focus on the A, B, and C variants with larger amino-acid differences at the N and/or C termini.

Although the physiological significance of multiple NBCe1 variants has yet to be fully elucidated, the modular splicing may impart the transporter with different modes of regulation under various conditions or stimuli. Indeed, N-terminal regions of NBCe1 regulate transporter activity themselves and through associations with other molecules. For example, the unique N terminus of the NBCe1-A contains an autostimulatory domain because its removal reduces transporter activity by ~50% (McAlear *et al.*, 2006). In contrast, the different N terminus of the -B and -C variants contains an autoinhibitory domain because its removal stimulates transporter activity by ~3 fold. Regarding interacting proteins, Shirakabe *et al.* (2006) found that the IP_3 receptor binding protein released with inositol triphosphate (IRBIT) binds to the N terminus and stimulates NBCe1-B, but not NBCe1-A. More recently, we found that IRBIT also stimulates the activity of NBCe1-C when co-expressed in *Xenopus* oocytes (Thornell *et al.*, 2010). NBCe1 variants can be modulated by traditional signaling molecules such as protein kinase A (PKA)/cAMP (Gross *et al.*, 2003;Gross *et al.*, 2001), protein kinase C (PKC) (Perry *et al.*, 2006), Ca^{2+} (Müller-Berger *et al.*, 2001), and ATP (Heyer *et al.*, 1999). One cAMP effect is variant specific as shown by Gross *et al.* (2003) who reported that a Thr at position 49 in the N terminus of human NBCe1-B (but not NBCe1-A) is required for a cAMP-stimulated increase in transporter activity. This increase however does not appear to involve a change in Thr's phosphorylation state.

We hypothesize that other regulatory pathways may differentially affect the activity of the NBCe1 variants. We recently discovered that the membrane phospholipid PIP_2 reduces the rate of rundown and stimulates activity of heterologously expressed rat NBCe1-A in excised macropatches from *Xenopus* oocytes (Wu *et al.*, 2009b). In the

current study, we used the 2-electrode voltage-clamp technique and pH/voltage-sensitive microelectrodes to characterize the effect of PIP_2 and its hydrolysis on the activity of all three rat NBCe1 variants heterologously expressed in intact oocytes. We find that injecting PIP_2 into oocytes stimulates the B and C variants —but not the A variant— through hydrolysis to IP_3. Stimulation by PIP_2 injection was eliminated by the PLC inhibitor U73122, and mimicked by either injecting IP_3 or activating the endogenous G_q-coupled receptor with LPA. PIP_2/IP_3 stimulation was mediated by an increase in $Ca^{2+}{}_i$ because the stimulation was eliminated by depleting ER Ca^{2+} stores, and mimicked by activating store-operated Ca^{2+} channels (SOCCs). The IP_3 stimulation involves a staurosporine-sensitive kinase.

Portions of this work have been published in preliminary form (Thornell *et al.*, 2010;Thornell & Bevensee, 2011;Wu *et al.*, 2009a).

Methods

Ethical Approval

The Institutional Animal Care and Use Committee (IACUC) at UAB reviewed and approved the protocol for harvesting oocytes from *Xenopus laevis* frogs.

Constructs and cRNA

cDNAs encoding NBCe1-A, -B, and -C, as well as $C_{\Delta N87}$, were previously subcloned into the oocyte expression vector pTLNII (McAlear *et al.*, 2006). $C_{\Delta N87}$ is an NBCe1-C construct with its N-terminal 87 residues deleted (McAlear *et al.*, 2006). All NBC constructs contained a nine residue hemagglutinin (HA) epitope (YPYDVPDYA) in

the exofacial loop between the fifth and sixth putative transmembrane domains that allowed us to analyze surface expression using single oocyte chemiluminescence (SOC) as described below. IRBIT constructs obtained from others were also HA tagged.

pTLNII plasmids were linearized with Mlu I, purified with the DNA Clean & Concentrator-5 Kit (Zymo Research, Irvine, CA), and then transcribed using the SP6 transcription kit (Ambion, Life Technologies, Grand Island, NY). cRNA was purified using the RNeasy Mini kit (Qiagen, Valencia, CA).

Oocytes

Oocytes were harvested from female *Xenopus laevis* frogs (Xenopus Express, Brooksville, FL) as previously described (McAlear *et al.*, 2006;McAlear & Bevensee, 2006). Segments of the ovarian lobe from anesthetized female frogs (with 0.2% tricaine) were extracted through an incision in the abdominal cavity, teased apart into ~0.5-cm^2 pieces, and then digested for 1-1.5 h in sterile Ca^{2+}-free ND96 containing 2 mg ml^{-1} collagenase A (Roche Applied Science, Indianapolis, IN). After the digested segments were washed in Ca^{2+}-free ND96 followed by Ca^{2+}-containing ND96, stage-V/VI oocytes were selected under a dissecting microscope (GZ6, Leica, Buffalo Grove, IL). Frogs were monitored during their recovery period after surgery; frogs were humanely euthanized after a final oocyte collection. Some stage V/VI oocytes were supplied from Ecocyte Bioscience (Austin, TX).

A Nanoject II microinjector (Drummond Scientific, Broomall, PA) was used to inject individual oocytes with 48 nl of either RNase-free H_2O (null control) or cRNA-

containing H_2O. Oocytes were incubated at 18°C in sterile ND96 supplemented with 10 mM Na/pyruvate and 10 mg ml^{-1} gentamycin.

2-electrode Voltage-clamp Experiments

Our technique for using the 2-electrode voltage-clamp technique to measure NBC currents has been previously described (McAlear *et al.*, 2006;Liu *et al.*, 2007). Briefly, voltage-sensitive and current-passing electrodes pulled from G83165T-4 borosilicate glass capillaries (Warner Instruments, Hamden, CT) were filled with saturated KCl and attached to the appropriate channels of an OC-725C voltage-clamp apparatus (Warner Instruments). For real-time current recordings, oocytes were voltage clamped at -60 mV and signals were filtered at 10–15 Hz with an 8-pole LFP-8 Bessel filter (Warner Instruments). The sampling frequency was 2 kHz; data were reduced by a factor of 100 using ClampFit (pClamp 8.2, Axon Instruments, Molecular Devices, San Jose, CA). For current-voltage (I-V) data, oocytes were voltage clamped at -60 mV between voltage-step protocols, and unfiltered amplifier signals (10 kHz) were sampled at 2 kHz. The voltage-step protocol consisted of 13 sweeps with a starting voltage of −60 mV for 12.5 ms, then a step to one of 13 voltages (-180 mV to 60 mV in increments of 20 mV) for 75 ms, and finally a return to −60 mV for 35 ms before the next sweep. ClampEx software (pClamp 8.2, Axon Instruments) controlled the acquisition, and a 1322A interface digitized the data (Axon Instruments). ClampFit software was used to analyze the data.

Experiments were performed at room temperature on oocytes at least 2 d after cRNA injection. Oocytes were placed in a continuous flow chamber connected to a custom-designed, gravity-fed, solution delivery system. Solutions delivered to the

chamber (500 μL volume) were controlled by a pair of 6-way rotary valves with outputs converging at a 2-position, 4-way Hamilton valve close to the chamber. This 2-position valve allowed us to alternate which 6-way rotary valve delivered solution to the perfusion chamber *vs*. waste (for priming purposes). The solution flow rate was 4-6 ml min^{-1}. In injection experiments, oocytes were also impaled at the vegetal-animal pole equator with a micropipettor attached to a Nanoject II microinjector to inject PIP_2, IP_3, or H_2O.

Simultaneous pH_i and Voltage-clamp Experiments

We measured pH_i using pH- and voltage-sensitive microelectrodes as previously described (McAlear *et al.*, 2006), but with a modified approach to voltage-clamp simultaneously. To make pH-sensitive microelectrodes, G200F-4 borosilicate glass capillaries (Warner Instruments) were first acid-washed and baked at 200°C. Capillaries were then pulled with a Brown-Flaming micropipette puller (P-80, Sutter Instruments, Novato, CA), and baked again before being silanized with *bis* (methylamino)-dimethylsilane (Fluka, Sigma-Aldrich, St. Louis, MO). Electrode tips were filled with hydrogen ionophore I-cocktail B (Fluka, Sigma-Aldrich), and the electrodes backfilled with a pH-7.0 solution containing 150 mM NaCl, 40 mM KH_2PO_4, and 23 mM NaOH. pH electrodes were then connected to one channel of an FD223 high-impedance electrometer (WPI, Sarasota, FL). The pH signal was obtained with a 4-channel electrometer (Biomedical Instrumentation Laboratory, Department of Cellular and Molecular Physiology, Yale University, New Haven, CT) that subtracted the 10× voltage output from the oocyte clamp (after split and relay through a 10× voltage divider) from the potential of the pH electrode. In voltage-clamp mode, the virtual ground clamps the

bath potential to 0 mV, so the voltage output (or V_m) equals the potential of the voltage electrode. Junction potentials were minimized with 3% agar/saturated KCl bridges (made of ~1-cm cut glass capillaries) between the virtual ground wires and bath solution. Digitized pH and voltage signals were acquired and plotted using custom-designed software written by Mr. Duncan Wong for the WF Boron laboratory (formerly in the Dept. of Cell. and Molec. Physiol., Yale Univ.). Before each experiment, the pH electrode was calibrated in the recording chamber with pH-6 and -8 buffer solutions (Fisher Scientific, Pittsburgh, PA).

Solutions

The standard ND96 solution (pH 7.5) contained (in mM): 96 NaCl, 2 KCl, 1 $MgCl_2$, 1.8 $CaCl_2$, 5 HEPES, and 2.5 NaOH. In the standard 5% CO_2/33 mM HCO_3^- solution, 33 mM NaCl was replaced with an equimolar amount of $NaHCO_3$, and the solution was equilibrated with 5% CO_2/95% O_2 to pH 7.5. In Ca^{2+}-free ND96 and 5% CO_2/33 mM HCO_3^- solutions, 1.8 mM $CaCl_2$ was replaced with 4 mM $MgCl_2$ + 1 mM EGTA. All chemicals and drugs were obtained from Sigma-Aldrich unless otherwise noted. All lipids were obtained from Avanti Polar Lipids (Pelham, AL).

Single-oocyte Chemiluminescence

Our technique for measuring surface expression of NBCe1 variants by SOC has been previously described (McAlear *et al.*, 2006;McAlear & Bevensee, 2006). Oocytes were fixed with 4% paraformaldehyde and incubated overnight in a 1% BSA-ND96 blocking solution, and then incubated for 1 h in a blocking solution containing a 1:100

dilution of the rat monoclonal α-hemagglutinin (HA) antibody (Roche), and then one containing a 1:400 dilution of the secondary antibody, goat α-rat IgG-HRP (Jackson ImmunoResearch Laboratories, Westgrove, PA). The aforementioned incubations were performed with sterile solutions at 4°C. Individual oocytes were incubated in 50 µl SuperSignal Elisa Femto substrate (Pierce, ThermoScientific, Rockford, IL) for ~1 min in an eppendorf tube before luminescence was measured with a TD-20/20 luminometer (Turner Designs, Sunnyvale, CA) for 15 s.

Immunoblotting of Oocyte Protein

Total protein was isolated by first homogenizing oocytes with a pestle in 20 µl/oocyte of a homogenization buffer (100 mM NaCl, 1% Triton X-100, 20 mM Tris-HCl, and 10 mM methionine) containing a Complete Protease Inhibitor Cocktail tablet (Roche). The homogenate was centrifuged at 13,400×*g* for 10 min at 4°C to separate the protein-containing intermediate layer from the lipid top layer and the cell-debris pellet. The protein suspension was stored at -80°C until use.

Proteins separated by gradient SDS-PAGE (4-12%) were transferred to a PVDF membrane using a Trans-Blot® SD semi-dry blotting apparatus (Bio-Rad Laboratories, Hercules, CA). The membrane was incubated for ~45 min at room temperature (RT) in TBS + 1% dry-milk powder. The membrane was subsequently incubated at RT for 1 h in TBS+1% BSA containing first the α-HA antibody (Roche), and then the secondary antibody goat α -rat-IgG:HRP (Jackson). Bound HRP was detected by chemiluminescence.

Statistics

Data are reported as means ± SEM. Means between groups of data were compared using one-factor analysis of variance (ANOVA), as well as paired or unpaired forms of the Student's *t* test (Microsoft® Excel 2002). $p < 0.05$ is considered significant. Rates of pH_i recoveries were determined by linear fits to pH_i *vs*. time using a least-squares method with custom-designed software written by Mr. Duncan Wong (Dept. of Molec. and Cell. Physiol., Yale Univ.) for the WF Boron laboratory.

Results

Injection of PIP_2

Using the 2-electrode voltage-clamp technique on whole oocytes, each expressing one of the three NBCe1 variants, we examined the effect of injecting PIP_2 on NBC-mediated, HCO_3^--induced outward currents. In an NBCe1-C-expressing oocyte clamped at -60 mV (Fig. 2A), briefly switching from the nominally CO_2/HCO_3^--free ND96 solution (pH 7.5) to one containing 5% CO_2/33 mM HCO_3^- (pH 7.5) elicited abrupt outward currents (Fig. 2A; *a*,*b*) due to the cotransport of Na^+, HCO_3^-, and net-negative charge into the oocyte. Injecting ~50 nl of a 100 μM PIP_2 stock solution, which increases intracellular PIP_2 by an estimated 10 μM[1], elicited an inward "sag" current (after arrow), which has previously been observed in oocytes injected with IP_3 (Oron *et al.*, 1985). The IP_3-mediated "sag" current arises from activation of Ca^{2+}-activated Cl^- channels (Yoshida & Plant, 1992) and can have two components: *i*) a fast inward current due to ER Ca^{2+} release, and *ii*) a slow inward current due to Ca^{2+} influx through SOCC activity. The

[1] This estimate is based on an average oocyte volume of 1 μL, and an aqueous compartment comprising 40% of the total volume (Zeuthen *et al.*, 2002).

magnitudes and time courses of these currents vary depending on factors including the depth and location of injection (Gillo *et al.*, 1987; Lupu-Meiri *et al.*, 1988). At 5 and 10 min after the PIP_2 injection, we assayed for NBC activity again by switching to the HCO_3^- solution, which elicited outward currents that were ~2-fold larger (Fig. 2A; *c*,*d*). In most experiments, the injected PIP_2[2]-stimulated, HCO_3^--induced outward current did not increase appreciably at 10 min. HCO_3^--induced currents were inhibited ~80% by 200 μM of the HCO_3^--transport inhibitor DIDS (Fig. 2A; *e*), similar to that previously reported for NBCe1-A without PIP_2 injection (Liu *et al.*, 2007). In four similar experiments, DIDS inhibited the injected PIP_2-stimulated, HCO_3^--induced outward current by 82 ± 1%. The slight outward current elicited by applying DIDS in ND96 may be due to inhibition of either an anionic conductance or NBC activity due to residual intracellular HCO_3^-.

Using the same protocol as described for Fig. 2A, we performed two types of control experiments. In one set of control experiments, injecting H_2O instead of PIP_2 failed to stimulate NBCe1-C (Fig. 2B). Therefore, the injection procedure and associated cell swelling did not alter the NBC current in our assay. In the other set of control experiments, injecting PIP_2 into a H_2O-injected null oocyte (Fig. 2C) had little effect on the small endogenous HCO_3^--induced currents in our assay (n=4).

Fig. 2A-type experiments were also performed on oocytes expressing NBCe1-A and -B, and the summary data are shown in Fig. 2D. PIP_2 injection failed to stimulate the A variant (bar 1), but stimulated the B variant by ~130% (bar 2) and the C variant by ~110% (bar 3). As described below, the A variant is more active than the B and C

[2] We use the term "injected PIP_2" rather than "PIP_2" because −as described in more detail below−injected PIP_2 stimulation is primarily indirect and operates through the IP_3/Ca^{2+} pathway.

variants expressed in oocytes. However, injected PIP_2 also failed to stimulate the A variant when we performed these experiments at a holding potential (-120 mV) where the A variant is less active (because of the reduced driving force favoring influx), but resembles the lower activity of the B and C variants (not shown). As described for Fig. 2B, injecting H_2O instead of PIP_2 failed to stimulate NBCe1-C activity (bar 4). We reasoned that the selective stimulation by PIP_2 injection of the B and C variants, but not the A variant is due to their common N terminus that differs in the A variant (Fig. 1). Indeed, as summarized by bar 5 in Fig. 2D, we found that injecting PIP_2 did not significantly stimulate an NBCe1-C construct with its N-terminal 87 residues deleted ($C_{\Delta N87}$)– a construct that our group has previously characterized (McAlear *et al.*, 2006). Similar results were obtained with the corresponding N terminal truncation of the B variant (data not shown). Therefore, stimulation by PIP_2 injection of the B and C variants requires their distinguishing N terminus.

In the absence of PIP_2 injection, the HCO_3^--induced outward currents are approximately 3-4 fold larger from the A vs B and C variants, and ~3-fold larger for mutant $C_{\Delta N87}$ vs wild-type C (McAlear *et al.*, 2006). According to Fig. 2D, PIP_2 injection had little effect on the relatively large A-variant current, but approximately doubled the size of the B/C-variant currents. Thus, PIP_2 injection increased the B/C-variant currents to resemble those of $C_{\Delta N87}$ and the A variant more closely.

We next examined the effect of injecting PIP_2 on the voltage dependence of the three NBCe1 variants, as well as $C_{\Delta N87}$ (Fig. 3 and Supplemental Fig. 1). HCO_3^--dependent I-V plots were generated by subtracting plots obtained from oocytes bathed in ND96 from those bathed in the CO_2/HCO_3^- solution for 5 min (to allow for intracellular

CO_2 to equilibrate). As expected, the injected PIP_2-stimulated, HCO_3^--dependent I-V plots in these experiments were largely inhibited by 200 μM DIDS (McAlear *et al.*, 2006) as determined by after switching back to ND96 briefly, applying DIDS, and then switching to the HCO_3^- solution for ~40s. For NBCe1-A-expressing oocytes, the HCO_3^--dependent I-V plot was nearly linear and displayed slight outward rectification (Fig. 3A) as previously reported (Sciortino & Romero, 1999;McAlear *et al.*, 2006). The I-V plot was minimally affected by injecting PIP_2, consistent with the summary data presented in Fig. 2D.

For both the C variant (Fig. 3B) and the B variant (Supplemental Fig. 1A), the near-linear shape of the HCO_3^--dependent I-V plots was similar to that of A, although the current magnitudes were less as previously reported (McAlear *et al.*, 2006). In contrast to that seen with the A variant, PIP_2 injection stimulated the HCO_3^--dependent outward currents of the B and C variants at V_m more positive than ~-100 mV. For the C-variant data, the mean I-V plots before and after $CO_2/HCO_3^- \pm PIP_2$ are shown in Supplemental Fig. 1B and Fig. 1C. The apparent sigmoidal nature of the injected PIP_2-stimulated I-V profiles at positive potentials is mostly likely due to time-dependent changes in the HCO_3^--independent current after PIP_2 injection rather than a PIP_2-induced shift in the voltage dependence of the NBC.[3] Consistent with lost stimulation by PIP_2 injection of

[3]We determined the effect of injected PIP_2 on the NBC (HCO_3^--dependent) I-V relationship by subtracting the I-V plot in ND96 (5 min after injection) from that obtained from oocytes bathed in CO_2/HCO_3^- for 5 min (i.e., 10 min after injection). The assumption is that the HCO_3^--independent I-V plot will not change during those 5 min extra minutes to allow for CO_2/HCO_3^- to equilibrate– an assumption that is historically reasonable. However, in separate experiments, we found that the ND96 currents were smaller, but variable at 10 vs. 5 min after PIP_2 injection. The difference was particularly pronounced at the more positive potentials (Supplemental Fig. 1D). In principle, a correction factor from these separate experiments could be determined and used to scale the ND96 I-V plots in the other experiments designed to estimate PIP_2's effect on the NBC I-V relationship. However, there are limitations to the reliability of such a correction primarily because the mean correction factor is obtained from unpaired experiments with considerable variability. The mean correction factor may not match the true correction factor for a given NBC I-V plot experiment. Nevertheless, in using this correction-factor approach, we estimated a more linear NBC I-V relationship than shown in Fig. 3 at the more positive potentials.

$C_{\Delta N87}$ shown in Fig. 2D, injecting PIP_2 failed to alter the HCO_3^--dependent I-V plot of $C_{\Delta N87}$ (Fig. 3C). H_2O-injected null oocytes did not exhibit HCO_3^--dependent currents before or after PIP_2 injection (Fig. 3D). In summary, injecting PIP_2 stimulates the B and C variants (but not the A variant) in a broad range of membrane potentials.

Role of IP_3, PLC Activity, and IRBIT

To determine the mechanism by which injecting PIP_2 stimulates NBCe1-B and -C, we tested the hypothesis that PIP_2 injected into oocytes is hydrolyzed by constitutively active PLC to the signaling molecules IP_3 and diacylglycerol (DAG). Prior to the experimental trace shown in Fig. 4A, an NBCe1-C-expressing oocyte was preincubated for 40 min in ND96 containing 10 μM of the membrane permeant PLC inhibitor U73122. Subsequently, the oocyte was voltage-clamped at -60 mV and NBC activity was assayed as described for Fig. 2A. The NBC-mediated, HCO_3^--induced outward currents at the beginning of the experiment were only slightly larger after injecting PIP_2. Similar experiments were performed on the A and B variants, and the data are summarized in Fig. 4B. For each variant, we determined the percent stimulation by PIP_2 injected into oocytes preincubated in either the inactive analog U73343 (solid bars) or the active U73122 (open bars). The inactive analog did not appreciably alter the mean percent stimulation by injected PIP_2 (Fig. 4B *vs*. Fig. 2D). In contrast, the PLC inhibitor U73122 reduced the injected PIP_2-induced percent stimulation by ~80% for the B and C variants. For the A variant, U73122 moderately increased the stimulation to ~30%. In the absence of PLC inhibition, PIP_2 injection did not stimulate the A variant presumably because the PIP_2 was rapidly hydrolyzed. In summary, PIP_2 in the absence of hydrolysis (i.e., with

U73122 pretreatment) significantly stimulated all three variants 20-30%— a finding that may reflect a direct stimulatory effect of PIP_2. As a control, H_2O injection did not stimulate the variants (hatched bars). In summary, stimulation of the B and C variants by PIP_2 injection requires PLC-mediated hydrolysis of PIP_2.

As described in Supplemental Fig. 2, U73122 pretreatment influences NBC surface expression and function independent of stimulation by PIP_2 injection. Specifically, U73122 pretreatment decreased the surface expression of the three variants by 30-60% based on SOC analysis (Supplemental Fig. 2A). Thus, constitutive PLC activity contributed to plasma-membrane expression of NBCe1. Regarding function, U73122 did not significantly alter the NBCe1-B/C current normalized to surface expression, but dramatically lowered the normalized NBCe1-A current by 80% (Supplemental Fig. 2B). Constitutive PLC activity is therefore required for the large A-variant currents.

The aforementioned U73122 data are consistent with PIP_2 hydrolysis to IP_3 and DAG being responsible for stimulation of the B and C variants. If IP_3 is responsible, then injecting IP_3 should mimic the stimulatory effect of injecting PIP_2. Using the experimental approached described for Fig. 2A, we found that injecting ~50 nl of a 100 μM IP_3 stock solution (which raised intracellular [IP_3] by an estimated 10 μM[1]) stimulated the HCO_3^--induced current in an NBCe1-C-expressing oocyte by ~150% (Fig. 5A). The maximal IP_3-stimulated, HCO_3^--induced current was evident 5-15 min after injection. The IP_3 stimulation required extracellular Na^+ (data not shown) as expected for increased NBC activity. We performed similar experiments on the A and B variants, as well as $C_{\Delta N87}$, and present the summary data in Fig. 5B. The IP_3 stimulatory profile for

the NBCs is identical to that for injected PIP_2 presented in Fig. 2D. More specifically, the IP_3 injection did not stimulate the A variant (bar 1), but stimulated the B variant by 190% (bar 2) and the C variant by ~170% (bar 3). Finally, full IP_3 stimulation of the C variant requires the N terminus because the percent stimulation of $C_{\Delta N87}$ was only ~50% (bar 4) compared to ~170% for wild-type.

We also performed Fig. 5A-type experiments and injected IP_3 stock concentrations of 10 μM and 1 μM that are predicted to raise intracellular concentrations to more physiological levels of 1 μM and 100 nM, respectively. These experiments were performed in 0 $Ca^{2+}{}_o$, which does not affect NBC-mediated HCO_3^--induced currents (Supplemental Fig. 3A). As summarized in Fig. 5C, all three IP_3 concentrations stimulated NBCe1-C to the same extent. Thus, injecting an amount of IP_3 that raises the intracellular concentration by only 100 nM mimics the effect of injecting PIP_2. Also, the stimulation was similar to that seen for oocytes bathed in the presence of external Ca^{2+} (Fig. 5B). Thus, the IP_3 stimulation did not require an influx of $Ca^{2+}{}_o$, for example, through SOCCs. In control experiments, injecting IP_3 did not stimulate the small HCO_3^--induced currents in H_2O-injected null oocytes bathed either in the presence of Ca^{2+} (Supplemental Fig. 3B) or its absence (Supplemental Fig. 3C).

The NBCe1 variant-specific IP_3-induced stimulation parallels the findings of Shirakabe *et al.* (2006) who found that co-expressing the IP_3 receptor binding protein IRBIT stimulates the B variant (but not A variant) in oocytes by binding to the N terminus. In similar experiments, IRBIT also stimulates NBCe1-C (Thornell *et al.*, 2010;Yang *et al.*, 2011). We considered the possibility that IP_3 injection in our experiments stimulates B/C by displacing endogenous IRBIT from its receptor. However,

this possibility appears unlikely due to low expression levels of endogenous *vs*. exogenously expressed IRBIT in oocytes (Shirakabe *et al.*, 2006). Using a more rigorous approach, we examined oocytes co-expressing NBCe1-C and the S68A mutant of IRBIT (Ando *et al.*, 2006), which has previously been shown not to stimulate NBCe1-B activity (Shirakabe *et al.*, 2006). This mutant only weakly binds to the IP_3 receptor because of the lost phosphorylation site. Furthermore, this mutant exerts a dominant-negative effect by multimerizing with wild-type IRBIT through interaction of the C-terminal tails independent of the aforementioned phosphorylation sites (Ando *et al.*, 2006).

In the co-injected oocyte shown in Fig. 6A, the IP_3-stimulated HCO_3^--induced outward currents were similar to those seen in Fig. 5A without mutant IRBIT. We used immunoblot analysis to confirm NBCe1-C and S68A IRBIT co-expression in batch-matched oocytes. According to the summary data, the mean IP_3-stimulated, HCO_3^--induced current was unaffected by co-expressing S68A IRBIT (Fig. 6B). Thus, IP_3 stimulation of NBCe1-C does not involve IRBIT. As presented in Supplemental Fig. 4, similar results were obtained with an S71A mutant of IRBIT, which also only weakly binds to the IP_3 receptor because of the lost phosphorylation site (Ando *et al.*, 2006), and likely also exerts a dominant-negative effect.

Role of Ca^{2+} and Kinases

Because stimulation by PIP_2 injection of NBCe1 is blocked by a PLC inhibitor, and mimicked by IP_3 without a requirement for Ca^{2+}_o, we hypothesized that IP_3-mediated Ca^{2+} release from intracellular stores is necessary. If so, then ER Ca^{2+} depletion should block the PIP_2/IP_3 stimulation. To test this hypothesis, we depleted ER Ca^{2+} using a

previously described protocol (Petersen & Berridge, 1994) in which oocytes were pretreated for 3-6 h in a modified Ca^{2+}-free ND96 solution containing 1 mM EGTA and 10 μM of the sarco/endoplasmic reticulum Ca^{2+}-ATPase (SERCA) inhibitor thapsigargin. The thapsigargin/0 Ca^{2+}-EGTA pretreatment did not affect surface expression of the NBCe1 variants (data not shown). Subsequently, oocytes were voltage-clamped at -60 mV and NBC activity assayed as described for Fig. 2A (i.e., in the presence of external Ca^{2+}). After an NBCe1-C-expressing oocyte was pretreated with thapsigargin/0 Ca^{2+}-EGTA, PIP_2 injection actually inhibited rather than stimulated the HCO_3^--induced outward current (Fig. 7A). Similar experiments were performed on all three NBCe1 variants and $C_{\Delta N87}$, and the summary data are shown in Fig. 7B. The injected PIP_2-induced percent stimulation of the B and C variants under control conditions with DMSO pre-incubation (solid bars) was eliminated by the thapsigargin/0 Ca^{2+}-EGTA pretreatment (open bars). The stimulation by PIP_2 injection remained absent for the pretreated A variant and $C_{\Delta N87}$ mutant.

As shown in Fig. 7C, we replicated the experimental protocol on the C variant described in Fig. 7A, but injected IP_3 instead of PIP_2. The thapsigargin/0 Ca^{2+}-EGTA pretreatment inhibited IP_3-stimulated NBC activity, similar to that seen for injected PIP_2. According to the summary data of the tested variants, the % stimulation profiles were similar for injected PIP_2 (Fig. 7B) and IP_3 (Fig. 7D). Note that the small IP_3-induced percent stimulation with $C_{\Delta N87}$ (also seen in Fig. 5B) was also inhibited by Ca^{2+}-store depletion. In summary, both injected PIP_2 and IP_3 stimulation of NBCe1-B/C require ER Ca^{2+} release.

We next tested the possibility that a rise in Ca^{2+}_i independent of intracellular stores can stimulate the B and C variants. We took advantage of our thapsigargin/0 Ca^{2+}-EGTA protocol that depletes ER Ca^{2+} stores, and in turn primes the activity of SOCCs in an attempt to replenish those stores. Thereafter, re-exposing an oocyte to Ca^{2+}_o triggers Ca^{2+} influx through the activated SOCCs (Petersen & Berridge, 1994). In the experiment shown in Fig. 8A, we pretreated the NBCe1-C-expressing oocyte in thapsigargin/0 Ca^{2+}-EGTA for 4-6 h, and then began the voltage-clamp experiment (-60 mV) with the oocyte still bathed in 0 Ca^{2+}-EGTA. The SERCA was still inhibited during the experiment because thapsigargin is irreversible. Note that the two NBC-mediated HCO_3^--induced outward currents in the continued absence of external Ca^{2+} were small. Returning external Ca^{2+} elicited a rapid, but transient inward current due to the influx of Ca^{2+} through the SOCCs stimulating Ca^{2+}-activated Cl^- channels. After returning the Ca^{2+}_o, the NBC-mediated, HCO_3^--induced outward currents were ~3-fold larger than at the beginning of the experiment. Furthermore, the magnitude of those currents decreased ~50% shortly after returning the oocyte to the 0 Ca^{2+}/EGTA solution— a result consistent with decreasing Ca^{2+}_i inhibiting NBCe1-C again. Similar experiments were performed on all three NBCe1 variants and $C_{\Delta N87}$, and the summary data are shown in Fig. 8B. The percent stimulation profile for the NBCs elicited by Ca^{2+} influx through activated SOCCs is nearly identical to that for IP_3 (Fig. 5B).

Using SOC analysis, we examined the possibility that Ca^{2+} stimulated the NBC current by increasing surface expression of the transporter. According to the summary data presented in Fig. 8C, returning Ca^{2+}_o in our SOCC-activation protocol had little effect on the A variant, and modestly decreased the surface expression of the B, C, and

$C_{\Delta N87}$ variants by 15-20% (open bars) compared to control conditions (closed bars) in the continued absence of $Ca^{2+}{}_o$. Therefore, the percent stimulation values for B, C, and $C_{\Delta N87}$ reported in Fig. 8B are actually underestimates because they are uncorrected for the modest decreases in surface expression. In summary, the Ca^{2+}-stimulatory effect is not due to an increase in NBC surface expression.

Using the non-specific kinase inhibitor staurosporine, we tested if the IP_3/Ca^{2+} stimulation of NBC activity involves kinase activity. Prior to the experimental trace shown in Fig. 9A, an NBCe1-C-expressing oocyte was preincubated for 4 h in ND96 containing 20 μM staurosporine. The oocyte was then voltage-clamped at -60 mV, and NBC activity assayed as described for Fig. 2A. The NBC-mediated, HCO_3^--induced outward current at the beginning of the experiment was only slightly larger after injecting IP_3. According to the summary data (Fig. 9B), pretreating with staurosporine eliminated the IP_3-induced percent stimulation (open bar) compared to pretreating with the vehicle DMSO (solid bar). Thus, the IP_3/Ca^{2+} stimulation of NBCe1-B/C requires activity of one or more kinases.

Endogenous Activation of a G-protein Coupled Receptor (GPCR)

According to our injection experiments, PIP_2 stimulates NBCe1-B and NBCe1-C through PLC-mediated hydrolysis to IP_3 and subsequent release of ER Ca^{2+}. We next used a less-invasive approach to hydrolyze PIP_2 to IP_3 by applying LPA to activate the endogenous GPCR in the oocyte (Durieux *et al.*, 1992).

For the experiment on an NBCe1-C-expressing oocyte shown in Fig. 10A, we used the same experimental protocol as described above (e.g., Fig. 2A), except that

solutions were Ca^{2+}-free and contained EGTA. At the beginning of the experiment, NBC-mediated, HCO_3^--induced outward currents were ~200 nA. Subsequently applying 1 μM LPA for ~15 s elicited the sag current consistent with IP_3-mediated Ca^{2+} release and Ca^{2+}-activated Cl^- channel activity. This transient LPA exposure stimulated the HCO_3^--induced outward currents by ~150%, similar to that observed with PIP_2 injection (Fig. 2A). Applying LPA to a control (null) oocyte did not elicit appreciable HCO_3^--induced currents (Supplemental Fig. 5A).

If the LPA-induced NBC stimulation involves IP_3-mediated ER Ca^{2+} release, then chelating Ca^{2+}_i with BAPTA should inhibit the stimulation. Pre-incubating NBC-expressing oocytes for ~5 h in ND96 containing 10 μM BAPTA-AM had no effect on the surface expression of the variants (Supplemental Fig. 5B), but caused a modest decrease (~35%) in the HCO_3^--induced currents for the B and C variants (Fig. 10B). This decrease may reflect sensitivity of the B and C variants to baseline Ca^{2+}_i.

BAPTA pretreatment had a large inhibitory effect on the LPA-induced stimulation of NBCe1-C. As shown in Fig. 10C, pretreating with BAPTA dramatically reduced the LPA-induced stimulation of the HCO_3^--induced current compared to Fig. 10A. Note that BAPTA pretreatment also eliminated the LPA-induced inward sag current attributed to Ca^{2+}-activated Cl^- channel activity. Similar Fig. 10A and 10C experiments were performed on all three NBCe1 variants and $C_{\Delta N87}$, and the summary data are shown in Fig. 10D. LPA increased the HCO_3^--induced currents of the B and C variants, but not the A variant (p=0.30) or $C_{\Delta N87}$ (p=0.10) (solid bars). BAPTA pretreatment reduced the LPA-stimulated currents from 90% to ~20% for the B variant, and ~140% to 30% for the C variant (open bars).

We examined the effect of LPA on NBC surface expression. As summarized in Supplemental Fig. 5C, transient LPA application increased surface expression (after 5 min) of NBCe1-B, but not the other variants, with or without pretreatment with BAPTA. The LPA-induced increase in surface expression of the B variant accounts for the majority of the stimulated current. In summary, transient LPA application increases the NBCe1-B current predominantly by increasing NBC surface expression through a Ca^{2+}-independent mechanism. In contrast, LPA increases the NBCe1-C current by stimulating transporter activity through a Ca^{2+}-dependent mechanism.

We have examined the effect of LPA not only on the electrogenicity of NBCe1, but also on HCO_3^- transport and associated mediated changes in pH_i. In the oocyte experiments presented in Fig. 11, we simultaneously measured pH_i using ion-sensitive microelectrodes (upper panels) and currents with the voltage-clamp technique (lower panels). For a voltage-clamped NBCe1-C-expressing oocyte (Fig. 11A), switching from ND96 to the CO_2/HCO_3^- solution elicited an initial pH_i decrease due to the influx of CO_2 and subsequent hydration to HCO_3^- and H^+ (*ab*). The HCO_3^- solution elicited the expected NBC-mediated outward current (*a′b′*). After the initial decrease, pH_i slowly increased (*bc*) due to NBC-mediated HCO_3^- entry, and the continual outward current slowly diminished (*b′c′*). Applying 1 μM LPA increased the rate of the pH_i recovery (*cd*) consistent with stimulation of NBC-mediated HCO_3^- transport. LPA generated a large, transient inward current —presumably due to IP_3/Ca^{2+}-stimulated Cl^- channels— followed by a larger outward current (*c′d′*). The LPA-stimulated pH_i recovery rate and larger outward current were both consistent with increased NBC activity because removing external Na^+ (*i*) blocked the pH_i recovery and caused the pH_i to decrease (*de*),

and (*ii*) reversed the outward current to an inward current (*d′e′*). Returning external Na^+ reinstated the pH_i recovery (*ef*) and outward current (*e′f′*). Finally, switching back to ND96 caused pH_i to increase and overshoot the initial pH_i (*fg*); the current also returned close to baseline (*f′g′*).

A similar experiment was performed on a null control H_2O-injected oocyte (Fig. 11B). As shown in the upper panel, the CO_2/HCO_3^- solution elicited the CO_2-induced pH_i decrease (*ab*), but no subsequent pH_i recovery (*bc*). The experimental maneuvers of applying LPA (*cd*), as well as removing and returning external Na^+ (*def*) had little effect on pH_i. All the aforementioned maneuvers did not elicit appreciable changes in current (lower panel).

From experiments similar to those presented in Fig. 11A and B, we calculated the mean dpH_i/dt during the initial segment-*bc* pH_i recovery (left pair of bars, Fig. 11C) for NBCe1-C-expressing oocytes (closed bars) and control oocytes (open bars). As expected, NBC-expressing oocytes displayed a HCO_3^--induced pH_i recovery rate greater than that seen in control oocytes. We also computed the mean LPA-stimulated dpH_i/dt (right pair of bars) for NBCe1-C-expressing oocytes (closed bars) and control oocytes (open bars) at the 5-min time point after applying LPA (to match LPA-stimulated NBC current measurements in the previous voltage-clamp experiments). The pH_i recovery rate was markedly greater in NBCe1-C-expressing oocytes exposed to LPA. Using the dpH_i/dt data from NBCe1-C-expressing oocytes in panel C, we subtracted the corresponding mean dpH_i/dt values from water-injected oocytes to calculate that LPA stimulated the NBCe1-C-mediated dpH_i/dt by ~80% (Fig. 11D). To analyze the current data, we determined the LPA-stimulated current at the 5 min time point relative to the current

immediately before applying LPA (point *c'*) after subtracting the corresponding currents from water-injected oocytes. LPA stimulated the NBCe1-C-mediated current by ~40%.

Discussion

Stimulation by PIP_2 Injection of the B and C Variants, But Not the A Variant of NBCe1

Our main conclusion is that PIP_2 injection stimulates the B and C variants —but not the A variant— expressed in oocytes through the classic IP_3/Ca^{2+} pathway that involves at least one staurosporine-sensitive protein kinase. There are six observations that support this conclusion. First, the PLC inhibitor U73122 eliminates the stimulation by PIP_2 injection (Fig. 4). Second, injecting IP_3 mimics the stimulation by PIP_2 injection (Fig. 5). Third, depleting ER Ca^{2+} eliminates both the injected PIP_2 and IP_3-induced stimulation (Fig. 7). Fourth, raising $Ca^{2+}{}_i$ by activating SOCCs mimics the PIP_2/IP_3 stimulation, and to a greater extent (Fig. 8). Fifth, applying LPA to activate the endogenous GPCR in oocytes resembles PIP_2/IP_3 in stimulating the C variant in a Ca^{2+}-dependent manner (Fig. 10), and also increases the pH_i recovery rate from a CO_2-induced acid load (Fig. 11). Sixth, pretreating with staurosporine eliminates the IP_3 stimulation (Fig. 9).

The aforementioned observations are consistent with injected PIP_2 being hydrolyzed to intracellular IP_3 by basal PLC activity in oocytes. In addition, the following two NBC-independent observations provide further evidence for such hydrolysis. First, injecting PIP_2 (Fig. 2A), but not water (Fig. 2B), triggered a prolonged IP_3-mediated, Ca^{2+}-activated Cl^- current (sag current) similar to that previously reported

in oocytes (Oron *et al.*, 1985;Yoshida & Plant, 1992). Second, the PLC inhibitor U73122 greatly inhibited this sag current (Fig. 4A).

The mechanism by which IP_3-mediated Ca^{2+} release stimulates the B and C variants is not entirely clear. Regarding Ca^{2+}, Müller-Berger *et al.* (2001) in a related study used the inside-out macropatch technique to characterize the activity of rat-kidney NBCe1-A expressed in oocytes. They reported that raising bath (cytosolic) Ca^{2+} from 100 nM to 500 nM stimulated the NBC current in most patches by increasing the Na^+:HCO_3^- stoichiometry from 1:2 to 1:3. Although PIP_2/IP_3/Ca^{2+} did not stimulate NBCe1-A in our study, injecting PIP_2 did elicit an apparent rightward shift of the HCO_3^--dependent reversal potential (E_{rev}) for oocytes expressing the B and C variants (e.g., Fig. 3). However, the observed E_{rev} shifts appear too small to result from an increase in transporter stoichiometry. There are other possible explanations, including a smaller HCO_3^- transmembrane gradient generated by a stimulated NBC that raises the HCO_3^- concentration on the inner surface of the membrane. Further studies are required to assess any IP_3/Ca^{2+}-mediated change in transporter stoichiometry.

IP_3/Ca^{2+} stimulation of NBCe1 variants may account for GPCR activation of NBCe1. For example, Perry *et al.* (2006) working on oocytes heterologously expressing NBCe1-A and the Ang-II receptor AT_{1B} reported that low concentrations of Ang II caused a modest (i.e., 20-30%) stimulation of the HCO_3^--induced current that is Ca^{2+}-dependent and perhaps partially inhibited by a PKC inhibitor. In our study however, the B and C variants —not the A variant— were stimulated by IP_3/Ca^{2+}. Furthermore, as described in more detail below, this stimulation is independent of PKC. Perhaps other components of receptor activation direct cell signaling to a specific NBC variant.

The mechanism by which IP_3-mediated Ca^{2+} release stimulates the B and C variants involves a staurosporine-sensitive kinase. Müller-Berger *et al.* (2001) hypothesized that kinase activation is responsible for Ca^{2+} stimulation of NBCe1-A in the macropatch. Our data support this hypothesis for the B and C variants. The general kinase inhibitor staurosporine blocks the IP_3 stimulation of the C variant. However, some of the more well-known kinases do not seem to be involved. In Fig. 9-type experiments (not shown), IP_3 stimulation of NBCe1-C was unaffected by the PKC inhibitors PKC (17-31) and GF109203X, a calmodulin inhibitory peptide, or the DAG kinase inhibitor R59949. Further studies are required to identify the specific kinase(s) responsible.

Requirement of the N Terminus for Full IP_3/Ca^{2+} Stimulation of NBCe1-B/C

The B and C variants share the same N terminus that differs in the A variant (Fig. 1). We therefore hypothesized that the different N terminus of B and C is required for full IP_3/Ca^{2+} stimulation. Indeed, the $PIP_2/IP_3/Ca^{2+}$ stimulation of a truncated NBCe1-C ($C_{\Delta N87}$) missing its 87 N-terminal residues was either eliminated or greatly inhibited. For example, injecting PIP_2 (Fig. 2) or applying LPA (Fig. 10) failed to stimulate $C_{\Delta N87}$. Furthermore, injecting IP_3 stimulated $C_{\Delta N87}$ by only 51% compared to 172% for wild-type C (Fig. 5B), and activating SOCCs stimulated $C_{\Delta N87}$ by only 133% compared to 364% for wild-type C (Fig. 8B). While the N terminus of B/C plays a major role in Ca^{2+} stimulation and a kinase is involved, the exact mechanism is not clear. Ca^{2+}-kinase stimulation presumably involves phosphorylation of either NBC itself or an associated protein. Such phosphorylation may remove the autoinhibitory domain (AID), either by targeting the AID itself within the N terminus, or the AID binding site elsewhere on the

molecule. However, there may also be Ca^{2+}/kinase-sensitive regulation of NBCe1-B/C independent of the N terminus based on the findings that both IP_3 injection and SOCC activation modestly stimulated $C_{\Delta N87}$. Such stimulation was not seen with the A variant, perhaps due its different N terminus. Although there was some variability, $PIP_2/IP_3/Ca^{2+}$ stimulated the B and C variants in a similar degree. Furthermore, $PIP_2/IP_3/Ca^{2+}$ stimulated the A, but not B variant even though both have the same C terminus. Therefore, the different C termini of NBCe1 do not appear to contribute substantially to this mode of regulation.

IP_3/Ca^{2+}-mediated Changes in Surface Expression

According to Fig. 8, our SOCC activation protocol, which promotes Ca^{2+} influx, stimulates the B and C variants even with a 15-20% decrease in surface expression (Fig. 8C). There is precedence for Ca^{2+}-activated internalization of NBCe1. For example, Perry *et al.* (2006, 2007) working on oocytes co-expressing NBCe1-A and the Ang-II receptor AT_{1B} reported that a high concentration of Ang II elicited a decreased in NBC activity due to PKC and Ca^{2+}-dependent internalization of the protein. However, we did not observe any $PIP_2/IP_3/Ca^{2+}$- or LPA-stimulated decrease in surface expression of the A variant. Furthermore, PKC inhibitors in our study did not inhibit the IP_3-mediated stimulation of the B and C variants (data not shown). Apparently, the effect of Ca^{2+} on NBCe1 expression is dependent on the NBCe1 variant studied and the receptor-signaling pathway activated. In fact, according to Supplemental Fig. 2, inhibiting basal PLC activity independent of receptor activation reduces surface expression and associated activity of NBCe1-A.

A curious finding in our study was the disparate mechanisms responsible for the LPA stimulation of the B *vs*. C variants. Although LPA stimulated the activity of both variants by at least 90% in a Ca^{2+}-dependent manner, the stimulation of the B but not the C variant was mainly attributed to an increase in surface expression (Supplemental Fig. 5C). Interestingly, the increase in NBCe1-B surface expression was not Ca^{2+}-dependent (i.e., not inhibited by BAPTA) (Fig. 10D). The simplest interpretation is that the LPA-induced increase in NBCe1-B surface expression does not require elevated $Ca^{2+}{}_i$, although the associated increase in transporter activity does. Apparently, GPCR activation can influence the activity and expression of NBCe1 variants.

IP_3/Ca^{2+} Stimulation Independent of IRBIT

As described in the Introduction, IRBIT binds to the N terminus and stimulates the B but not A variant (Shirakabe *et al.*, 2006) by removing the AID as proposed by the authors. Furthermore, IRBIT also stimulates the C variant (Thornell *et al.*, 2010;Yang *et al.*, 2011). The PIP_2/IP_3/Ca^{2+} stimulatory effect on the B and C variants, but not the A variant reported in this study is consistent with IRBIT's stimulatory profile. However, we believe that the PIP_2/IP_3/Ca^{2+} and IRBIT stimulatory pathways are distinct for the following four reasons. First, relative to heterologous expression, endogenous expression of IRBIT is low in oocytes (Shirakabe *et al.*, 2006). Second, injecting IP_3 into ER Ca^{2+}-depleted oocytes that are returned to bath Ca^{2+} failed to stimulate NBCe1-B/C (Fig. 8). In these experiments, primed SOCC activity would provide sufficient cytosolic Ca^{2+} for IP_3-displaced IRBIT activity. Third, IP_3 stimulation of NBCe1-C is not abolished by a Ca^{2+}/calmodulin kinase inhibitor (data not shown). Ca^{2+}/calmodulin-mediated

phosphorylation is required for IRBIT activity (Ando *et al.*, 2006). Fourth, and most convincingly, co-expressing either the dominant-negative S68A IRBIT mutant (Fig. 6) or the less-characterized S71A IRBIT mutant (Supplemental Figure 4) inhibits neither the HCO_3^--induced NBCe1-C current (which reinforces the first point above) nor its IP_3 stimulation. However, this fourth point relies on the following two assumptions: *i*) exogenous human IRBIT multimerizes with any endogenous *Xenopus* IRBIT, and *ii*) the dominant-negative nature of S68A IRBIT characterized in IP_3-receptor binding and Ca^{2+} responses studies (Ando *et al.*, 2006) would extend to IRBIT stimulation of NBCe1.

Although the IP_3/Ca^{2+} and IRBIT stimulatory pathways are distinct, there may be some crosstalk. In oocytes expressing NBCe1-B/C, co-expressing IRBIT markedly inhibited the PIP_2-induced stimulation of the HCO_3^--induced NBC current (Thornell *et al.*, 2010). However, we can not exclude the possibility that elevated expression of IRBIT competes with injected PIP_2-generated IP_3 for the IP_3 receptor, thereby reducing Ca^{2+} release and NBC stimulation.

Physiological Significance of $PIP_2/IP_3/Ca^{2+}$ Regulation of NBCe1-B/C Activity

Our finding that PIP_2 stimulates NBCe1 activity through hydrolysis to IP_3 and subsequent ER Ca^{2+} release may have important implications for understanding receptor-mediated effects on acid-base transporter activity and pH_i regulation, as well as functional coupling to Ca^{2+}_i physiology in tissues such as heart and brain. In brain, glutamate-induced metabotropic receptor activation and subsequent IP_3/Ca^{2+}-stimulated NBCe1 activity in glial cells would be expected to dampen extracellular alkaline shifts or augment acid shifts associated with neuronal activity (Chesler, 2003). PIP_2 regulation of

NBCe1 activity may also contribute to important secretory or reabsorptive processes of epithelia. In the pancreas for example, secretin acting through an increase in cAMP is the primary stimulator of HCO_3^- secretion. However, other synergistic mechanisms appear to be involved as reviewed by Lee *et al.* (2010). IP_3/Ca^{2+} induced stimulation of NBCe1-B on the basolateral membrane may be responsible for additional PLC-mediated cholingeric and CCK_A stimulation of ductal HCO_3^- secretion.

PIP_2 Regulation of NBCe1 Activity by a Dual Mechanism

The effect of PIP_2 on NBCe1 activity in oocytes is complex and appears to involve dual pathways based on results presented here and in our previous publication (Wu *et al.*, 2009b). In the current study, we report that injecting PIP_2 into an intact oocyte heterologously expressing NBCe1 stimulates transporter current. The injected-PIP_2 stimulation is indirect and requires hydrolysis to IP_3, ER Ca^{2+}, and one or more kinases. Furthermore, this effect is variant specific and seen with the B and C variants, but not the A variant— a finding that supports the hypothesis that different bicarbonate transporter variants have different modes of regulation. This IP_3/Ca^{2+} regulation requires the 85 N-terminal residues of the B/C variants for full stimulation.

However, in a previous study, our group found that PIP_2 directly stimulates NBCe1 activity and reduces the rate of transporter rundown in excised patches from oocytes expressing the A variant (Wu *et al.*, 2009b). Data presented in the current study also provide support for direct PIP_2 stimulation of expressed NBCe1 variants in whole oocytes. More specifically, in the presence of PLC inhibition, injecting PIP_2 stimulated all three variants —including the A variant— by 20-30% (Fig. 4B). However, we can not

exclude the possibility that residue PLC activity is responsible for the small stimulation of the B/C variants, although this possibility does not explain the stimulation of the A variant that is insensitive to PIP_2/IP_3 injection. Also, indirect effects of altering PIP_2 metabolism by PLC inhibition may be responsible. Finally, according to recent preliminary data (not shown) on oocytes, activating a heterologously expressed voltage-sensitive phosphatase to reduce PIP_2 levels without IP_3 production inhibited NBCe1-C activity. Thus, it appears that PIP_2 itself is required for NBCe1 activity, and depleting PIP_2 independent of the IP_3/Ca^{2+} pathway reduces activity.

We are currently characterizing PIP_2 regulation of all NBCe1 variants at both the functional and molecular levels to understand if/how these two pathways regulate variant-specific NBCe1 activity either in concert or differentially. The dominance of one pathway over another may depend not only on the NBCe1 variant and its apparent PIP_2 affinity, but also on PIP_2 concentration, particular signaling pathways, and perhaps PIP_2 microdomains or lipid rafts (Gamper & Shapiro, 2007). Physiologically, PIP_2 regulation of NBCe1 activity may explain pH changes linked to GPCR activation and PLC-mediated cellular processes as described above, as well as pathological conditions leading to ATP deficiency and associated PIP_2 degradation.

Acknowledgements

We thank Drs. Katsuhiko Mikoshiba and Hideaki Ando (RIKEN Brain Science Institute, Japan) providing the mutant S68A IRBIT construct and relevant information. We also thank Drs. Mark D. Parker and Walter F. Boron (Department of Physiology and Biophysics, Case Western Reserve University) for providing the mutant S71A IRBIT

construct. This work was supported by an award from the American Heart Association, and by NIH/NINDS R01 NS046653.

References

Abuladze N, Song M, Pushkin A, Newman D, Lee I, Nicholas S, & Kurtz I (2000). Structural organization of the human NBC1 gene: kNBC1 is transcribed from an alternative promoter in intron 3. *Gene* 251, 109-122.

Ando H, Mizutani A, Kiefer H, Tsuzurugi D, Michikawa T, & Mikoshiba K (2006). IRBIT suppresses IP_3 receptor activity by competing with IP_3 for the common binding site on the IP_3 receptor. *Mol Cell* 22, 795-806.

Bevensee MO, Schmitt BM, Choi I, Romero MF, & Boron WF (2000). An electrogenic Na^+-HCO_3^- cotransporter (NBC) with a novel COOH-terminus, cloned from rat brain. *Am J Physiol Cell Physiol* 278, C1200-C1211.

Boron WF, Chen L & Parker MD (2009). Modular structure of sodium-coupled bicarbonate transporters. *J Exp Biol* 212, 1697-1706.

Chesler M (2003). Regulation and modulation of pH in the brain. *Physiol Rev* 83, 1183-1221.

Durieux ME, Salafranca MN, Lynch KR, & Moorman JR (1992). Lysophosphatidic acid induces a pertussis toxin-sensitive Ca^{2+}-activated Cl^- current in *Xenopus laevis* oocytes. *Am J Physiol* 263, C896-C900.

Gamper N & Shapiro MS (2007). Target-specific PIP_2 signalling: how might it work? *J Physiol* 582, 967-975.

Gillo B, Lass Y, Nadler E, & Oron Y (1987). The involvement of inositol 1,4,5-triphosphate and calcium in the two-component response to acetylcholine in *Xenopus* oocytes. *J Physiol* 392, 349-361.

Gross E, Fedotoff O, Pushkin A, Abuladze N, Newman D, & Kurtz I (2003). Phosphorylation-induced modulation of pNBC1 function: distinct roles for the amino- and carboxy-termini. *J Physiol* 549, 673-682.

Gross E, Hawkins K, Pushkin A, Sassani P, Dukkipati R, Abuladze N, Hopfer U, & Kurtz I (2001). Phosphorylation of Ser^{982} in the sodium bicarbonate cotransporter kNBC1 shifts the HCO_3^-:Na^+ stoichiometry from 3:1 to 2:1 in murine proximal tubule cells. *J Physiol* 537, 659-665.

Heyer M, Müller-Berger S, Romero MF, Boron WF, & Frömter E (1999). Stoichiometry of the rat kidney Na^+-HCO_3^- cotransporter expressed in *Xenopus laevis* oocytes. *Pflügers Arch* 438, 322-329.

Lee MG, Ohana E, Park HW, Yang D, & Muallem S (2012). Molecular mechanism of pancreatic and salivary gland fluid and HCO_3^- secretion. *Physiol Rev* 92, 39-74.

Liu X, Williams JB, Sumpter BR, & Bevensee MO (2007). Inhibition of the Na/bicarbonate cotransporter NBCe1-A by diBAC oxonol dyes relative to niflumic acid and a stilbene. *J Membr Biol* 215, 195-204.

Liu Y, Xu JY, Wang DK, Wang L, & Chen LM (2011). Cloning and identification of two novel NBCe1 splice variants from mouse reproductive tract tissues: A comparative study of NCBT genes. *Genomics* 98, 112-119.

Lupu-Meiri M, Shapira H, & Oron Y (1988). Hemispheric asymmetry of rapid chloride responses to inositol trisphosphate and calcium in *Xenopus* oocytes. *FEBS Let* 240, 83-87.

McAlear SD & Bevensee MO (2006). A cysteine-scanning mutagenesis study of transmembrane domain 8 of the electrogenic Na/bicarbonate cotransporter NBCe1. *J Biol Chem* 281, 32417-32427.

*McAlear SD, *Liu X, Williams JB, McNicholas-Bevensee CM, & Bevensee MO (2006). Electrogenic Na/HCO_3 cotransporter (NBCe1) variants expressed in *Xenopus oocytes*: functional comparison and roles of the amino and carboxy termini. *J Gen Physiol* 127, 639-658. [*equal contributors]

Müller-Berger S, Ducoudret O, Diakov A, & Frömter E (2001). The renal Na-HCO_3^- cotransporter expressed in *Xenopus laevis* oocytes: change in stoichiometry in response to elevation of cytosolic Ca^{2+} concentration. *Pflügers Arch* 442, 718-728.

Oron Y, Dascal N, Nadler E, & Lupu M (1985). Inositol 1,4,5-trisphosphate mimics muscarinic response in *Xenopus* oocytes. *Nature* 313, 141-143.

Perry C, Blaine J, Le H, & Grichtchenko II (2006). PMA- and ANG II-induced PKC regulation of the renal Na^+-HCO_3^- cotransporter (hkNBCe1). *Am J Physiol Renal Physiol* 290, F417-F427.

Perry C, Le H, & Grichtchenko II (2007). ANG II and calmodulin/CaMKII regulate surface expression and functional activity of NBCe1 via separate means. *Am J Physiol Renal Physiol* 293, F68-F77.

Petersen CC & Berridge MJ (1994). The regulation of capacitative calcium entry by calcium and protein kinase C in *Xenopus* oocytes. *J Biol Chem* 269, 32246-32253.

Romero MF, Fulton CM, & Boron WF (2004). The SLC4 family of HCO_3^- transporters. *Pflügers Arch* 447, 495-509.

Sciortino CM & Romero MF (1999). Cation and voltage dependence of rat kidney electrogenic Na^+- HCO_3^- cotransporter, rkNBC, expressed in oocytes. *Am J Physiol* 277, F611-F623.

Shirakabe K, Priori G, Yamada H, Ando H, Horita S, Fujita T, Fujimoto I, Mizutani A, Seki G, & Mikoshiba K (2006). IRBIT, an inositol 1,4,5-trisphosphate receptor-binding protein, specifically binds to and activates pancreas-type Na^+/HCO_3^- cotransporter 1 (pNBC1). *Proc Natl Acad Sci USA* 103, 9542-9547.

Thornell IM & Bevensee MO (2011). Role of Ca^{2+} in phosphatidylinositol 4,5-bisphosphate (PIP_2)/IP_3-induced stimulation of the electrogenic Na/bicarbonate cotransporter NBCe1-C heterologously expressed in *Xenopus laevis* oocytes. *FASEB J* 25, #656.6.

Thornell I, Wu J, & Bevensee MO (2010). The IP_3 receptor-binding protein IRBIT reduces phosphatidylinositol 4,5-bisphosphate (PIP_2) stimulation of Na/bicarbonate cotransporter NBCe1
variants expressed in *Xenopus laevis* oocytes. *FASEB J* 24, #815.6.

Wu J, Liu X, Thornell IM, & Bevensee MO (2009a). Phosphatidylinositol 4,5-bisphosphate stimulation of electrogenic Na/bicarbonate cotransporter NBCe1 variants expressed in *Xenopus laevis* oocytes. *FASEB J* 23, #800.13.

Wu J, McNicholas CM, & Bevensee MO (2009b). Phosphatidylinositol 4,5-bisphosphate (PIP_2) stimulates the electrogenic Na/HCO_3 cotransporter NBCe1-A expressed in *Xenopus* oocytes. *Proc Natl Acad Sci USA* 106, 14150-14155.

Yang D, Shcheynikov N, & Muallem S (2011). IRBIT: it is everywhere. *Neurochem Res* 36, 1166-1174.

Yoshida S & Plant S (1992). Mechanism of release of Ca^{2+} from intracellular stores in response to ionomycin in oocytes of the frog *Xenopus laevis*. *J Physiol* 458, 307-318.

Zeuthen T, Zeuthen E, & Klaerke DA (2002). Mobility of ions, sugar, and water in the cytoplasm of *Xenopus* oocytes expressing Na^{+}-coupled sugar transporters (SGLT1). *J Physiol* 542, 71-87.

Zhu Q, Kao L, Azimov R, Newman D, Liu W, Pushkin A, Abuladze N, & Kurtz I (2010). Topological location and structural importance of the NBCe1-A residues mutated in proximal renal tubular acidosis. *J Biol Chem* 285, 13416-13426.

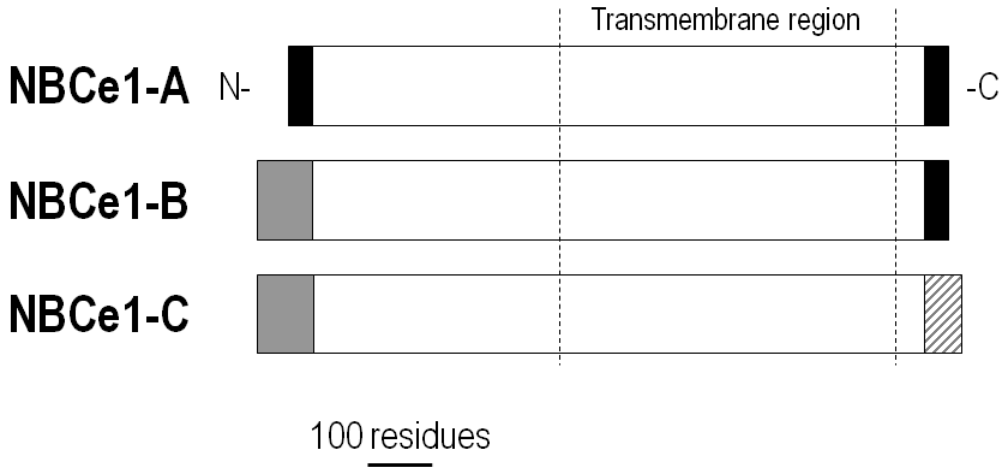

Figure 1. NBCe1-A, -B, and -C variants are identical except at the amino and/or carboxy termini. 85 N-terminal residues of the B and C variants (grey) replace the unique 41 N-terminal residues of the A variant (black), and 61 C-terminal residues of the C variant (striped) replace the 46 C-terminal residues of the A and B variants (black). The transmembrane region denoted by the dotted lines contains as many as 14 transmembrane domains (Boron *et al.*, 2009; Zhu *et al.*, 2010).

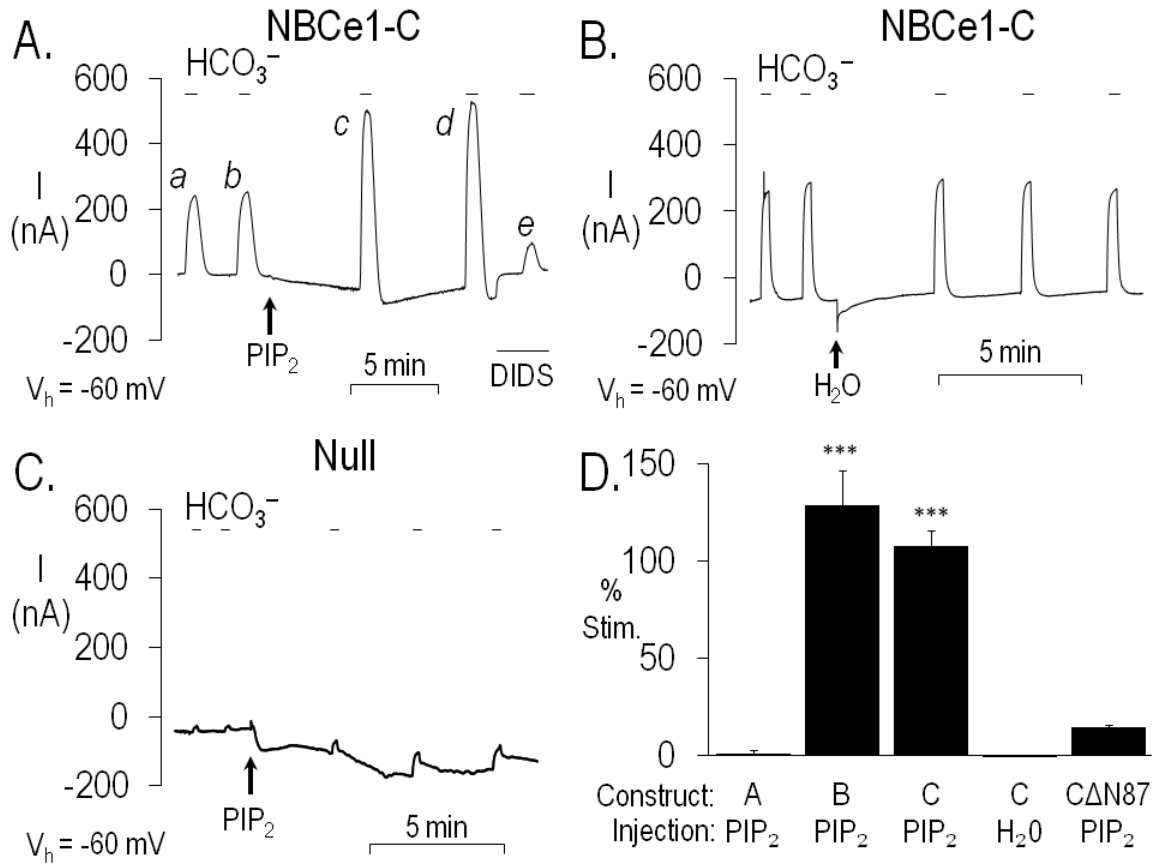

Figure 2. Injecting PIP_2 stimulates the HCO_3^--induced outward currents of the B and C variants. *A*, Switching from ND96 to CO_2/HCO_3^- elicited NBC-mediated, HCO_3^--induced outward currents (*a*, *b*) in an NBCe1-C-expressing oocyte voltage clamped at -60 mV. Injecting 100 μM PIP_2 (~10 μM final concentration) increased the HCO_3^--induced outward currents ~2-fold (*c*, *d*), and these currents were inhibited ~80% by 200 μM DIDS (*e*). *B*, A similar experiment to that described in panel *A* was performed on an NBCe1-C-expressing oocyte, but H_2O instead of PIP_2 was injected. H_2O injection did not alter the HCO_3^--induced outward currents. *C*, In another control experiment on a H_2O-injected null oocyte, injecting PIP_2 did not appreciably stimulate endogenous HCO_3^--induced outward currents. *D*, Summary data from panel *A*- and *B*-type experiments performed on all three variants, as well as a C variant missing its N-terminal 87 residues ($C_{\Delta N87}$). $^{***}P \leq .001$ for the mean current pre *vs*. post injection. $n \geq 4$ for each bar.

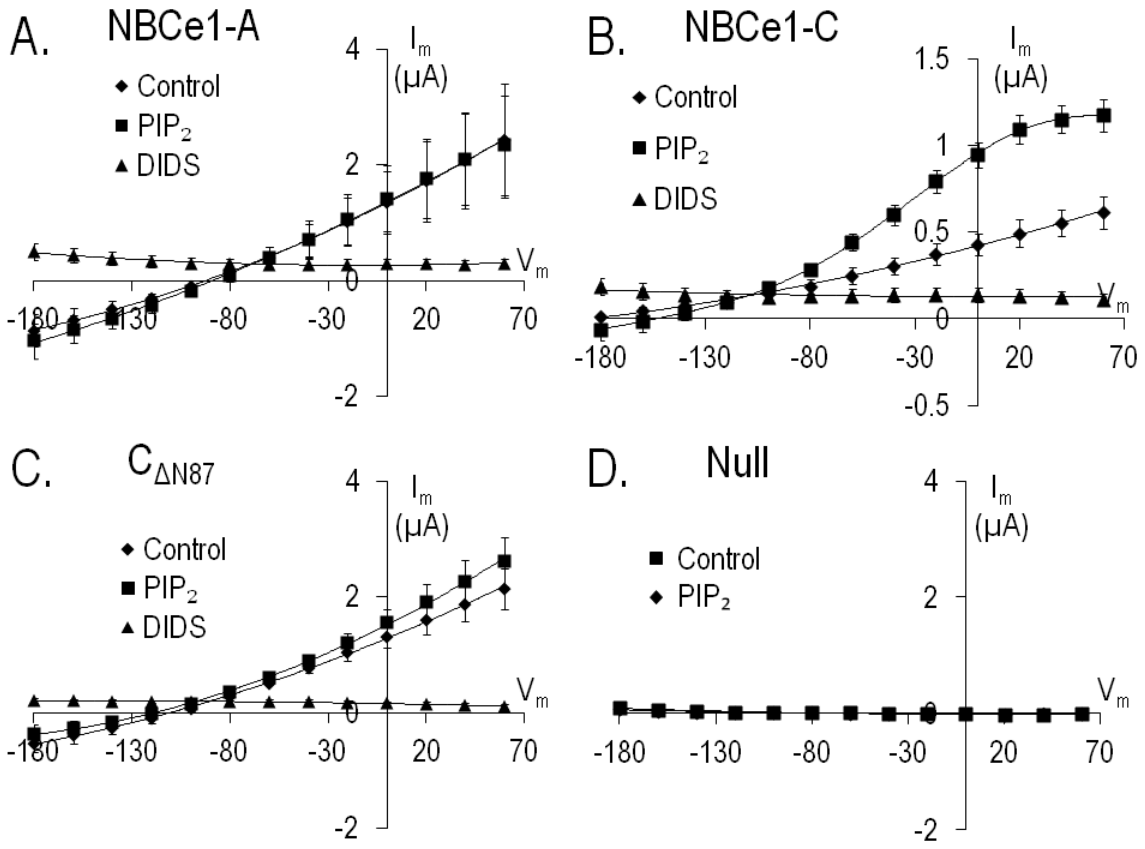

Figure 3. Injecting PIP_2 stimulates the voltage-dependent HCO_3^--induced currents of the B and C variants. *A*, The mean HCO_3^--dependent I-V plots from NBCe1-A-expressing oocytes were similar before injecting PIP_2 (diamonds) and after (squares). 200 μM DIDS inhibited the currents (triangles). *B*, The mean HCO_3^--dependent currents from NBCe1-C-expressing oocytes at potentials more positive than ~-100 mV were smaller before injecting PIP_2 (diamonds) than after (squares). 200 μM DIDS inhibited the currents (triangles). *C*, The mean HCO_3^--dependent I-V plots for $C_{\Delta N87}$ were similar to those for the A variant (panel *A*). *D*, Negligible currents were observed in H_2O-injected null oocytes. The upward-shifted I-V plots with DIDS in panels A-C presumably reflect different baseline currents inherent in these experiments designed to minimize the delay between HCO_3^--induced currents ± DIDS after PIP_2 injection. For each panel, n = 3 from 1 batch of oocytes, and the data were repeated in a second batch.

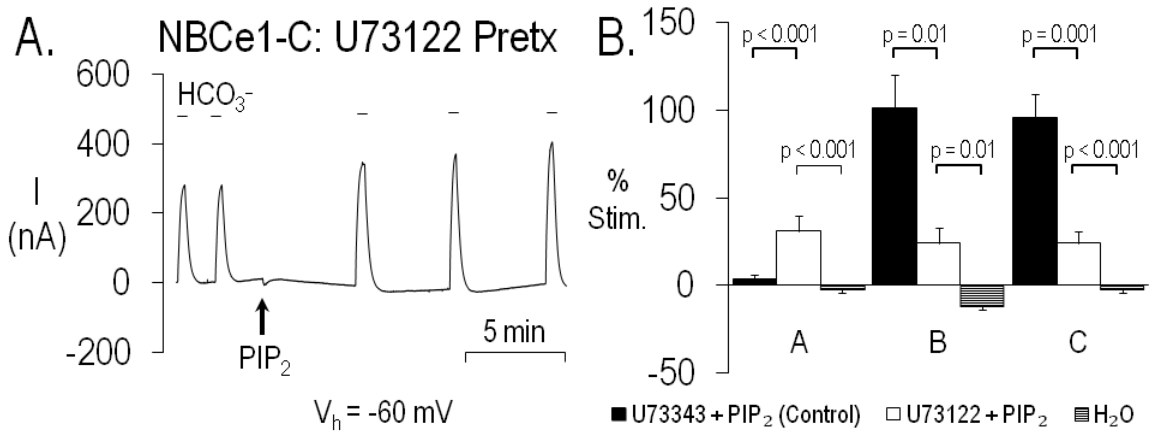

Figure 4. Full stimulation by PIP_2 injection of the B and C variants requires PLC activity. *A*, PIP_2 injection elicited only a modest stimulation of the HCO_3^--induced outward current in an oocyte pre-incubated for 30 min in 10 μM of the PLC inhibitor U73122. *B*, Summary data of the mean injected PIP_2-induced % NBC stimulation from panel *A*-type experiments on the three variants. For oocytes pre-incubated in the inactive analog U73343, subsequent PIP_2 injection had little effect on the A variant, but stimulated the B and C variants by ~100% (closed bars). Pre-incubating oocytes in U73122 reduced the stimulation by PIP_2 injection of the B and C variants to ~35%, and increased the stimulation of the A variant by the same extent (open bars). H_2O injection failed to stimulate any of the variants (hatched bars). $n \geq 3$ for each bar. Pretx, pretreatment.

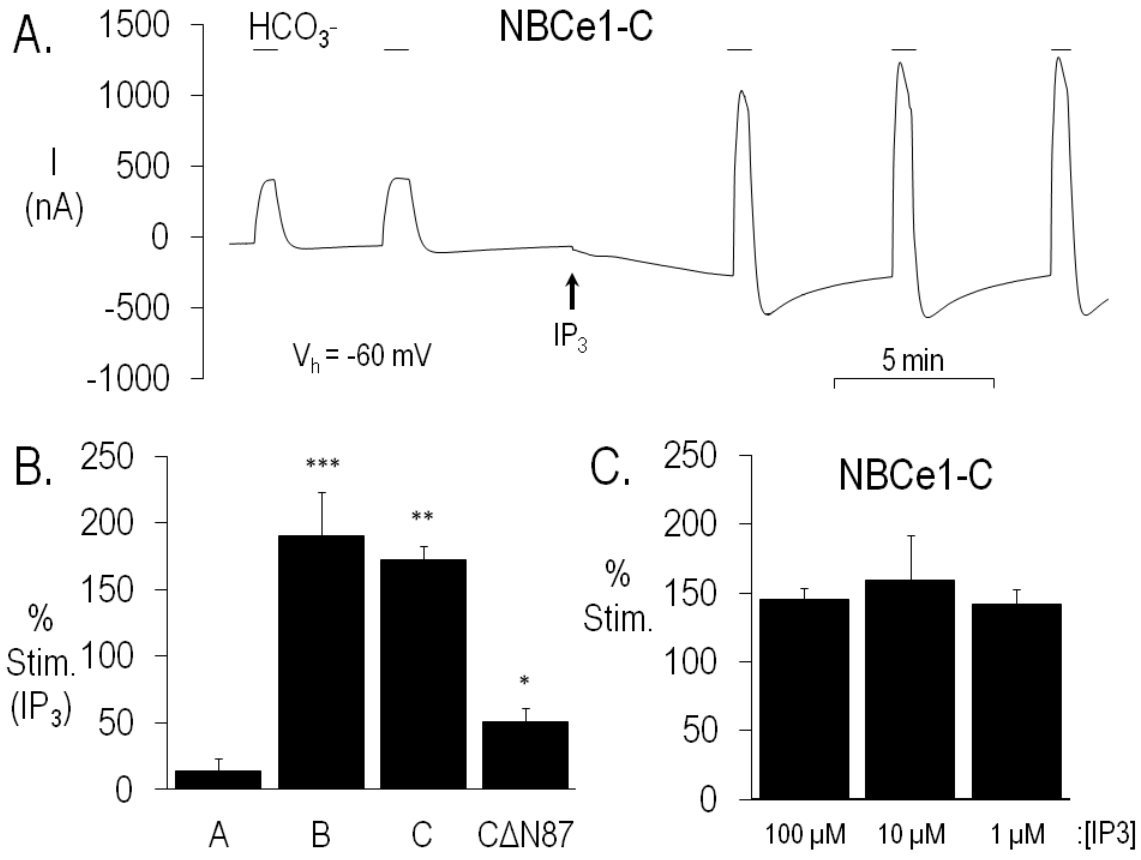

Figure 5. Injecting IP_3 —even at a low concentration— stimulates the HCO_3^--induced outward currents of the B and C variants. *A*, IP_3 injection stimulated the HCO_3^--induced outward currents by ~3-fold in an NBCe1-C-expressing oocyte. *B*, Summary data of the mean IP_3-induced % NBC stimulation from panel *A*-type experiments on the three variants, as well as $C_{\Delta N87}$. $^{***}P \leq .001$, $^{**}P \leq .01$, and $^{*}P \leq .05$ for the mean current pre *vs*. post injection. n = 5 for each bar. *C*, Summary data of the mean IP_3-induced % NBC stimulation from panel *A*-type experiments on NBCe1-C-expressing oocytes injected with one of three different concentrations of IP_3. These experiments with different IP_3 injections were performed in Ca^{2+}-free solutions containing 1 mM EGTA. $n \geq 5$ for each bar.

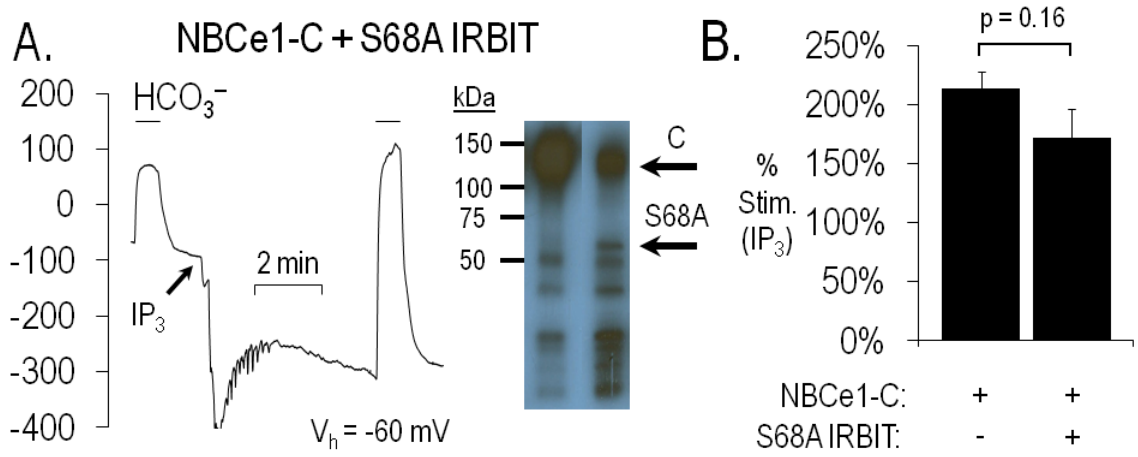

Figure 6. Co-expressing S68A IRBIT does not inhibit the IP_3-induced stimulation of NBCe1-C. *A*, As shown on the left, IP_3 injection stimulated the HCO_3^--induced outward current by ~3-fold in an oocyte co-injected with equal amounts of NBCe1-C and S68A IRBIT cRNA. As shown by an immunoblot on the right, an individual oocyte injected with NBCe1-C cRNA expressed ~130 kDa NBCe1-C (left column), whereas an oocyte co-injected with both cRNAs expressed ~130 kDa NBCe1-C and ~60 kDa S68A IRBIT (right column). *B*, Summary data of the mean IP_3-induced % NBC stimulation from panel *A*-type experiments on oocytes expressing NBCe1-C with or without S68A IRBIT (n = 7 for each bar).

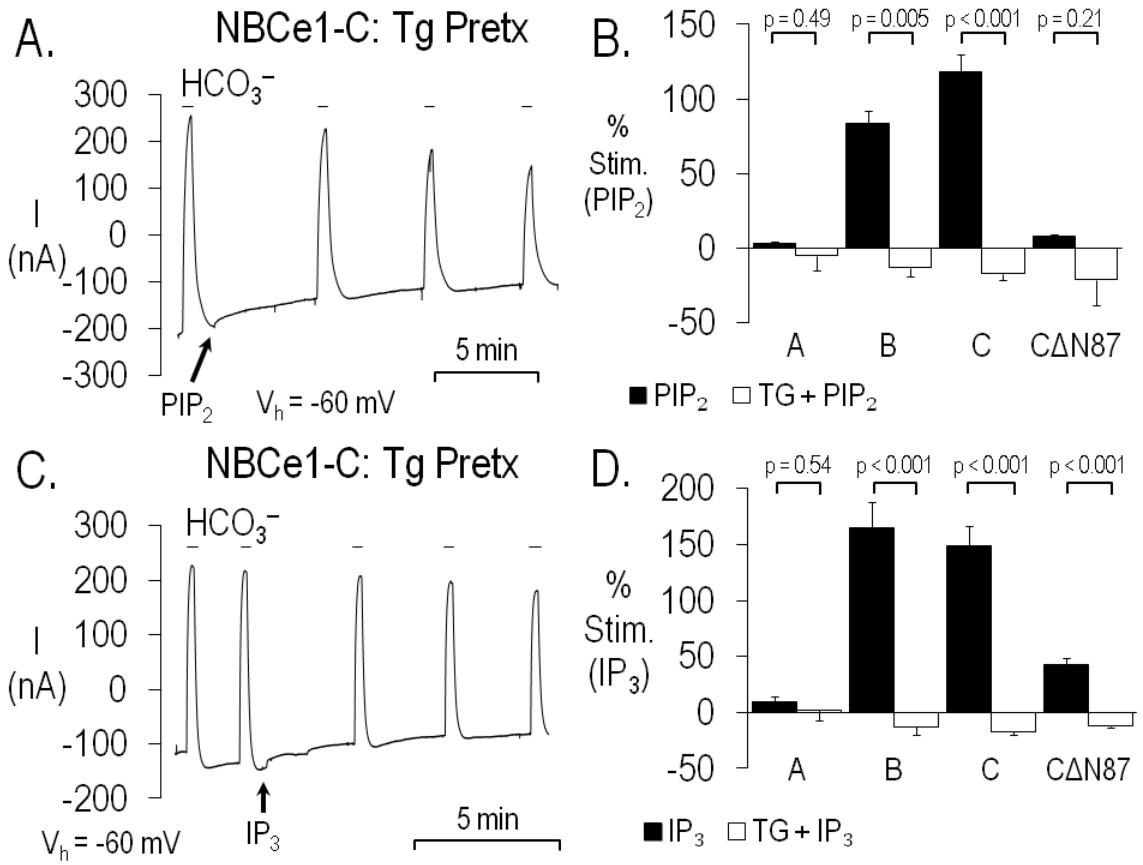

Figure 7. Depletion of ER Ca^{2+} blocks the injected PIP_2- and IP_3-stimulated HCO_3^--induced currents of the B and C variants. *A*, Pre-incubating an NBCe1-C-expressing oocyte in a 0 Ca^{2+}/EGTA solution containing 10 μM thapsigargin (Tg) for ~4 h to deplete ER Ca^{2+} stores eliminated the injected PIP_2 stimulation of the HCO_3^--induced outward current. *B*, Summary data of the mean PIP_2-induced % NBC stimulation from panel *A*-type experiments on the three variants, as well as $C_{\Delta N87}$ with the oocytes pre-incubated in 0 Ca^{2+}/EGTA plus either DMSO (closed bars) or Tg (open bars). n ≥ 3 for each bar. *C*, The 0 Ca^{2+}/EGTA/Tg pre-incubation also eliminated the injected-IP_3 stimulation of the HCO_3^--induced outward current of NBCe1-C. *D*, Summary data of the mean IP_3-induced % NBC stimulation from panel *C*-type experiments on the variants with the oocytes pre-incubated in 0 Ca^{2+}/EGTA plus either DMSO (closed bars) or Tg (open bars). n ≥ 3 for each bar.

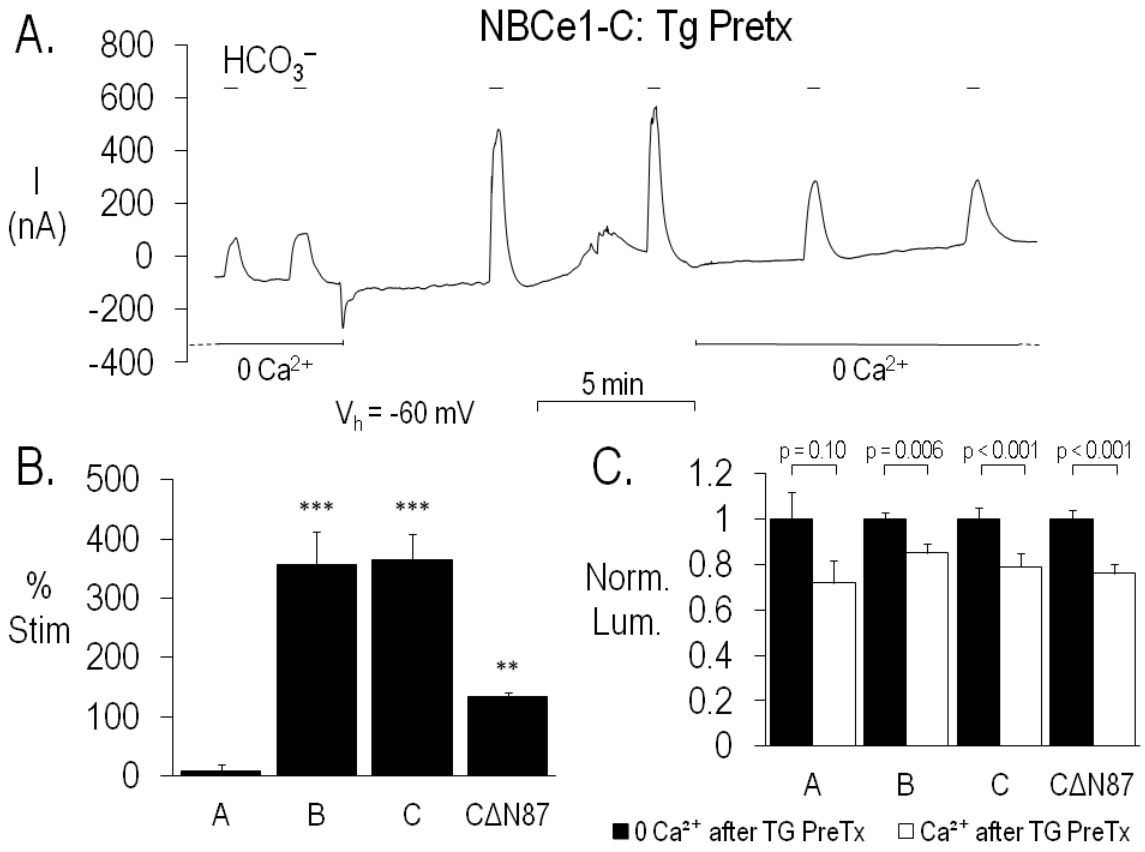

Figure 8. Activating store-operate Ca^{2+} channels stimulates the HCO_3^--induced outward current of the B and C variants. *A*, The NBCe1-C-expressing oocyte was pre-incubated for ~4 h in a 0 Ca^{2+}/EGTA solution containing 10 μM thapsigargin (Tg) and maintained in the 0 Ca^{2+}/ETGA solution at the beginning of the experiment. Subsequently returning Ca^{2+}_o stimulated the HCO_3^--induced outward currents by ~3-fold compared to the currents in the absence of Ca^{2+}_o. These stimulated currents were reversed by removing Ca^{2+}_o. *B*, Summary data of the mean % NBC stimulation from panel *A*-type experiments on the three variants, as well as $C_{\Delta N87}$. $^{***}P \leq .001$ and $^{**}P \leq .01$ for the mean current pre *vs*. post injection. n ≥ 3 for each bar. *C*, Summary of mean single-oocyte chemiluminescence (SOC) from oocytes first pretreated with the 0 Ca^{2+}/EGTA/Tg solution, and then either maintained in 0 Ca^{2+} (closed bars) or re-exposed to Ca^{2+}_o for 5 min (open bars). n ≥ 20 (2 oocyte batches) for each bar.

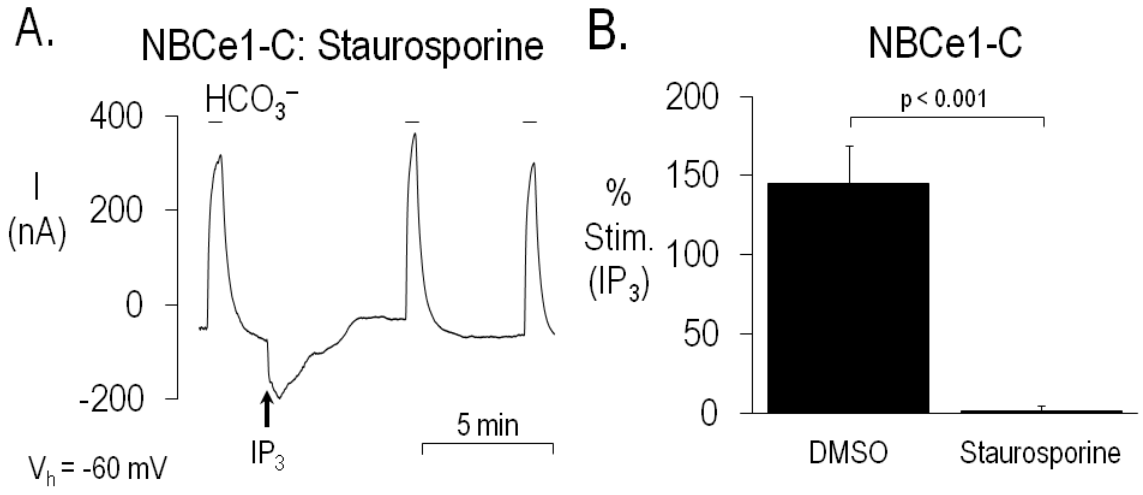

Figure 9. Staurosporine blocks the IP_3-induced stimulation of NBCe1-C. *A*, Pre-incubating an NBCe1-C-expressing oocyte in ND96 containing 20 μM staurosporine for ~4 h to inhibit kinase activity eliminated the injected-IP_3 stimulation of the HCO_3^--induced outward current. *B*, Summary data of the mean IP_3-induced % NBC stimulation from panel *A*-type experiments from oocytes pretreated with DMSO (closed bar) or staurosporine (open bar). n ≥ 5 for each bar.

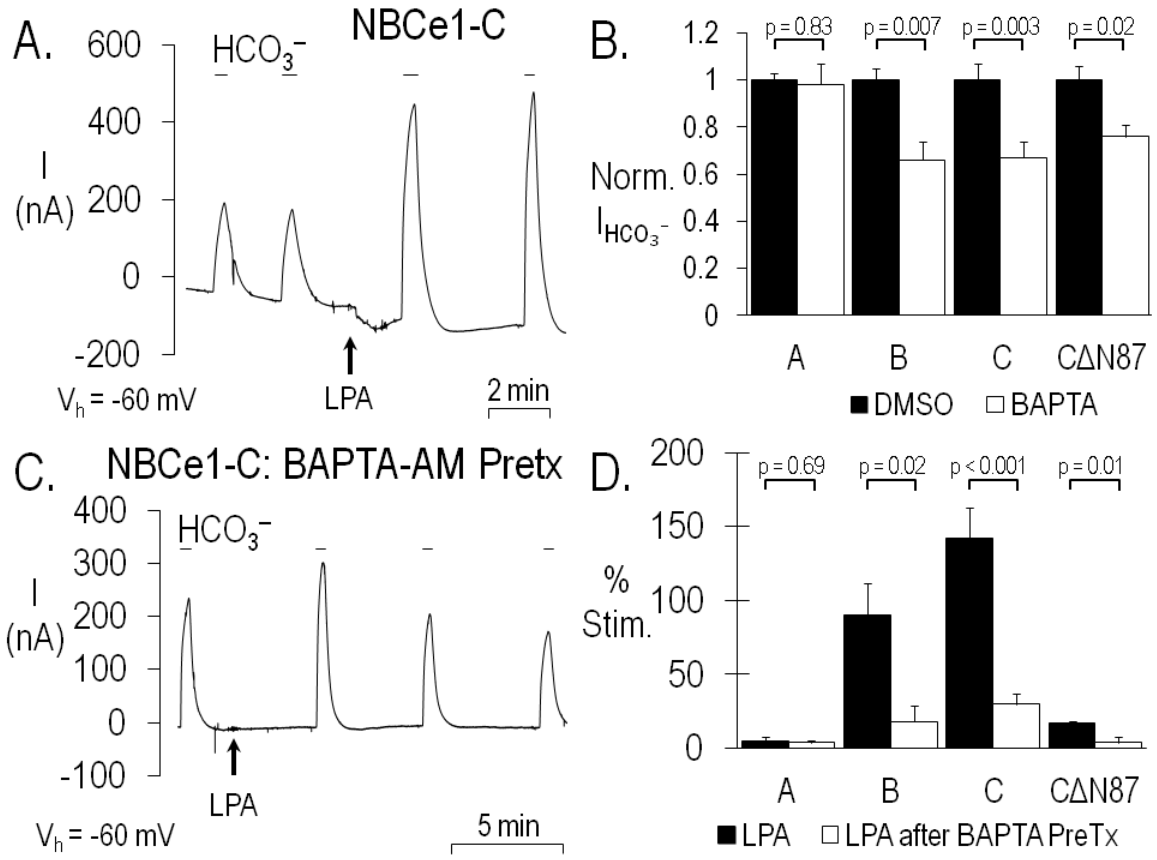

Figure 10. Lysophosphatidic acid (LPA) stimulates the HCO_3^--induced outward current of the B and C variants. *A*, Transiently exposing an NBCe1-C-expressing oocyte to 1 μM LPA for ~15 s stimulated the HCO_3^--induced outward currents by ~2.3-fold. *B*, Summary data of the normalized HCO_3^--induced outward currents for variant-expressing oocytes pre-incubated for 5-7 h in DMSO (closed bars) *vs*. 10 μM BAPTA-AM (open bars). n ≥ 4 for each bar. *C*, BAPTA-AM pre-incubation inhibited the LPA-stimulated, HCO_3^--induced currents in an NBCe1-C-expressing oocyte. *D*, Summary data of the mean LPA-induced % NBC stimulation from panel *A*-type experiments on oocytes pretreated with DMSO (closed bars) or BAPTA-AM (open bars). n ≥ 4 for each bar.

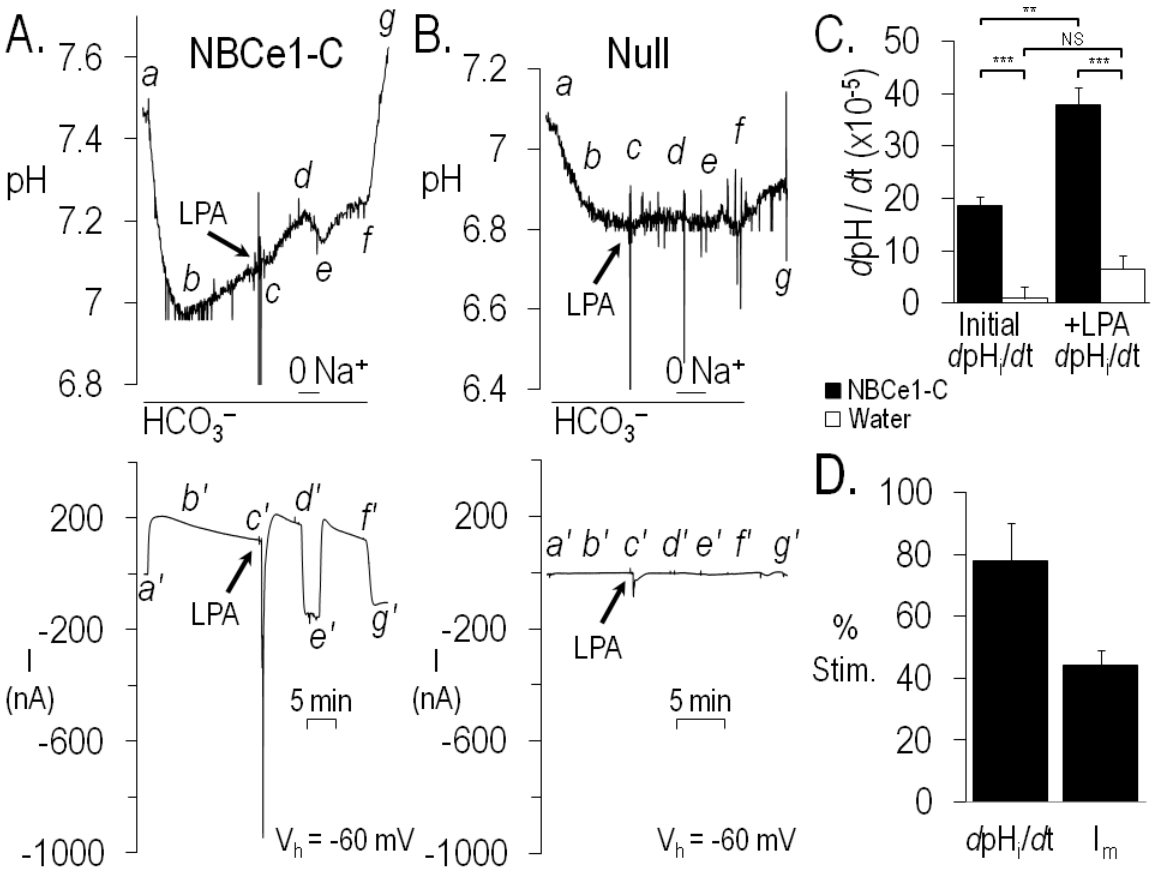

Figure 11. LPA stimulates both a HCO_3^--dependent pH_i recovery and outward current in an NBCe1-C-expressing oocyte voltage clamped at -60 mV. *A*, As shown in the top panel, switching from ND96 to CO_2/HCO_3^- elicited a pH_i decrease (*ab*) due to CO_2 influx, followed by a recovery (*bc*) due to NBC activity. Applying 1 μM LPA for ~15 s increased the pH_i recovery rate shortly thereafter (*cd*) consistent with NBC stimulation. Removing and returning external Na^+ caused pH_i to decrease and then increase again (*def*). Switching back to ND96 caused pH_i to increase (*fg*). In the simultaneous current recording, the HCO_3^- solution elicited the characteristic NBC-mediated outward current (*a′b′c′*). LPA induced a transient inward current presumably due to Ca^{2+}-activated Cl^- channel activity, followed by a pronounced outward current (*c′d′*) due to NBC stimulation. Removing and returning external Na^+ reversed and then reinstated the outward current (*d′e′f′*). Switching back to ND96 eliminated the outward current (*f′g′*). *B*, A similar experiment was performed on a H_2O-injected null oocyte. As shown in the upper panel, the CO_2/HCO_3^- solution elicited the expected decrease in pH_i (*ab*), but no subsequent pH_i recovery (*bc*). Subsequent experimental maneuvers had little effect on pH_i (*c*-*f*). As shown in the lower panel, the solutions had little effect on current (*a′*-*g′*). *C*, Left pair of bars summarizes the mean dpH_i/dt from segment-*bc* pH_i recoveries for oocytes expressing NBCe1-C (closed bar) or injected with H_2O (open bar). Right pair of bars summarizes the mean dpH_i/dt obtained 5 min after applying LPA to oocytes expressing NBCe1-C (closed bar) or injected with H_2O (open bar). n ≥ 4 for each bar. $^{***}P < .001$, $^{**}P < .01$, NS = not significant. *D*, LPA stimulated the NBCe1-C-mediated dpH_i/dt (calculated from panel-C data) by ~80% and current by ~40%.

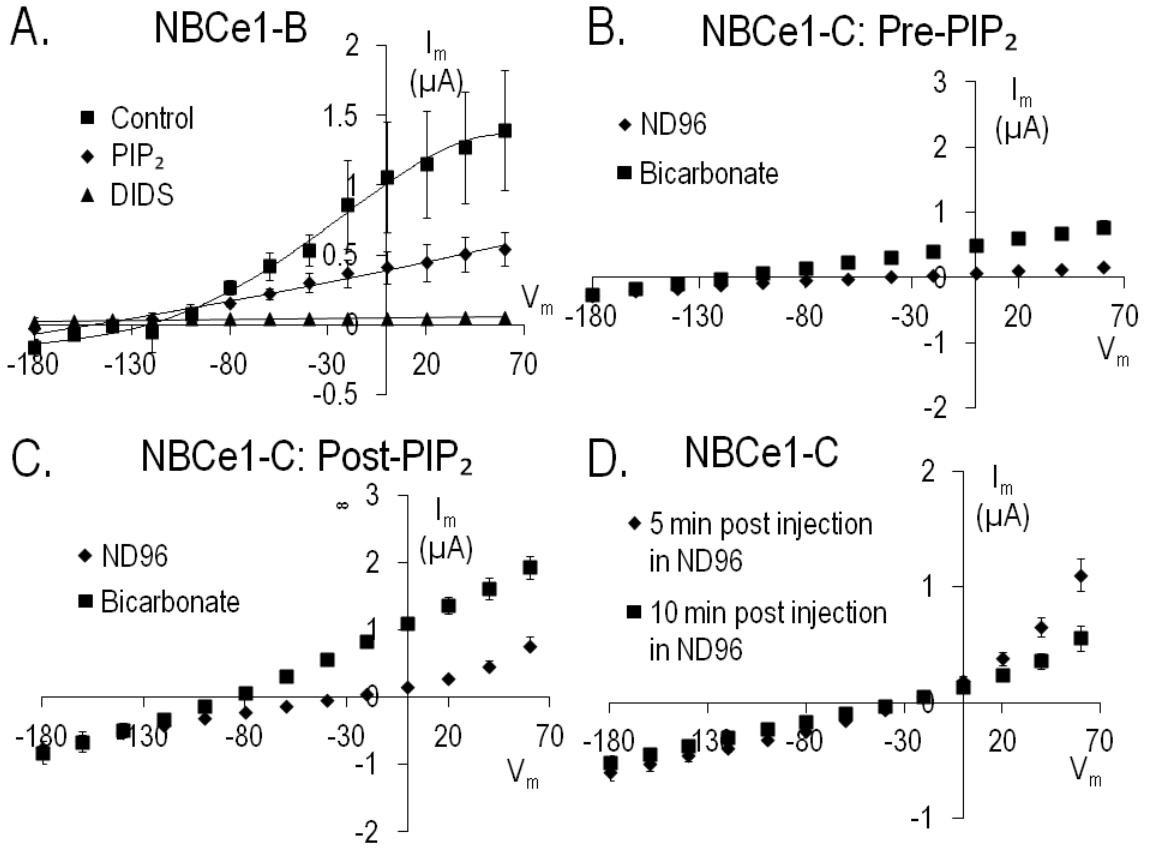

Supplemental Figure 1. Injecting PIP_2 stimulates the voltage-dependent HCO_3^--induced currents of the B and C variants. *A*, Fig. 3-type experiments were performed on oocytes expressing NBCe1-B. The mean HCO_3^--dependent currents at potentials more positive than ~-100 mV were smaller before injecting PIP_2 (diamonds) than after (squares). 200 μM DIDS inhibited the currents (triangles). *B*, The mean I-V plots NBCe1-C-expressing oocytes bathed in ND96 (diamonds), and then CO_2/HCO_3^- (squares) prior to PIP_2 injection were used to generate the HCO_3^--dependent I-V plot (Control, diamonds) shown in Fig. 3B. *C*, The mean I-V plots of NBCe1-C-expressing oocytes bath in ND96 (diamonds), and then CO_2/HCO_3^- (squares) after PIP_2 injection were used to generate the HCO_3^--dependent I-V plot (PIP_2, squares) shown in Fig. 3B. *D*, According to mean I-V plots obtained from NBCe1-C-expressing oocytes (different batch) bathed in ND96, outward currents were larger at positive potentials 5 min (diamonds) vs. 10 min (squares) after PIP_2 injection. n = 4 from 1 batch of oocytes, and similar results were obtained from a second batch of oocytes. Similar results were also obtained from NBCe1-B-expressing oocytes.

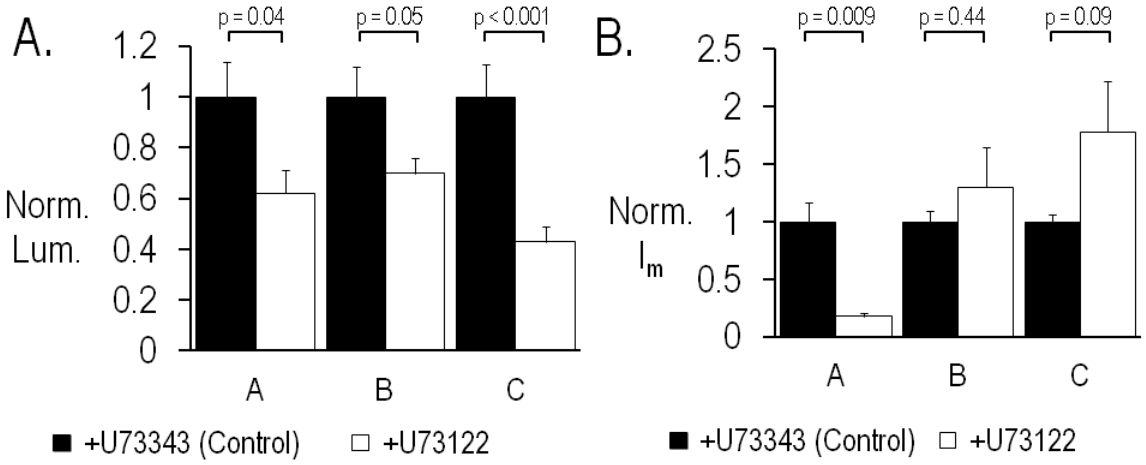

Supplemental Figure 2. PLC inhibition decreases the surface expression of the three variants, and reduces the activity of NBCe1-A. *A*, Summary of mean single-oocyte chemiluminescence (SOC) from NBCe1-A, -B, or -C-expressing oocytes preincubated for 30 min in ND96 containing 10 μM of the inactive analog U73343 (closed bars) or the PLC-inhibitor U73122 (open bars). For each variant, SOC was normalized to the mean from batch-matched control experiments (i.e., U73343 pretreated). The U73122 pretreatment decreased the mean surface expression of the three variants by 30-57%. $n \geq 18$ from 2 oocyte batches. *B*, For each variant, the SOC data from panel *A* were used to normalize the HCO_3^--induced outward currents to surface expression in oocytes pretreated with U73343 (closed bars) or U73122 (open bars). $n \geq 3$. More specifically, the outward currents from the U73122-treated variants were normalized to their reduced expression, and then all values were normalized to the mean from batch-matched control experiments (i.e., U73343 pretreated). U73122 pretreatment decreased the activity of the A variant by ~80%, but not the B or C variants.

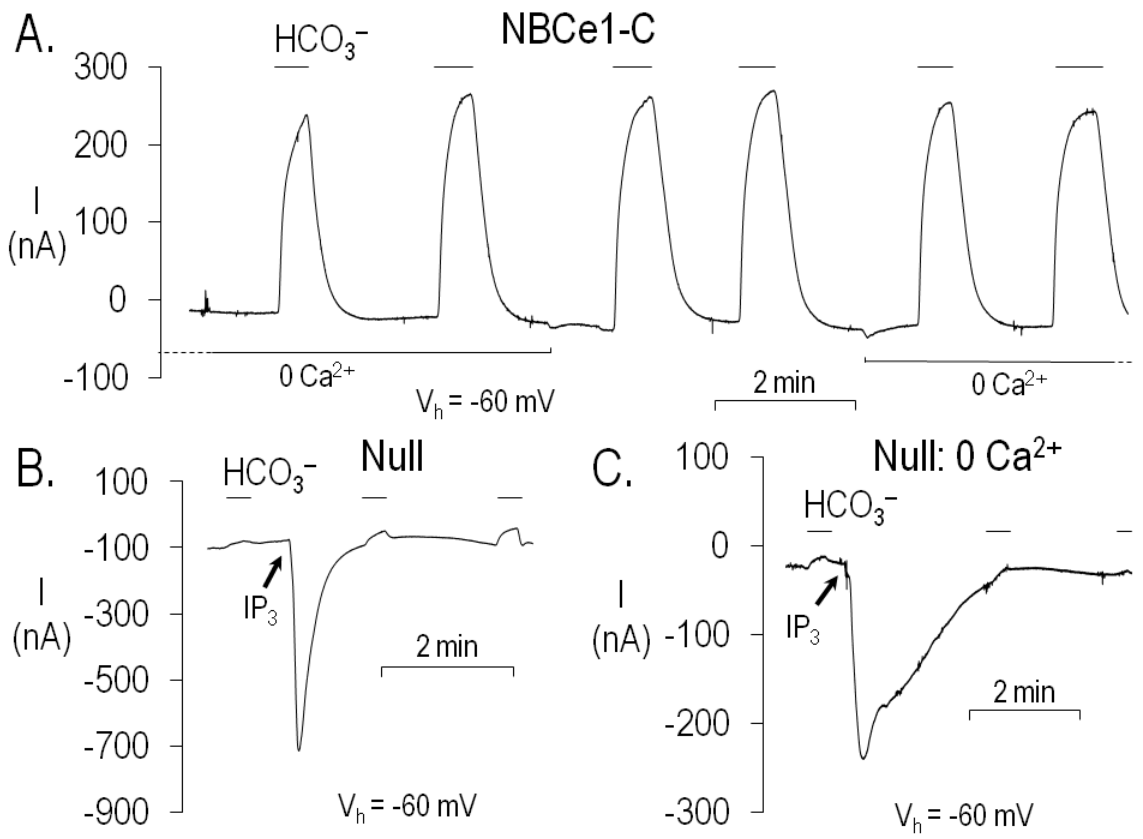

Supplemental Figure 3. Pretreating oocytes in 0 Ca^{2+}/EGTA does not inhibit NBCe1-C activity, and injecting IP_3 does not stimulate endogenous HCO_3^--induced currents. *A*, For an NBCe1-C-expressing oocyte pre-incubated in ND96 containing 0 Ca^{2+}/EGTA for 3 h, the HCO_3^--induced outward currents were similar before and after returning external Ca^{2+}. *B*, In a control experiment on a H_2O-injected null oocyte bathed in Ca^{2+}-containing solutions, injecting IP_3 did not appreciably stimulate endogenous HCO_3^--induced outward currents. *C*, In another control experiment on a H_2O-injected null oocyte bathed in 0 Ca^{2+}/EGTA solutions, injecting IP_3 also did not stimulate HCO_3^--induced outward currents. The large, transient inward current elicited by IP_3 injection reflects pronounced ER Ca^{2+}-induced stimulation of the Ca^{2+}-activated Cl^- channels. The time course of these transient currents was variable; the faster recovery seen in Ca^{2+} vs. 0 Ca^{2+} conditions was not a consistent finding. For all panels, n = 3.

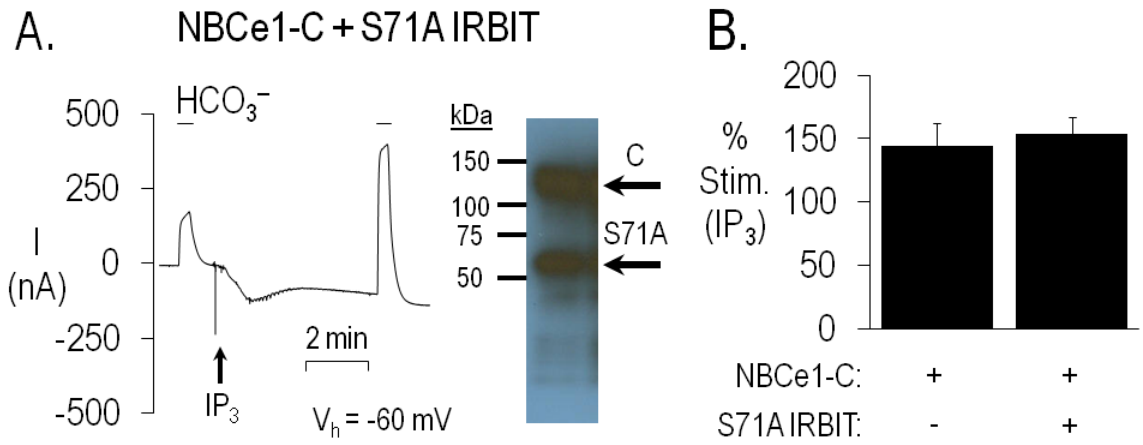

Supplemental Figure 4. Co-expressing S71A IRBIT does not inhibit the IP_3-induced stimulation of NBCe1-C. *A,* As shown on the left, IP_3 injection stimulated the HCO_3^--induced outward current by ~3-fold in an oocyte co-injected with equal amounts of NBCe1-C and S71A IRBIT cRNA. As shown by an immunoblot on the right, an individual oocyte co-injected with cRNA expressed ~130 kDa NBCe1-C and ~60 kDa S71A IRBIT (arrows). *B,* Summary data of the mean IP_3-induced % NBC stimulation from panel *A*-type experiments on oocytes expressing NBCe1-C with or without S71A IRBIT (n=6 for each bar).

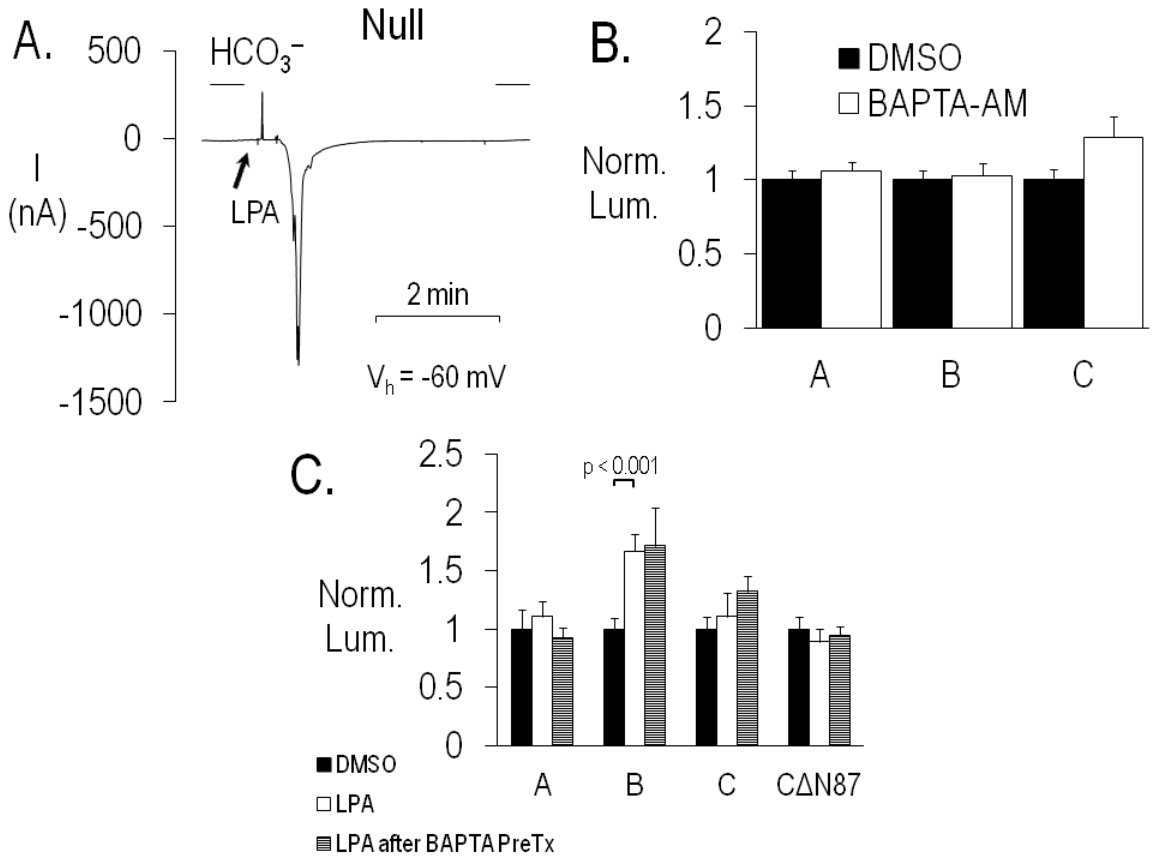

Supplemental Figure 5. LPA increases the surface expression of NBCe1-B independent of Ca^{2+}. *A*, In a control experiment on a H_2O-injected null oocyte, 1 μM LPA did not stimulate an endogenous HCO_3^--induced outward current. n=3. *B*, Summary of mean SOC from NBCe1-A, -B, or -C-expressing oocytes pre-incubated for 5 h in ND96 containing 10 μM DMSO (closed bars) or BAPTA-AM (open bars). n ≥ 18. For each variant, SOC was normalized to the mean from batch-matched DMSO control experiments. BAPTA-AM pretreatment did not affect the mean surface expression of the three variants. *C*, Summary of mean SOC from oocytes expressing one of the three variants or $C_{\Delta N87}$, and pre-incubated for 5 h in ND96 containing either 10 μM DMSO (closed and open bars) or BAPTA-AM (hatched bars). To stimulate the endogenous G-protein coupled receptor, LPA was applied for 15 s to one group of oocytes pre-incubated in DMSO (open bars) or BAPTA-AM (hatched bars). For each variant, SOC was normalized to the mean from batch-matched DMSO control experiments (i.e., without LPA stimulation). LPA only increased the surface expression of NBCe1-B through a BAPTA-insensitive mechanism. This increase in surface expression accounts for most of the % LPA = stimulation of NBCe1-B reported in Fig. 10D.

PIP_2 DEGRADATION INHIBITS THE Na/BICARBONATE COTRANSPORTER NBCe1-B AND -C VARIANTS EXPRESSED IN *XENOPUS* OOCYTES

Ian M. Thornell and Mark O. Bevensee

In preparation for *Journal of Physiology*

Format adapted for dissertation

Abstract

The electrogenic Na/bicarbonate cotransporter (NBCe1) of the *slc4* gene family is a powerful regulator of intracellular pH (pH_i) and extracellular pH (pH_o), and contributes to solute reabsorption and secretion in many epithelia. Using *Xenopus laevis* oocytes expressing NBCe1 variants, we have previously reported that the phospholipid phosphatidylinositol 4,5-bisphosphate (PIP_2) directly stimulates NBCe1-A in an excised macropatch, and indirectly stimulates NBCe1-B and -C in the intact oocyte primarily through $InsP_3/Ca^{2+}$. In the current study, we used the 2-electrode voltage-clamp technique alone or in combination with pH/voltage-sensitive microelectrodes or confocal fluorescence imaging of plasma-membrane PIP_2 to characterize the PIP_2 sensitivity of NBCe1-B and -C in whole oocytes by co-expressing a voltage-sensitive phosphate (VSP) that decreases PIP_2 and bypasses the $InsP_3/Ca^{2+}$ pathway. An oocyte depolarization that activated VSP only transiently stimulated the NBCe1-B/C current, consistent with an initial rapid depolarization-induced NBCe1 activation, and then a subsequent slower VSP-mediated NBCe1 inhibition. Upon repolarization, the NBCe1 current decreased, and then slowly recovered with an exponential time course that paralleled PIP_2 resynthesis as measured with a PIP_2-sensitive fluorophore and confocal imaging. A subthreshold depolarization that minimally activated VSP caused a more sustained increase in NBCe1 current, and did not lead to an exponential current recovery following repolarization. Similar results were obtained with oocytes expressing a catalytically dead VSP mutant at all depolarized potentials. Depleting ER Ca^{2+} did not inhibit the NBCe1 current recovery following repolarization from VSP activation, demonstrating that changes in $InsP_3/Ca^{2+}$ were not responsible. This study demonstrates for the first time that depleting PIP_2 per se

inhibits NBCe1 activity. The data in conjunction with previous findings implicate a dual PIP_2 regulatory pathway for NBCe1 involving both PIP_2 itself and generated $InsP_3/Ca^{2+}$.

Abbreviations

I_{HCO3-}, HCO_3^--dependent current; IRBIT, $InsP_3$ receptor-binding protein released with $InsP_3$; mutVSP, C366S mutant VSP; NBCe1, electrogenic Na/bicarbonate cotransporter; PH-GFP, GFP conjugated to the pleckstrin homology of PLC-δ; PIP_2, phosphatidylinositol 4,5-bisphosphate; PLC, phospholipase C; VSP, voltage-sensitive phosphatase; wtVSP, wild-type VSP; % NBC_{depol}, percent of the initial depolarization-induced current; % NBC_{init}, percent of the initial NBC current before the depolarization pulse

Introduction

The electrogenic Na/bicarbonate cotransporter (NBCe1) regulates intracellular pH (pH_i) by moving 2 or 3 HCO_3^- ions (or $CO_3^{2-} \pm HCO_3^-$) for each Na^+ ion across the plasma membrane. In the process of regulating pH_i, NBCe1 also contributes to important solute handling and pH physiology of tissues. In many epithelia for instance, NBCe1 promotes absorption or secretion of solutes (Parker & Boron, 2013), including Na^+ and HCO_3^- reabsorption by the kidney proximal tubule (Boron & Boulpaep, 1983), HCO_3^- secretion by the pancreas (Muallem & Loessberg, 1990), and HCO_3^- secretion by both the proximal colon (Sullivan & Smith, 1986) and distal colon (Vidyasagar *et al.*, 2004). In the nervous system, NBCe1 modulates extracellular pH (pH_o) that impacts neuronal activity (Chesler, 1990, 2003; Ransom, 2000). Although NBCe1 is found in neurons (Svichar *et al.*, 2011), it is predominantly expressed in glial cells, such as astrocytes (Majumdar & Bevensee, 2010), where it responds to activity-evoked increases in extracellular potassium. Subsequent astrocyte depolarization stimulates NBC-mediated inward transport of HCO_3^-, thereby acidifying the extracellular space and dampening excessive neuronal activity.

At the molecular level, NBCe1 is a member of the bicarbonate-transporter gene superfamily (*slc4*) , which includes the anion exchangers (AE1-3), a borate transporter (BTR1), and the following Na-coupled bicarbonate transporters (NCBTs): the electrogenic NBCs (NBCe1 and NBCe2), the electroneutral NBCs (NBCn1 and NBCn2/NCBE), and the electroneutral Na-driven Cl-HCO_3 exchanger (NDCBE) (Parker & Boron, 2013). For nearly all of the NCBTs, alternative splicing produces proteins with different cytoplasmic amino (N) or carboxy (C) termini (Boron *et al.*, 2009; Parker &

Boron, 2013). There are 5 identified variants of NBCe1 (A-E). For the B, C, and E variants, 85 N-terminal residues replace the 41 different N-terminal residues of the A and D variants. The D and E variants are identical to the A and B variants, respectively, with the exception of a missing 9-amino acid cassette within the cytoplasmic N terminus. Although the physiological significance of such variants has yet to be fully elucidated, the alternative N terminus of the A vs. B/C variant confers different functional and regulatory properties. Regarding function for instance, the A variant with an autostimulatory domain (ASD) in its N terminus is more functionally active than the B/C variant with an autoinhibitory domain (AID) in its different N terminus (McAlear *et al.*, 2006). Regarding regulation, the inositol 1,4,5-trisphosphate ($InsP_3$) receptor-binding protein released with $InsP_3$ (IRBIT) stimulates NBCe1-B, but not NBCe1-A, by binding to its different N terminus and likely removing the AID (Shirakabe *et al.*, 2006; Parker *et al.*, 2007), at least in part (Lee *et al.*, 2012). IRBIT also stimulates NBCe1-C (Parker *et al.*, 2007; Thornell *et al.*, 2010; Yang *et al.*, 2011), presumably through the same mechanism.

Membrane phospholipids also influence NBCe1 activity. Although phosphatidylinositol 4,5-bisphosphate (PIP_2) comprises only 0.2-1% of total cellular phospholipids, its hydrolysis following receptor-mediated activation of phospholipase C generates the signaling molecules DAG and $InsP_3$ (Balla, 2013). Furthermore, PIP_2 is a signaling molecule itself and regulates many cellular processes, including plasma membrane dynamics (e.g., associated with endo/exocytosis and cell motility), cell adhesion, microtubule assembly, and the function of channels and transporters (Di Paolo & De Camilli, 2006; Balla, 2013). Previously, we found that PIP_2 stimulates NBCe1

current and reduces transporter rundown when applied to a macropatch of membrane from a *Xenopus laevis* oocyte expressing NBCe1-A (Wu *et al.*, 2009). However, direct PIP_2 stimulation of NBCe1 in the intact oocyte has been less apparent. Injecting PIP_2 into a whole oocyte stimulates the B and C variants, but not the A variant, mainly through PIP_2 hydrolysis to $InsP_3$, and requires intracellular Ca^{2+} release and a staurosporine-sensitive kinase (Thornell *et al.*, 2012). However, does PIP_2 directly stimulate the B and C variants independent of the $InsP_3/Ca^{2+}$ pathway in the intact cell? Such a direct effect may explain the modest ~25% stimulation of NBC current in the presence of a PLC inhibitor (Thornell *et al.*, 2012).

A direct PIP_2 effect is further supported by the recent finding that the delivery of PIP_2 by pipette (particularly in a Na^+-free solution) or as a histone-carrier complex stimulated NBCe1-B transiently transfected in HeLa cells (Hong *et al.*, 2013). However, these data on the HeLa cells might also be explained by an increase in $InsP_3/Ca^{2+}$ signaling. Indeed, the stimulation requires the N terminus of NBCe1-B (Hong *et al.*, 2013), although this requirement is also the case for $InsP_3/Ca^{2+}$ stimulation of the B and C variants (Thornell *et al.*, 2012). Furthermore, the A variant without this specific N terminus is stimulated by PIP_2 directly in the macropatch (Wu *et al.*, 2009). Therefore, the effect of intracellular PIP_2 per se on NBCe1 variant activity in the intact cell needs to be further evaluated.

For the current study, our goal was to examine PIP_2 regulation of NBCe1-B and -C activity in the intact oocyte, and independent of changes in $InsP_3/Ca^{2+}$. We were particularly interested in how NBCe1 activity is altered by a PIP_2 decrease, which is a more physiological change than an imposed PIP_2 increase. To decrease PIP_2, we

heterologously co-expressed a voltage-sensitive phosphatase (VSP) cloned from the sea squirt *Ciona intestinalis* (Murata *et al.*, 2005) along with NBCe1-B or -C in *Xenopus laevis* oocytes. VSP is a 5′-specific phosphatase (Iwasaki *et al.*, 2008; Halaszovich *et al.*, 2009). Upon activation by a threshold cell depolarization, VSP converts $PI(4,5)P_2$ to PI(4)P, and therefore decreases PIP_2 independent of PLC-mediated hydrolysis.

In 2-electrode voltage-clamp experiments, depolarizing oocytes co-expressing either NBCe1-B or -C, and either the wild-type VSP (wtVSP) or the catalytically dead C366S VSP mutant (mutVSP) elicited an expected NBC-mediated outward current. However, this NBC current was transient when wtVSP was activated by a pronounced depolarization to +60 mV known to activate VSP (Murata & Okamura, 2007). Subsequent repolarization to -60 mV caused a pronounced, transient decrease in the NBC current in oocytes co-expressing wtVSP vs. mutVSP, followed by an exponential NBC current recovery (τ = ~30 s). In voltage-clamp experiments with simultaneous PIP_2 fluorescence readings by confocal microscopy, the NBC current recovery mirrored PIP_2 regeneration at the plasma membrane with similar time constants. Longer VSP activation produced greater NBC current inhibition. Depleting ER Ca^{2+} stores did not affect the NBC current recovery, indicating that PIP_2 hydrolysis was not involved. In voltage-clamp experiments with simultaneous pH_i measurements, activated wtVSP at +20 mV inhibited the depolarization-stimulated, NBC-mediated pH_i recovery that was observed in other control experiments with mutVSP. These findings demonstrate unequivocally that both NBCe1-B and -C are PIP_2 sensitive. Furthermore, this is the first study to demonstrate that a decrease in PIP_2 inhibits NBCe1-B and -C in a whole cell.

Portions of this work have been published in preliminary form (Thornell & Bevensee, 2013).

Materials and Methods

Ethical Approval

The Institutional Animal Care and Use Committee (IACUC) at the University of Alabama at Birmingham reviewed and approved the protocol for harvesting oocytes from *Xenopus laevis* frogs. After a maximum of 3 surgeries, frogs were humanely euthanized.

Chemicals

All reagents were purchased from Sigma-Aldrich unless otherwise noted. The ND96 solution contained (in mM): 96 NaCl, 2 KCl, 1 $MgCl_2$, 1.8 $CaCl_2$, 5 HEPES, and 2.5 NaOH to pH 7.5. In 2-electrode, voltage-clamp experiments, the ND96 solution was bubbled with 21% O_2/balance N_2 to eliminate nominal levels of CO_2 and HCO_3^-. For the 5% CO_2-33 mM HCO_3^- solution (pH 7.5), 33 mM $NaHCO_3$ was replaced with an equimolar amount of NaCl, and the solution was equilibrated with 5% CO_2/95% O_2. In Ca^{2+}-free solutions, 1.8 mM $CaCl_2$ was replaced with 4 mM $MgCl_2$ and 1 mM EGTA.

Constructs and cRNA

Rat NBCe1-B and -C cDNAs were previously subcloned into the pTLNII oocyte-expression vector (McAlear *et al.*, 2006), which contains a *Mlu*I restriction site for linearization and an SP6 promotor for transcription. *Ciona intestinalis* VSP and the C366S mutant (provided by Y. Okamura, Osaka University, Osaka, Japan) were

previously subcloned into the pSD64TF oocyte-expression vector (Murata *et al.*, 2005; Murata & Okamura, 2007), which contains a *Not*I restriction site for linearization and an SP6 promotor site for transcription. GFP conjugated to the pleckstrin homology of PLC-δ (PH-GFP) was subcloned into the pGEMsh oocyte expression vector (both provided by D. Logothetis, Virginia Commonwealth University, Richmond, VA), which contains a *Spe*I restriction site for linearization and a T7 promotor for transcription. All restriction enzymes were purchased from New England BioLabs Inc. Linearized DNA was purified using the DNA Clean & Concentrator-5 Kit (Zymo Research), and then transcribed using either the SP6 or T7 transcription kit (Ambion Life Technologies). cRNA was purified using the RNeasy Mini kit (Qiagen).

Frog Oocytes

Oocytes were obtained from albino *Xenopus laevis* frogs (from Xenopus Express) as previously described (McAlear *et al.*, 2006; Thornell *et al.*, 2012). In brief, a female frog was anaesthetized (0.2% tricaine) and segments of the ovarian lobe were extracted from the abdominal cavity. The segments were teased apart into ~0.5 cm^2 pieces and subsequently digested for 1-2 h in sterile Ca^{2+}-free ND96 containing 2 mg ml^{-1} collagenase A (Roche). Oocytes were first washed in Ca^{2+}-free ND96, and then Ca^{2+}-containing ND96. Stage-V/VI oocytes were selected under a dissecting microscope (Leica). Oocytes were injected with cRNA in a volume of ~50 nl using a nanoinjector (Drummond), and then incubated in ND96 solution supplemented with 10 mM sodium pyruvate and 50 µg ml^{-1} gentamicin sulfate (Lonza) at 18°C for at least 2 days. In co-expressing experiments with 2 constructs, 250 ng ml^{-1} of each cRNA was injected. In co-

expressing experiments with 3 constructs for simultaneous voltage clamping and confocal imaging, 67 ng ml^{-1} of PH-GFP cRNA and ~170 ng ml^{-1} of each of the other two cRNAs were injected.

2-electrode Voltage-clamp Technique

Our approach for measuring NBC current using the 2-electrode voltage-clamp technique has been previously described (McAlear *et al.*, 2006; Liu *et al.*, 2007; Thornell *et al.*, 2012). Voltage-sensitive and current-passing electrodes were pulled from G83165T-4 borosilicate glass capillaries (Warner Instruments), filled with saturated KCl, and attached to an OC-725C amplifier (Warner Instruments). Signals were filtered at 10 Hz with an eight-pole LFP-8 Bessel filter (Warner Instruments). For gapfree experiments, the sampling frequency was 2 kHz and data were reduced by a factor of 100 using ClampFit (pCLAMP 8.2, Molecular Devices). In experiments with either wtVSP or mutVSP, the sampling frequency was ~400 Hz. The automated experimental protocol clamped an oocyte at -60 mV for 10 ms, then depolarized the cell (to either +60 mV, +20 mV, or -20 mV) for 10 s (except for Fig. 3 F), and finally returned the oocyte to -60 mV for ~3.75 min. Traces were data reduced by a factor of 10 for analysis. All data were acquired using ClampEx software (pClamp 8.2, Molecular Devices) and digitized using a 1322A digital to analog converter (Molecular Devices).

Oocytes were placed in a perfusion chamber (~500 µL volume) connected to a custom gravity-fed perfusion system. Solutions were controlled by a pair of six-way rotary valves that feed into a two-position, four-way Hamilton valve. The Hamilton valve allows the experimenter to alternate which rotary valve delivers solution to the chamber

while the other delivers to waste. Priming solution to waste before delivery assures properly equilibrated CO_2 solutions to the chamber. The rate of solution flow was 4-6 ml min^{-1}.

Simultaneous Confocal Imaging and 2-electrode Voltage Clamping

The aforementioned voltage-clamp setup was merged with a Nikon Eclipse TE2000-U inverted confocal microscope and fluorescence imaging. A coverslip formed the base of a RC-25 (Warner Instruments) perfusion chamber, and then a piece of appropriately sized mesh was secured by vacuum grease on the coverslip to stabilize oocytes. PH-GFP was excited with a 488 argon-krypton laser (Melles Griot) of a Perkin-Elmer ERS 6FE spinning disk confocal. Epifluorescence through a 10.5 mm long working distance 10× objective (0.25 NA; Nikon) was captured using a 525 (W50) bandpass filter and a CCD camera (Hamamatsu C9100). Imaging acquisition was controlled by Volocity software (v.6.1.1). Exposure time was set to 200 ms and laser intensity to 50%; sensitivity was adjusted to reach a sub-saturation count of ~14,000. The oocyte was imaged at the equator. Images were acquired at 0.1-1 Hz, except during rapid fluorescence changes (e.g., with VSP activation) when images were acquired at 3 Hz. Intensity-over-time plots were constructed with the Volocity software, and represent the mean fluorescence from a line region of interest (ROI) over the most stationary area of membrane and a background area. Plots were imported into Excel (Microsoft) for further analysis, including subtraction of background fluorescence.

Measurement of pH_i Under Voltage-clamp Conditions

Our approach has been previously described (Thornell *et al.*, 2012). pH-sensitive microelectrodes were fabricated from G200F-4 borosilicate glass capillaries (Warner Instruments) that were acid washed and baked at 200°C. Capillaries were subsequently pulled with a Brown-Flaming micropipette puller (P-80, Sutter Instruments Co.) and baked upright for at least 1 h. After capillaries were silanized with bis(dimethylamino)-dimethylsilane, the pipette tips were filled with hydrogen ionophore I-cocktail B and backfilled with a pH-7.0 solution containing (in mM): 150 NaCl, 40 KH_2PO_4, and 23 NaOH. pH electrodes were then connected to a FD223 high-impedance electrometer (WPI). The pH signal was obtained with a four-channel electrometer (Yale Biomedical Instrumentation Laboratory) that subtracts the potential from the voltage electrode from that of the pH electrode. The voltage signal was obtained from the 10× voltage output from the oocyte clamp after passing through a 10× voltage divider. Junction potentials were minimized by using 1-3% agar/saturated KCl bridges (fabricated from ~1 cm cut glass capillaries) between the virtual ground wires and bath solution. Digitized signals were acquired and analyzed using custom-designed software written by Mr. Duncan Wong for the WF Boron laboratory (previously at Yale U.). Before each experiment, the pH electrode was calibrated with pH-6 and -8 buffer solutions (Fisher Scientific).

Analysis

Data are reported as means ± SEM. Means between groups of data were compared using either ANOVA with Bonferroni correction or a *t*-test using Origin. $P \leq$

0.05 is considered significant. Figures were generated using Excel 2002 (Microsoft), except for scatterplots that were generated using Prism 5 (GraphPad). Intensity-over-time plots for imaging experiments were constructed in Volocity version 6.1.1 software (Perkin Elmer) and imported into Excel 2002 (Microsoft). Origin was used to fit the following first exponential association equation to both NBC current and PH-GFP fluorescence recoveries: $y = y_o + A\left(1 - e^{x/\tau}\right)$, where y is the instantaneous current or intensity, y_o is the current or intensity at time x, A is the amplitude of the fit, and τ is the time constant. A fast endogenous off current that rapidly decayed was seen in all +60-mV experiments; fitting to the markedly slower NBC current began at 3τ ($3 \times$ 25-30 ms) of this endogenous decay current. pH_i recovery rates were calculated as dpH_i/dt from a least-squares linear fit of pH_i vs. time using custom designed software (Mr. Duncan Wong in the WF Boron laboratory [previously at Yale Univ.]).

Results

Activating VSP Inhibits NBCe1-C

In our experiments, we evaluated the effect of lowering PIP_2 independent of $InsP_3$ generation on NBCe1 activity by using a VSP. In 2-electrode voltage-clamp experiments to measure NBC current, we co-injected oocytes with cRNA encoding NBCe1 and either wtVSP or the catalytically inactive mutVSP (with the single amino acid substitution C366S) for control experiments. VSP contains a voltage-sensing domain comprised of positive residues in a transmembrane domain (Fig. 1). VSP is minimally active at negative potentials (e.g., -60 mV) (Fig. 1A), but changes its conformation and becomes considerably more active at positive potentials (e.g., +60 mV) and dephosphorylates PIP_2

to PIP (Fig. 1C) (Murata & Okamura, 2007). A depolarization to +60 mV raises wtVSP's activation probability to ~40% (Murata & Okamura, 2007). We predicted that activated wtVSP would inhibit NBCe1 function through a decrease in PIP_2. The associated voltage-dependent conformational changes also occur with mutVSP, but the catalytically inactive phosphatase domain fails to dephosphorylate PIP_2 at either negative potentials (Fig. 1B) or positive potentials (Fig. 1D). We predicted that neither active nor inactive mutVSP would inhibit NBCe1 because PIP_2 levels would be unaffected. As such, experiments with mutVSP at each potential (in addition to inactive/weakly active wtVSP at negative potentials) served as controls.

Control oocytes co-expressing NBCe1-C and the catalytically inactive mutVSP were allowed to equilibrate with a 5% CO_2/33 mM HCO_3^- solution for 5 min while voltage clamped to -60 mV (Fig. 2A). For each group, grey traces represent individual experiments and the black trace represents their mean. In separate experiments, depolarizing oocytes to -20 mV (left panel), +20 mV (middle panel), or +60 mV (right panel) for 10 s elicited outward currents that were progressively larger with greater depolarizations. These outward currents were much smaller for the same oocytes initially bathed in ND96 (Fig. 2B). For each oocyte, we subtracted the ND96 current trace (Fig, 2B) from the corresponding HCO_3^- trace (Fig. 2A) to compute the HCO_3^--dependent current trace (Fig. 2C).

We repeated this experimental protocol on oocytes co-expressing NBCe1-C and wtVSP in both the presence and absence of CO_2/HCO_3^-. Similar to control experiments with mutVSP, progressively greater depolarizations produced progressively larger outward currents, and these currents were larger in CO_2/HCO_3^- (Fig. 2D) than ND96

(Fig. 2E). The HCO_3^--dependent traces are presented in Fig. 2F. There were two notable observations when comparing the HCO_3^--dependent traces from oocytes co-expressing mutVSP (Fig. 2C) vs. wtVSP (Fig. 2F). First, the HCO_3^--dependent currents induced by depolarization to -20 mV for mutVSP (Fig. 2C; left panel) and wtVSP (Fig. 2F; left panel) were similar. This observation is not surprising because -20 mV does not appreciably activate VSP. The second more striking observation is that for HCO_3^--dependent current, currents induced by depolarizations to positive potentials for wtVSP (Fig. 2F; middle and right panels) vs. mutVSP (Fig. 2C, middle and right panels) were only transient and decayed rapidly. The transient nature of these outward currents is consistent with VSP-induced inhibition of NBC.

To determine and characterize the NBCe1-specific currents from Fig.-2 experiments, we also needed to subtract the corresponding endogenous HCO_3^--dependent currents seen in the absence of NBCe1. Therefore, we performed similar experiments and analyses on control oocytes injected with water (instead of NBCe1 cRNA) and either wtVSP (Fig. 3A-C) or mutVSP cRNA (Fig. 3D-F). We found that wtVSP-expressing oocytes depolarized to +20 mV elicited unexplained CO_2/HCO_3^--dependent inward currents that were large and variable. Thus, for the remainder of this manuscript we focus on the currents obtained at -20 and +60 mV— potentials where the endogenous currents are smaller and less variable.

Subtracting the mean HCO_3^--dependent current traces obtained from wtVSP- or mutVSP-expressing oocytes without NBCe1 (Fig. 3C and 3E) from individual HCO_3^--dependent current traces with NBCe1 (Fig. 2C and 2E) yielded NBC-specific current traces. These control and NBCe1 data were obtained from the same oocyte batches.

Traces are reported as the % of the initial NBC current before the depolarization pulse (% NBC_{init}), and are shown for +60 mV (Fig. 4A) and -20 mV (Fig. 4B). As shown in Fig. 4A, depolarizing wtVSP-expressing oocytes to +60 mV (a potential where ~40% of the VSPs are active [Murata and Okamura, 2007]) momentarily increased the mean % NBC_{init} to ~330%, followed by a rapid decay to only ~130% after 10 s (Fig. 4A; black trace) as activated VSP inhibited NBC. Repolarizing oocytes to -60 mV caused % NBC_{init} to decrease to ~25%, and then to exhibit a slow single-exponential recovery, presumably due to PIP_2 re-synthesis in the plasma membrane (Falkenburger *et al.*, 2010; Sakata *et al.*, 2011). In control mutVSP experiments (Fig. 4A; grey trace), there was a sustained depolarization-induced increase in mean % NBC_{init} to ~300%, but without the subsequent decay, and no repolarization-induced exponential recovery. Smaller depolarizations that did not appreciably activate wtVSP did not elicit the % NBC_{init} decay seen in Fig. 4A. For example, a depolarization to -20 mV (a potential where VSPs are relatively inactive [Murata and Okamura, 2007]) increased the mean % NBC_{init} that was sustained and no different with either wtVSP (Fig. 4B; black trace) or mutVSP (Fig. 4B; grey trace). From the current traces used to generate Fig. 4A and B, we calculated the NBC current remaining at the end of the 10-s depolarization phase as a % of the initial depolarization-induced current (% NBC_{depol}). According to the summary data presented in Fig. 4C, only the +60 mV depolarization that activated wtVSP reduced the mean % NBC_{depol} to 39.4 ± 5.2% ($P < 0.001$, $n = 7$). In these +60 mV experiments, the slow recovery following the repolarization was fit by a single exponential function with a mean τ of 29.3 ± 1.5 s ($n = 7$). A representative trace and fit are shown in Fig. 4D. Extrapolating the fits to the moment of repolarization yielded a mean % NBC_{init} of 33.7 ± 3.5%, which is no different

than the mean % NBC_{depol} of ~39% in Fig. 4C (P = 0.06). Furthermore, for all similar water-subtracted NBC data presented in this manuscript, the % NBC_{depol} of 37.8 ± 5.7% was no different than the % NBC_{init} of 35.2 ± 6.1% back extrapolated from the repolarization phase (P = 0.53; *n* = 17). A plot of % NBC_{depol} vs. % NBC_{init} back extrapolated to the moment of repolarization (Fig. 4E) reveals a slope of near unity (0.93), which indicates that NBC inhibition is approximately the same at +60 mV and at -60 mV (i.e., immediately before and following repolarization). However, there is some variability with this correlation (R^2 = 0.18) that likely arises from subtracting mean currents from a group of water-injected oocytes to calculate NBC currents from individual oocytes. In summary, VSP activation that decreases PIP_2 inhibits NBCe1-C activity, as evident by a decrease in % NBC_{init} during depolarization, as well as a recovery of % NBC_{init} following repolarization.

We next explored the possibility that varying the duration of the +60 mV depolarization (and hence extent of PIP_2 degradation) would influence the degree of NBCe1 inhibition. Therefore, we repeated Fig. 4A-type experiments on NBCe1-C with wtVSP, but varied the duration of the depolarization from 1 s to 30 s, and then calculated % NBC_{init} back extrapolated to the moment of repolarization. Because currents following repolarization in control water-injected oocytes are minimal (Fig. 3), we analyzed the un-subtracted HCO_3^--dependent recoveries. The 1-s depolarization protocol did not generate an exponential current recovery (not shown). For protocols with longer depolarizations, there was an inverse relationship between the depolarization duration and NBC activity (Fig. 4F). Thus, longer depolarizations that reduced PIP_2 to a greater extent inhibited more NBC activity.

We have previously shown that injecting PIP_2 into a whole oocyte stimulates NBCe1-B and -C through PLC-mediated PIP_2 hydrolysis to $InsP_3/Ca^{2+}$ (Thornell *et al.*, 2012). We therefore considered the possibility that the observed wtVSP-mediated changes in NBCe1 activity seen in Fig. 4 are caused by altered ambient $InsP_3$ levels rather than changes in PIP_2 per se. If so, then our previously used thapsigargin/0 Ca^{2+}/EGTA protocol to deplete ER Ca^{2+} (Thornell *et al.*, 2012) should inhibit the NBCe1 current recovery following repolarization from wtVSP activation. However, as shown in Fig. 4G, oocytes preincubated in 0 Ca^{2+}/EGTA and either thapsigargin (which depletes ER Ca^{2+}) or DMSO exhibited similar recoveries of % NBC_{init} following repolarization as seen under control conditions (Fig. 4D).

Activating VSP Inhibits NBCe1-B.

Fig.-2 experiments and Fig.-4 analyses were also performed on NBCe1-B-expressing oocytes, and nearly identical results were obtained. Depolarizing wtVSP-expressing oocytes to +60 mV produced a transient increase in mean % NBC_{init} followed by a rapid decay (Fig. 5A; black trace); only a sustained increase was observed in depolarized mutVSP-expressing oocytes (Fig. 5A; grey trace). Following the repolarization to -60 mV, a slow single-exponential recovery of the mean % NBC_{init} was evident for oocytes co-expressing wtVSP (Fig. 5A; black trace), but not mutVSP (Fig. 5A; grey trace). The smaller depolarization to -20 mV elicited a relatively sustained increase in the mean % NBC_{init} that was similar with wtVSP (Fig. 5B; black trace) and mutVSP (Fig. 5B; grey trace). According to the summary data presented in Fig. 5C, only the +60 mV depolarization that activated wtVSP reduced the mean % NBC_{depol} to 35.2 ±

6.1% ($P < 0.001$, $n = 5$). In these +60 mV experiments, a single exponential fit to the slow recovery following repolarization had a mean τ of 30.2 ± 1.5 s. A representative trace and fit are shown in Fig. 5D. Extrapolating the fits to the moment of repolarization yielded a mean % NBC_{init} of 37.9 ± 5.7% ($n = 5$), which is no different than the corresponding mean % NBC_{depol} ($P = 0.67$). % NBC_{depol} vs. % NBC_{init} at repolarization for the NBCe1-B-expressing oocytes are included in Fig. 4E as discussed above. In summary, VSP activation, which decreases PIP_2, inhibits both NBCe1-B and -C.

Activating/inactivating VSP Causes Parallel Changes in Plasma-membrane PIP_2 and NBCe1 Activity

The results from our previous experiments are consistent with a VSP-induced decrease in PIP_2 inhibiting NBCe1 activity at the plasma membrane. If so, then changes in membrane PIP_2 should parallel changes in NBCe1 activity. We therefore simultaneously used confocal imaging with a PIP_2-reporting fluorophore (PH-GFP) and the voltage-clamp technique to correlate changes in plasma-membrane PIP_2 and NBCe1 currents. Experiments were performed on oocytes co-expressing NBCe1-C, PH-GFP, and either wtVSP or mutVSP. Oocytes co-expressing NBCe1-C and wtVSP exhibited a decrease in plasma membrane PH-GFP when depolarized from -60 mV to +60 mV (Fig. 6A; first pair of images), but not to -20 mV (Fig. 6A; second pair of images). Such a decrease in PH-GFP was not observed in oocytes co-expressing NBCe1-C and mutVSP with either voltage change (Fig. 6A; bottom 2 pairs of images). As an aside, we noticed that the PH-GFP fluorescence signal progressively increased with time after cRNA injection (even over the course of a single day), and correlated with a decrease in the

percentage of VSP-activated probe translocation. This observation is consistent with a progressive increase in PH-GFP background fluorescence either at or near the plasma membrane.

From Fig. 6A-type experiments, we correlated the PH-GFP fluorescence intensity at the plasma membrane (top trace) with the whole-cell current (bottom trace) in the same oocyte (Fig. 6B). For the oocyte in the ND96 solution, depolarization to +60 mV for 10 s elicited a decrease in membrane fluorescence, followed by a recovery after repolarization. Switching to the CO_2/HCO_3^- solution caused a slight decrease in fluorescence (perhaps due altered pH_i and pH sensitivity of PH-GFP), and elicited the expected NBCe1-mediated outward current. The subsequent depolarization to +60 mV caused a simultaneous decrease in membrane fluorescence, as well as a transient increase in outward current (arrow) as shown in Figs. 4 and 5. Immediately after repolarization, both the membrane fluorescence and current decreased, and then slowly recovered with similar time courses.

In control experiments performed on oocytes co-expressing NBCe1-C and mutVSP, depolarization to +60 mV had little effect on the membrane fluorescence, and caused a sustained outward current (arrow) without the pronounced exponential recovery following repolarization (Fig. 6C). Not surprisingly, and in agreement with Figs. 4B and 5B, depolarizing oocytes co-expressing NBCe1-C and either wtVSP or mutVSP to -20 mV had little effect on membrane fluorescence, and elicited a sustained outward current (arrow) without any current recovery after repolarization (Fig. 6D and E). According to results from similar experiments performed on oocytes co-injected with water (Fig. 6F-I), only wtVSP-expressing oocytes depolarized to +60 mV elicited a transient decrease in

fluorescence (Fig. 6F). No depolarization-induced NBC current or subsequent repolarization-stimulated recovery was evident in any of these water-injected oocytes.

Using the approach outlined for Figs. 4 and 5, we computed the NBCe1 current recovery following the repolarization from +60 mV, and plotted the % NBC_{init} shown in Fig. 6J for a single experiment. The mean time constant for six similar experiments was 42.8 ± 3.6 s. We also plotted the corresponding time course of the PH-GFP fluorescence recovery for oocytes bathed in either the absence (not shown) or presence of the HCO_3^- solution for the same experiment (Fig. 6K). For the six experiments combined, the mean time constants were 52 ± 6.8 s in the absence of HCO_3^-, and 43.8 ± 4.5 s in the presence of HCO_3^-. Fluorescence changes were typically smaller in the absence vs. presence of HCO_3^-, perhaps due to a CO_2/HCO_3^--mediated pH_i effect on PH-GFP fluorescence. The mean time constants for these three data sets (Fig. 5L) were not significantly different (P = 0.37). In summary, the NBCe1-C current recovery following wtVSP inactivation (from a +60 mV depolarization) paralleled the PIP_2 recovery at the membrane.

Activating VSP Inhibits NBCe1-C-mediated pH_i Changes

Because NBCe1 transports HCO_3^- and changes pH_i, we examined the effect of the VSP-induced PIP_2 decrease on the NBCe1-mediated pH_i recovery in oocytes exposed to CO_2/HCO_3^-. We measured pH_i using ion-sensitive microelectrodes while holding oocytes at either -60 mV or +20 mV (to activate wtVSP). The depolarization to +20 mV is expected to increase the NBCe1-mediated pH_i recovery in the absence of a functional VSP (i.e., with mutVSP that serves as our positive control). However, in light of our voltage-clamp data presented above, this stimulation should be blunted in the presence of

a functional VSP (i.e., wtVSP). For oocytes initially held at -60 mV and co-expressing NBCe1-C and either mutVSP (grey trace) or VSP (black trace), switching from ND96 to the CO_2/HCO_3^- solution (arrow) elicited an initial pH_i decrease due to the influx of CO_2, followed by a slower pH_i increase due to NBCe1 activity (Fig. 7A). Such NBCe1-mediated pH_i recoveries have been well characterized (Parker and Boron, 2013). After a constant pH_i-recovery rate was established, each oocyte was then depolarized to +20 mV, which stimulated the pH_i-recovery rate to a greater extent in the oocyte co-expressing mutVSP than wtVSP. pH_i-recovery rates (dpH_i/dt) from panel A-type experiments are summarized in Fig. 7B. dpH_i/dt from oocytes co-expressing mutVSP or wtVSP were no different at the initial potential of -60 mV ($P = 0.86$). However, depolarization to +20 mV stimulated the mean dpH_i/dt from $17 \pm 2 \times 10^{-5}$ pH units s^{-1} to $31 \pm 4 \times 10^{-5}$ pH units s^{-1} with mutVSP ($P < 0.001$, $n = 8$), but failed to stimulate the mean dpH_i/dt ($17 \pm 2 \times 10^{-5}$ pH units s^{-1} or $19 \pm 3 \times 10^{-5}$ pH units s^{-1}) with wtVSP ($P = 0.28$, $n = 7$). Oocytes co-injected with H_2O and either mutVSP or wtVSP exhibited minimal mean dpH_i/dts at -60 mV or +20 mV (Fig. 7C). Thus, a VSP-induced decrease in PIP_2 not only inhibits NBCe1-mediated currents, but also inhibits the NBCe1-mediated pH_i recovery from a CO_2-induced acid load.

Discussion

General Findings

In this study, we explored the effect of selectively decreasing PIP_2 on the activity of NBCe1-B/C heterologously expressed in oocytes by co-expressing wtVSP that dephosphorylates PIP_2 to PIP. We conclude that PIP_2 is required for NBCe1-B/C activity based on the following observations:

(1) For oocytes co-expressing NBCe1 and wtVSP, a depolarization to +60 mV that raises wtVSP's activation probability to ~40% (Murata & Okamura, 2007) caused a transient stimulation of NBCe1 current, followed by a pronounced inhibition (Figs. 4A, C and 5A, C; black traces). A depolarization to -20 mV that does not appreciably alter wtVSP's activation probability caused a more sustained stimulation (Figs. 4B, C and 5B, C; black traces).

(2) Depolarization-induced inhibition of NBCe1 in oocytes co-expressing VSP requires a catalytically active VSP. Indeed, a sustained NBCe1 current stimulation without the subsequent inhibition was observed with the catalytically dead mutVSP at all voltages tested (Figs. 4A-C and 5A-C; grey traces).

(3) For oocytes expressing NBCe1 and wtVSP, repolarization from +60 mV back to -60 mV caused a transient decrease followed by a slow recovery of the initial steady-state NBCe1 current (Figs. 4D and 5D). This repolarization-induced recovery was minimal with wtVSP-expressing oocytes first depolarized to only -20 mV (Figs. 4B and 5B; black traces), or mutVSP-expressing oocytes first depolarized to any of the voltages tested (Figs. 4A, B and Figs. 5A, B; grey traces).

(4) The time course of the NBCe1 current recovery following repolarization correlated with the time course of PIP_2 recovery at the plasma membrane (Fig. 6B and J-L). In these experiments, our PIP_2 recovery time constants of ~52 s (in ND96) and ~44 s (in HCO_3^-) are similar to ~45 s previously reported for *Xenopus* oocytes under similar conditions

with the two-electrode voltage-clamp technique (Sakata *et al.*, 2011). For reasons that are not entirely clear, Sakata *et al.* (Sakata *et al.*, 2011) obtained shorter time constants (~16 s) in patch-clamp studies on the oocytes. The faster recovery in these patch studies could in part be due to localized VSP activation and lateral diffusion of unaffected PIP_2 (Sakata *et al.*, 2011). Shorter time constants have also been reported with mammalian cells (Falkenburger *et al.*, 2010). Differences in techniques (spatial voltage clamp) and PI5K activity (Sakata *et al.*, 2011) may account for these different time constants in the oocyte and mammalian cells.

(5) VSP-mediated effects appear independent of changes in $InsP_3/Ca^{2+}$ because NBC current recoveries following repolarization were observed in oocytes depleted of ER Ca^{2+} (Fig. 4G).

(6) A depolarization-stimulated, NBCe1-mediated pH_i recovery from a CO_2-induced acid load was inhibited by activated wtVSP, but not mutVSP (Fig. 7A, B).

Based on the aforementioned points, we conclude that $PI(4,5)P_2$ itself regulates NBCe1-B and -C, with a decrease in PIP_2 inhibiting transporter activity in the intact cell. We cannot rule out the involvement of PIP_3, which activated VSP (a 5′ phosphatase) would dephosphorylate to a different form of PIP_2— $PI(3,4)P_2$ (Iwasaki *et al.*, 2008; Halaszovich *et al.*, 2009). However, an appreciable VSP-induced PIP_3 decrease in oocytes is only evident after an insulin-induced PIP_3 increase as monitored by translocation of the PIP_3–specific probe PH_{Btk}-GFP (Murata & Okamura, 2007). In

agreement with a minimal contribution of baseline PIP_3, preliminary macropatch data (unpublished data) demonstrate that a low concentration of PIP_3 (e.g., 1 μM) does not stimulate NBCe1-A (and 10 μM $PI(3,4)P_2$ is less effective than $PI(4,5)P_2$ in stimulating the transporter). Thus, $PI(4,5)P_2$ vs. PIP_3 is likely the dominant regulator of NBCe1 in these here experiments.

Endogenous Current

In our study, VSP activation required large cell depolarizations, which we expected would elicit endogenous currents. Thus, we performed many control experiments on oocytes expressing wtVSP or mutVSP alone to determine any NBCe1-independent HCO_3^--dependent current, which we then subtracted from the corresponding currents obtained from NBCe1-expressing oocytes (Fig. 3). There are three notable observations about the endogenous current in our assay. First, the current is voltage-activated and CO_2/HCO_3^--dependent, but its specific identity remains to be determined. Curiously, this CO_2/HCO_3^--dependent endogenous current on average was larger at +20 mV than +60 mV. Second, this endogenous current was transient in oocytes expressing wtVSP, and therefore also sensitive to PIP_2. Finally, upon oocyte repolarization from +60 mV back to -60 mV, the reversal of this current coincided with a fast transient inward current (Fig. 3) with a time constant (τ_{endo}) of 25-30 ms that was VSP-independent (i.e., observed in oocytes expressing either wtVSP or mutVSP) and reminiscent of a tail current. In corresponding NBCe1-expressing oocytes, we were careful to begin each exponential fit to an NBCe1-dependent current recovery at $3\times\tau_{endo}$ following repolarization.

PIP_2 Regulation of NBCe1 Activity: Permissive vs. Signaling Role

According to our data, PIP_2 per se is required for NBCe1 activity, and independent of changes in $InsP_3/Ca^{2+}$. However, our study doesn't address PIP_2's mode of regulation, and whether PIP_2 plays either an 'on/off' permissive role or a more dynamic signaling role, as discussed for ENaC (Ma *et al.*, 2007). The K_M for PIP_2 would be expected to be relatively low in a permissive role (and NBCe1 fully active unless PIP_2 decreases significantly), but higher and closer to a physiological concentration in a signaling role (and NBCe1 activity more dynamically altered by small changes in PIP_2). Although our results do not directly distinguish between these two possibilities, they do expand on our previous findings (Thornell *et al.*, 2012) in providing some insight. Previously, we increased intracellular PIP_2 by injecting PIP_2 into NBCe1-expressing oocytes after PLC inhibition (to eliminate PIP_2 hydrolysis). We found that the injected PIP_2 modestly stimulated all three variants by ~25%. The stimulation of NBCe1-A was particularly informative because this variant is not stimulated by the $InsP_3/Ca^{2+}$ pathway. This modest PLC-independent PIP_2 stimulation indicates that the transporter's K_M for PIP_2 is likely below the ambient plasma membrane PIP_2 level, which is probably near the upper end of the dose-response profile. These findings are consistent with PIP_2 playing a dynamic signaling role in regulating NBCe1, especially with decreases in PIP_2. It is interesting to note that the phosphates at positions 4 and 5 of PIP_2 have pK_a values (6.7, 7.7) in the physiological range (McLaughlin *et al.*, 2002). Perhaps at least some pH sensitivity of NBCe1 is mediated by pH-induced conformational changes of PIP_2 that modulate transporter activity. The physiological significance of such regulation is discussed further below.

Mechanism of PIP_2 Regulation of NBCe1

PIP_2 regulation of NBCe1 could be either indirect or direct. An indirect interaction may involve PIP_2 interacting with an auxiliary protein that directly stimulates NBCe1. Proteins that directly interact with NBCe1 include IRBIT (Shirakabe *et al.*, 2006) and the microsomal-associated protein chaperone stress 70 protein (Bae *et al.*, 2013), although neither protein has been shown to bind PIP_2. IRBIT is discussed further below.

A direct interaction could involve PIP_2 binding to a region of basic amino acids often found in proteins with Pleckstrin homology domains (McLaughlin *et al.*, 2002). Such binding accounts for PIP_2 regulation of other channels and transporters, including specific K^+ channels (Hansen *et al.*, 2011; Whorton & Mackinnon, 2011) and the Na-H exchanger NHE1 (Barret *et al.*, 2000). The following four candidate regions of NBCe1-A, -B, and -C are putative PIP_2 binding sites: KDKKKKEDEKKKKKKK at the cytosolic C terminus of these 3 NBCe1 variants (*Region 1*), RRRRRHKRK at the cytosolic N terminus of the B and C variants, but not the A variant (*Region 2*), RKHRH in the cytosolic N terminus of these 3 variants (*Region 3*), and RKEHKLKK before transmembrane domain 8 of these 3 variants (*Region 4*). In preliminary studies, NBCe1 mutants devoid of the first 5 K, the last 7 K, or all 12 K within *Region 1* still exhibited PIP_2 sensitivity in oocytes co-expressing VSP (unpublished data). *Region 2* does not appear to be involved because an N terminal truncation of NBCe1 (ΔN43) lacking this region is still inhibited by activated VSP (unpublished data). Hong et al. have recently reported that a trimer of Arg in *Region 2* is required for both PIP_2 and IRBIT (WNK/SPAK) regulation of NBCe1-B transiently transfected into HeLa cells. Although

we are in agreement that this region is required for IRBIT regulation of NBCe1-B/C (Thornell *et al.*, 2010), we believe that the binding sites for PIP_2 and IRBIT are distinct. This region is not found in NBCe1-A, which is stimulated by PIP_2 (Wu *et al.*, 2009). An alternative explanation for PIP_2 stimulation of NBCe1-B reported by Hong et al. is involvement of the $InsP_3/Ca^{2+}$ pathway. Indeed, we find that ΔN43 is not stimulated by injected PIP_2 (Thornell *et al.*, 2010), which activates wild-type NBCe1-B/C through hydrolysis to $InsP_3/Ca^{2+}$ (Thornell *et al.*, 2012). Furthermore, the stimulatory effect of this injected PIP_2 on wild-type NBCe1-B/C is inhibited by IRBIT overexpression (Thornell *et al.*, 2010).

PIP_2 binding to *Regions 3* and *4* of NBCe1 have yet to be explored. *Region 4* is near TMD 8 that contributes to the ion translocation pathway (McAlear & Bevensee, 2006). If PIP_2 binds to this region, then it may modulate ion accessibility of the translocation pathway. *Region 4* also contains an intracellular binding site for DIDS, raising the possibility that DIDS may disrupt PIP_2 binding and regulation. Further studies are required to explore the potential involvement of one or more of the aforementioned putative PIP_2-binding sites.

Physiological Relevance: PIP_2 vs. $InsP_3/Ca^{2+}$

Collectively, our work (Wu, 2009, Thornell et al., 2012, this study) and that of Hong et al. (Hong et al., 2013) provide evidence that PIP_2 itself stimulates NBCe1-A, -B, and -C, and PIP_2 hydrolysis to $InsP_3$ with subsequent Ca^{2+} release stimulates the B and C variants. What is the physiological relevance of this dual regulation, and which pathway dominates? The answers may lie in a similar dual regulatory PIP_2 pathway that exists for

the KCNQ-mediated M current. In superior cervical ganglion cells, activating an endogenous G_q-coupled receptor inhibits the M current through either a Ca^{2+}-dependent mechanism (Gamper *et al.*, 2004) or a PIP_2-dependent mechanism (Suh & Hille, 2002; Zhang *et al.*, 2003; Winks *et al.*, 2005). The Ca^{2+}-dependent mechanism involves PIP_2 hydrolysis to $InsP_3$ and subsequent Ca^{2+} release from nearby intracellular stores (Zaika *et al.*, 2011). There is no appreciable drop in PIP_2 because the Ca^{2+} release stimulates Ca^{2+}-activate PI4K, which rapidly resynthesizes PIP_2 in the membrane (Zaika *et al.*, 2011). In contrast, the PIP_2-dependent mechanism involves PIP_2 hydrolysis to $InsP_3$, but no subsequent Ca^{2+} release because of the absence of nearby intracellular stores or IRBIT competition for $InsP_3$ receptors. Without Ca^{2+} activation of PI4K, the PIP_2 level falls and is not rapidly replenished (Zaika *et al.*, 2011). The mechanism that dominates depends on the degree of G_q receptor activation as determined by ligand concentration and receptor density rather than dissimilar G_q subunit signaling (Dickson *et al.*, 2013; Falkenburger *et al.*, 2013). Further experiments are required to determine if a similar differential response and mechanistic basis is responsible for PIP_2-$InsP_3$/Ca^{2+} regulation of NBCe1, particularly in a native environment. Such a dual regulatory pathway following G_q activation would lead to either NBCe1 activation by $InsP_3$/Ca^{2+} or inhibition by PIP_2 hydrolysis.

Alternatively, $InsP_3$/Ca^{2+} stimulation of NBCe1 may be the dominant regulatory pathway with G_q activation (as seen in oocytes, Thornell et al., 2012), and PIP_2 regulation may occur under more specific conditions. In one example proposed by Hilgemann (Hilgemann et al., 2001), the PIP_2 requirement may serve to inactivate newly synthesized channels and transporters as they traffic through PIP_2-barren organellar membranes to the

PIP_2-containing plasma membrane (Hilgemann et al., 2001). It is perhaps logical for a plasma-membrane acid-base transporter such as NBCe1 to remain inactive during its maturation through organellar membranes. In another example, PIP_2 regulation of NBCe1 may be particularly important during pathological conditions such as ischemia or hypoxia that deplete cellular energy sources. Decreases in ATP that in turn reduce PIP_2 levels and inhibit NBCe1 may be protective in delaying or minimizing large increases in intracellular Na^+ that can promote intracellular Ca^{2+} overload and cellular damage. As such, PIP_2 may function as an energy sensor that regulates NBCe1 activity. Overall, given the myriad of G_q receptors and mechanisms that alter PIP_2 and/or $InsP_3/Ca^{2+}$ levels, associated regulation of NBCe1 and corresponding changes in pH are likely to have a significant impact on many subsequent cellular responses.

Author Contributions

All experiments were performed in the laboratory of Mark O. Bevensee in the Department of Cell, Developmental and Integrative Biology at the University of Alabama at Birmingham. The authors contributed the following ways. IMT: data collection. IMT and MOB: experimental conception design, data analysis and interpretation, manuscript drafting and editing. All authors approved the final version of the manuscript.

Funding

This work was supported by an award from the NIH/NINDS (R01 NS046653 to M.O.B.), and by an award from the NIH/NIGMS (T32 GM008111 to

I.M.T.). This work was supported by an award from the American Heart Association (Southeast Affiliate, 0755255B to M.O.B.). The authors declare no competing interests.

Acknowledgements

We thank Dr. Yasushi Okamura (Department of Integrative Physiology, Osaka University) for providing the wtVSP and mutVSP constructs, and Dr. Diomedes E. Logothetis (Department of Physiology and Biophysics, Virginia Commonwealth University) for providing the PH-GFP construct. We also thank Dr. Bradley K. Yoder, Dr. Erik B. Malarkey, and Wesley R. Lewis (Department of Cell, Developmental and Integrative Biology, University of Alabama at Birmingham) for generous use and assistance with their confocal microscope. We thank Dr. Mark Parker (Department of Physiology and Biophysics, University at Buffalo) for providing a batch of oocytes and sharing information.

References

Bae JS, Koo NY, Namkoong E, Davies AJ, Choi SK, Shin Y, Jin M, Hwang SM, Mikoshiba K & Park K (2013). Chaperone stress 70 protein (STCH) binds and regulates two acid/base transporters NBCe1-B and NHE1. *J Biol Chem* **288,** 6295–6305.

Balla T (2013). Phosphoinositides: tiny lipids with giant impact on cell regulation. *Physiol Rev* **93,** 1019–1137.

Barret C, Roy C, Montcourrier P, Mangeat P & Niggli V (2000). Mutagenesis of the phosphatidylinositol 4,5-bisphosphate (PIP_2) binding site in the NH_2-terminal domain of ezrin correlates with its altered cellular distribution. *J Cell Biol* **151,** 1067–1080.

Boron WF & Boulpaep EL (1983). Intracellular pH regulation in the renal proximal tubule of the salamander basolateral HCO_3^- transport. *J Gen Physiol* **81,** 53–94.

Boron WF, Chen L & Parker MD (2009). Modular structure of sodium-coupled bicarbonate transporters. *J Exp Biol* **212,** 1697–1706.

Chesler M (1990). The regulation and modulation of pH in the nervous system. *Prog Neurobiol* **34,** 401–427.

Chesler M (2003). Regulation and modulation of pH in the brain. *Physiol Rev* **83,** 1183–1221.

Dickson EJ, Falkenburger BH & Hille B (2013). Quantitative properties and receptor reserve of the IP_3 and calcium branch of G_q-coupled receptor signaling. *J Gen Physiol* **141,** 521–535.

Falkenburger BH, Dickson EJ & Hille B (2013). Quantitative properties and receptor reserve of the DAG and PKC branch of G_q-coupled receptor signaling. *J Gen Physiol* **141,** 537–555.

Falkenburger BH, Jensen JB & Hille B (2010). Kinetics of PIP_2 metabolism and KCNQ2/3 channel regulation studied with a voltage-sensitive phosphatase in living cells. *J Gen Physiol* **135,** 99–114.

Gamper N, Reznikov V, Yamada Y, Yang J & Shapiro MS (2004). Phosphatidylinositol 4,5-bisphosphate signals underlie receptor-specific $G_{q/11}$-mediated modulation of N-type Ca^{2+} channels. *J Neurosci* **24,** 10980–10992.

Halaszovich CR, Schreiber DN & Oliver D (2009). Ci-VSP is a depolarization-activated phosphatidylinositol-4,5-bisphosphate and phosphatidylinositol-3,4,5-trisphosphate 5'-phosphatase. *J Biol Chem* **284,** 2106–2113.

Hansen SB, Tao X & MacKinnon R (2011). Structural basis of PIP_2 activation of the classical inward rectifier K^+ channel Kir2.2. *Nature* **477,** 495–498.

Hong JH, Yang D, Shcheynikov N, Ohana E, Shin DM & Muallem S (2013). Convergence of IRBIT, phosphatidylinositol (4,5) bisphosphate, and WNK/SPAK kinases in regulation of the Na^+-HCO_3^- cotransporters family. *Proc Natl Acad Sci USA* **110,** 4105–4110.

Iwasaki H, Murata Y, Kim Y, Hossain MI, Worby CA, Dixon JE, McCormack T, Sasaki T & Okamura Y (2008). A voltage-sensing phosphatase, Ci-VSP, which shares sequence identity with PTEN, dephosphorylates phosphatidylinositol 4,5-bisphosphate. *Proc Natl Acad Sci USA* **105,** 7970–7975.

Kao L, Sassani P, Azimov R, Pushkin A, Abuladze N, Peti-Peterdi J, Liu W, Newman D & Kurtz I (2008). Oligomeric structure and minimal functional unit of the electrogenic sodium bicarbonate cotransporter NBCe1-A. *J Biol Chem* **283,** 26782–26794.

Lee SK, Boron WF & Parker MD (2012). Relief of autoinhibition of the electrogenic Na-HCO_3 cotransporter NBCe1-B: role of IRBIT vs.amino-terminal truncation. *Am J Physiol Cell Physiol* **302,** C518–26.

Liu X, Williams JB, Sumpter BR & Bevensee MO (2007). Inhibition of the Na/bicarbonate cotransporter NBCe1-A by diBAC oxonol dyes relative to niflumic acid and a stilbene. *J Membr Biol* **215,** 195–204.

Ma HP, Chou CF, Wei SP & Eaton DC (2007). Regulation of the epithelial sodium channel by phosphatidylinositides: experiments, implications, and speculations. *Pflügers Arch* **455,** 169–180.

Majumdar D & Bevensee MO (2010). Na-coupled bicarbonate transporters of the solute carrier 4 family in the nervous system: function, localization, and relevance to neurologic function. *Neuroscience* **171,** 951–972.

McAlear SD & Bevensee MO (2006). A cysteine-scanning mutagenesis study of transmembrane domain 8 of the electrogenic sodium/bicarbonate cotransporter NBCe1. *J Biol Chem* **281,** 32417–32427.

McAlear SD, Liu X, Williams JB, McNicholas-Bevensee CM & Bevensee MO (2006). Electrogenic Na/HCO_3 cotransporter (NBCe1) variants expressed in *Xenopus* oocytes: functional comparison and roles of the amino and carboxy termini. *J Gen Physiol* **127,** 639–658.

McLaughlin S, Wang J, Gambhir A & Murray D (2002). PIP_2 and proteins: interactions, organization, and information flow. *Annu Rev Biophys Biomol Struct* **31,** 151–175.

Muallem S & Loessberg PA (1990). Intracellular pH-regulatory mechanisms in pancreatic acinar cells. I. Characterization of H^+ and HCO_3^- transporters. *J Biol Chem* **265,** 12806–12812.

Murata Y, Iwasaki H, Sasaki M, Inaba K & Okamura Y (2005). Phosphoinositide phosphatase activity coupled to an intrinsic voltage sensor. *Nature* **435,** 1239–1243.

Murata Y & Okamura Y (2007). Depolarization activates the phosphoinositide phosphatase Ci-VSP, as detected in *Xenopus* oocytes coexpressing sensors of PIP_2. *J Physiol* **583,** 875–889.

Di Paolo G & De Camilli P (2006). Phosphoinositides in cell regulation and membrane dynamics. *Nature* **443,** 651–657.

Parker MD, Skelton LA, Daly CM & Boron WF (2007). IRBIT binds to and functionally enhances the electroneutral Na-coupled bicarbonate transporters NBCn1, NDCBE and NCBE (Abstract). *FASEB J* **21,** A1285.

Parker MD & Boron WF (2013). The divergence, actions, roles, and relatives of sodium-coupled bicarbonate transporters. *Physiol Rev* **93,** 803–959.

Ransom B (2000). Glial modulation of neural excitability mediated by extracellular pH: a hypothesis revisited. *Progress Brain Res* **125,** 217–228.

Sakata S, Hossain MI & Okamura Y (2011). Coupling of the phosphatase activity of Ci-VSP to its voltage sensor activity over the entire range of voltage sensitivity. *J Physiol* **589,** 2687–2705.

Sergeev M, Godin AG, Kao L, Abuladze N, Wiseman PW & Kurtz I (2012). Determination of membrane protein transporter oligomerization in native tissue using spatial fluorescence intensity fluctuation analysis. *PLoS One* **7,** e36215.

Shirakabe K, Priori G, Yamada H, Ando H, Horita S, Fujita T, Fujimoto I, Mizutani A, Seki G & Mikoshiba K (2006). IRBIT, an inositol 1, 4, 5-trisphosphate receptor-binding protein, specifically binds to and activates pancreas-type Na^+/HCO_3^- cotransporter 1 (pNBC1). *Proc Natl Acad Sci USA* **103,** 9542–9547.

Suh BC & Hille B (2002). Recovery from muscarinic modulation of M current channels requires phosphatidylinositol 4,5-bisphosphate synthesis. *Neuron* **35,** 507–520.

Sullivan SK & Smith PL (1986). Bicarbonate secretion by rabbit proximal colon. *Am J Physiol Gastrointest Liver Physiol* **251,** 436–445.

Svichar N, Esquenazi S, Chen HY & Chesler M (2011). Preemptive regulation of intracellular pH in hippocampal neurons by a dual mechanism of depolarization-induced alkalinization. *J Neurosci* **31,** 6997–7004.

Thornell IM & Bevensee MO (2013). Activating a voltage-sensitive 5' phosphatase (VSP) that decreases phosphatidylinositol 4,5-bisphosphate (PIP_2) inhibits electrogenic Na/bicarbonate cotransporter NBCe1-B and -C variants expressed in *Xenopus laevis* oocytes (Abstract). *FASEB J* **27,** 730.7.

Thornell IM, Wu J & Bevensee MO (2010). The IP_3 receptor-binding protein IRBIT reduces phosphatidylinositol 4,5-bisphosphate (PIP_2) stimulation of Na/bicarbonate cotransporter NBCe1 variants expressed in *Xenopus laevis* oocytes (Abstract). *FASEB J* **24,** 815.6.

Thornell IM, Wu J, Liu X & Bevensee MO (2012). PIP_2 hydrolysis stimulates electrogenic Na/bicarbonate cotransporter NBCe1-B and -C variants expressed in *Xenopus laevi*s oocytes. *J Physiol* **590,** 5993–6011.

Vidyasagar S, Rajendran VM & Binder HJ (2004). Three distinct mechanisms of HCO_3^- secretion in rat distal colon. *Am J Physiol Cell Physiol* **287,** C612–21.

Whorton MR & Mackinnon R (2011). Crystal structure of the mammalian GIRK2 K^+ channel and gating regulation by G proteins, PIP_2, and sodium. *Cell* **147,** 199–208.

Winks JS, Hughes S, Filippov AK, Tatulian L, Abogadie FC, Brown DA & Marsh SJ (2005). Relationship between membrane phosphatidylinositol-4,5-bisphosphate and receptor-mediated inhibition of native neuronal M channels. *J Neurosci* **25,** 3400–3413.

Wu J, McNicholas CM & Bevensee MO (2009). Phosphatidylinositol 4, 5-bisphosphate (PIP_2) stimulates the electrogenic Na/HCO_3 cotransporter NBCe1-A expressed in *Xenopus* oocytes. *Proc Natl Acad Sci USA* **106,** 14150–14155.

Yang D, Shcheynikov N & Muallem S (2011). IRBIT: it is everywhere. *Neurochem Res* **36,** 1166–1174.

Zaika O, Zhang J & Shapiro MS (2011). Combined phosphoinositide and Ca^{2+} signals mediating receptor specificity toward neuronal Ca^{2+} channels. *J Biol Chem* **286,** 830–841.

Zhang H, Craciun LC, Mirshahi T, Rohács T, Lopes CMB, Jin T & Logothetis DE (2003). PIP_2 activates KCNQ channels, and its hydrolysis underlies receptor-mediated inhibition of M currents. *Neuron* **37,** 963–975.

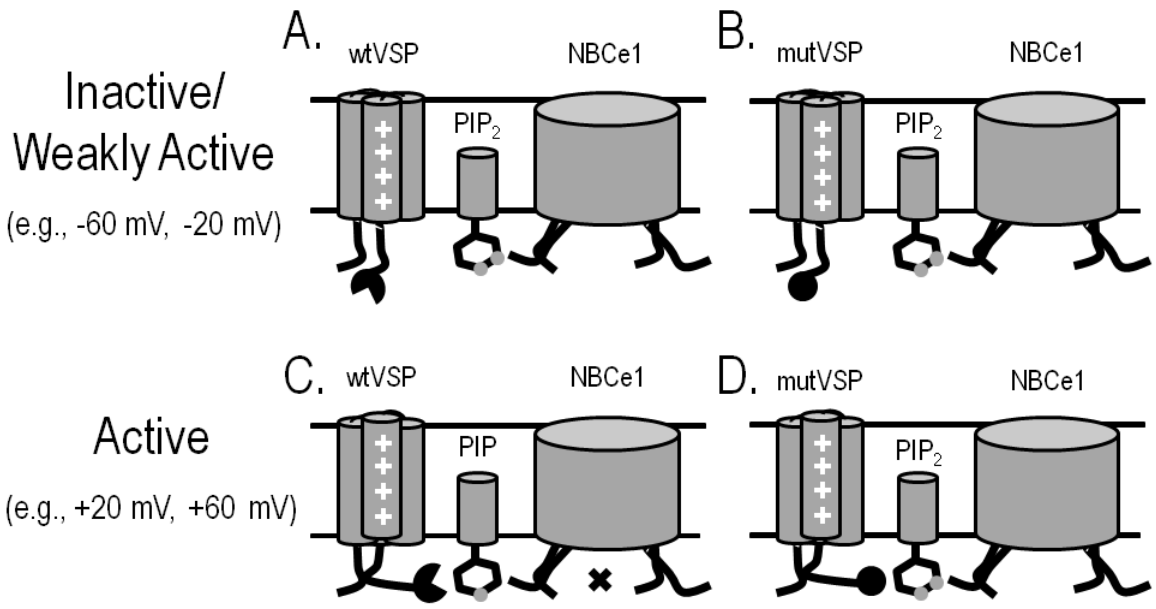

Figure 1. Wild-type VSP (wtVSP), but not mutant (mutVSP), can be voltage activated to dephosphorylate PIP_2 and probe for PIP_2 sensitivity of NBCe1. Negative voltages such as -60 mV and -20 mV fail to activate wtVSP (A) and mutVSP (B) appreciably. Positive voltages such as +20 mV and +60 mV activate wtVSP, which decreases PIP_2 and inhibits NBCe1 (C). Although positive voltages also activate mutVSP, its catalytically dead phosphatase domain fails to dephosphorylate PIP_2 (D). NBCe1 is represented as a dimer as described by the Kurtz group (Kao *et al.*, 2008; Sergeev *et al.*, 2012).

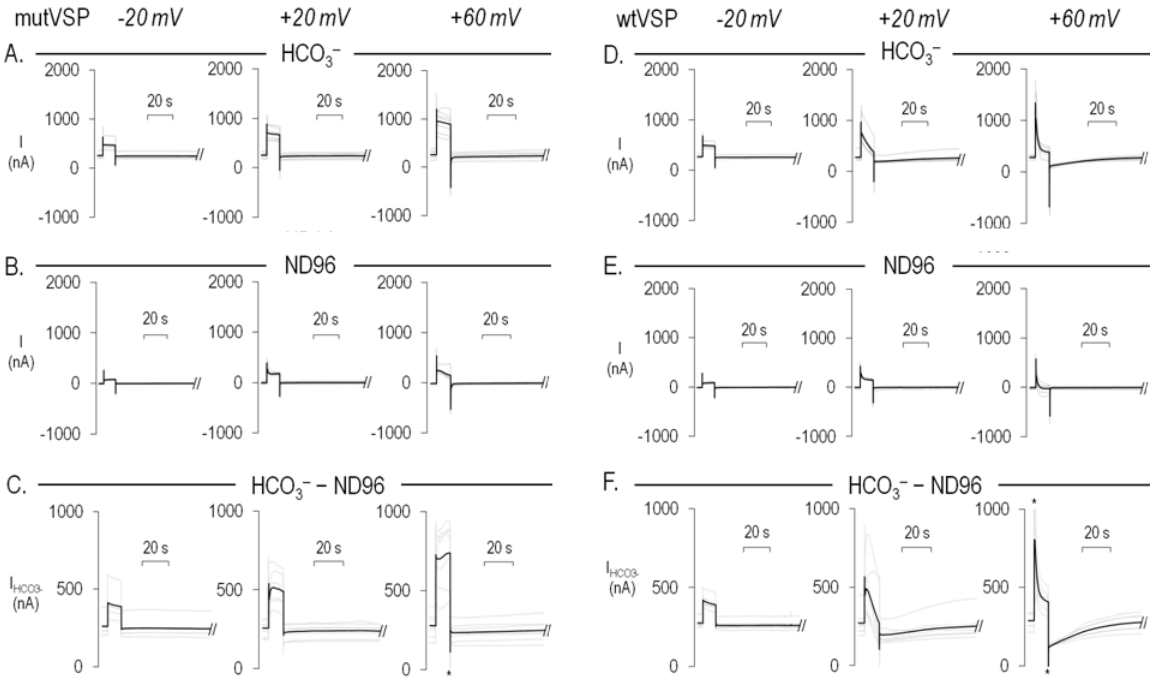

Figure 2. Activated wtVSP inhibits currents for NBCe1-expressing oocytes bathed in HCO_3^- and ND96 solutions. In each panel, individual traces are shown in grey, and the average is shown in black. Oocytes were initially voltage clamped at -60 mV. (A) Control oocytes co-expressing mutVSP and NBCe1-C and bathed in 5% CO_2/33 mM HCO_3^- depolarized to -20 mV (n = 5), +20 mV (n = 7), or +60 mV (n = 7). (B) Smaller currents obtained from the same panel-A oocytes bathed in ND96 prior to the HCO_3^- solution for each depolarization. (C) HCO_3^--dependent current (I_{HCO3-}) traces obtained by subtracting panel-B traces from corresponding panel-A traces. The outward currents were sustained and greater at larger depolarizations (-20 mV < +20 mV < +60 mV). (D) Oocytes co-expressing wtVSP and NBCe1-C and bathed in 5% CO_2/33 mM HCO_3^- depolarized to -20 mV (n = 6), +20 mV (n = 7), or +60 mV (n = 7). (E) Smaller currents obtained from the same panel-D oocytes bathed in ND96 prior to the HCO_3^- solution for each depolarization. (F) HCO_3^--dependent current (I_{HCO3-}) traces obtained by subtracting panel-E traces from corresponding panel-D traces. The outward currents were transient and decayed rapidly for the +20 mV and +60 mV depolarizations, but not for the -20 mV depolarization. For the +20 mV and +60 mV depolarizations, repolarization back to -60 mV elicit a decrease in I_{HCO3-} that gradually recovered back to the initial steady-state I_{HCO3-}. *Transient was truncated.

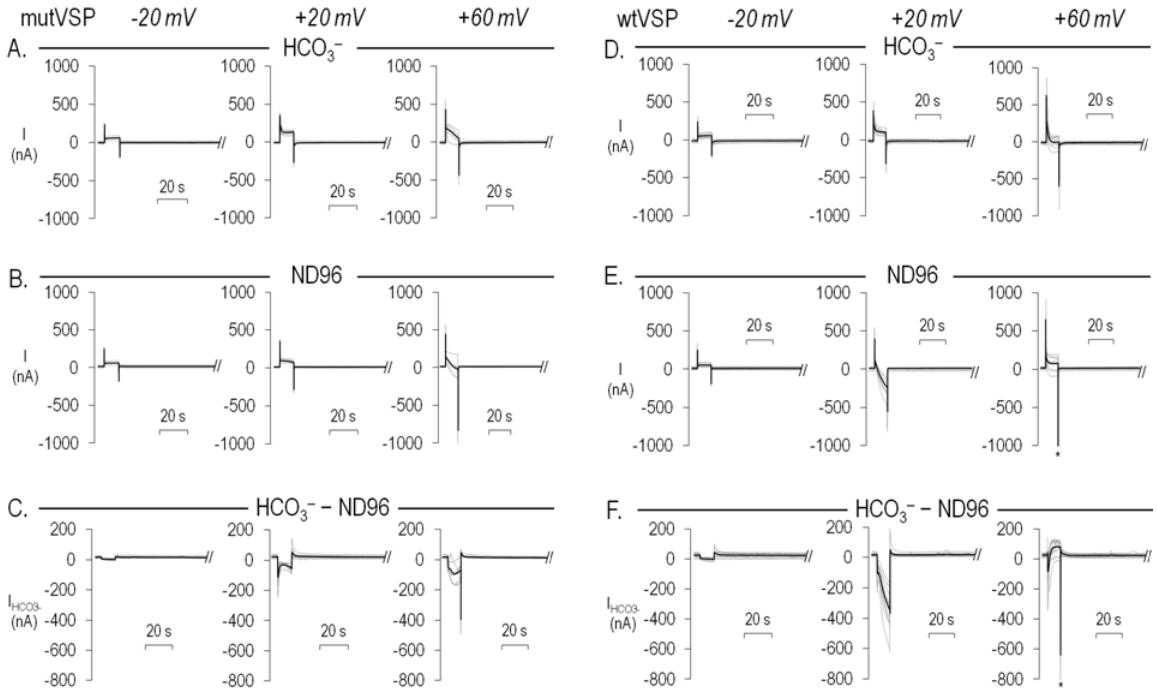

Figure 3. Depolarization of wtVSP- and mutVSP-expressing oocytes elicits HCO_3^--dependent endogenous currents. In each panel, individual traces are shown in grey, and the average is shown in black. Oocytes were initially voltage clamped at -60 mV. (A) Oocytes co-injected with water and mutVSP cRNA, equilibrated for 5 min in the 5% CO_2/33 mM HCO_3^- solution, and depolarized to either -20 mV (n = 8), +20 mV (n = 9), or +60 mV (n = 9). (B) Currents obtained from the same mutVSP-expressing oocytes bathed in ND96 prior to the 5% CO_2/33 mM HCO_3^- solution. (C) HCO_3^--dependent current (I_{HCO3-}) traces obtained by subtracting panel-B traces from corresponding panel-A traces.-Depolarizing control oocytes expressing mutVSP alone caused an inward HCO_3^--dependent current (I_{HCO3-}), which was reversible upon repolarization to -60 mV. This inward current was greater at larger depolarizations (-20 mV < +20 mV < +60 mV). (D) Panel A-experiments performed on oocytes co-injected with water and wtVSP cRNA, and subjected to depolarizations of -20 mV (n = 8), +20 mV (n = 7), or +60 mV (n = 6). (E) Currents also obtained from the same wtVSP-expressing oocytes bathed in ND96 prior to the 5% CO_2/33 mM HCO_3^- solution. (F) HCO_3^--dependent current (I_{HCO3-}) traces obtained by subtracting panel-E traces from corresponding panel-D traces. Depolarizing oocytes co-expressing wtVSP alone had more variable effects on I_{HCO3-}. In all panels above, repolarization back to -60 mV caused a rapid return to the initial steady-state I_{HCO3-} without any slow recovery.

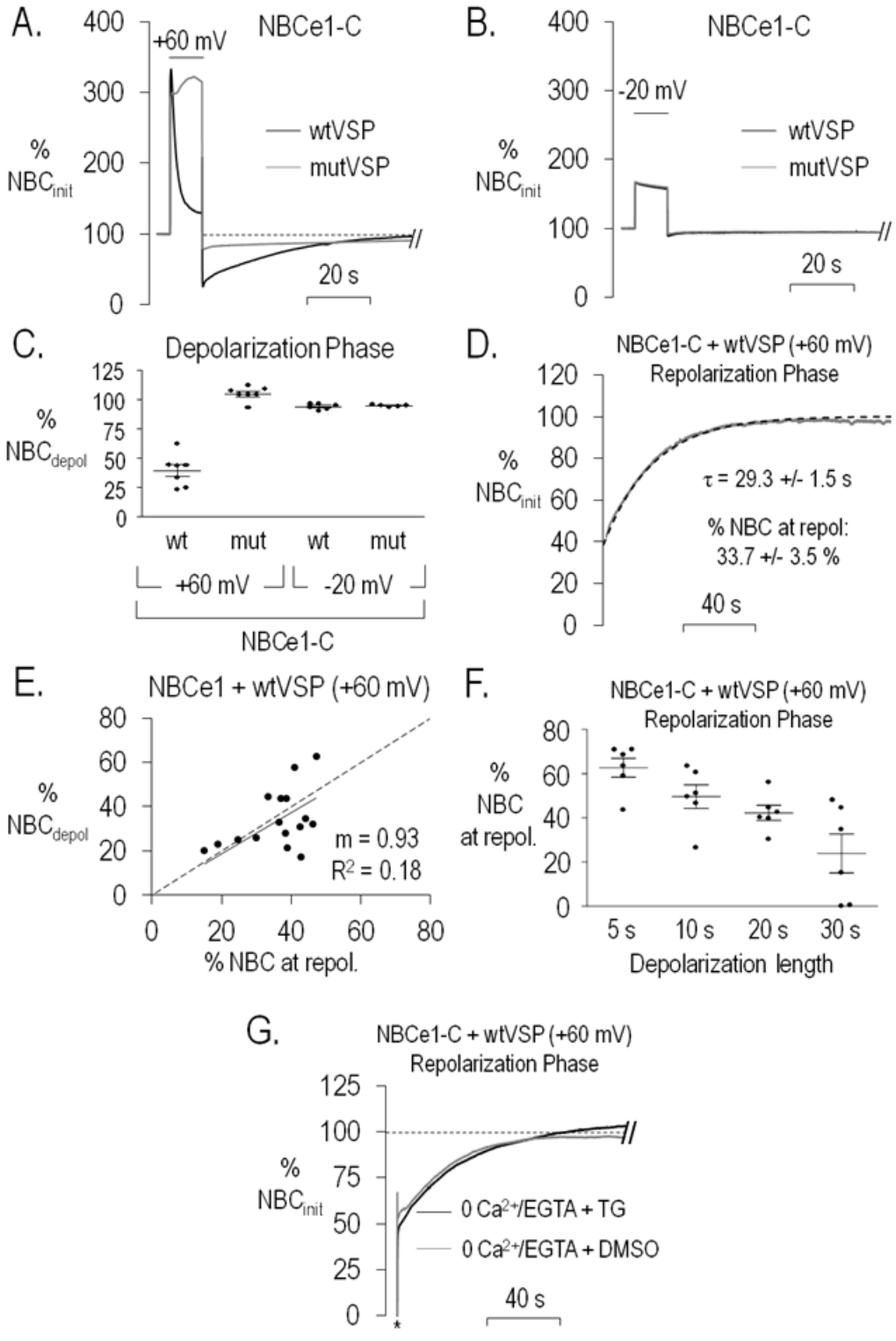
A.
NBCe1-C
+60 mV
wtVSP
mutVSP
% NBC$_{init}$
20 s
B.
NBCe1-C
-20 mV
wtVSP
mutVSP
% NBC$_{init}$
20 s
C.
Depolarization Phase
% NBC$_{depol}$
wt
mut
wt
mut
+60 mV
-20 mV
NBCe1-C
D.
NBCe1-C + wtVSP (+60 mV)
Repolarization Phase
% NBC$_{init}$
τ = 29.3 +/- 1.5 s
% NBC at repol:
33.7 +/- 3.5 %
40 s
E.
NBCe1 + wtVSP (+60 mV)
% NBC$_{depol}$
m = 0.93
R^2 = 0.18
% NBC at repol.
F.
NBCe1-C + wtVSP (+60 mV)
Repolarization Phase
% NBC at repol.
5 s
10 s
20 s
30 s
Depolarization length
G.
NBCe1-C + wtVSP (+60 mV)
Repolarization Phase
% NBC$_{init}$
0 Ca^{2+}/EGTA + TG
0 Ca^{2+}/EGTA + DMSO
40 s

Figure 4. Activated wtVSP inhibits NBCe1-C. (A) Mean NBCe1-C currents for oocytes co-expressing either VSP (*n* = 7) or mutVSP (*n* = 7), and plotted as the % of the initial NBC current before the depolarization from -60 mV to +60 mV (% NBC_{init}). (B) Mean % NBC_{init} for oocytes co-expressing either VSP (*n* = 6) or mutVSP (*n* = 5), and depolarized from -60 mV to -20 mV. (C) The NBC current remaining at the end of the 10-s depolarization (+60 mV or -20 mV) as a % of the initial depolarization-induced current (% NBC_{depol}) calculated from panel-A and -B experiments. (D) The % NBC_{init} during the current recovery after a +60 mV depolarization for an oocyte co-expressing NBCe1-C and wtVSP (grey trace). The recovery was fit with a single exponential equation (dashed trace). (E) % NBC_{depol} vs. % NBC_{init} back extrapolated to the moment of repolarization for NBCe1-C and -B combined (*n* = 16). (F) The % NBC_{init} back extrapolated to the moment of repolarization for oocytes co-expressing wtVSP and NBCe1-C that were depolarized to +60 mV for various durations (*n* = 6 for each). The mean % NBC inhibition was greater with longer wtVSP activation (5 s vs. 30 s, $P < 0.001$; 10 s vs. 30 s, $P = 0.03$ (Bonferroni)). (G) % NBC_{init} recoveries following the +60 mV depolarization of oocytes co-expressing wtVSP and NBCe1-C pre-incubated in 0 Ca^{2+}/EGTA with either DMSO (grey trace; *n* = 3) or thapsigargin (black trace, *n* = 5). *Transient was truncated. TG = thapsigargin.

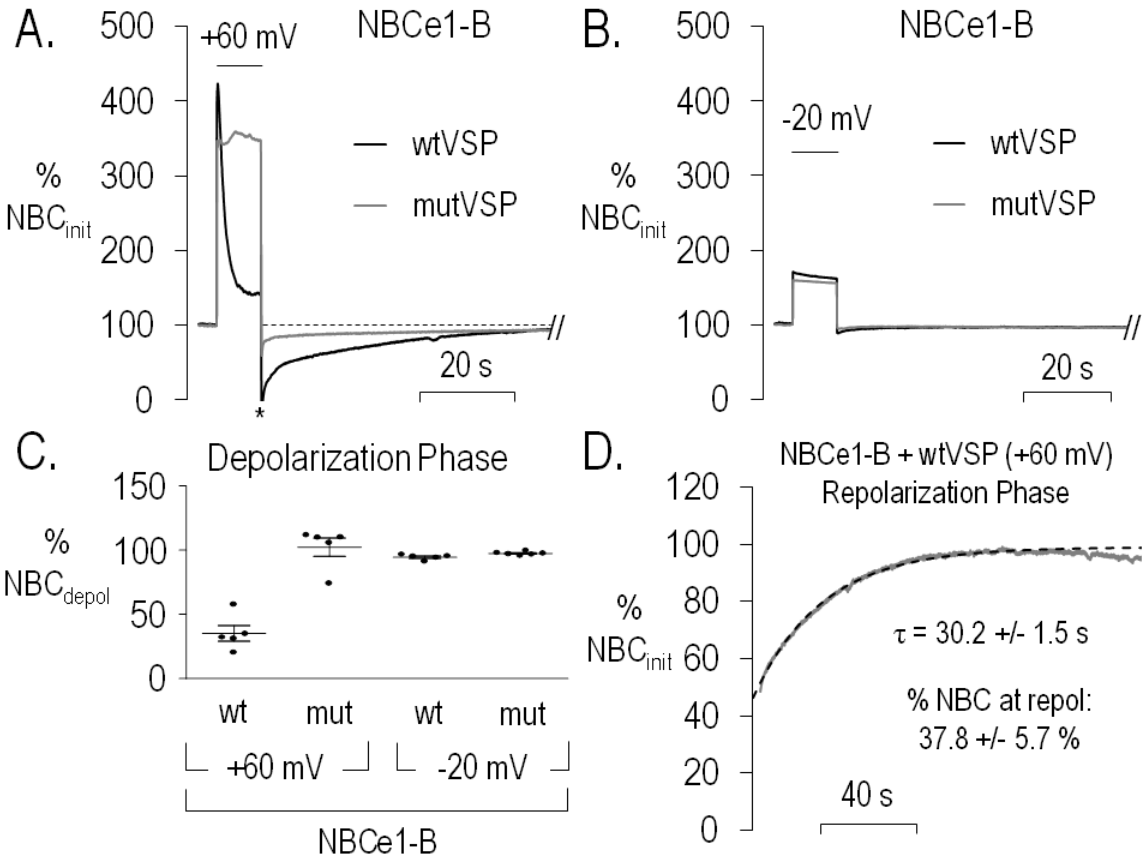

Figure 5. Activated wtVSP inhibits NBCe1-B. (A) Mean NBCe1-B currents for oocytes co-expressing either VSP (*n* = 5) or mutVSP (*n* = 5), and plotted as the % NBC_{init}. *Transient was truncated. (B) Mean % NBC_{init} for oocytes co-expressing either VSP (*n* = 5) or mutVSP (*n* = 6), and depolarized from -60 mV to -20 mV. (C) The NBC current remaining at the end of the 10-s depolarization (+60 mV or -20 mV) calculated as the % NBC_{depol} from panel-A and -B experiments. (D) The % NBC_{init} during the current recovery after a +60 mV depolarization for an oocyte co-expressing NBCe1-C and wtVSP (grey trace). The recovery was fit with a single exponential equation (dashed trace).

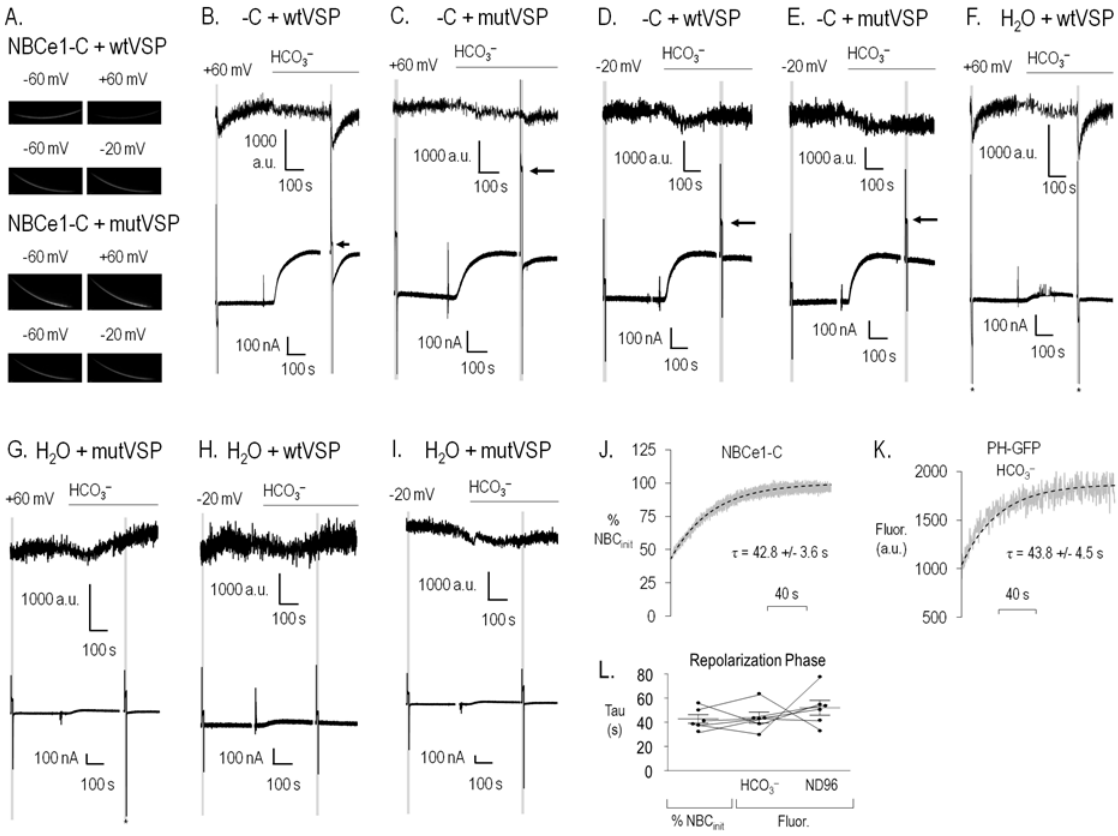

Figure 6. Activating/inactivating VSP causes parallel changes in plasma-membrane PIP_2 and NBCe1 activity. (A) Representative changes in the plasma-membrane PH-GFP fluorescence for oocytes co-expressing NBCe1-C and either wtVSP (top 4-panel image set) or mutVSP (bottom 4-panel image set) depolarized from -60 mV to either +60 mV or -20 mV. (B) A representative PH-GFP signal trace (above) and current trace (below) from an oocyte co-expressing PH-GFP, wtVSP, and NBCe1-C and transiently depolarized (grey shaded region) with the oocyte bathed in either ND96 or a HCO_3^- solution (n = 6). (C-E) Panel B-type experiments performed on oocytes co-expressing NBCe1-C and either mutVSP depolarized to +60 mV (n = 4), wtVSP depolarized to -20 mV (n = 5), or mutVSP depolarized to -20 mV (n = 4). (F) Panel B-type experiment performed on a wtVSP-expressing oocyte without NBCe1-C (n = 3) and displaying fluorescence changes similar to those in panel B, but no NBC currents. (G-I) Control experiments in which the +60 mV or -20 mV depolarization of oocytes expressing mutVSP, or the -20 mV depolarization of oocytes expressing wtVSP had little effect on both membrane fluorescence and the CO_2/HCO_3^--stimulated currents (n = 3 or 4). (J) Representative current recovery plotted as the % NBC_{init} from an oocyte co-expressing PH-GFP, NBCe1-C, and wtVSP (grey trace) fitted with a single exponential equation (dashed black trace). (K) Representative PH-GFP fluorescence recovery (grey trace) associated with the current recovery shown in panel J, and also fitted with a single exponential equation (dashed black trace). (L) Similar mean time constants (τ) for panel J/K-type experiments. Gaps in some current traces (B-I) represent discontinuity when

switching between gap-free and programmed depolarization protocols during continuous fluorescence recordings.

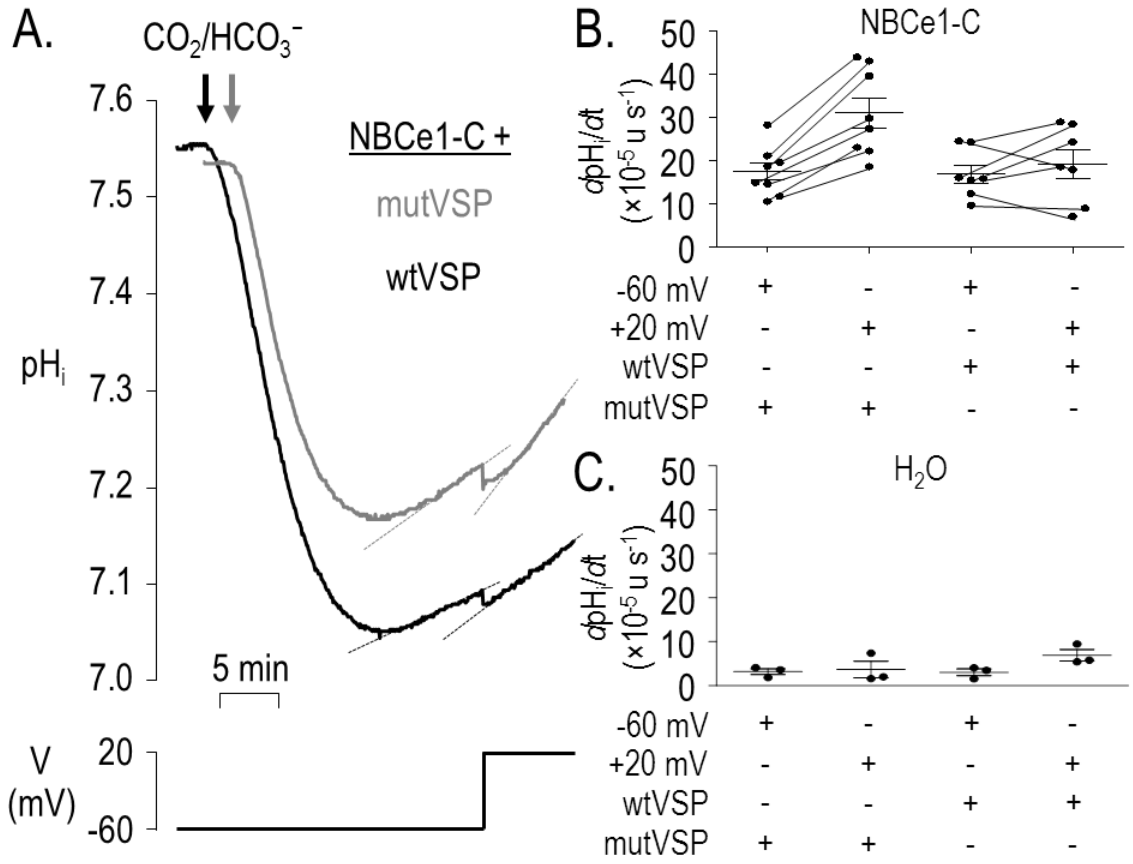

Figure 7. Activated VSP inhibits a depolarization-stimulated, NBCe1-C-mediated pH_i recovery from an acid load. (A) Oocytes initially voltage clamped at -60 mV and co-expressing NBCe1-C and either mutVSP (grey trace) or wtVSP (black trace). Switching to a 5% CO_2/33 mM HCO_3^- solution elicited a fall in pH_i due to CO_2 influx, followed by a slow pH_i recovery due to NBC. Subsequent depolarization to +20 mV stimulated the pH_i recovery to a greater extent in oocytes co-expressing mutVSP than wtVSP. (B) Summary dpH_i/dt data from pH_i recoveries at -60 mV and +20 mV in panel A-type experiments. (C) Similar water-injected control experiments. The mean dpH_i/dt was minimal for oocytes expressing either mutVSP or wtVSP and clamped at either -60 mV or +20 mV (n = 3 each).

DISCUSSION

The goal of this dissertation was to characterize phosphatidylinositol 4,5-bisphosphate (PIP_2)-mediated regulation of cloned variants of the electrogenic Na/bicarbonate cotransporter (NBCe1) in an intact cell. PIP_2 regulated NBCe1 by 2 distinct mechanisms. First, PIP_2 hydrolysis to IP_3/Ca^{2+} stimulated NBCe1-B and -C, but not NBCe1-A (Chapter 3). Second, PIP_2 depletion per se inhibited NBCe1-B and -C (Chapter 4). The next two sections discuss each of these signaling pathways. The combined data from Chapter 3 and Chapter 4 reveal that PIP_2 regulates NBCe1-B and -C through a dual mechanism involving both PIP_2 itself and the classic IP_3/Ca^{2+} signaling pathway—similar to that seen for the K^+ channel KCNQ.

PIP_2 Hydrolysis

NBCe1-B and -C, but not NBCe1-A, were stimulated by an injection of PIP_2 into *Xenopus* oocytes (Chapter 3). This PIP_2 stimulation was caused by PIP_2 hydrolysis and was mimicked by several components of the PIP_2 hydrolysis pathway (e.g., PIP_2, inositol trisphosphate (IP_3), Ca^{2+}, and lysophosphatidic acid (LPA)). The PIP_2 hydrolysis-induced simulation required the N-terminus of NBCe1-B and -C and was independent of the signaling protein IRBIT (IP_3 receptor binding protein released with inositol trisphosphate), which is a previously described NBCe1 regulator.

PIP_2 Injection

As detailed in Chapter 3 and briefly summarized here, NBCe1-B and -C, but not NBCe1-A, were stimulated by PIP_2 hydrolysis and subsequent Ca^{2+} release. Experiments were performed using the 2-electrode voltage clamp technique on *Xenopus* oocytes expressing an NBCe1 variant. Injecting 100 μM PIP_2 (estimated 10 μM final concentration) stimulated NBCe1-B and -C current by ~125%, but failed to stimulate NBCe1-A current. These findings were initially surprising because NBCe1-A was PIP_2 sensitive in a membrane macropatch from *Xenopus* oocytes expressing the same NBCe1-A clone (Wu *et al.*, 2009). Additional experiments demonstrated that injected PIP_2 was hydrolyzed to IP_3 and this hydrolysis, not PIP_2 per se, provided the differential stimulation among the 3 variants. The injected PIP_2 failed to stimulate NBCe1-B and -C after ER Ca^{2+} depletion. Further, the PIP_2 injection-induced stimulation was reduced to ~30% when oocytes expressing NBCe1-B or -C were pretreated with the phospholipase C (PLC) inhibitor U73122. For the PLC inhibitor experiments, NBCe1-A was also stimulated ~30%. These modest stimulations likely resulted from a stimulatory effect of PIP_2 per se because the IP_3/Ca^{2+}-insensitive NBCe1-A was also stimulated by PIP_2 injection with PLC-mediated PIP_2 hydrolysis inhibited. The modest PIP_2-induced stimulation for all variants in the PLC inhibitor experiments provided the rationale for selectively decreasing PIP_2 in Chapter 4 experiments.

IP_3 Injection

Injecting IP_3 mimicked the PIP_2 injection results. Specifically, IP_3 injection stimulated NBCe1-B and -C by ~175% and was inhibited by ER Ca^{2+} depletion. The

NBCe1 stimulation profile was unaffected by lowering the IP_3 concentration to a more physiological concentration (~100 nM).

Involvement of a Kinase

Pretreating the oocytes with staurosporine inhibited the IP_3 injection-induced stimulation, which is consistent with the involvement of a Ca^{2+}-sensitive kinase. As summarized in Figure 1, the staurosporine-sensitive kinase was not phosphokinase C (PKC), calmodulin, or diacylglycerol (DAG) kinase, which are common Ca^{2+}-sensitive kinases associated with the PLC pathway. There are several untested possibilities for the roles of Ca^{2+} and a kinase in this mode of NBCe1 regulation. In regards to Ca^{2+}, there are no known Ca^{2+} binding motifs on either variant; therefore Ca^{2+} is likely a requirement for another regulator. In regards to the role of the kinase, it is possible that NBCe1-B and -C are regulated by an untested Ca^{2+}-induced kinase that phosphorylates NBCe1 (i.e., not PKC, calmodulin, or DAG kinase). Alternatively, the staurosporine-sensitive kinase and the Ca^{2+}-sensitive regulator may be distinct. For example, the kinase may phosphorylate NBCe1, priming NBCe1 for a Ca^{2+}-sensitive regulator. Finally, staurosporine may have inhibited an upstream component of the signaling pathway (e.g., the IP_3 receptor or PLC), which may require staurosporine-sensitive phosphorylation. This final scenario is unlikely because the Ca^{2+}-induced Cl^- conductance resulting from IP_3-induced ER Ca^{2+} release was still observed after staurosporine pretreatment.

Endogenous Regulation

Consistent with the injection data, activation of an endogenous oocyte G_q-coupled receptor with LPA stimulated NBCe1-B by ~100% and -C by ~150%, but not NBCe1–A. After pretreatment with BAPTA-AM to chelate Ca^{2+}, NBCe1-B and -C currents were reduced by ~35%, consistent with ambient Ca^{2+} stimulation of NBCe1. In BAPTA-AM pretreated oocytes, LPA-induced stimulation was inhibited, consistent with the involvement of Ca^{2+} in the G_q receptor-mediated response. The difference in LPA stimulation of NBCe1-B and -C may result from separate mechanisms. LPA stimulated NBCe1-C activity independent of surface expression. However, LPA stimulated NBCe1-B predominantly by an increase in membrane expression that was Ca^{2+}-independent and not blocked by BAPTA. The LPA receptor is not exclusively G_q-coupled, but can also couple to $G_{i/o}$ as characterized in *Xenopus* oocytes (Guo *et al.*, 1996). The Ca^{2+}-independent regulation of NBCe1-B may arise from LPA-induced $G_{i/o}$ signaling.

NBCe1 transports HCO_3^- and therefore PIP_2 hydrolysis should also affect pH_i physiology, such as an NBCe1-mediated recovery from an acid load. In simultaneous 2-electrode voltage clamp and pH_i experiments on NBCe1-C expressing oocytes, LPA application stimulated NBCe1-mediated pH_i recovery by ~80% and current by ~40%.

A rise in Ca^{2+} without PIP_2 injection was sufficient to provide stimulation of NBCe1. Ca^{2+} was increased through store operated Ca^{2+} channels (SOCC) and stimulated NBCe1-B and -C by ~350%. Therefore, PIP_2 hydrolysis is sufficient, but not necessary for this mode of NBCe1 regulation.

N-terminus Requirement

NBCe1-B and NBCe1-C have an N-terminus that is distinct from NBCe1-A. Therefore, we tested whether the N-terminus of NBCe1-B and -C was required for full PIP_2 injection stimulation. Truncation of the N-terminus of NBCe1-C produced a more active NBCe1 because the truncation removed the autoinhibitory domain (AID) (McAlear *et al.*, 2006). Further, stimulation by PIP_2 injection, IP_3 injection, SOCCs, or LPA were all reduced by an N-terminus truncation of NBCe1-C. These findings support that the final step of this regulatory pathway may involve a conformational change in NBCe1-C that relieves the AID. However, there may be other components involved because removing the N-terminus did not completely inhibit PIP_2 stimulation of NBCe1.

IRBIT Independence

In our experiments, an increase in IP_3 could in principle displace IRBIT from the IP_3 receptor and stimulate NBCe1. Indeed, IRBIT stimulates NBCe1-B and -C, but not -A, just as we observed with our PIP_2 injection study (Shirakabe *et al.*, 2006; Parker *et al.*, 2007; Thornell *et al.*, 2010). However, there were several reasons to exclude that endogenous IRBIT regulated NBCe1-B and -C in our experiments as discussed in Chapter 3. Our strongest evidence against the involvement of IRBIT was from oocytes co-expressing a dominant negative IRBIT mutant and NBCe1-C, where the IP_3 injection still stimulated NBCe1-C to the same extent as in the absence of the mutant. These data are consistent with a novel NBCe1 stimulator in the IP_3 pathway that is independent of IRBIT.

PIP_2 Per Se

In the first study (Chapter 3), injecting PIP_2 in the presence of a PLC inhibitor stimulated all 3 NBCe1 variants modestly, consistent with direct PIP_2 stimulation. In the second study (Chapter 4), we used a co-expressed voltage-sensitive phosphatase (VSP) to unequivocally demonstrate that PIP_2 per se regulates NBCe1-B and -C expressed in *Xenopus* oocytes. VSP is a 5' phosphatase and dephosphorylates PIP_2 to PIP. This was a useful probe for assessing NBCe1 sensitivity to PIP_2 per se because dephosphorylation of PIP_2 circumvents the PIP_2 hydrolysis pathway characterized in Chapter 3. In our VSP co-expression experiments, activated wild type VSP, but not a catalytically dead VSP mutant, inhibited NBCe1-B and -C. This VSP study combined with the PIP_2 injection study support the novel finding that NBCe1-B and -C can be regulated by two components of the PIP_2 signaling pathway— PIP_2 itself and IP_3/Ca^{2+}.

We have preliminary data from whole oocytes that an NBCe1-A mediated pH_i recovery from a CO_2-induced acid load is inhibited by activated VSP. This finding supports our previous report that PIP_2 stimulates NBCe1-A in the membrane patch (Wu *et al.*, 2009). However, it was difficult to evaluate whole oocyte NBCe1-A currents using VSP. NBCe1-A mediated currents become extremely large when oocytes are depolarized to potentials necessary for substantial VSP activity (e.g. +60 mV). This depolarized-induced NBCe1-A current is expected to create an unstirred layer, which slows NBCe1-mediated transport due to the accumulation of Na^+ and HCO_3^- on the cytosolic side of the membrane. Upon repolarization, the ion gradient is gradually reestablished as reflected in the gradual return of the transporter current to the pre-depolarization steady-state current. These unstirred layer effects on NBCe1-A currents are in the same direction as VSP-

mediated inhibition of NBCe1 and make these experiments difficult to evaluate for the highly active A variant. To control for this effect, we reduced NBCe1-A expression to mimic the magnitude of the whole-cell HCO_3^- currents seen with the B and C variants, and minimize the unstirred layer effect. In these experiments, wtVSP effects consistent with PIP_2 inhibition were observed, however similar effects were observed with the control mutant VSP. This depolarization-induced inhibition of NBCe1-A needs to be further characterized before evaluating PIP_2 regulation using the +60 mV VSP assay.

Location of the PIP_2 Binding Site

This study did not evaluate if PIP_2 binds NBCe1 directly or through an NBCe1 associated protein. IRBIT (Shirakabe *et al.*, 2006) and chaperone stress 70 protein (Bae *et al.*, 2013) bind and regulate NBCe1-B and -C, however both are predominantly cytosolic proteins and are unlikely to directly bind PIP_2. Four candidate binding regions that are consistent with an electrostatic PIP_2/NBCe1 interaction are discussed in Chapter 4. As discussed in Chapter 1, GIRK/PIP_2 and K_{ir}/PIP_2 crystal structures show that PIP_2 binding to these K^+ channels induces a change in their conformation, which opens the channel gate. Based on the amino acid sequence for PIP_2 binding to the K^+ channel, the most likely location in NBCe1 is RKEHKLKK near TMD8, which is involved in the ion translocation pathway (McAlear & Bevensee, 2006).

Role of PIP_2

PIP_2 may play a permissive role (i.e., NBCe1 function depends on the presence of PIP_2) or a dynamic signaling role (i.e., receptor-mediated changes profoundly inhibit

NBCe1) as discussed in Chapter 4. The K_m of NBCe1 for PIP_2 is likely lower than the physiological PIP_2 level based on the finding that PIP_2 injection in the presence of a PLC inhibitor modestly stimulated NBCe1 (Chapter 3). The K_m value should be close to the level of PIP_2 after a 10s-VSP activation because NBCe1 was inhibited ~40% (Chapter 4). Calibrating the PH-GFP fluorescence to quantitate PIP_2 concentration in these experiments is challenging for 3 reasons. (1) It is unknown if the initial fluorescence (PIP_2 concentration) in our intact oocyte experiments matched the oocyte PIP_2 concentration quantitated from an oocyte extract. (2) It is hard to obtain a fluorescence minimum in the absence of PIP_2 because VSP activation will not deplete PIP_2 entirely, as indicated by the presence of subsequent PIP_2 hydrolysis following prolonged VSP activation (Kohout *et al.*, 2010; Dickson *et al.*, 2013). (3) The relationship between VSP-activation and PIP_2 depletion is non-linear (Murata *et al.*, 2005) and requires many known calibration points. There is currently no technique to clamp membrane PIP_2 at known levels for such a calibration. One alternative calibration method would be to calibrate PH-GFP membrane fluorescence of oocytes with membrane vesicles loaded with known concentrations of PIP_2. This calibration would have to assume that the fluorescent properties of PH-GFP are the same in both preparations.

In these experiments, we demonstrate that PIP_2 is stimulatory or required for NBCe1, and this effect may involve a PIP_2 binding site. However, the detailed mechanism by which PIP_2 stimulates NBCe1 needs to be explored. The simplest explanation is that PIP_2 stimulates NBCe1 through a conformational change that increases the rate of ion translocation. For example, PIP_2 may make the mouth or translocation path of the transporter more accessible to Na^+ and/or HCO_3^-. Additionally,

PIP_2 may induce a conformation that increases the transporter's ion affinities for Na^+ and HCO_3^-. We can't rule out the possibility that PIP_2's stimulatory role may be independent from the biophysics of NBCe1 transport. For example, PIP_2 may be required for NBCe1 expression, and possibly promote dimerization. On the other hand, any PIP_2-mediated change in NBC surface expression would have to be extremely fast to account for marked VSP-stimulated inhibition of NBC activity within 10 s (Chapter 4). Also, in the whole oocyte, PLC inhibition that would be expected to increase baseline PIP_2 at least somewhat actually causes a decrease in surface expression of all three variants (Chapter 3). However, interpreting these data is complex because IP_3/Ca^{2+} is also affected.

Two Distinct PIP_2 Regulatory Modes

As discussed in Chapter 4, dual pathway PIP_2 regulation exists for endogenous KCNQ potassium channel-mediated M-current in superior cervical ganglion (SCG) neurons. Briefly, G_q-stimulated PIP_2 hydrolysis *with Ca^{2+} release* (e.g. by bradykinin or purinergic receptor activation) does not appreciably deplete PIP_2 due to Ca^{2+}-sensitive phosphatidylinositol 4-kinase (PI4K) activation. The Ca^{2+} released from ACh-induced PIP_2 hydrolysis inhibits the M current through calmodulin. However, G_q-stimulated PIP_2 hydrolysis *without Ca^{2+} release* (e.g. by muscarinic acetylcholine receptor, mAChR, activation) does appreciably deplete PIP_2 and inhibits the M current through PIP_2. The data from Chapters 3 and 4 are consistent with potential PIP_2 dual regulation of NBCe1-B and -C. However, the resultant activity (i.e., stimulation vs. inhibition) from these G_q-coupled pathways would be expected to be different for NBCe1than KCNQ. For example, extending our findings to what is characterized for the SCG neuron, NBCe1

placed in the same cellular location as KCNQ would be stimulated by bradykinin or purinergic receptor activation and inhibited by mAChR activation (Figure 2).

Significance

PIP_2 regulation of NBCe1 has important physiologically implications for NBCe1-mediated pH_i regulation and epithelial transport in mammalian cells as described in Chapter 1. In this section, I highlight the implications for PIP_2 regulation of NBCe1 in general tissue hypoxia, epithelial physiology, and neuronal firing. Furthermore, preliminary data are presented that support PIP_2 regulation of NBCe1 in a mammalian cell. Any cell type that expresses NBCe1 is likely to be modulated by at least one mode of PIP_2 regulation because PIP_2 is ubiquitous.

Hypoxic Tissue

The role of PIP_2 regulation on NBCe1 activity may also be relevant for pathological states such as hypoxia, where a decrease in PIP_2 and subsequent fall in pH_i are observed. A decrease in PIP_2 that inhibit NBCe1-B will contribute to a hypoxia-induced decline in pH_i. Tissue reperfusion that restores PIP_2 levels would be expected to reactivate NBCe1 and promote a pH_i recovery. However, such a reactivation may be detrimental as NBCe1-mediated Na^+ loading can reverse the Na^+-Ca^{2+} exchanger, elevate intracellular Ca^{2+}, and activate apoptosis pathways.

Pancreas

In the pancreatic duct, PIP_2 regulation of NBCe1-B likely coordinates apical HCO_3^- secretion to basolateral HCO_3^- transport. Briefly, NBCe1, which is located in the basolateral membrane, is largely responsible for raising intracellular HCO_3^-, which is then secreted across the apical membrane . Intriguingly, secretin and acetylcholine (ACh) stimulate apical HCO_3^- secretion without a change in pH_i (Evans *et al.*, 1996). Thus, basolateral NBCe1-B is likely simultaneously stimulated by secretin and ACh. IRBIT also plays a role in coordinating this HCO_3^- secretion because siRNA targeting IRBIT transfected into pancreatic duct cells lowers both NBCe1 activity and HCO_3^- secretion (Yang *et al.*, 2009). In addition to IRBIT stimulation, the IP_3/Ca^{2+} generated from ACh or secretin may stimulate NBCe1-B by the mechanism described in Chapter 3.

Direct PIP_2 stimulation is unlikely to a play a role in the physiological receptor-mediated responses because PIP_2 hydrolysis that depletes PIP_2 would be expected to inhibit NBCe1-B. Therefore, PIP_2 may be rapidly replenished by a lipid kinase, such as described for SCG neurons (Chapter 1). Alternatively, IRBIT binding to NBCe1 may lower NBCe1's K_m for PIP_2, which is consistent with IRBIT stimulation of NBCe1, thereby making physiological decreases in PIP_2 inconsequential to NBCe1 activity. However, PIP_2 per se may play a role in pancreatic pathology in addition to the general hypoxia mechanism described above. Pancreatitis is associated with an increase in PLC and PLC-activating receptors (Korc *et al.*, 1994). This increase in G_q-signaling components may decrease PIP_2 levels, thereby inhibiting NBCe1 and subsequent HCO_3^- secretion in the duodenum.

Brain

NBCe1 activity has been reported in both mammalian astrocytes (O'Connor *et al.*, 1994; Pappas & Ransom, 1994; Bevensee *et al.*, 1997*b*; Majumdar *et al.*, 2008) and neurons (Majumdar *et al.*, 2008; Svichar *et al.*, 2011). As described in Chapter 1, NBCe1 can modulate pH_o shifts in the brain because of the voltage-dependence of NBCe1 (Chesler, 2003). Briefly, depolarization of neurons by voltage-gated channels or depolarization of astrocytes by astrocytic K^+ buffering, will increase NBCe1 activity and lower pH_o, which inhibits hippocampal population spikes. Glutamate released from excitatory neurons can modulate neuronal firing through metabotropic glutamate receptors (mGluRs). The G_q-coupled group I mGluRs have the potential to inhibit NBCe1 activity by PIP_2 depletion, or stimulate activity by PIP_2 hydrolysis and IP_3/Ca^{2+}. In the following section, we present preliminary data that NBCe1 is inhibited by mGluR activation in cultured astrocytes. NBCe1 inhibition would increase pH_o, and possibly facilitate the activation of NMDA receptors that are pH sensitive. Thus, this NBCe1 inhibition with reduced PIP_2 following receptor stimulation may augment the extracellular alkaline shift and mitigate the subsequent acid shift previously characterized with neuronal activity (Chesler, 2003).

Preliminary Data

Exogenous PIP_2

This section discusses preliminary data from experiments utilizing PIP_2 manipulation strategies explained in Chapter 1 on dissociated rat hippocampal astrocytes. Briefly, the pH_i of cultured dissociated astrocytes was monitored by BCECF fluorescence

(Figure 3A). Astrocytes were first bathed in a HEPES buffered ACSF. An NH_4^+ prepulse was used to acid load the cell (Boron & De Weer, 1976; Roos & Boron, 1981). When a cell is exposed to an NH_4^+/NH_3 solution, the gas NH_3 crosses the cell membrane and combines with protons to form NH_4^+, which causes the upstroke in pH_i. During the plateau, additional NH_4^+ enters the cell and NH_3 leaves the cell causing a slight acidification. When the NH_4^+/NH_3 solution is removed, the excess protons produced from the additional NH_4^+ are trapped in the astrocyte, causing the rapid pH_i decrease (acid load). The addition of HCO_3^- during the subsequent pH_i recovery activates NBCe1(Bevensee *et al.*, 1997*a*). The first control pH_i recovery was slower than the pH_i recovery after addition of the PIP_2-histone complex. Histone alone did not stimulate the pH_i recovery in HCO_3^- (Figure 3B). Further, PIP_2 was elevated throughout the PIP_2 recovery phase in Figure 3A because we observed that histone delivered PIP_2 incorporated into and remained in the membrane greater than 1 hr as monitored by the delivery of rhodamine-conjugated PIP_2 (Figure 4). These data are consistent with PIP_2 stimulating the endogenous NBCe1 in astrocytes.

Additionally, we have perfused PIP_2 into a patch pipette attached to an astrocyte. PIP_2 perfusion stimulated the NBCe1 current, however it was unclear whether the perfused PIP_2 stimulated Ca^{2+} release. As detailed below, DHPG-mediated PIP_2 hydrolysis inhibited NBCe1 consistent with the PIP_2 per se mode of NBCe1 regulation. Therefore, hydrolysis that may occur by raising PIP_2 may not affect NBCe1 in the astrocyte and the delivered PIP_2 stimulations of NBCe1 are likely an effect of PIP_2 per se.

PIP_2 Hydrolysis

Astrocyte G_q-coupled signaling was activated using the group I metabotropic glutamate receptor (mGluR) agonist DHPG (Figure 5) using a similar 2 pulse protocol as Figure 3. These experiments were performed with the cells exposed to amiloride to eliminate the contribution of the sodium-proton exchanger (NHE) to the pH_i recovery. pH_i recoveries in HCO_3^- were slower after DHPG application. Calculated acid extrusion rates as a function of pH_i are shown in Figure 6. The pH_i dependence of acid extrusion was reduced by mGluR activation. These findings are consistent with an inhibitory effect of reduced PIP_2 overriding any stimulatory effect of activating the IP_3/Ca^{2+} pathway.

Future Experiments

Xenopus Oocytes

Identity of the kinase in PIP_2 injection experiments. Injecting PIP_2 resulted in a staurosporine-sensitive stimulation of NBCe1-B and -C. To further identify the kinase, we can use a pharmacological approach and use more specific serine/threonine kinase inhibitors, such as PKG inhibitor (protein kinase G), ML-7 (myosine light chain kinase), KN-93 (calmodulin kinase), and H-89 (protein kinase A). If we obtain positive results with one of these inhibitors, then more specific inhibitors can be used to identify the kinase subtype (e.g., PKG-1 or PKG-2).

Identity of the phosphorylation site. It was unclear whether staurosporine inhibited a kinase that phosphorylates NBCe1 or an NBCe1 regulator. A phosphorylation assay, such as used by Gross *et al.*, 2003, can be used to determine if staurosporine changes the phosphorylation state of NBCe1. If there is a change in NBCe1

phosphorylation, then we can perform systematic mutagenesis on staurosporine-sensitive phosphorylation sites (serines and threonines) in the N-terminus of NBCe1-B and -C because NBCe1-A, which has a different N-terminus, is insensitive to the staurosporine-induced stimulation. Each mutant would be expressed in oocytes and tested for changes in baseline NBC current and/or expression. Subsequently, the IP_3/Ca^{2+} mode of regulation of each mutant would be assayed with IP_3 injections.

PIP_2 binding site. To assess if PIP_2 directly binds to NBCe1, PIP_2 coated nitrocellulose strips can be incubated with protein from oocytes expressing an NBCe1 variant tagged with an epitope for detection by immunofluorescence. We have preliminary data that NBCe1 weakly binds all phosphorylated PIPs to varying degrees, but not PI. Based on these preliminary data, future studies should target regions on NBCe1 as potential targets for membrane PIP_2 regulation. As discussed in Chapter 4 and above, the crystallized structures of PIP_2 binding to GIRK and K_{ir} reveal a PIP_2-mediated change in gate conformation. Mutagenesis studies should first target RKEHKLKK (underlined residues are potential binding sites) near TMD8 of NBCe1. Point and combination mutants can be tested for altered PIP_2 sensitivity using the VSP assay as detailed in Chapter 4.

NBCe1 K_m for PIP_2. To verify that NBCe1's K_m for PIP_2 is physiological, a dose-response curve can be constructed from experiments where varying PIP_2 concentrations are applied to NBCe1-expresssing patches. Based on data from this dissertation, we predict that the K_m obtained from these experiments would be in the physiological PIP_2 range, consistent with dynamic PIP_2 regulation of NBCe1 as opposed to a permissive role for PIP_2.

It is possible that the apparent K_m for PIP_2 in the patch is lower (i.e., NBCe1 has a high affinity for PIP_2) because of missing cytosolic regulators. These patch experiments make it possible to test how missing regulators, such as Mg^{2+} or IRBIT, could change NBCe1's K_m for PIP_2. As described in Chapter 2, Mg^{2+} inhibits NBCe1 likely through charge screening because the inhibition is less potent in the presence of other charge screeners (Yamaguchi & Ishikawa, 2008). In addition, IRBIT also alters the Mg^{2+}-mediated NBCe1 inhibition (Yamaguchi & Ishikawa, 2012). Based on these data, Mg^{2+} should raise the K_m for PIP_2 in the patch by acting as a charge screener. IRBIT disrupts the Mg^{2+} regulation; therefore, IRBIT should decrease the K_m for PIP_2. These experiments would evaluate the relative contribution of each regulator to the K_m for PIP_2, and may provide insight into a novel mechanism whereby NBCe1 activity is regulated not only by PIP_2, but by modulators of the transporter's apparent affinity for PIP_2.

Astrocytes

Activating mGluR with DHPG inhibited NBCe1 in astrocytes. This inhibition is consistent with PIP_2 per se regulating NBCe1, but further control experiments need to be performed to rule out Ca^{2+} involvement, particularly in the PIP_2 loading experiments described above. For example, applying PIP_2-histone after BAPTA or DMSO vehicle incubation would assess the potential involvement of Ca^{2+} in these experiments. A similar experiment could be performed in the PIP_2 dialysis experiments. These control experiments are also important in determining dual PIP_2 regulation of NBCe1 in astrocytes. If Ca^{2+} chelation does not affect any of these protocols, then it is likely that

the Ca^{2+} mode of regulation is absent in these cells and NBCe1 does not undergo dual PIP_2 regulation in astrocytes.

By monitoring the fluorescence of the PIP_2 probe tubby-GFP, which is a high affinity PIP_2 binding domain conjugated to GFP (Balla & Várnai, 2009), Hughes *et al.* demonstrated that activating the G_q-coupled receptor for bradykinin on SCG neurons did not deplete PIP_2 (Hughes *et al.*, 2007). Only when PIP_2 resynthesis was blocked was there an apparent PIP_2 decrease in response to bradykinin. Tubby-GFP can be transfected into astrocytes to determine if mGluR activation elicits a decrease in PIP_2 or not (i.e., PIP_2 is rapidly resynthesized). We found that mGluR activation inhibited NBCe1 in astrocytes (Figure 4). Thus, the primary effect of mGluR activation on NBCe1 activity appears to be through a decrease in PIP_2 that should be measurable.

Conclusion

The data presented in this dissertation demonstrate that PIP_2 hydrolysis to IP_3/Ca^{2+} stimulates NBCe1-B and -C, but not NBCe1-A and all 3 variants are stimulated by PIP_2 per se. These data demonstrate for the first time a dual PIP_2 regulation mode for a transporter (NBCe1-B and NBCe1-C) similar to the dual PIP_2 regulation modes demonstrated for KCNQ. Through characterization in *Xenopus* oocytes, these studies can now be extended to mammalian cells to predict PIP_2 regulation modes. Based on these data, we predict that the activation of a G_q-coupled receptor that inhibits NBCe1-B or -C regulates NBCe1 through PIP_2 per se, whereas G_q-coupled receptor activation that stimulates NBCe1 regulates NBCe1 through Ca^{2+} released by PIP_2 hydrolysis (Figure 2). Further, regulation by PIP_2 per se may explain NBCe1 inhibition in energy deficient

states (e.g., hypoxia), where decreased ATP (the phosphate source for PIP_2 synthesis) inhibits NBCe1. The finding that NBCe1 variants are regulated by the powerful signaling phospholipid PIP_2 in an intact cell may represent a key mechanism whereby acid-base transporter activity and pH_i physiology is tightly regulated by G_q-coupled receptors under various physiological and pathological conditions. Given the ubiquitous expression of NBCe1 and PIP_2, this mechanism has potential physiological relevance in many organ systems. In addition, the work presented in this dissertation provides the foundation for examining the regulation of other bicarbonate transporters by PIP_2 and other phosphoinositides.

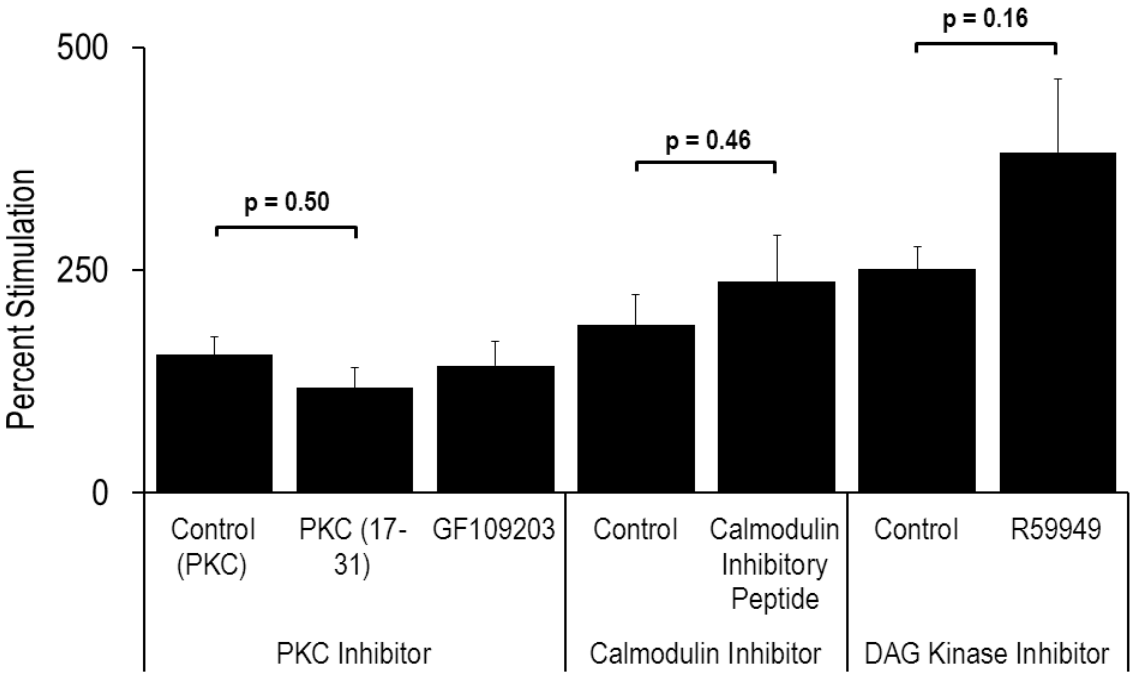

Figure 1. IP_3 stimulation of NBCe1-C is not mediated by common Ca^{2+}-dependent kinases. IP_3 stimulation of NBCe1-C was unaffected after PKC inhibition by an inhibitory peptide PKC (17-31) or inhibitor compound GF1092013, calmodulin inhibition by calmodulin inhibitory peptide, or DAG kinase inhibition by R59949.

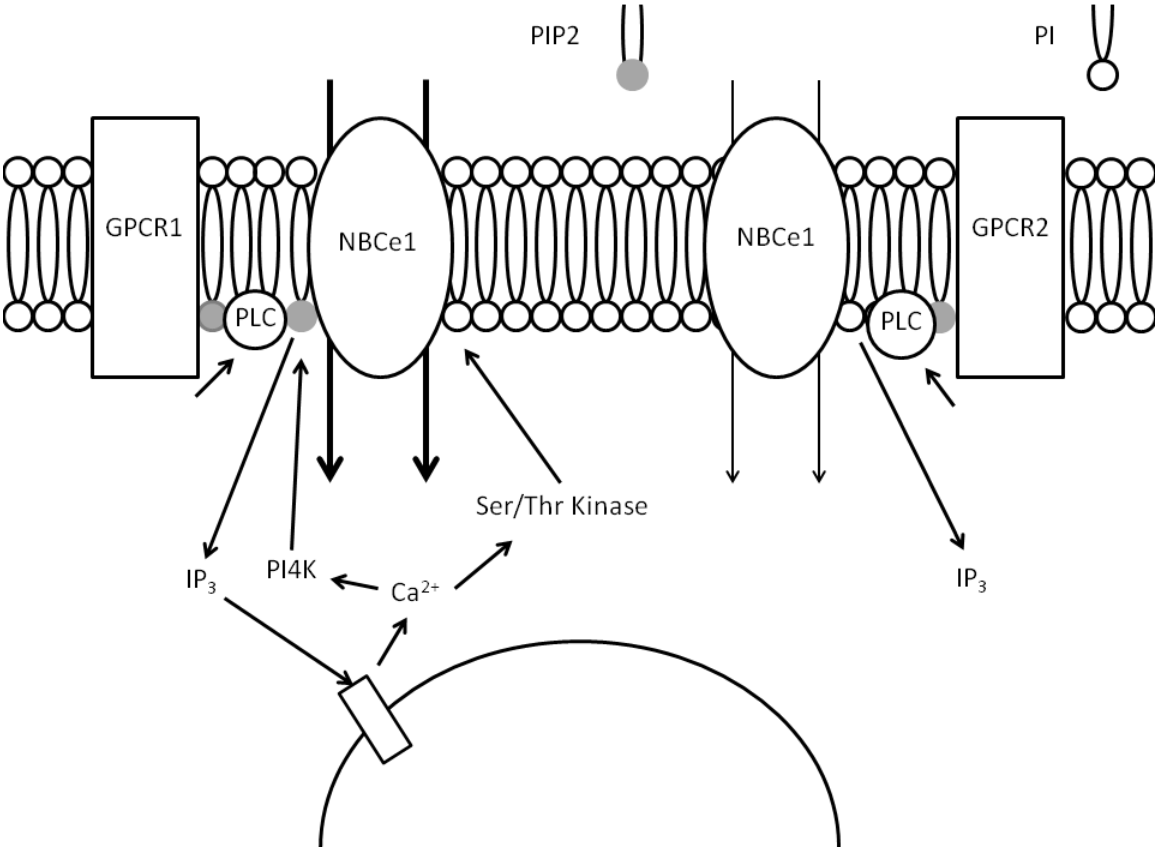

Figure 2. Summary of PIP_2 regulation of NBCe1. Activation of GPCR1 stimulates PLC-mediated PIP_2 hydrolysis to IP_3. IP_3 binds to the IP_3 receptor on the ER and releases Ca^{2+}. Ca^{2+} stimulates PI4K that replenishes PIP_2 in the membrane and there is no effective decrease in PIP_2. In this scenario, NBCe1-B or -C is stimulated by an unknown Ser/Thr kinase. Activation of GPCR2 stimulates PLC-mediated PIP_2 hydrolysis to IP_3. However, IP_3 does not bind to the IP_3 receptor and Ca^{2+} is not released. In this scenario, PIP_2 depletion inhibits all NBCe1 variants.

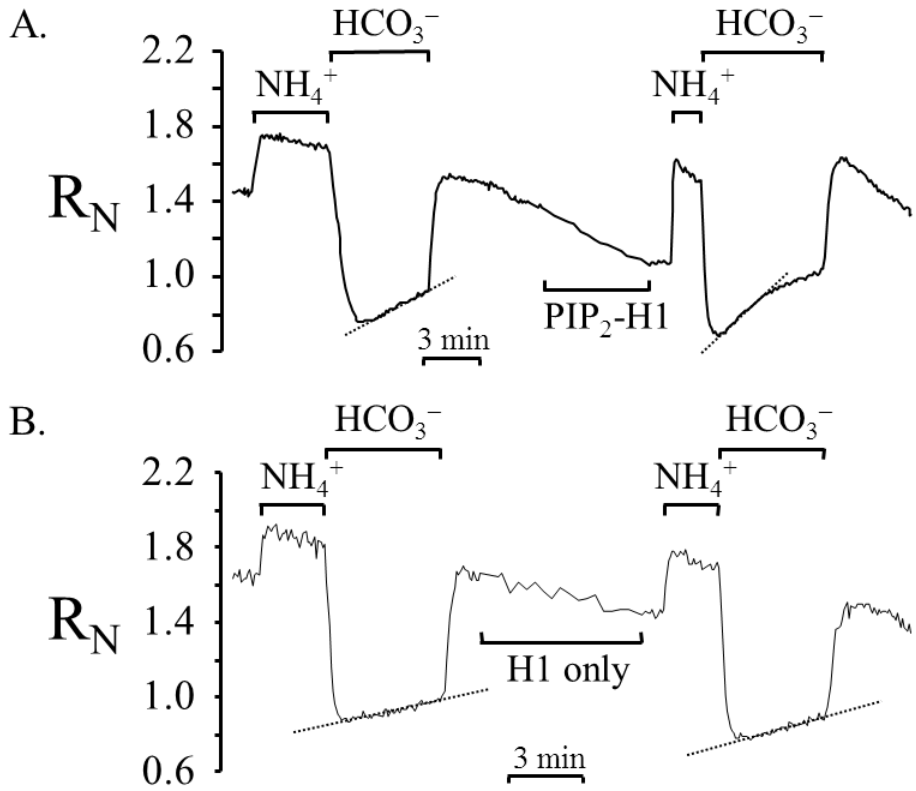

Figure 3. PIP_2-H1 complex stimulates pH_i recovery in HCO_3^-. (A) A control pH_i recovery (first dotted line) after an ammonium prepulse was obtained in HCO_3^-. Addition of the PIP_2-H1 complex decreased pH_i the histone was then removed and the pH_i recovery after the subsequent ammonium prepulse was stimulated. (B) Panel A-type experiment. Exposure to the histone complex without PIP_2 did not stimulate the pH_i recovery in HCO_3^-.

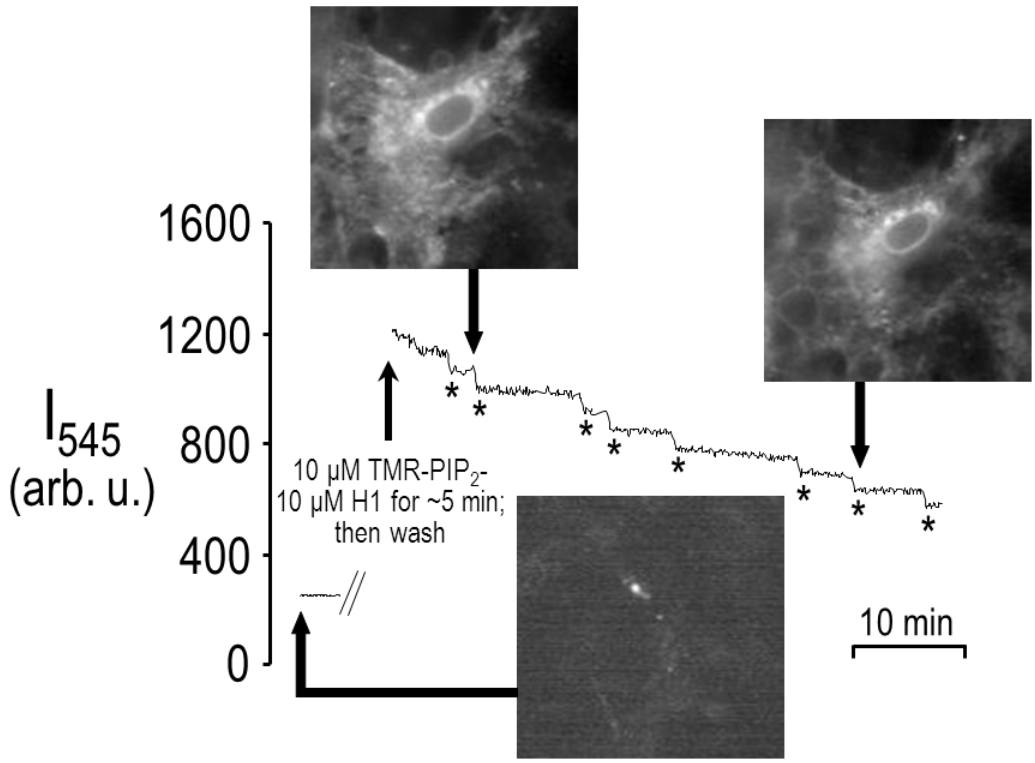

Figure 4. PIP_2-H1 complex increases PIP_2 in astrocytes over a prolonged period. Background fluorescence was obtained before incubating astrocytes with the H1/rhodamine-conjugated PIP_2 (TMR-PIP_2) complex. After a 5-minute wash fluorescence intensity was monitored. Fluorescence initially increased from baseline then gradually declined to ~33% of this increase over 50 min. Arrows depict a background image and images ~10 min and ~40 min post complex incubation. * = refocus

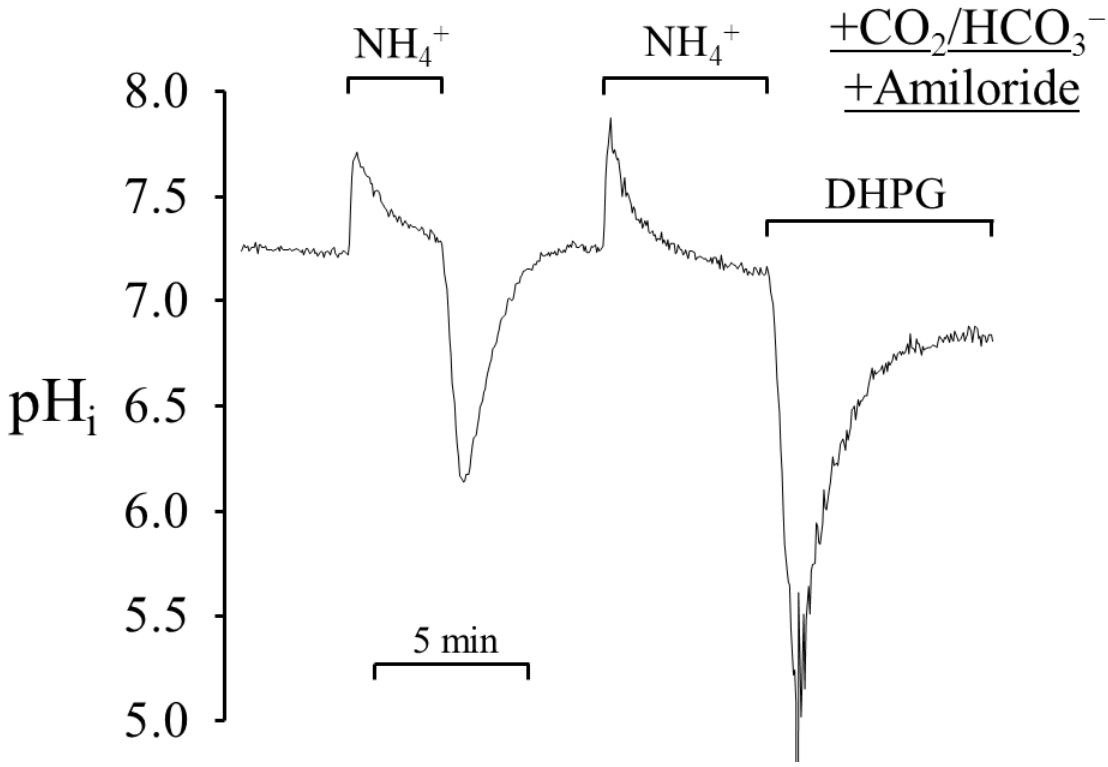

Figure 5. DHPG inhibits the endogenous NBCe1 in astrocytes. Astrocytes in CO_2/HCO_3^- and amiloride (to block NHE recovery) were acid-loaded by ammonium prepulse technique. The pH_i recovery in CO_2/HCO_3^- in the absence of DHPG (the first pH_i recovery) was faster than in the presence of DHPG (the second pH_i recovery).

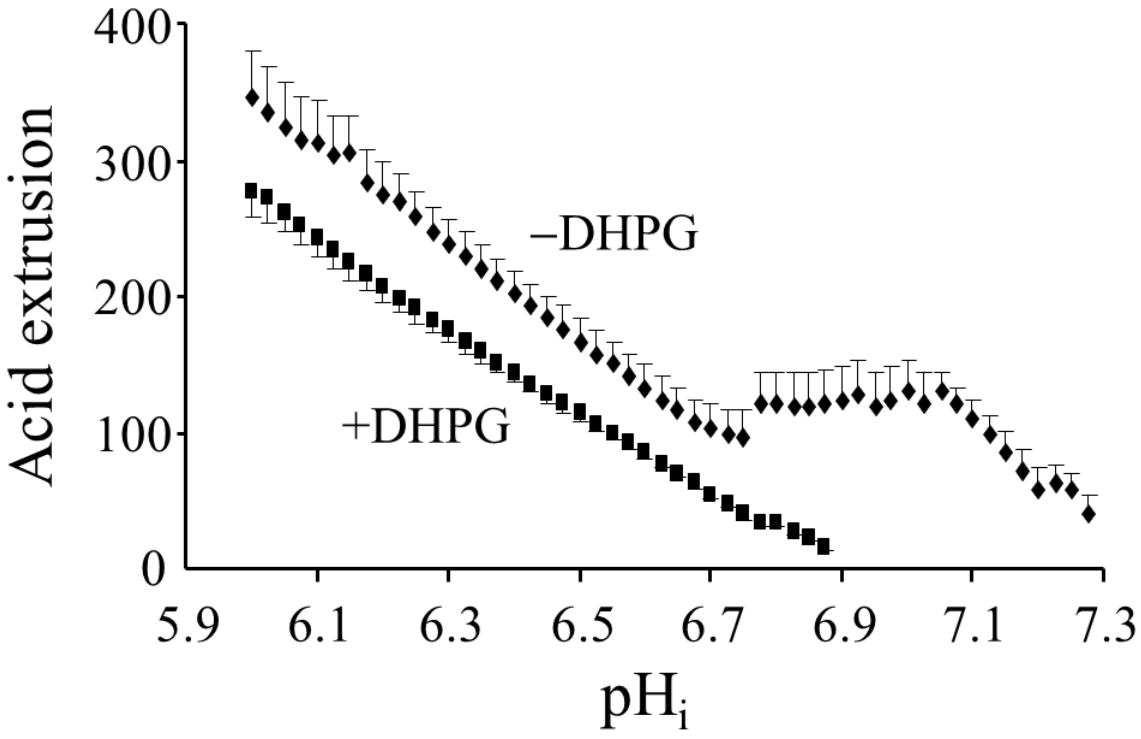

Figure 6. DHPG inhibits the endogenous NBCe1-mediated acid-extrusion in astrocytes. pH_i matched summary data for NBCe1-mediated acid extrusion from Figure 5-type experiments. Acid extrusion was inhibited in the presence (squares) vs. the absence (diamonds) of DHPG across all pH_i data points.

GENERAL LIST OF REFERENCES

Abuladze N, Lee I, Newman D, Hwang J, Boorer K, Pushkin A & Kurtz I (1998). Molecular cloning, chromosomal localization, tissue distribution, and functional expression of the human pancreatic sodium bicarbonate cotransporter. *J Biol Chem* **273,** 17689–17695.

Abuladze N, Song M, Pushkin A, Newman D, Lee I, Nicholas S & Kurtz I (2000). Structural organization of the human NBC1 gene: kNBC1 is transcribed from an alternative promoter in intron 3. *Gene* **251,** 109–122.

Aharonovitz O, Zaun HC, Balla T, York JD, Orlowski J & Grinstein S (2000). Intracellular pH regulation by Na^+/H^+ exchange requires phosphatidylinositol 4,5-bisphosphate. *J Cell Biol* **150,** 213–224.

Alper SL (2002). Genetic diseases of acid-base transporters. *Annu Rev Physiol* **64,** 899–923.

Alper SL (2009). Molecular physiology and genetics of Na^+-independent SLC4 anion exchangers. *J Exp Biol* **212,** 1672–1683.

Bae JS, Koo NY, Namkoong E, Davies AJ, Choi S-K, Shin Y, Jin M, Hwang S-M, Mikoshiba K & Park K (2013). Chaperone stress 70 protein (STCH) binds and regulates two acid/base transporters NBCe1-B and NHE1. *J Biol Chem* **288,** 6295–6305.

Balestrino M & Somjen G (1988). Concentration of carbon dioxide, interstitial pH and synaptic transmission in hippocampal formation of the rat. *J Physiol* **396,** 247–266.

Balla T (2013). Phosphoinositides: tiny lipids with giant impact on cell regulation. *Physiol Rev* **93,** 1019–1137.

Balla T & Várnai P (2003). Visualization of cellular phosphoinositide pools with GFP-fused protein-domains. *Sci STKE* **123,** pl3

Berridge MJ & Irvine RF (1984). Inositol trisphosphate, a novel second messenger in cellular signal transduction. *Nature* **312,** 315–321.

Bevensee MO, Apkon M & Boron WF (1997*a*). Intracellular pH regulation in cultured astrocytes from rat hippocampus. II. Electrogenic Na/HCO_3 cotransport. *J Gen Physiol* **110,** 467–483.

Bevensee MO & Boron WF (2007). Control of intracellular pH. In *The Kidney: Physiology and Pathophysiology*, pp. 1429–1480.

Bevensee MO, Schmitt BM, Choi I, Romero MF & Boron WF (2000). An electrogenic Na^+-HCO_3^- cotransporter (NBC) with a novel COOH-terminus , cloned from rat brain. *Am J Physiol Cell Physiol* **278,** C1200–C1211.

Bevensee MO, Weed RA & Boron WF (1997*b*). Intracellular pH regulation in cultured astrocytes from rat hippocampus. I. Role Of HCO_3^-. *J Gen Physiol* **110,** 453–465.

Boron WF & Boulpaep EL (1983). Intracellular pH regulation in the renal proximal tubule of the salamander basolateral HCO_3 transport. *J Gen Physiol* **81,** 53–94.

Boron WF & De Weer P (1976). Intracellular pH transients in squid giant axons caused by CO_2, NH_3, and metabolic inhibitors. *J Gen Physiol* **67,** 91–112.

Brown DA, Hughes SA, Marsh SJ & Tinker A (2007). Regulation of M(Kv7.2/7.3) channels in neurons by PIP_2 and products of PIP_2 hydrolysis: significance for receptor-mediated inhibition. *J Physiol* **582,** 917–925.

Burnham C, Amlal H, Wang Z, Shull G & Soleimani M (1997). Cloning and functional expression of a human kidney Na^+:HCO_3^- cotransporter. *J Biol Chem* **272,** 19111–19114.

Burnham CE, Flagella M, Wang Z, Amlal H, Shull GE & Soleimani M (1998). Cloning, renal distribution, and regulation of the rat Na^+-cotransporter. *Am J Physiol Ren Physiol* **274,** F1119–F1126.

Chesler M (1990). The regulation and modulation of pH in the nervous system. *Prog Neurobiol* **34,** 401–427.

Chesler M (2003). Regulation and modulation of pH in the brain. *Physiol Rev* **83,** 1183–1221.

Chever O, Djukic B, McCarthy KD & Amzica F (2010). Implication of Kir4.1 channel in excess potassium clearance: an *in vivo* study on anesthetized glial-conditional Kir4.1 knock-out mice. *J Neurosci* **30,** 15769–15777.

Choi I, Romero MF, Khandoudi N, Bril A & Boron WF (1999). Cloning and characterization of a human electrogenic Na^+- cotransporter isoform (hhNBC). *Am J Physiol Cell Physiol* **276,** C576–C584.

Clapham D (1995). Calcium signaling. *Cell* **80,** 259–268.

Deitmer J & Schlue W (1989). An inwardly directed electrogenic sodium-bicarbonate co-transport in leech glial cells. *J Physiol*179–194.

Deitmer J & Szatkowski M (1990). Membrane potential dependence of intracellular pH regulation by identified glial cells in the leech central nervous system. *J Physiol* **421,** 617–631.

Deitmer JW & Schlue W-R (1987). The regulation of intracellular pH by identified glial cells and neurones in the central nervous system of the leech. *J Physiolgy* **388,** 261–283.

Dickson EJ, Falkenburger BH & Hille B (2013). Quantitative properties and receptor reserve of the IP_3 and calcium branch of G_q-coupled receptor signaling. *J Gen Physiol* **141,** 521–535.

Ding W-G, Toyoda F & Matsuura H (2004). Regulation of cardiac IKs potassium current by membrane phosphatidylinositol 4,5-bisphosphate. *J Biol Chem* **279,** 50726–50734.

Evans RL, Ashton N, Elliott AC, Green R & Argent BE (1996). Interactions between secretin and acetylcholine in the regulation of fluid secretion by isolated rat pancreatic ducts. *J Physiol* **496,** 265–273.

Falkenburger BH, Jensen JB & Hille B (2010). Kinetics of PIP_2 metabolism and KCNQ2/3 channel regulation studied with a voltage-sensitive phosphatase in living cells. *J Gen Physiol* **135,** 99–114.

Ford CP, Stemkowski PL, Light PE & Smith PA (2003). Experiments to test the role of phosphatidylinositol closure in bullfrog sympathetic neurons. *J Neurosci* **23,** 4931–4941.

Gamper N, Reznikov V, Yamada Y, Yang J & Shapiro MS (2004). Phosphatidylinositol 4,5-bisphosphate signals underlie receptor-specific $G_{q/11}$-mediated modulation of N-type Ca^{2+} channels. *J Neurosci* **24,** 10980–10992.

Gamper N & Shapiro MS (2007). Regulation of ion transport proteins by membrane phosphoinositides. *Nat Rev Neurosci* **8,** 921–934.

Gross E, Fedotoff O, Pushkin A, Abuladze N, Newman D & Kurtz I (2003). Phosphorylation-induced modulation of pNBC1 function: distinct roles for the amino- and carboxy-termini. *J Physiol* **549,** 673–682.

Guo Z, Liliom K, Fischer DJ, Bathurst IC, Tomei LD, Kiefer MC & Tigyi G (1996). Molecular cloning of a high-affinity receptor for the growth factor-like lipid mediator lysophosphatidic acid from Xenopus oocytes. *Proc Natl Acad Sci USA* **93,** 14367–14372.

Halaszovich CR, Schreiber DN & Oliver D (2009). Ci-VSP is a depolarization-activated phosphatidylinositol-4,5-bisphosphate and phosphatidylinositol-3,4,5-trisphosphate 5'-phosphatase. *J Biol Chem* **284,** 2106–2113.

Hansen SB, Tao X & MacKinnon R (2011). Structural basis of PIP_2 activation of the classical inward rectifier K^+ channel Kir2.2. *Nature* **477,** 495–498.

Hilgemann DW & Ball R (1996). Regulation of cardiac Na^+/Ca^{2+} exchange and K_{ATP} potassium channels by PIP_2. *Science* **273,** 956–959.

Hobiger K, Utesch T, Mroginski MA & Friedrich T (2012). Coupling of Ci-VSP modules requires a combination of structure and electrostatics within the linker. *Biophys J* **102,** 1313–1322.

Hong JH, Yang D, Shcheynikov N, Ohana E, Shin DM & Muallem S (2013). Convergence of IRBIT, phosphatidylinositol (4,5) bisphosphate, and WNK/SPAK kinases in regulation of the Na^+-HCO_3^- cotransporters family. *Proc Natl Acad Sci USA* **110,** 4105–4110.

Hossain MI, Iwasaki H, Okochi Y, Chahine M, Higashijima S, Nagayama K & Okamura Y (2008). Enzyme domain affects the movement of the voltage sensor in ascidian and zebrafish voltage-sensing phosphatases. *J Biol Chem* **283,** 18248–18259.

Hughes S, Marsh SJ, Tinker A & Brown DA (2007). PIP_2-dependent inhibition of M-type (Kv7.2/7.3) potassium channels: direct on-line assessment of PIP_2 depletion by G_q-coupled receptors in single living neurons. *Pflugers Arch* **455,** 115–124.

Hurley J & Misra S (2000). Signaling and subcellular targeting by membrane binding domains. *Annu Rev Biophys Biomol Struct* **29,** 49–79.

Ishiguro H, Steward MC, Wilson RW & Case RM (1996). Bicarbonate secretion in interlobular ducts from guinea-pig pancreas. *J Physiol* **495,** 179–191.

Iwasaki H, Murata Y, Kim Y, Hossain MI, Worby C a, Dixon JE, McCormack T, Sasaki T & Okamura Y (2008). A voltage-sensing phosphatase, Ci-VSP, which shares sequence identity with PTEN, dephosphorylates phosphatidylinositol 4,5-bisphosphate. *Proc Natl Acad Sci USA* **105,** 7970–7975.

Kohout SC, Bell SC, Liu L, Xu Q, Minor DL & Isacoff EY (2010). Electrochemical coupling in the voltage-dependent phosphatase Ci-VSP. *Nat Chem Biol* **6,** 369–375.

Korc M, Friess H, Yamanaka Y, Kobrin MS, Buchler M & Beger HG (1994). Chronic pancreatitis is associated with increased concentrations of epidermal growth factor receptor, transforming growth factor alpha, and phospholipase C gamma. *Gut* **35,** 1468–1473.

Lee MG, Ohana E, Park HW, Yang D & Muallem S (2012). Molecular mechanism of pancreatic and salivary gland fluid and HCO_3 secretion. *Physiol Rev* **92,** 39–74.

Lee SK, Grichtchenko II & Boron WF (2011). Distinguishing HCO_3^- from CO_3^{2-} transport by NBCe1-A. *FASEB J*656.9.

Liu Y, Xu J-Y, Wang D-K, Wang L & Chen L-M (2011). Cloning and identification of two novel NBCe1 splice variants from mouse reproductive tract tissues: a comparative study of NCBT genes. *Genomics* **98,** 112–119.

Lopes CMB, Rohács T, Czirják G, Balla T, Enyedi P & Logothetis DE (2005). PIP_2 hydrolysis underlies agonist-induced inhibition and regulates voltage gating of two-pore domain K^+ channels. *J Physiol* **564,** 117–129.

Madshus IH (1988). Regulation of intracellular pH in eukaryotic cells. *Biochem J* **250,** 1–8.

Majumdar D, Maunsbach AB, Shacka JJ, Williams JB, Berger UV, Schultz KP, Harkins LE, Boron WF, Roth KA, Bevensee MO (2008). Localization of electrogenic Na/bicarbonate cotransporter NBCe1 variants in rat brain. *Neuroscience* **155,** 818–832.

McAlear SD & Bevensee MO (2006). A cysteine-scanning mutagenesis study of transmembrane domain 8 of the electrogenic sodium/bicarbonate cotransporter NBCe1. *J Biol Chem* **281,** 32417–32427.

McAlear SD, Liu X, Williams JB, McNicholas-Bevensee CM & Bevensee MO (2006). Electrogenic Na/HCO_3 cotransporter (NBCe1) variants expressed in *Xenopus* oocytes: functional comparison and roles of the amino and carboxy termini. *J Gen Physiol* **127,** 639–658.

McLaughlin S, Wang J, Gambhir A & Murray D (2002). PIP_2 and proteins: interactions, organization, and information flow. *Annu Rev Biophys Biomol Struct* **31,** 151–175.

Muallem S & Loessberg P (1990). Intracellular pH-regulatory mechanisms in pancreatic acinar cells. I. Characterization of H^+ and HCO_3^- transporters. *J Biol Chem* **265,** 12806–12812.

Murata Y, Iwasaki H, Sasaki M, Inaba K & Okamura Y (2005). Phosphoinositide phosphatase activity coupled to an intrinsic voltage sensor. *Nature* **435,** 1239–1243.

Murata Y & Okamura Y (2007). Depolarization activates the phosphoinositide phosphatase Ci-VSP, as detected in *Xenopus* oocytes coexpressing sensors of PIP_2. *J Physiol* **583,** 875–889.

Nasuhoglu C, Feng S, Mao J, Yamamoto M, Yin HL, Earnest S, Barylko B, Albanesi JP & Hilgemann DW (2002). Nonradioactive analysis of phosphatidylinositides and other anionic phospholipids by anion-exchange high-performance liquid chromatography with suppressed conductivity detection. *Anal Biochem* **301,** 243–254.

O'Connor E, Sontheimer H & Ransom B (1994). Rat hippocampal astrocytes exhibit electrogenic sodium-bicarbonate co-transport. *J Neurophysiol* **72,** 2580–2589.

Okamura Y, Murata Y & Iwasaki H (2009). Voltage-sensing phosphatase: actions and potentials. *J Physiol* **587,** 513–520.

Ozaki S, DeWald DB, Shope JC, Chen J & Prestwich GD (2000). Intracellular delivery of phosphoinositides and inositol phosphates using polyamine carriers. *Proc Natl Acad Sci USA* **97,** 11286–11291.

Di Paolo G & De Camilli P (2006). Phosphoinositides in cell regulation and membrane dynamics. *Nature* **443,** 651–657.

Pappas C & Ransom B (1994). Depolarization-induced alkalinization (DIA) in rat hippocampal astrocytes. *J Neurophysiol* **72,** 2816–2826.

Parker MD, Skelton LA, Daly CM & Boron WF (2007). IRBIT binds to and functionally enhances the electroneutral Na-coupled bicarbonate transporters NBCn1, NDCBE and NCBE (Abstract). *FASEB J* **21,** A1285.

Parker MD & Boron WF (2013). The Divergence, actions, roles, and relatives of sodium-coupled bicarbonate transporters. *Physiol Rev* **93,** 803–959.

Ratzan WJ, Evsikov AV, Okamura Y & Jaffe LA (2011). Voltage sensitive phosphoinositide phosphatases of *Xenopus*: their tissue distribution and voltage dependence. *J Cell Physiol* **226,** 2740–2746.

Romero MF, Hediger M, Boulpaep E & Boron WF (1997). Expression cloning and characterization of a renal electrogenic Na^+/HCO_3^- cotransporter. *Nature* **387,** 409–413.

Romero MF, Fong P, Urs VB, Hediger MA & Boron WF (1998). Cloning and functional expression of rNBC, an electrogenic Na^+-cotransporter from rat kidney. *Am J Physiol Ren Physiol* **274,** F425–F432.

Roos A & Boron WF (1981). Intracellular pH. *Physiol Rev* **61,** 296–434.

Sakata S, Hossain MI & Okamura Y (2011). Coupling of the phosphatase activity of Ci-VSP to its voltage sensor activity over the entire range of voltage sensitivity. *J Physiol* **589,** 2687–2705.

Shirakabe K, Priori G, Yamada H, Ando H, Horita S, Fujita T, Fujimoto I, Mizutani A, Seki G & Mikoshiba K (2006). IRBIT, an inositol 1,4,5-trisphosphate receptor-binding protein, specifically binds to and activates pancreas-type Na^+/HCO_3^- cotransporter 1 (pNBC1). *Proc Natl Acad Sci USA* **103,** 9542–9547.

Sinđić A, Sussman CR & Romero MF (2010). Primers on molecular pathways: bicarbonate transport by the pancreas. *Pancreatology* **10,** 660–663.

Steward MC & Ishiguro H (2009). Molecular and cellular regulation of pancreatic duct cell function. *Curr Opin Gastroenterol* **25,** 447–453.

Suh BC & Hille B (2002). Recovery from muscarinic modulation of M current channels requires phosphatidylinositol 4,5-bisphosphate synthesis. *Neuron* **35,** 507–520.

Suh BC & Hille B (2008). PIP_2 is a necessary cofactor for ion channel function: how and why? *Annu Rev Biophys* **37,** 175–195.

Suh BC, Inoue T, Meyer T & Hille B (2006). Rapid chemically induced changes of PtdIns(4,5)P_2 gate KCNQ ion channels. *Science* **314,** 1454–1457.

Sussman CR, Zhao J, Plata C, Lu J, Daly C, Angle N, Dipiero J, Drummond IA, Liang JO, Boron WF, Romero MF, Chang M, Ia D, Jo L, Wf B & Mf R (2009). Cloning , localization , and functional expression of the electrogenic Na/ bicarbonate cotransporter (NBCe1) from zebrafish. 865–875.

Svichar N, Esquenazi S, Chen HY & Chesler M (2011). Preemptive regulation of intracellular pH in hippocampal neurons by a dual mechanism of depolarization-induced alkalinization. *J Neurosci* **31,** 6997–7004.

Tang CM, Dichter M & Morad M (1990). Modulation of the N-methyl-D-aspartate channel by extracellular H^+. *Proc Natl Acad Sci USA* **87,** 6445–6449.

Thévenod F, Roussa E, Schmitt BM & Romero MF (1999). Cloning and immunolocalization of a rat pancreatic Na^+ bicarbonate cotransporter. *Biochem Biophys Res Commun* **264,** 291–298.

Thornell IM, Wu J & Bevensee MO (2010). The IP_3 receptor-binding protein IRBIT reduces phosphatidylinositol 4,5-bisphosphate (PIP_2) stimulation of Na/bicarbonate cotransporter NBCe1 variants expressed in *Xenopus* laevis oocytes (Abstract). *FASEB J* **24,** 815.6.

Thornell IM, Wu J, Liu X & Bevensee MO (2012). PIP_2 hydrolysis stimulates electrogenic Na/bicarbonate cotransporter NBCe1-B and -C variants expressed in *Xenopus laevis* oocytes. *J Physiol* **590,** 5993–6011.

Tombaugh G & Somjen G (1996). Effects of extracellular pH on voltage-gated Na^+, K^+ and Ca^{2+} currents in isolated rat CA1 neurons. *J Physiolgy* **493,** 719–732.

Traynelis S & Cull-Candy S (1990). Proton inhibition of N-methyl-D-aspartate receptors in cerebellar neurons. *Nature* **345,** 347 – 350.

Trivedi B & Danforth WH (1966). Effect of pH on the kinetics of frog muscle phosphofructokinase. *J Biol Chem* **241,** 4110–4112.

Vaughan-Jones RD, Spitzer KW & Swietach P (2009). Intracellular pH regulation in heart. *J Mol Cell Cardiol* **46,** 318–331.

Waldmann R, Champigny G, Bassilana F, Heurteaux C & Lazdunski M (1997). A proton-gated cation channel involved in acid-sensing. *Nature* **386,** 173–177.

Whorton MR & Mackinnon R (2011). Crystal structure of the mammalian GIRK2 K^+ channel and gating regulation by G proteins, PIP_2, and sodium. *Cell* **147,** 199–208.

Winks JS, Hughes S, Filippov AK, Tatulian L, Abogadie FC, Brown D a & Marsh SJ (2005). Relationship between membrane phosphatidylinositol-4,5-bisphosphate and receptor-mediated inhibition of native neuronal M channels. *J Neurosci* **25,** 3400–3413.

Wu J, McNicholas CM & Bevensee MO (2009). Phosphatidylinositol 4,5-bisphosphate (PIP_2) stimulates the electrogenic Na/HCO_3 cotransporter NBCe1-A expressed in *Xenopus* oocytes. *Proc Natl Acad Sci U S A* **106,** 14150–14155.

Yamaguchi S & Ishikawa T (2008). The electrogenic Na^+-HCO_3^- cotransporter NBCe1-B is regulated by intracellular Mg^{2+}. *Biochem Biophys Res Commun* **376,** 100–104.

Yamaguchi S & Ishikawa T (2012). IRBIT reduces the apparent affinity for intracellular Mg^{2+} in inhibition of the electrogenic Na^+-HCO_3^- cotransporter NBCe1-B. *Biochem Biophys Res Commun* **424,** 433–438.

Yang D, Shcheynikov N, Zeng W, Ohana E, So I, Ando H, Mizutani A, Mikoshiba K & Muallem S (2009). IRBIT coordinates epithelial fluid and HCO_3^- secretion by

stimulating the transporters pNBC1 and CFTR in the murine pancreatic duct. **119,** 193–202.

Zaika O, Zhang J & Shapiro MS (2011). Combined phosphoinositide and Ca^{2+} signals mediating receptor specificity toward neuronal Ca^{2+} channels. *J Biol Chem* **286,** 830–841.

Zhang H, Craciun LC, Mirshahi T, Rohács T, Lopes CMB, Jin T & Logothetis DE (2003). PIP_2 activates KCNQ channels, and its hydrolysis underlies receptor-mediated inhibition of M currents. *Neuron* **37,** 963–975.

APPENDIX

INSTITUTIONAL ANIMAL CARE AND USE COMMITTEE APPROVAL FORM

THE UNIVERSITY OF ALABAMA AT BIRMINGHAM

Institutional Animal Care and Use Committee (IACUC)

NOTICE OF APPROVAL

DATE: June 16, 2014

TO: MARK OLIVER BEVENSEE, Ph.D.
MCLM-812
(205) 975-9084

FROM:

Robert A. Kesterson, Ph.D., Chair
Institutional Animal Care and Use Committee (IACUC)

SUBJECT: Title: Na/Bicarbonate Cotransporters in Brain
Sponsor: NIH
Animal Project_Number: 140608765

As of June 29, 2014 the animal use proposed in the above referenced application is approved. The University of Alabama at Birmingham Institutional Animal Care and Use Committee (IACUC) approves the use of the following species and number of animals:

Species	Use Category	Number In Category
Rats	B	34
Frogs	C	13

Animal use must be renewed by June 28, 2015. Approval from the IACUC must be obtained before implementing any changes or modifications in the approved animal use.

Please keep this record for your files, and forward the attached letter to the appropriate granting agency.

Refer to Animal Protocol Number (APN) 140608765 when ordering animals or in any correspondence with the IACUC or Animal Resources Program (ARP) offices regarding this study. If you have concerns or questions regarding this notice, please call the IACUC office at (205) 934-7692.

Institutional Animal Care and Use Committee (IACUC)
CH19 Suite 403
933 19th Street South
(205) 934-7692
FAX (205) 934-1188

Mailing Address:
CH19 Suite 403
1530 3rd Ave S
Birmingham, AL 35294-0019